In vitro Antidiabetic and Antimicrobial properties of *Ocimum* species (*Ocimum basilicum* and *Ocimum sanctum*) (L.)

by

Veshara Malapermal

Submitted in fulfilment of the requirements of the degree of

Master in Technology

At

Durban University of Technology

Faculty of Health Sciences

Biomedical Technology and Clinical Technology

Supervisor: Ms J.N. Mtshali	Date: 26/02/2016
Co-supervisor: Dr I. Botha	Date: 26/02/2016
Co-supervisor: Dr K.S.B. Naidu	Date: 26/02/2016

February 2016

DECLARATION

I, **Veshara Malapermal**, hereby declare that this dissertation entitled **"*In vitro* antidiabetic and antimicrobial properties of *Ocimum* species (*Ocimum basilicum* and *Ocimum sanctum*) (L.)"**, submitted to the Durban University of Technology, in fulfilment of the requirements for the award of the Degree of Master of Technology, Biomedical Technology, in the Faculty of Health Sciences, is the result of my own work and that all sources used or quoted have been indicated and acknowledged by means of complete references.

…… ……

Veshara Malapermal Date of signature

…… ……

Signature of supervisor Date of signature

Mrs. Joyce N. Mtshali M Med Sc.: Medical Micro (UKZN)

…… ……

Signature of co-supervisor Date of signature

Dr. Izel Botha D.Tech: Homeopathy (DUT)

…… ……

Signature of co-supervisor Date of signature

Dr. K. Suresh Babu Naidu PhD (Research Associate, DUT)

ACKNOWLEDGEMENTS

I would like to convey my sincere gratitude to my supervisor Ms J.N. Mtshali, co-supervisors Dr I. Botha and Dr K.S.B. Naidu for their patience and continued support throughout this study.

Dr N. Somaru for assisting and teaching me the techniques involved in the preparation of the various extracts.

My humble appreciation to Dr K. Anand (Department of Chemistry, DUT) for his continued expertise, without you this research could have never have been accomplished.

Mr D. Singh (Statistician-DUT) for his assistance regarding the statistical aspects of this research.

I am sincerely grateful to the following individuals: Mr G. Nursayhe (Department of Chemistry, DUT), Ms E. Rampersad (Department of Biotechnology, DUT), Mr A. Ramsaroop (Department of Mechanical Engineering, DUT), Mr N.K. Broomhead (Department of Chemistry, UKZN), and Mr C. Phillip (Electron Microscope Unit, UKZN).

My regards to the kind staff of the Biomedical and Clinical Technology Department for their help and encouragement, especially Mrs P. Pillay, Ms T.S. Ndolvu and Prof. J.K. Adams. Special thanks to Mrs H. Ramphal for always motivating me and for her constant interest in my personal well-being.

I offer my humble appreciation and blessings to my dear family and friends who supported me throughout this study.

This study is dedicated to my loving Father (K. Malapermal), Mother (T. Malapermal) and my late Aunt Mrs A. Naidoo, thank you for always instilling in me the importance of an education.

Above all, I wish to thank GOD in all forms and name for divine guidance and blessing to start and complete this project.

ABSTRACT

Introduction

In Africa, use of phytotherapy for treatment of diabetes mellitus is a common form of practice. Considering the increasing burden of non-communicable diseases in South Africa efforts are directed at simple, cost effective, non-hazardous and efficient methods to treat cancer, cardiovascular diseases and diabetes. The role of phytonanotherapy is an attractive proposition for advancing new therapies. Metal nanoparticles are a possible means for delivery of such therapies. However, this requires investigation on interactions, mechanisms and therapeutic efficacy upon co-administering ethnobotanicals with metal nanoparticles and existing drug therapy in human beings.

Aim

The primary aim of the study was to test the *in vitro* antidiabetic and antibacterial activity of *Ocimum sanctum* (leaf extracts and flower extracts), *Ocimum basilicum* (leaf extracts and flower extracts), and a combination of the leaf extracts of both, and to observe whether any antidiabetic and antibacterial activity was enhanced in due to phyto-synthesised bimetallic gold-silver (Au-Ag) nanoparticles and silver nanoparticles.

Methods

Aqueous and ethanol extracts of *O. sanctum* and *O. basilicum* leaf and flowers alone and combined (leaf + flower) were prepared using hot vs cold water extraction techniques and 60% and 70% ethanol as polar solvents.

A simple, rapid, cost effective and reproducible green chemistry method synthesised alloyed bimetallic (Au-Ag) nanoparticles using *O. basilicum* leaf and flower aqueous extracts and prepared silver nanoparticles (AgNps) using *O. basilicum* and *O. sanctum* leaf aqueous extracts singly and in combination (*O. sanctum* + *O. basilicum*). The size, shape and elemental analysis of the nanoparticles was carried out using UV-Visible spectroscopy, transmission electron microscopy (TEM), scanning electron microscopy coupled with energy-dispersive X-ray (SEM-EDX), dynamic light scattering (DLS) and zeta potential.

Fourier transform infrared spectroscopy (FT-IR) supported by gas chromatography mass spectroscopy (GC-MS) identified the bio-capping agents.

Antidiabetic carbohydrate metabolising enzymes, α-amylase (porcine) and *Bacillus stearothermophilus* α-glucosidase as models tested the *in vitro* inhibitory potential of the aqueous and ethanol plant extracts and the phyto-synthesised (Au-Ag) bimetallic and AgNps. In addition, the study investigated the antibacterial potential for the aqueous plant preparations and their respective phyto-synthesised bimetallic and AgNps against the bacterial species *Staphylococcus aureus, Escherichia coli, Bacillus subtilis, Salmonella* species and *Pseudomonas aeruginosa* compared to gentamycin and vancomycin.

Results

Bimetallic nanoparticles (synthesised from leaf and flower aqueous extracts) displayed inhibitory activity that showed uncompetitive inhibition (leaf extract), and non-competitive inhibition (flower extract) of α-amylase and competitive (leaf extract) and uncompetitive inhibition (flower extract) of α-glucosidase. Bimetallic nanoparticles were higher in inhibitory activity than acarbose and the crude *O. basilicum* ethanol and aqueous leaf and flower extracts. In the antibacterial analysis, bimetallic nanoparticles derived from *O. basilicum* leaf showed inhibition against *Staphylococcus aureus, Escherichia coli, Bacillus subtilis* and *Pseudomonas aeruginosa* and were greater in activity compared to the crude aqueous leaf extract from *O. basilicum*.

The *in vitro* inhibitory effect of AgNps derived from *O. sanctum* and AgNps derived from *O. basilicum* on both enzymes was higher in activity than acarbose and their respective crude extracts. However, in combination (*O. sanctum* + *O. basilicum*), the derived AgNps appeared to be a less potent inhibitor of α-amylase and α-glucosidase enzyme and was lower than acarbose. AgNps synthesised from the combination of *O. sanctum* and *O. basilicum* showed the highest percentage inhibition against *Bacillus stearothermophilus* α-glucosidase, and AgNps derived from *O. sanctum* and AgNps derived from *O. basilicum* displayed competitive type of inhibition. In the antibacterial analysis, AgNps derived from the various extracts showed zones of inhibition against the Gram negative and Gram positive bacterial test strains. However, AgNps synthesised from the *O. sanctum* leaf extract showed higher inhibition against *Escherichia coli* than the positive control gentamycin and higher inhibition against *Staphylococcus aureus* compared to vancomycin. In addition, AgNps from *O.*

sanctum leaf extract displayed inhibition against *Bacillus subtilis*, *Pseudomonas aeruginosa* and *Salmonella* species, thus representing the highest antibacterial potential.

Conclusion

The results demonstrate the possibility of synthesis of stable silver and bimetallic nanoparticles of *Ocimum* sp. The synthesised silver nanoparticles and first time synthesis of bimetallic (Au-Ag) nanoparticles displayed enhanced antihyperglycaemic properties compared to their respective crude extracts and, therefore, show promising effects in lowering postprandial hyperglycaemia in diabetic patients with dual potential for antibacterial treatment. However, the antidiabetic and antibacterial effect will need to be further affirmed in a clinical context. Medicinal plants with therapeutic value may create a new platform for further research to explore the potential for herbal medicine and nanoscience as effective biomedical and industrial applications, and for improving existing drug delivery systems in diabetic patients. Investigations into the cytotoxicity of these extracts and phytosynthesised nanoparticles is recommended.

TABLE OF CONTENTS

LIST OF FIGURES

LIST OF SCHEMES

LIST OF TABLES

LIST OF APPENDIXES

ACRONYMS AND ABBREVIATIONS

α	Alpha
Aq	Aqueous
AIDS	Acquired Immunodeficiency Syndrome
Asymp. Sig.	Asymptotic Significance
B. subtilis	*Bacillus subtilis*
β	Beta
BP	Blood pressure
CAM	Complementary and Alternative Medicine
Conc	Concentration
Dist	Distillation
DLS	Dynamic Light Scattering
DM	Diabetes mellitus
E. coli	*Escherichia coli*
EtOH	Ethanol
FBG	Fasting blood glucose
FFA	Free fatty acids
FID	Flame Ionisation Detector
FT-IR	Fourier Transform Infrared Spectroscopy
g	Grams
GC-MS	Gas Chromatography Mass Spectrophotometry
GK	Glucokinase
G6P	Glucose-6-phosphate

G6PDH	Glucose-6-phosphate dehydrogenase
HK	Hexokinase
HIV	Human Immunodeficiency Virus
HPA	Human pancreatic α-amylase
IC_{50}	Concentration inhibiting 50% of the effect
IDDM	Insulin-dependent diabetes mellitus
L	Lamiaceae/Labiatae
MBC	Minimum Bactericidal Concentration
MF	Molecular Formula
MH agar	Mueller Hinton agar
MIC	Minimum Inhibitory Concentration
mg	Milligrams
ml	Millilitres
mM	Millimolar
Min	Minute
MOA	Mechanism of action
MODY	Maturity onset diabetes of the young
MRSA	Methicillin-resistant *Staphylococcus aureus*
MW	Molecular Weight
NIDDM	Non-insulin dependent diabetes mellitus
NIST	National Institute of Standards and Technology
Nps	Nanoparticles
OS	*Ocimum sanctum*

OB	*Ocimum basilicum*
P. aeruginosa	*Pseudomonas aeruginosa*
PFK	Phosphofructokinase
PPA	Porcine pancreatic α-amylase
PPHG	Postprandial hyperglycaemia
ROH	Alcohol
ROS	Reactive oxygen species
RT	Room temperature
S. aureus	*Staphylococcus aureus*
SA	South Africa
SEM-EDX	Scanning Electron Microscopy-Energy Dispersed X-ray
Sp	Species
TB	Tuberculosis
TEM	Transmission Electron Microscopy
TG	Triglycerides
TM	Traditional medicine
UV	Ultraviolet
UV-Vis	Ultraviolet-Visible radiation
VLDL	Very low density lipoprotein
vs	Versus
WHO	World Health Organisation

CHAPTER 1 : INTRODUCTION TO PRESENT STUDY

1.1 Introduction

Africa has a rich diversity of indigenous medicinal plants (Fang 2011). Developing countries such as South Africa (SA) give high priority to eco-friendly, non-hazardous and cost effective healthcare including the use of medicinal plants to treat various illnesses, including human immunodeficiency virus infection and acquired immune deficiency syndrome (HIV/AIDS), tuberculosis (TB), malaria, diabetes mellitus and cancer (Gurib-Fakim 2006; van Huyssteen 2007). Reports show that more than 80% of the southern African population use complementary and alternative medicines (CAM) (Maduna 2006), with a high proportion using it together with conventional prescription drugs (Maduna 2006; Fang 2011). This high level of usage is for three main reasons: improving quality of life, relief of symptoms and prevention of long-term complications (Maduna 2006). Despite the advances and advantages of conventional pharmaceutical medication such medications can be associated with long-term side effects and pose risks of inefficacy for treatment of chronic diseases such as diabetes (Wadkar *et al.* 2007).

In phytonanotherapy, the synergistic features of plant and metal nanoparticles (Nps) offer potential healing properties that may be the clinical bioequivalence of many synthetic drugs, with minimal side effects (Grace and Pandian 2007; Sinha 2006). This could provide alternative approaches to treatment of chronic diseases, overcoming the disadvantages of synthetic monotherapy allowing medicinal plant therapy to co-exist with current synthetic treatments (Subramania *et al.* 2012; Durai *et al*. 2014). This creates a much needed paradigm shift as the base for further clinical studies in diabetes research.

Numerous *in vitro* and *in vivo* studies have reported several South African medicinal plants with antidiabetic properties (Afolayan and Sunmonu 2010; van de Venter *et al*. 2008; Deutschländera *et al*. 2009). However, there exists a lack of information about the antidiabetic efficacy and safety of phyto-synthesised Nps. Plants consist of multiple bioactive compounds (phenols, alkaloids, flavonoids, terpenes, terpenoids etc.) (Bilal *et al.* 2012) therefore it is necessary that the biological effectiveness of these compounds be substantiated.

The present study investigates the *in vitro* antidiabetic and antibacterial activity of *Ocimum sanctum* (*O. sanctum*) and *Ocimum basilicum* (*O. basilicum*) singly and in combination (O. *sanctum* + *O. basilicum*). The inhibitory potential of the crude extracts and bio-synthesised Nps was tested using α-amylase and α-glucosidase enzymes and their antibacterial properties were tested against *Staphylococcus aureus*, *Escherichia coli*, *Bacillus subtilis*, *Salmonella* species (sp.) and *Pseudomonas aeruginosa*. Inhibition of α-amylase and α-glucosidase enzymes retards the rate of carbohydrate digestion providing an alternative and less invasive strategy for reducing postprandial hyperglycaemia (PPHG) in diabetic patients (Subramanian *et al.* 2008). Furthermore, the emerging rate of bacterial infections in diabetic patients validates the need for the discovery of dual diabetes therapies (Shankar *et al*. 2005).

Since the present study focused on the potential antidiabetic and antibacterial activity of medicinal plants and phyto-synthesised Nps as a treatment of diabetes, a description of diabetes is provided in Chapter 1, and the medicinal plants to treat this disease is included as these aspects apply to this study. A comprehensive literature survey specific to phytonanotherapy a major focus on the present study, is detailed in Chapter 2 as well as the rationale for using carbohydrate metabolising enzymes and diabetic related bacteria.

1.2 Diabetes mellitus

1.2.1 Characterisation of diabetes mellitus

Diabetes is one of the most common metabolic disorders worldwide (Wild *et al.* 2004), characterised by a loss of glucose homeostasis with disturbances in carbohydrate, fat and protein metabolism resulting from defects in insulin secretion, insulin action, or both (Katzung *et al.* 2009). Without adequate insulin, body tissues, in particular the liver, muscular and adipose tissues fail to take up and use glucose from the blood circulation. The resultant elevated blood glucose level is known as hyperglycaemia (Jarald *et al.* 2008). Figure 1 shows the many factors contributing to hyperglycaemia.

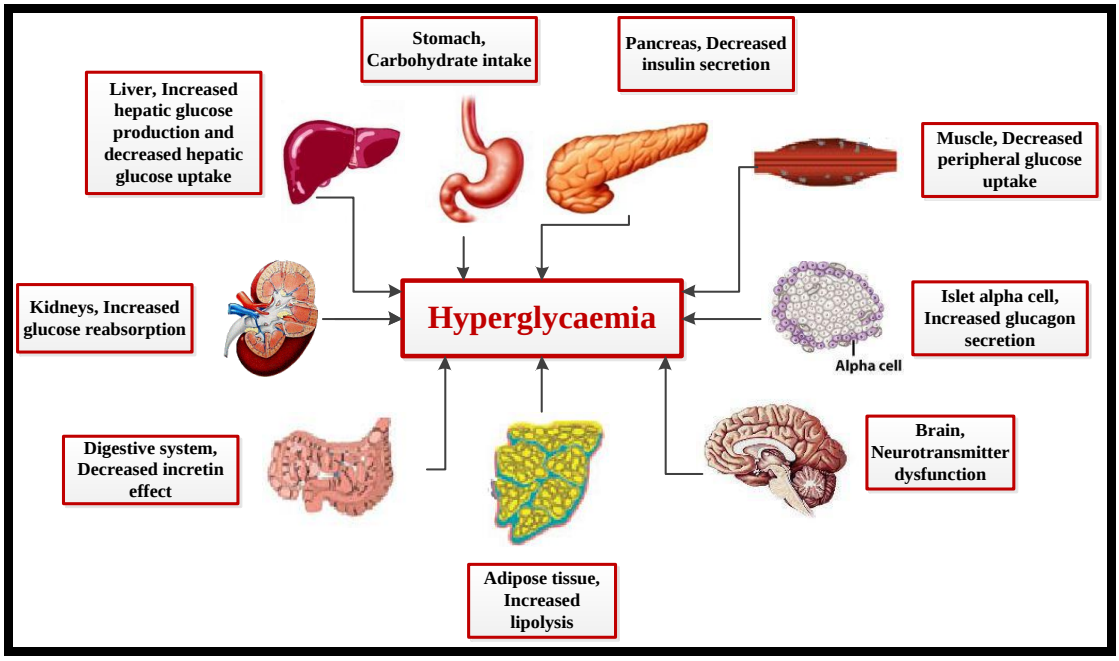

Figure 1: Factors causing hyperglycaemia
Source: Katzung *et al.* 2009

Diabetes occurs predominantly in two forms, namely: Type 1 and Type 2. These two forms differ in terms of pathogenesis but produce essentially similar metabolic derangements (Nowak and Handford 2004). On the basis of aetiology, the term Type 1 is widely used to describe insulin dependent diabetes mellitus (IDDM) (Nowak and Handford 2004). This type is the more severe of the two forms, which typically is picked up at a young age, and is less common. It develops following viral infection, exposure to environmental chemicals, abuse of and/or exposure to therapeutic drugs or a strong genetic predisposition leading to antigen alteration and subsequent immune attack, causing Beta-cell (β-cell) destruction and leading to zero functioning of the β-cells, therefore resulting in no secretion of insulin (Katzung *et al.* 2009). Type 2 diabetes mellitus, formerly known as non-insulin dependent diabetes mellitus (NIDDM), is characterised by chronic hyperglycaemia as a consequence of insulin deficiency caused by insufficient synthesis or secretion of insulin from the β-cells, however many contributing factors remain uncertain (Figure 2) (Nowak and Handford 2004).

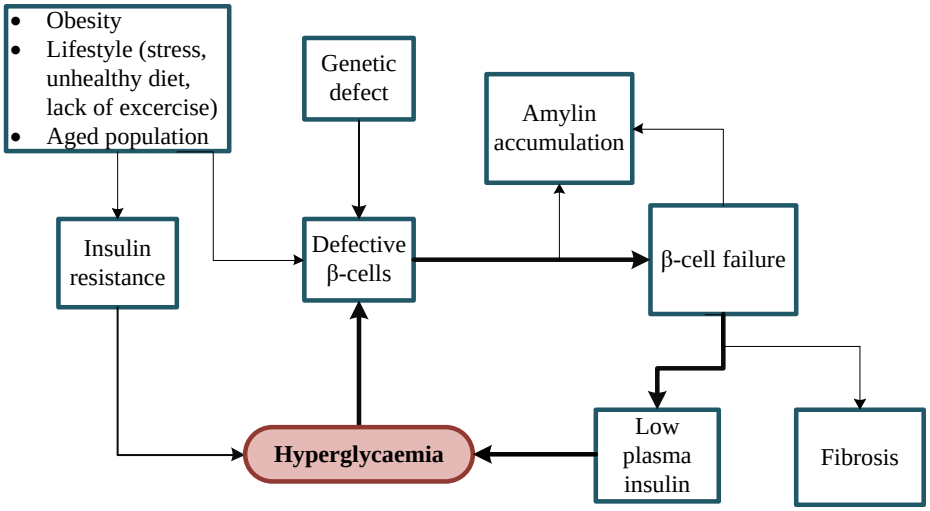

Figure 2: Pathogenesis of NIDDM
Adapted from: Nowak and Handford (2004)

Type 2 diabetes is by far the most common form of diabetes (Hannan *et al.* 2006), accounting for more than 90% of population cases (Nguyen *et al.* 2011). This form of diabetes has a slow progression or development of symptom; often years will pass without the victim being aware of any change (Nowak and Handford 2004). Insulin therapy is required less often in this type of diabetes, with the exception being patients that fail to achieve proper glycaemic control, during severe bacterial infections, ketoacidosis, during pregnancy and in patients with impaired renal or hepatic function (Mizuno *et al.* 2008). A minority of cases of Type 3 and Type 4 are due to various specific metabolic or genetic causes presented in Figure 3 (Bastaki 2005).

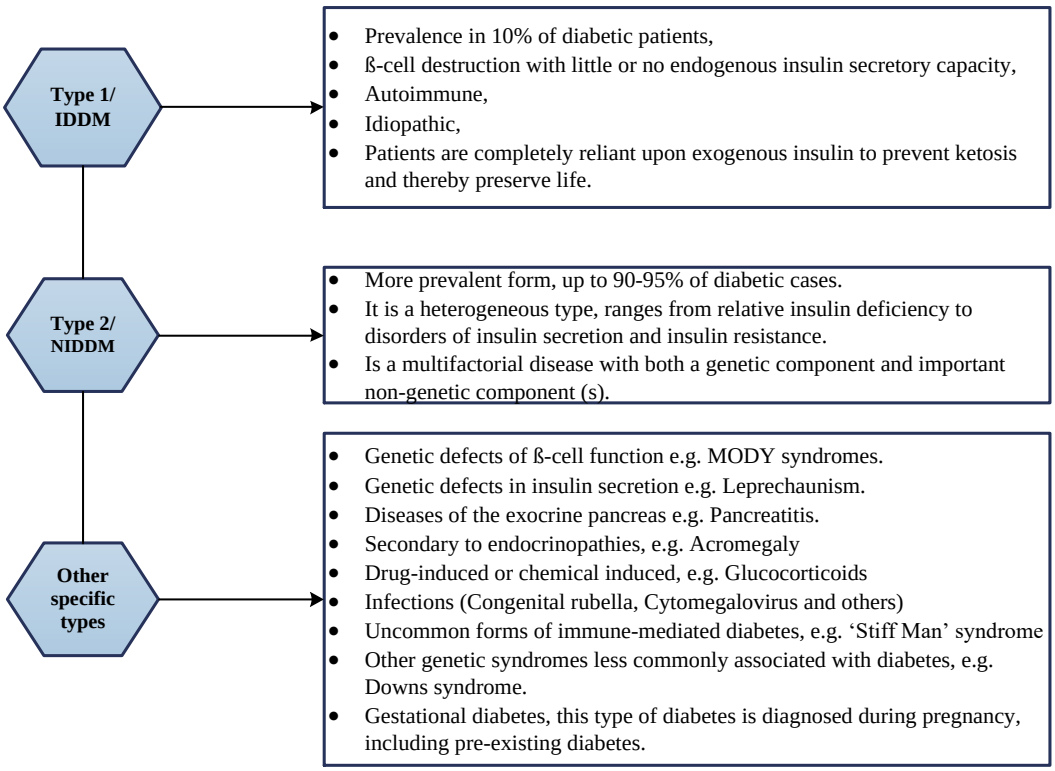

Figure 3: Classification of diabetes mellitus
Source: Bastaki 2005; Lokesh and Amit 2006

1.2.2 Complications of diabetes mellitus

Patients with diabetes experience significant morbidity and mortality from micro- and/or macrovascular complications (Tayyab *et al.* 2012). Microvascular disease is defined as damage to the small blood vessels while macrovascular disease is damage to the larger arteries (Nowak and Handford 2004). The relationship between glycaemic control and diabetic microvascular disease has been established in both Type 1 and Type 2 diabetes. Acute complications include diabetic ketoacidosis common to Type 1 diabetic patients, and non-ketotic hyperosmolar coma, common in Type 2 diabetic patients (Tayyab *et al.* 2012). Regardless of common diabetic treatment regimens, chronic hyperglycaemia has been implicated as the main cause of the adverse effects experienced by patients such as polydipsia, polyphagia and lingering complications over a significant period (McCue *et al.* 2005). The resultant long-term complications are caused by damage to organs including the eyes, kidneys, nervous system and blood vessels, causing various pathologies such as atherosclerotic vascular disease (Gan *et al.* 1999; Bastaki 2005), ketoacidosis, nephropathy,

neuropathy, ulceration, eye complications including retinopathy (most common cause of blindness), 'diabetic foot' and limb amputation (Bastaki 2005; Lewis *et al.* 2010).

Oxidative stress induced by chronic hyperglycaemia (Kil *et al.* 2004) has been shown to be a major underlying mechanism for the formation of harmful byproducts that accumulate and contribute to development of the long-term complications associated with diabetes (Neri *et al.* 2005). Oxidative stress reflects an imbalance between the systemic manifestations of reactive oxygen species (ROS) constantly formed in the human body and the quantities of antioxidant products required to restore balance, causing vasoconstriction (Kuyvenhoven and Meinders 1999). Excess production of ROS leads to the impairment of equilibrium between pro-oxidants and antioxidant systems (Sharma and Kar 2014). The activation of a number of metabolic pathways induced by chronic hyperglycaemia produce end products that contribute to the development of long-term complications associated with diabetes (Kuyvenhoven and Meinders 1999). For example, the activation of the polyol pathway causes decreased nitric oxide and prostaglandin synthesis, which results in endothelial dysfunction and hypertension. Increased polyol pathway activity can induce retinopathy and neuropathy. Similarly, increased protein kinase C (PKC) pathway activity and the formation of non-enzymatic glycation of proteins can lead to the increased risk of developing nephropathy, neuropathy and retinopathy. In addition, increased hexosamine pathway activity can potentiate macromolecular damage. Proper glycaemic control, blood pressure management and lipid modification are important to consider as they may independently slow the progression of diabetic related micro- and macrovascular complications, and thus reduce the rates of diabetic retinopathy, neuropathy, nephropathy, diabetic foot infections, atherosclerosis and other associated cardiovascular events, including dyslipidaemia, hypertension, hypercoagulability and obesity (Ratner 2001; Mizuno *et al.* 2008).

1.2.3 Incidence of diabetes mellitus

Diabetes is a major health problem with its frequency increasing every day from most developed and developing countries (Wild *et al*. 2004). In SA, the prevalence is between 4% and 6%. The global prevalence was estimated at 2.8% in 2000 (171 million people affected) (Wild *et al.* 2004), 382 million people in 2013 and is estimated to reach 592 million people by the year 2035, with a prevalence of 8.3% (Guariguata *et al*. 2014). The World Health Organisation (WHO) predicts that diabetes will be the 7th leading cause of death by 2030 (WHO 2011). The reasons for this global rise have been linked to changes in lifestyle

associated with urbanisation, modernisation (Hamdan and Afifi 2004), growth of aged population, increasing trends towards obesity, unhealthy diet, and sedentary lifestyles (Hannan *et al.* 2006). Hypertension, coronary heart disease, stroke, genetics and various forms of cancer are amongst the reasons for the global rise in diabetes (Omran 1983; Reddy *et al.* 1998).

The WHO emphasised the rise over a projected time frame of non-communicable diseases worldwide (WHO 2011). Many countries, including SA, are undergoing health and epidemiological transition that pose significant threats involving the emergence of debilitating diseases and their associated long-term complications (Omran 1983), and will increase with or without the impact of HIV/AIDS in SA (Mollentze and Levitt 2005). The prevalence of diabetes and obesity is an increasing concern affecting the developing countries to a greater extent than the developed world (Wild *et al.* 2004). Obesity is a major concern because it indirectly affects or exacerbates the incidence of diabetes, worsening the severity of side effects or accelerating the incidence of diabetic related complications (Mollentze and Levitt 2005; National Department of Health 2006). These data shows that reliable, cost saving therapy is necessary to lower the global rise of diabetes (Chiha *et al.* 2012). Medicinal plants contain enormous potential to provide alternative medicines for treating diabetes, but it is necessary that their effectiveness is researched and substantiated.

1.2.4 Treatment and management of diabetes mellitus

Over the years, concerted efforts to treat diabetes have evoked breakthrough discoveries, which have facilitated suitable management. The primary aim is to save a life and alleviate diabetic symptoms and secondary aims are to prevent long-term diabetic complications which encompass a variety of metabolic abnormalities. Insulin replacement therapy is the mainstay for patients with Type 1 diabetes while diet and lifestyle modifications are considered the foundation for the treatment and management of Type 2 diabetes (Bastaki 2005). If diet and exercise fail to control blood glucose at the desired level, pharmacological treatments such as insulin or oral hypoglycaemic drugs for management of Type 2 diabetes are then evoked. Yet, due to the rise and progress of the disease, and modernisation of lifestyle, opinion is divided regarding the primary use of conventional hypoglycaemic agents (Wadkar *et al.* 2007; Mizuno *et al.* 2008). In addition, patients placed on restricted diets and instructed to exercise in order to lose weight, do not always comply (Jarald *et al.* 2008).

Proposed goals of treatment intervention have been to improve β-cell function to increase pancreatic insulin decrease hepatic glucose production, increase glucose uptake peripherally and reduce absorption of carbohydrates (Houghton and Raman 1998). In addition, novel treatment strategies suggest prescribing according to the individual's genetic pathogenic profile (Bastaki 2005; van Huyssteen 2007).

The overall treatment of diabetes depends on the severity of hyperglycaemia and the lifestyle of the patient. Oral administered hypoglycaemic drugs e.g., sulfonylureas, metformin, thiazolidinediones (TZDs), meglitinides and α-glucosidase inhibitors are prescribed first, either alone or in combination. Often medical professionals are inclined to suggest combination therapy for patients failing to achieve normal glucose levels (South African Medical Association 2005). The most common combination is sulfonylurea plus metformin. However, if combination therapy fails to attain glycaemic control, patients are placed on insulin monotherapy or combined with oral hypoglycaemic agents (Mizuno *et al.* 2008). Common mechanistic classes of hypoglycaemic drugs in use exert their glucose lowering effects by means of: (1) Enhancement of insulin secretion by pancreatic β-cells (insulin secretagogues) (sulfonylureas and potassium-ATP channel stimulators); (2) Decreasing hepatic glucose production through inhibition of gluconeogenesis and promoting insulin-stimulated glucose uptake in muscle and changes lipid metabolism by decreasing plasma triglycerides and free fatty acids (metformin, a biguanide); (3) Increase muscle and adipose tissue glucose uptake by potentiating insulin action; PPARγ activates genes that regulate insulin action, glucose uptake and energy expenditure (thiazolidinediones (TZDs)); (4) Increase β-cell insulin secretion (meglitinides); and (5) Inhibition of intestinal glucose digestion and absorption (α-glucosidase inhibitors such as acarbose and migitol competitive inhibitors of intestinal α-glucosidases) (Appendix 1) (Bastaki 2005).

Modern antidiabetic drugs pose many limitations (Mizuno *et al.* 2008). The main drawback of insulin is that it has to be administered by injection (Wadkar *et al.* 2007) and research shows that most of the oral hypoglycaemic agents cannot maintain normal levels of blood glucose for an extended period (Mizuno *et al.* 2008). For example, glibenclamide is effective for patients that do not lack endogenous insulin but the side effects of this drug are hypoglycaemia with increased cardiovascular risk, especially in the elderly and patients with renal problems, and weight gain (Reid *et al.* 2012). In addition, gastrointestinal (GI) disturbances (severe lactic acidosis) are associated with metformin; weight gain, GI disturbances and liver injury with thiazolidinediones; GI disturbances, weight gain and

hypersensitivity reactions with meglitinides. Given the association of obesity and insulin resistance, weight gain is problematic, particularly in that that are overweight to start with (Mizuno *et al.* 2008). In pregnancy-induced diabetes, synthetic agents are vigorously used, however, continuous use is prohibited due to the development of hypoglycaemia, weight gain, GI disturbances and liver toxicity (Swarnalatha *et al.* 2012). Therefore, prolonged use of such agents can cause serious long-term complications. The current mainstay of treatments fail to alter the course of diabetic complications, do not restore glucose homeostasis and pose risks of high secondary failure rates (Mizuno *et al.* 2008). Drug compliance and accurate regulation of blood glucose is a difficult to control (Rang *et al.* 2003). It is therefore essential to look for other means of treatment that will be as efficacious in the mechanism of action (MOA) as synthetic agents but with minimal side effects and which can delay the chronic complications associated with diabetes. Apart from the current therapeutic options, many herbal medicines have been proposed for the treatment of diabetes (Jarald *et al.* 2008). The use of medicinal plants are part of traditional practice in many countries and cultures (Soumyanath 2006) including South Africa (van de Venter *et al.* 2008), because of their availability, effectiveness, minimal side effects and low cost. Investigation into antidiabetic agents from traditional medicinal plants is a major driver of research (Palatty *et al.* 2013).

1.3 The use of traditional medicine in the treatment of diabetes

In Africa, many plants are traditionally used for the management and control of various ailments (Baynes 2006) including diabetes (Kavishankar *et al.* 2011). Globally, approximately 85,000 medicinal plant species (sp.) are reported as medicinally useful (Liu and Wang 2008); however, few have received scientific scrutiny despite medical and scientific recommendation from the WHO (WHO 2007).

In South Africa, victims of chronic diseases are turning to herbal medicines as alternative sources of treatment as recommended by the National Department of Health (2006). This renewed interest in plant medicines as alternative therapy to restore health or treat diseases is believed to be motivated by factors such as their effectiveness, that they are more specific and that they contain diverse secondary metabolites which provide numerous health benefits. The orchestra of chemical compounds within the plants work together synergistically allowing active compounds to be available to produce maximal therapeutic efficiency that are less toxic than high doses of individual components (van Huyssteen 2007).

Traditional medicine (TM) may provide an effective solution to the threat of diabetes worldwide, thus helping to reduce chronic disease complications and deaths (Fang 2011). World ethnobotanical information on medicinal plants has reported up to 800 plants used for the treatment of diabetes (Udayakumar *et al.* 2009). Numerous medicinal plants offer sustainable management of the sugar levels among diabetic patients and validated for their hypoglycaemic potential using experimental animal models (Yeh *et al.* 2003). Plants such as *Momordica charantia* and *Eugenia jambolana* have been shown to ameliorate diabetic complications such as neuropathy, nephropathy, fructose-induced insulin resistance, and cataracts in experimental animals (Premila and Conboy 2007). Diabetes is thus a common disease for investigation using natural products. However, the mechanism of action and/or the components that specifically exert blood glucose lowering effects on tissues or organs remain unknown (Prabhakar and Doble 2011; Palatty *et al.* 2013). Diabetic research on the therapeutic effectiveness of natural plant products of SA is limited (Afolayan and Sunmonu 2010), therefore, this study is aimed at improving the management of diabetes by investigating novel compounds and the synergistic action of medicinal plants, marking a promising future and better usage of South Africa's medicinally important plants.

1.4 Ethnobotanical properties of *Ocimum* sp.

Safety, therapeutic effectiveness, economic benefits and availability are advantages claimed for medicinal plants in the treatment of various ailments therefore need to be subject to scientific study. The genus *Ocimum* is among those plants recognised for their medicinal attributes being rich in phenolic compounds. The genus *Ocimum* belongs to the family Lamiaceae/Labiatae and is presently one of the most studied genera worldwide (Kaya *et al.* 2008) with more than 150 sp. distributed in both subtropical and tropical regions worldwide, and are used to treat and manage a variety of human ailments (Tchoumbougnang *et al.* 2006). The plants selected for this study are *Ocimum sanctum* (*O. tenuiflorum*) commonly referred to as Holy basil/Tulsi, and *Ocimum basilicum*, commonly referred to as Sweet basil. Figure 4 illustrates *O. basilicum* and *O. sanctum* leaves and flowers.

Figure 4: Medicinal plants selected for the present study (A) *Ocimum sanctum* and (B) *Ocimum basilicum* (photographed by V. Malapermal)

Indian and African communities are identified as leading users of traditional plants (Afolayan and Sunmonu 2010; Grover *et al.* 2002). India is the leading manufacturer of Ayurvedic medicine, using genera such as *Ocimum* sp. for effective treatment and management of various diseases (Kuldeep *et al.* 2013). *Ocimum* sp. have been studied intensively, and reveal that many subspecies and varieties are globally distributed (Carović-Stanko *et al.* 2011). This is due to the recurring polymorphism of plants all of which produce essential oils with varying chemical composition of the genus (Carović-Stanko *et al.* 2011) due to edaphic and geographic factors (Tchoumbougnang *et al.* 2006). This is a useful indicator for plant improvement and an effective means of maintaining genetic resources of *Ocimum* sp., besides their effective medicinal uses (Harisaranraj *et al.* 2008). Despite many efforts, taxonomy and phylogenetic relationships within the *Ocimum* genus are still in question due to the recurring genetic, chemical and geographical variability. In South Africa this crop has adapted to many geographic regions and climates, making it reliable for large scale production (Fang 2011).

1.4.1 *Ocimum basilicum* (Sweet basil)

Ocimum basilicum (Sweet basil) is often used as a medicine worldwide (Tchoumbougnang *et al.* 2006) with a vast range of bioactive compounds (Bilal *et al.* 2012). In many countries, essential oils extracted from the leaves and flowering parts of this plant are used for culinary

purposes, pharmaceutics and cosmetics (Bilal *et al.* 2012). Traditionally, the plant is used to treat fever, nausea, abdominal cramps, gastroenteritis, migraines, insomnia, depression, gonorrhoea, dysentery, chronic diarrhoea, exhaustion (Usman *et al* 2013; Kaya *et al.* 2008), acne, loss of smell, insect stings, snake bites and skin infections (Martin and Ernst 2004). Studies indicate ethanol extracts which display antilipidaemic and anticholesterol properties (Zeggwagh and Eddouks 2007). Phytochemical screening of the leaf extract has revealed several flavonoids, tannins, steroids, cardiac glycosides and reducing sugars that contribute to its medicinal properties (El-Beshbishy and Bahashwan 2012). Studies conducted by Benalla *et al.* (2010), Jaiganesh *et al.* (2012), Usman *et al.* (2013) and Zeggwagh and Eddouks (2007) indicate that *O. basilicum* could play a significant role in improving hyperglycaemia in diabetic patients as well as having antimicrobial potential for diabetic induced infections (Kaya *et al*. 2008). The current research study focuses on this medicinal plant for treatment of type 2 diabetes mellitus and is further motivated by its effectiveness, bioactive chemical variability and negligible toxicity.

1.4.2 *Ocimum sanctum/Ocimum tenuiflorum* (Tulsi/Holy basil)

Ocimum sanctum also known as Tulsi or Holy Basil (syn. *Ocimum tenuiflorum*) is cultivated in many parts of the world, such as Asia and Africa, to treat various disorders and has contributed to the field of science from ancient times to modern research, due to its diverse medicinal properties (Mondal *et al.* 2009). The leaves of *O. sanctum* possesses numerous pharmacological properties including immunomodulatory, antistress, analgesic, antipyretic, antiinflammatory, antiulcerogenic, antihypertensive, central nervous system (CNS) depressant, radioprotective, antitumor, antibacterial (Kadian and Parle 2012), hepatoprotective, cardioprotective, antiemetic and antispasmodic (Dineshkumar *et al.* 2010). Extensive studies using *O. sanctum* leaf extract on fibrosarcoma cells in culture have demonstrated anticancer activity (Karthikeyan *et al*. 1999). *O. sanctum* is highly recommended and is one of the most effective traditional plants to manage diabetes (Govind and Madhuri 2010). In a study conducted by Hannan *et al.* (2006), oral administration of ethanol-based leaf extracts and five partition fractions led to marked lowering of blood sugar and increased plasma insulin in type 2 diabetic rats and demonstrated that leaf extracts exerted prominent stimulatory effects on insulin secretion from β-cells via physiological pathways. *O. sanctum* has aldose reductase activity, which may help in reducing complications of diabetes such as cataract and retinopathy (Govind and Madhuri 2010). *In*

vivo toxicity studies using aspirin-, indomethacin-, alcohol-, histamine-, reserpine-, serotonin- and stress-induced ulceration in experimental animal models conducted by Singh and Majumdar (1994) indicate that the effect of the fixed oil from *O. sanctum* did not cause ulcerogenic effects or histopathological alterations. No behavioural and histological changes in the brain, lungs, liver and kidneys were reported by Mondal *et al.* (2009). Bhargava and Singh (1981) reported *O. sanctum* increased the physical endurance (increased survival time) of swimming mice, prevented stress-induced ulcers in rats, protected mice and rats against carbon tetrachloride-induced hepatotoxicity and prevented milk-induced leucocytosis in mice. There are many reports on biological and pharmacological investigations and analyses of chemical ingredients and essential oils produced from *Ocimum* sp. (Tchoumbougnang *et al.* 2006), but studies in South Africa on the chemical investigation of volatile constituents or the biological activity of *O. sanctum* is non-existent. *O. sanctum* was selected for its antidiabetic and antimicrobial properties with negligible toxicity, and for being an ideal agent to promote health and to prevent and treat disease.

1.5 The study aims and objectives

1.5.1 Aims

The primary aim of the study was to test the *in vitro* antidiabetic and antibacterial activity of *Ocimum sanctum* (leaf extracts and flower extracts), *Ocimum basilicum* (leaf extracts and flower extracts), and a combination of the leaf extracts of both, and to observe whether any antidiabetic and antibacterial activity was enhanced in due to phyto-synthesised bimetallic gold-silver (Au-Ag) nanoparticles and silver nanoparticles.

1.5.2 Objectives

1. To extract chemical compounds from *O. basilicum* and *O. sanctum* leaf and flowers using water and ethanol (60% and 70%) (Ahmad and Beg 2001; German Homoeopathic Pharmacopoeia 2005; Sivaranjani and Meenakshisundaram 2013; Khogare and Lokhande 2011) and to identify the chemical compounds using gas chromatography mass spectrophotometry (GC-MS).

2. To synthesise bimetallic (Au-Ag) Nps using *O. basilicum* aqueous leaf and flower extracts.

3. To synthesise silver nanoparticles (AgNps) using aqueous leaf extracts derived from *O. sanctum* and *O. basilicum* singly and in combination (*O. sanctum* plus *O. basilicum*).

4. To characterise the stability and formation of the Nps via UV-Vis spectroscopy, transmission electron microscopy (TEM), scanning electron microscopy and energy dispersive X-ray analysis (SEM-EDX), Fourier transform infrared spectroscopy (FT-IR), dynamic light scattering (DLS) and zeta potential analysis.

5. To investigate the antibacterial activity of the aqueous extracts from *O. basilicum* and *O. sanctum* utilising pathogenic bacterial strains (*S. aureus* ATCC 25923, *E. coli* ATCC 26922, *P. aeruginosa* ATCC 27853, *Salmonella* sp. ATCC UKQC 9990 and *B. subtilis* ATCC 6051) using an agar-diffusion method, and in terms of the Minimum Inhibitory Concentration (MIC) and Minimum Bactericidal Concentration (MBC).

6. To investigate the *in vitro* inhibitory potency of the resultant crude extracts (aqueous and ethanol), bimetallic (Au-Ag) Nps and AgNps, using α-amylase (from porcine) and *Bacillus stearothermophilus* α-glucosidase enzymes as models.

7. To compare the effectiveness of the test samples showing enzyme inhibitory activity to standard reference acarbose, and compare the samples that inhibit the bacteria to available antibacterial standards.

1.6 The Research Hypotheses

1. It was hypothesised that *O. sanctum* and *O. basilicum* (aqueous and ethanol) leaf and flower extracts will be effective in delaying carbohydrate digestion via inhibition of selected diabetic related enzymes and will show effective antibacterial activity.

2. It was hypothesised that *O. basilicum* leaf and flower aqueous extracts could be used to synthesise bimetallic (Au-Ag) Nps and display antidiabetic and antibacterial activity. In addition, the synthesis of AgNps from *O. sanctum* and *O. basilicum* singly and in combination will display antidiabetic and antibacterial activity.

CHAPTER 2 : LITERATURE REVIEW

2.1 The link between nanotechnology and phytotherapy in the treatment of diabetes

Individuals with diabetes and other debilitating diseases have been treated via traditional folk medicine with a variety of plant extracts from many years (Barnes *et al.* 2007). Natural medicinal drugs are reclaiming their position as the primary source of treatment as compared to the current and main forms of synthetic treatment (Mizuno *et al.* 2008). The most popular antidiabetic plants studied belong to the following families: Anacardiaceae, Alliaceae, Asphodelaceae, Asteraceae, Apocynaceae, Bombacaceae, Caesalpiniaceae, Combretaceae, Cucurbitaceae, Fabaceae, Hypoxydaceae, Lamiaceae, Lauraceae, Linaceae, Liliaceae, Menispermaceae, Moraceae, Myrtaceae, Pedaliaceae, Piperaceae, Rutaceae and Zingiberaceae (Appendixes 2-4).

In the quest for innovative and eco-friendly healthcare, nanobiotechnology is now an active field of research, concentrating on the rapid biosynthesis of benign Nps using highly acclaimed antidiabetic medicinal plants possessing active compounds that serve as natural reducing agents (Rao *et al.* 2013). This has led to many researchers developing newer and more efficient green methods of synthesis of biocompatible and inert Nps (Ramteke *et al.* 2013). Chemical, physical and microbial methods of synthesising gold (Au), silver (Ag), palladium (Pd), platinum (Pt), indium oxide (In_2O_3), magnetite (Fe_3O_4) and zinc oxide (ZnO) Nps currently exist (Iravani 2011; Naik 2002), however, these methods are toxic, costly, time consuming and difficult, especially in relation to preserving microbial cultures (Jayapriya and Lalitha 2013). In light of this, nanomedicine is making use of the vast reserves of phytotherapy to synthesise Nps using various noble metals such as gold, silver and palladium in nanoform.

2.1.1 Green synthesis of metal Nps using medicinal plants

The biosynthesis of silver and gold Nps using medicinal plants has received considerable attention as a suitable alternative to using hazardous chemical and physical techniques (Iravani 2011). Plants are being exploited for their unique metal tolerance and effective production of metal Nps. A single medicinal plant contains an orchestra of chemical elements

(e.g. proteins, vitamins, enzymes, amino acids, polysaccharides and organic compounds) that are "environmentally benign, yet chemically complex" (Iravani 2011) and therefore serve as ideal tools for enhanced medicinal applications. It is reported that polyols such as terpenoids, polysaccharides and flavones take part in the bio-reduction, stabilisation and bio-capping mechanisms to form stable silver (Huang *et al.* 2007), gold (Shankar *et al.* 2003) and bimetallic Nps (Shankar *et al*. 2004). The importance of plant constituents have been shown in the bio-reduction of Ag ions to AgNps using an aqueous (aq.) preparation of *Cinnamon zeylanicum* bark which is rich in terpenoids such as linalool, methyl chavicol and eugenol as well as cinnamaldehyde, ethylcinnamate and β-caryophyllene. Proteins from *C. zeylanicum* bark capped and further stabilised the particles of free amine groups and/or cysteine residues (Sathishkumar *et al.* 2009). Phenolic compounds play an important role in the bio-reduction and stabilisation of metal Nps. Phenols/phenolics are a class of compounds comprising a hydroxyl functional group (-OH) attached to an aromatic hydrocarbon group (Harborne 1998). Recent interest in phenolic compounds is because of their potential antioxidant action against oxidative damage related diseases such as diabetes, cancer, coronary heart disease and stroke. Phenolic compounds have a high affinity with chelating metals that may inactivate iron ions by chelating and supressing the superoxide driven Fenton reaction, which is the sole source of ROS (Iravani 2011). Therefore, plants with high content of phenolic compounds such as *Ocimum* sp. are suitable candidates for nanoparticle synthesis.

Specific characteristics such as size, morphology, physicochemical properties (charge interaction and surface properties) and dispersity play significant roles in improving the stability and compatibility of Nps (Song and Kim 2009). By controlling the metal nanoparticle structure at a precise nanoscale level measured in nanometres (one billionth of a metre), a standard control and modification can be set to change their surface layer for enhanced aq. solubility, biocompatibility or bio-conjugation (Grace and Pandian 2007). This enables greater biological activity due to their relatively high surface area to volume ratios compared to their larger counterparts (Mubarak *et al.* 2011). For example, remarkable size-dependent properties were presented in the facile green synthesis of AuNps, with a size range of 15-25 nm, using the antidiabetic plant *Cassia auriculata* (Ganesh *et al.* 2011); a similar nanorange was reported by Arunachalam *et al.* (2013) forming biocompatible AgNps and AuNps from *Memecylon umbellatu.* Bimetallic Au core-Ag shells Nps was reported by Sheny *et al.* (2011), with a size range below 10 nm synthesised from *Anacardium occidentale*, and a

size range of 50-100 nm was achieved using Neem (*Azadirachta indica*) with a large percentage of Au Nps exhibiting remarkable flat, platelike morphology (Shankar *et al.* 2004).

The medical applications of AgNps, AuNps and bimetallic Nps synthesised by living plants has advanced dramatically, focusing on improving diagnosis, treatment, drug development and targeted drug delivery systems (Raman *et al.* 2012; Adekoya *et al.* 2014). The applications have huge potential for treating major diseases such as cancer (Anand *et al.* 2015), diabetes (Daisy and Saipriya 2012) and HIV/AIDS (Raman *et al.* 2012) in the near future. Recent trends in diabetic research suggest the potential antidiabetic activity of Nps synthesised using antidiabetic plants as the reducing and stabilising agents (Ganesh *et al.* 2011) and raise the question of their potential for improving drug delivery of existing synthetic drugs for enhanced antidiabetic treatment (Subramania *et al.* 2012). In this study the properties of metal Nps synthesised from *O. sanctum* (Philip and Unni 2011) and *O. basilicum* (Sivaranjani and Meenakshisundaram 2013) will be further extended to investigate their possibly enhanced antidiabetic activity.

2.1.2 *In vitro* inhibition of carbohydrate metabolising enzymes

A range of *in vitro* models is available to study the potential antidiabetic activity of plant extracts. Both α-amylase and α-glucosidase enzyme models can be used to explain many reported herbal interactions (Kim *et al.* 2005).

The enzyme α-amylase is present in pancreatic juice and saliva and its main role is to start the breakdown of dietary carbohydrates (a major constituent of the human diet) in the gastrointestinal tract (GIT) via hydrolysis of dietary polysaccharides, to produce oligosaccharides and disaccharides (McCue *et al.* 2005). The resulting disaccharides are further hydrolysed to produce glucose and other monosaccharides (fructose and galactose) by the enzymatic action of α-glucosidase (Sudha *et al.* 2011). After digestion the liberated glucose and other resulting monosaccharides are absorbed through the small intestine into the hepatic portal vein and this results in an elevated blood glucose levels known as PPHG. Glucose is now available for the body cells to use it for energy (Nowak and Handford 2004).

Even though the aetiology of diabetes does not relate to the metabolism of carbohydrates (Lebovit 1998), the inhibition of α-amylase activity (Funke and Melzig 2006) and inhibition of α-glucosidase activity and other key enzymes (Table 1) (Akkarachiyasit *et al.* 2010) have

long been targeted as potential avenues for better glycaemic control in type 2 diabetic patients or as alternative treatment choice for many borderline patients (Subramanian *et al.* 2008).

Table 1: The role of selected carbohydrate metabolising enzymes in the digestion and absorption of carbohydrates

Enzyme	Catalytic function
Alpha amylase	Produced in the pancreas this enzyme hydrolyses dietary starch into disaccharides and trisaccharides.
Alpha glucosidase	Present in the brush border of the small intestines, this membrane bound enzyme hydrolyses oligosaccharides, tri- and disaccharides to glucose and other monosaccharides.
Hexokinase (glucokinase)	First enzyme to change glucose during the energy investment phase of glycolysis, allows glucose to remain in the cells.
Glucose-6-phosphatase (G-6-P)	Plays a role in homeostatic regulation of blood glucose levels. Hydrolyses G-6-P to glucose and inorganic phosphate.

Source: (Akkarachiyasit *et al.* 2010; Ugochukwu and Babady 2003; Udayakumar *et al.* 2009)

Currently in the market there are several established enzyme inhibitors which are conventionally used to manage diabetes, including miglitol, voglibose, nojirimycin, 1-deoxynojirimycin and acarbose, commercially known as Glucobay® (South African Medical Association 2005; Nickavar and Yousefian 2009). However, studies have proven that many of these drugs possess limitations, are non-specific, produce serious side effects and fail to alleviate diabetic complications (McCue *et al.* 2005; Bhat *et al.* 2011). For example, long-term repercussions of acarbose include GIT side effects, such as bloating, abdominal pain/discomfort, diarrhoea, flatulence and abdominal bacterial fermentation of undigested carbohydrates in the colon (Bhat *et al.* 2011; Sudha *et al.* 2011).

Research shows that certain plant sources show prominent α-amylase and α-glucosidase inhibition and are able to mimic the MOA of standard commercial agents such as acarbose and provide better inhibition without the associated side effects (Kim *et al.* 1999), in particular those possessing important natural producing hypoglycaemic bioactive compounds (Appendix 5) (Kim *et al.* 2005; McCue *et al.* 2005; Mogale *et al.* 2011b). Several chemical compounds exhibit α-amylase and α-glucosidase inhibition (Subramanian *et al.* 2008), namely: alkaloids; stilbenoids (polyphenol); triterpene; phytosterol; myoinositol; flavonoids; flavonolignans; anthraquinones; anthrones; xanthones; feruloylglucosides; flavanone glucosides; acetophenone glucosides; glucopyranoside derivatives; genine derivatives; flavonol and anthocyanin (Benalla *et al.* 2010). Thus, diabetic studies are ongoing with the aim of obtaining clinically useful enzyme inhibitors in order to better control diabetes (Jung *et al.* 1996).

2.1.3 Antidiabetic potential of AgNps and AuNps synthesised via the green route

One of the first attempts at assessing the antidiabetic activity of AgNps was demonstrated using *Sphaeranthus amaranthoides* extract as a natural reducing agent, the results of which showed a dose-response inhibitory activity on α-amylase and an IC_{50} result lower than the standard drug acarbose (Swarnalatha *et al.* 2012). Biogenic AgNps synthesised by *Halymenia poryphyroides* showed significant *in vitro* antidiabetic efficacy in a dose-dependent manner with an increase in the percentage inhibitory activity against α-amylase enzyme, at a concentration of 1.0 mg/ml, 91.30% ± 0.02% inhibition, similarly a significant increase in percentage inhibitory activity against α-glucosidase enzyme at a concentration of 1.0 mg/ml with 89.10% ± 0.01% inhibition (Vishnu and Murugesan 2013). More recently, Vishnu and Murugesan (2014) reported the biological green synthesis of AgNps from marine algae *Colpomenia sinuosa* that displayed *in vitro* α-amylase and α-glucosidase inhibitory activity.

The high biological activity can be explained by the properties of the metal Nps. For example, AgNps possess a high surface area to volume ratio plus the charge they carry is useful in catalytic studies, as they can easily interact with protein molecules (Swarnalatha *et al.* 2012).

As mentioned ROS is a major potentiating factor in diabetic related complications (Iravani 2011). Barathmanikanth *et al*. (2010) found that AuNps displayed prominent antioxidant properties, inhibiting the formation of ROS and scavenging free radicals, therefore increasing the antioxidant enzymes and creating a sustained control over hyperglycaemic conditions revealing the potential of biocompatible AuNps as a safe therapeutic form of treatment for diabetes and its associated complications. The main functionalised property associated with AuNps is that they bind readily to a large range of biomolecules such as proteins/enzymes, DNA, amino acids, and expose a large surface area for the immobilisation of ions of such biomolecules (Ganesh *et al*. 2011). The biomedical applications of AuNps include diagnostic assays, thermal ablation, radiotherapy enhancement, gene therapy and improving drug delivery systems. They are increasingly being researched due to their low toxicity in humans, ease of biodegradability, and chemical stability as evidenced by Anand *et al.* (2015). However, there is a lack of catalytic studies testing the antidiabetic potential for AuNps and bimetallic Nps. In relation to carbohydrate metabolising enzymes, the exact mode of the binding of nanoscale molecules to α-amylase and α-glucosidase (Hamdan *et al.* 2004) and the consequent inhibition requires further investigation.

Studies of the biological applications of metal have focused mainly on how matter behaves at a nanoscale level. The limitation of these studies is that they have not addressed the question of how Nps will react in the human body (Vishnu and Murugesan 2014). The current study investigates the *in vitro* effect of bimetallic (Au-Ag) Nps and AgNps against α-amylase (derived from porcine) and *B. stearothermophilus* α-glucosidase that mimics the catalytic activity of the human pancreatic α-amylases (HPA) and intestinal brush border α-glucosidases. The rationale for the synthesis of bimetallic (Au-Ag) Nps were twofold: (1) to combine AuNps (chemically inert and less toxicity) with AgNps (higher bioactive properties), (2) increase the surface phenomenon in the reduction reaction (higher surface area to volume ratio) to achieve greater biological activity in the enzyme assay.

2.2 Antibacterial screening: infectious diseases

2.2.1 Diabetic related infections

Diabetic induced infections are increasing globally at an alarming rate, adding to associated complications and worsening the effects of the disease (Reid *et al.* 2012). Previously, diabetes was treated as a single disease; now medical professionals are aware that diabetes covers a wide range of heterogeneous diseases and is itself an environmental factor that leads to the development of a wider range of disorders (Bastaki 2005; Mizuno *et al.* 2008). In both developed and developing countries, the disabling complications from diabetes are rapidly draining health care resources. Admissions for diabetic foot-related complications is the most common reason for hospital bed occupancies in this patient population (Tudhope 2008).

In sub-Saharan Africa, the increased incidence of infections in diabetic patients (van Huyssteen 2007) is indirectly affected by the increased incidence of HIV/AIDS, and TB, where up to 22.9 million people are infected with HIV/AIDS (Reid *et al.* 2012). This increase is attributed to several factors, including the growing incidence of antimicrobial resistance to hospital-acquired and community-acquired infections, poorer socioeconomic conditions, inaccessibility to modern health care needs especially in rural areas, and poorly controlled diabetic cases (Shankar *et al.* 2005). Management of infections in diabetic patients is more complex and therefore of greater concern compared to infections in non-diabetic patients (Larkin *et al.* 1985).

Immunological deficiency in diabetic patients is triggered because of poor glycaemic control. Defects in their defence system may increase the risk and severity of developing diabetic

induced infections (Larkin *et al.* 1985). Infections of the skin (particularly *staphylococcal*), periodontal disease, postoperative infections, pneumonia caused by *Staphylococcus aureus* or *Klebsiella pneumonia*, urinary tract infections (UTIs) and foot infections can further result in immunological deficiency in the diabetic patient population. Diabetic peripheral neuropathy (polyneuropathy) among all the other associated co-morbid diabetic conditions is reported to be the primary reason underlying the severity of bacterial related diabetic foot trauma and ulceration. Delayed recognition of symptoms due to lack of sensation because of neuropathy together with poor peripheral circulation may delay healing and encourage opportunistic infections (Shankar *et al.* 2005). The worst outcome of infection gangrene which may lead to amputation of the foot or limb and even death if prompt treatment is not instituted (Hall *et al.* 2011).

In a study by Shankar *et al.* (2005) diabetic polyneuropathy was found to be common, with the incidence of Gram negative (predominant in chronic diabetes) induced infections being higher than Gram positive (predominant in acute diabetes) induced infections. In addition, polymicrobial infections caused by combinations of bacteria such as *Staphylococcus, E. coli, P. aeruginosa*, and/or Methicillin-resistant *Staphylococcus aureus* (MRSA) in diabetic foot infections are increasingly becoming a problem in patients previously hospitalised.

Despite the existence of conventional antimicrobial agents on the market, resistant strains are continuously surfacing (Adwan *et al.* 2010). Multidrug resistance is developed due to the indiscriminate use of antimicrobial drugs. In addition, there are side effects of antimicrobials including hypersensitivity, immune-suppression and/or allergic reactions (Sánchez-Borges *et al.* 2013).

Ever since humankind suffered from infectious diseases, herbal medicine has been pursued as an effective source of treatment. New research is ongoing in the fight against the constant mutation and upgrading of bacteria (Adwan *et al.* 2010). A major emphasis of industrial antibiotic production is toward screening programmes for new potent antimicrobial producing agents.

Plants or natural products still appear to be the most promising source of future antimicrobials because of their availability and chemical diversity (Ahmad and Beg 2001). Historically, plants have created a platform to create new biologically active components, specifically focusing on the isolation and characterisation of unknown compounds expressing interesting properties regarding their antimicrobial activity.

2.2.2 Antimicrobial potential of AgNps and AuNps synthesised via the green route

Plant extracts mediated synthesis of AgNps and their antimicrobial activity against clinically isolated pathogens has been reported on in relation to most prevalent and pathogenic Gram positive, Gram negative bacterial and fungal microorganisms (Ramteke *et al.* 2013; Rout *et al.* 2012). Medically, silver is commonly incorporated into many topical ointments and creams. This antimicrobial agent prevents infections caused by burns or open wounds (Singhal *et al.* 2011). Improving the properties of silver by altering their physicochemical properties (charge interaction, surface properties and size i.e. nanorange) nanomedicine has generated the facile green synthesis of biocompatible AgNps which are reported to possess antifungal, antibacterial, antiinflammatory, antiangiogenesis, antiplatelet and antiviral properties, thus amplifying the existing medicinal properties of silver ions. The AgNps formed from *Phyllanthusniruri* sp. displayed antibacterial properties against *Staphylococcus* sp., *Salmonella* sp., *Proteus* sp. and *Bacillus* sp. (Krishnamoorthy and Jayalakshmi 2012); AgNps from *Artocarpus heterophyllus* Lam. seed displayed potent antibacterial activity towards *B. cereus, B. subtilis, S. aureus* and *P. aeruginosa* (Jagtap and Bapat 2013); AgNps from *O. sanctum* and *Vitex negundo,* showed enhanced antibacterial activity against *S. aureus, E. coli* and *P. aeruginosa* (Ramteke *et al* 2013) and antifungal properties against *C. albicans, C. kefyr* and *A. niger* (Rout *et al.* 2012); AgNps from *Andrographis paniculata* has shown prominent antifungal properties (Kotakadi *et al.* 2014). A study by Singhal *et al.* (2011) found that AgNps from *O. sanctum* displayed greater activity against *E. coli* and *S. aureus* than silver nitrate and standard antibiotic ciprofloxacin and a study by Sivaranjani and Meenakshisundaram (2013) found that AgNps derived from *O. basilicum* displayed high antibacterial activity against *P. aeruginosa.*

Antimicrobials are produced naturally by bacteria, fungi, actinomycetes, algae, lichens and green plants (Peláez 2006). Thousands of antimicrobials have been identified, but few natural sources have been commercially used to treat human diseases (Hackl *et al.* 2004). Plant communities are among the most complex, diverse and important assemblages of chemical compounds in the biosphere and participate in various biological activities. They are an important source material in the search for novel antimicrobial agents and molecules with biotechnological importance (Hackl *et al.* 2004). Together with nanomedicine the rich abundance of plants in Africa and South Africa makes it a promising avenue for investigation and discovery of therapeutic drugs.

2.3 Selection of pathogens used in this study

Studies that investigate the antimicrobial efficacy of new plants or drugs use a combination of Gram negative and Gram positive bacteria as test microorganisms, due to the selective toxicity that the agent may have for a specific pathogen or class of pathogens (van Huyssteen 2007). A general characteristic of Gram positive pathogens is that the disease symptoms exhibited often result from the exotoxins they secrete. In contrast, Gram negative pathogens do not secrete exotoxins but have a toxic outer membrane that result in life threatening disease states in human beings (Bauman 2007).

2.3.1 *Bacillus subtilis* (*B. subtilis*)

B. subtilis are endospore-forming Gram positive, aerobic, rod-shaped bacteria found in soil (Bauman 2007). Due to their habitat, the chances of finding *B. subtilis* in medicinal plant remedies are high. *Bacillus* causes diarrhoea (van Huyssteen 2007). *B. subtilis* is one of the most sensitive bacterial microorganisms to most current antimicrobial drugs on the market therefore, if an antimicrobial agent does not inhibit this bacterial microorganism it is unlikely to do so against any other microorganism so may be disregarded, which makes it suitable as a reference strain on this study (Sivaranjani and Meenakshisundaram 2013).

2.3.2 *Salmonella* species

Salmonella sp. is a genus of motile, Gram negative peritrichous bacilli that live in the intestines of birds, reptiles and mammals and is eliminated in their faeces. This bacterium is a common contaminant found in food contaminated with animal faeces and may be found in poultry, eggs or inadequately pasteurised milk. Salmonellosis is characterised by non-bloody diarrhoea, nausea and vomiting (Tortora *et al.* 2007). This GI pathogen from food causes "food poisoning" emanating from restaurants. Natural plant products have been recommended to produce an effective and safe disinfectant among immunodeficient patients (Lee and Lee 1994; Dorman and Deans 2000).

2.3.3 *Staphylococcus aureus (S. aureus)*

Staphylococcus is a genus of Gram positive pyogenic cocci which is facultatively anaerobic and arranged in grape-like clusters. They are found in soil and the mucous membranes of animals. The pathogenicity of *S. aureus* results from the production of specific enzymes or

virulence factors such as cell-free coagulase, hyaluronidase, staphylokinase, lipases, and beta-lactamase. *S. aureus* produces cytotoxic toxins such as leukocidin, haemolysins, enterotoxins and exfoliatin (Honeyman *et al.* 2001). Therefore, it is categorised as a highly virulent form of Gram positive bacteria resulting in a variety of diseases and symptoms. The infections it causes depend on the site of infection, immune state of its host and the specific toxins and enzymes it secretes (Bauman 2007), and can be categorised as non-invasive (enterotoxin resulting in food poisoning); cutaneous (scalded skin syndrome, impetigo, furuncles, and carbuncles); and systemic which could be potentially fatal when they are introduced into deeper tissues of the body. If introduced into blood it can cause toxic shock syndrome (TSS); or affect the heart (endocarditis), lungs (pneumonia and empyema) and bones (osteomyelitis) (Tortora *et al.* 2007).

S. aureus is a common cause of bacteraemia especially in immunocompromised individuals, and nosocomial (hospital-acquired) infections account for half the cases of *Staphylococcus* bacteraemia. South Africa has experienced the emergence of MRSA (van Huyssteen 2007) which has become a major problem in the health care setting. Since vancomycin is used to treat MRSA infections, a concern has been raised by many physicians regarding the emergence of vancomycin-resistant strains of *S. aureus* (Honeyman *et al.* 2001). Due to its natural presence on skin in variable proportions it may be classified as a potential agent that can cause complications in diabetic patients. In a diabetic patient, any systemic or abscess infection requires long-term therapy with antimicrobial drugs, which can potentiate further resistance; it is therefore a suitable choice in this study.

2.3.4 *Escherichia coli* (*E. coli*)

E. coli is a Gram negative, rod-shaped bacterium that is a facultative anaerobe and is the most common pathogenic Enterobacteriaceae, and is well known as a laboratory research microorganism. This bacterium is found as normal flora in the intestinal tract of animals and humans and may be present in soil, plants and decaying vegetation. Infections occur because of contaminated water due to poor sewage disposal (Bauman 2007). The pathogenicity of specific strains is associated with specific antigens. Using fimbriae to facilitate adherence to mucosal surfaces of the intestinal and urinary tract, *E. coli* produces endotoxins and exotoxins resulting in different disease states, including septicaemia, UTIs, neonatal meningitis (capsular antigens), fatal haemorrhagic colitis, gastroenteritis and diarrhoeal diseases (Tortora *et al.* 2007).

Treatment includes phthalysulphathiazole, neomycin, doxycycline, trimethoprim, norfloxacin, chloramphenicol and other fluroquinolones (Sabir *et al.* 2014). However, the incidence of multidrug resistant *E. coli* has increased in SA, and due to the continuous use of antibiotics against *E. coli* the organism has developed resistance to these antibiotics (van Huyssteen 2007). Infections with this microorganism can be fatal in children and immunocompromised adults (Tortora *et al.* 2007). As a result of poor sanitation this infection is encountered mainly by patients in the lower socioeconomic groups (van Huyssteen 2007). Selection of this bacterium in the current study was deemed vital due to the emergence of resistant strains and because it is one of the isolated causes of polymicrobial induced diabetic foot infection (Shankar *et al.* 2005). Studies show that not all AgNps derived from the green method of synthesis can eliminate this bacterium (Sivaranjani and Meenakshisundaram 2013).

2.3.5 *Pseudomonas aeruginosa (P. aeruginosa)*

P. aeruginosa is a Gram negative bacterium, strictly aerobic, non-motile, non-capsulate, rough mucoid colony that produces a bluish-green pigment. *P. aeruginosa* has fimbriae, mucoid polysaccharide capsule and other adhesions that contribute to its pathogenicity, as it enables attachment to host cells and shields the bacteria from phagocytosis. The microorganism produces elastase, protease, collagenase, lipase, haemolysins, leukocidin, exotoxin A and exoenzyme S and pigment called pyocyanin that contributes to tissue damage and spread of *Pseudomonas* infections (Robert and Fick 1993).

The natural habitat is water and moist soil and is rarely part of normal human microbiota. Due to its ubiquity and virulence, it causes inherent resistance to a wide range of antimicrobial drugs. This opportunistic pathogen colonises in immunocompromised or debilitated patients, therefore is a growing concern in hospital-acquired infections. It can be involved in bacteraemia, endocarditis, urinary, ear, eye, septicaemia, CNS, GI, muscle and skeletal infections. Infections in burn victims and cystic fibrosis patients are common (Bauman 2007). Physicians treat *Pseudomonas* with combination therapy (aminoglycosides such as gentamycin, amikacin, tobramycin; and beta-lactam drugs with piperacillin), however, treatment is frustrating as this bacterium is notoriously resistant to a wide range of antimicrobial drugs such as amikacin, gentamycin, cefotaxime or ciprofloxacin (Karlowsky *et al.* 2003).

P. aeruginosa may cause severe tissue damage in diabetic patients, and should never be disregarded as insignificant in the event of acquiring diabetic foot ulcers (Shankar *et al.* 2005). The importance of considering these bacteria as contaminants or commensals is that they may cause sepsis leading to amputation. *P. aeruginosa* displayed a mixed involvement in other microorganisms such as *S. aureus* and *E. coli* in contrast to supporting evidence that most diabetic related foot infections are mono-microbial (Shankar *et al.* 2005). Selection of this bacterium in this study is necessary due to its common occurrence in diabetic induced infections.

2.4 Conclusion

The primary challenge to treating chronic diseases such as diabetes is the resultant widespread multi-organ complications. Even after introducing novel antidiabetic and antimicrobial drugs, there have been no major leads to find proper drugs for overall treatment of diabetes. Safety, therapeutic effectiveness, economic benefits and availability are important advantages of medicinal (Dineshkumar *et al.* 2010). Their bioactive compounds offer many additive benefits such as natural hypoglycaemic, antiobesity, wound healing properties (Nickavar and Yousefian 2009; Nguyen *et al.* 2011) and offer a natural source of antioxidants capable of neutralising free radicals and reducing the severity of diabetic micro- and macrovascular complications (Swarnalatha *et al.* 2012). The significance of finding natural α-amylase and α-glucosidase inhibitors and which are also antibacterial agents are discussed.

CHAPTER 3 : METHODOLOGY

3.1 Research design

This is an experimental study based on a quantitative method. The laboratory analysis includes investigating the inhibitory activity of bimetallic (Au-Ag) Nps, AgNps and the respective crude aq. and ethanol extracts of *O. sanctum*, and *O. basilicum* alone and in combination on α-amylase and α-glucosidase enzymes and on the bacterial species *S. aureus*, *E. coli*, *P. aeruginosa*, *Salmonella* sp. and *B. subtilis.*

3.2 The data

This research comprises primary and secondary data. The primary data were collected through experiments. Data were collected from *O. basilicum* and *O. sanctum* leaf and flower aq. and ethanol extracts that were subjected to GC-MS evaluation; green synthesis of bimetallic and silver Nps followed by characterisation techniques using SEM-EDX, TEM, FT-IR, DLS and zeta potential with subsequent *in vitro* antidiabetic investigation and antibacterial studies. The secondary data were obtained through published research from journals, books and manuals.

3.3 Materials

Fresh leaves and flowers from *O. sanctum* and *O. basilicum* were collected from Tropical Garden Nursery originating from Peters Gate Nursery in KwaZulu Natal (KZN), South Africa and planted in a medicinal garden made for this study. The medicinal garden (grid ref: 29°47’59” S, 30°56’48” E), conditions includes soil (sand); moisture (running water) and exposure (partial shade). Time for collection was from October 2012-July 2013 with minimal seasonal variation. The plants were immature (*O. sanctum*: 20 cm height, no flowers; *O. basilicum*: 30 cm height, no flowers) when purchased and 12 weeks mature (*O. sanctum*: 48 cm height, purple flowers, ± 4 leaves/node, ± 14 leaves/stem; *O. basilicum*: 60 cm height, white flowers, ± 3 leaves/node, ± 17 leaves/stem) when harvested. The plants were botanically identified at the KZN Herbarium Durban, by Mr M.A. Ngwenya where voucher

specimens were deposited (Voucher 1: *O. tenuiflorum* (*sanctum*) L., Det: Malapermal, V., NH0137400; Voucher 2: *O. basilicum* L., Det: Malapermal, V., NH0137401).

The solvents included absolute ethanol (Merck, SA), used for extraction and were of analytical grade. Silver nitrate and Gold (III) chloride trihydrate ($HAuCl_4 \cdot 3H_2O$) were ACS reagents purchased from Sigma-Aldrich, SA. Acarbose (Glucobay®, BXG1W51, Germany) was purchased from a local pharmacy. The following Sigma-Aldrich products were obtained from Capital Lab Supplies, SA: Type Vi-B from porcine pancreas, SLBB0391V; Potato starch, BCBG8131V; maltose, 071M0259V; *Bacillus stearothermophilus* α-glucosidase, SLBD2144V; sodium carbonate (Na_2CO_3), SZBC244BV; and p-nitrophenyl α-D glucopyranoside (pNPG), BCBK1879V.

3.4 Methods

3.4.1 Extraction and medicinal plant preparation

Distilled water and ethanol (60% and 70%) were used as the extraction solvents to prepare medicinal plant stock solutions (Figure 5). Prior to each extraction method, the leaves and flowers were separated and cleaned by dusting any contaminants or diseased parts. Once this was completed a simple process of shredding of the plant parts was carried out by hand.

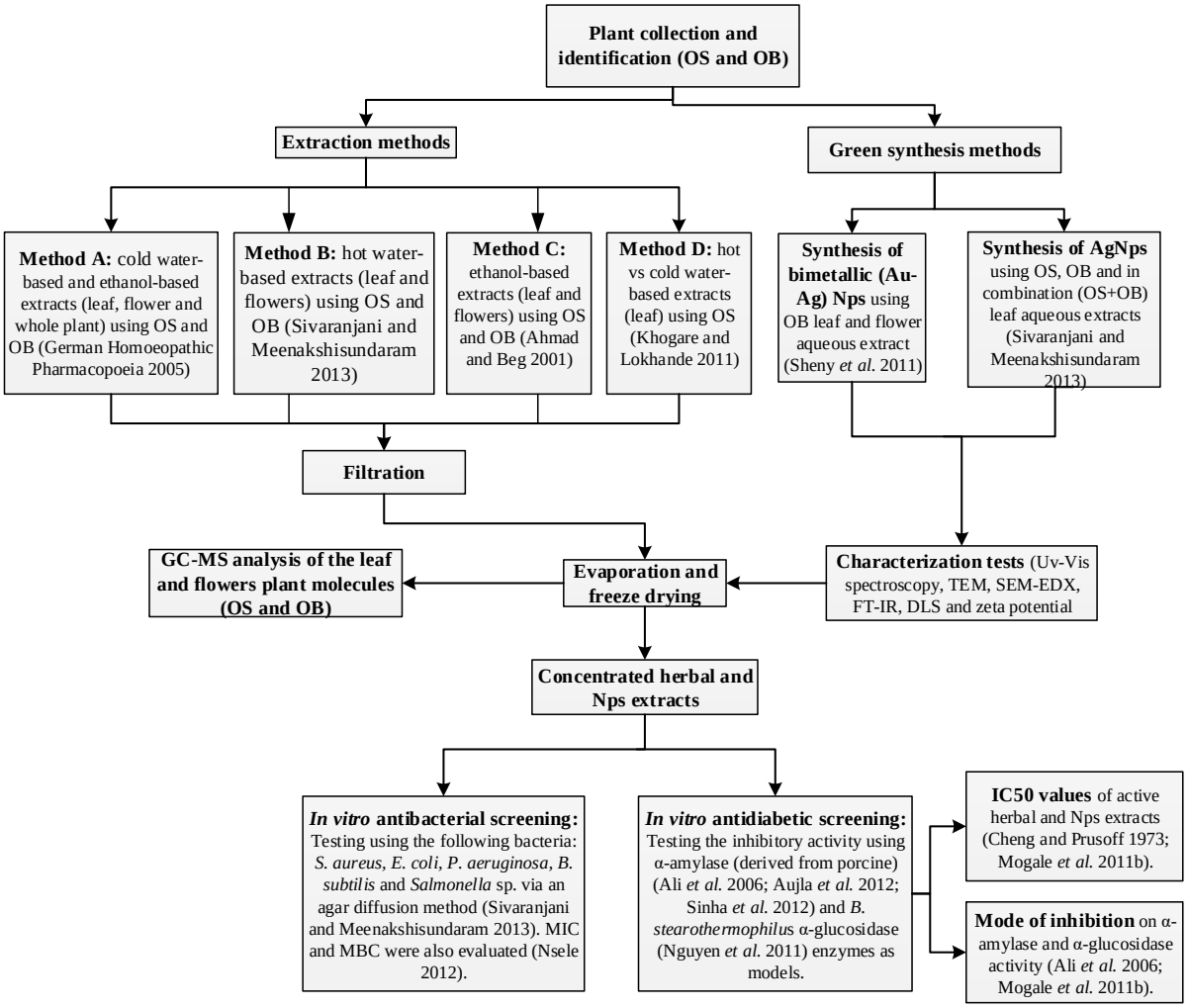

Figure 5: Summary of methods
Key: OS = *O. sanctum*; OB = *O. basilicum*

3.4.1.1 Method A: Cold Water-based and ethanol-based extracts using *O. sanctum* and *O. basilicum*)

Fresh *O. sanctum* and *O. basilicum* leaves, flowers were used to prepare the filtered and unfiltered homoeopathic 150 g mother tinctures (leaf extract, flower extract and leaf + flowers extract). The maceration method 2a (German Homoeopathic Pharmacopoeia 2005), a common extraction technique (Govender 2011), was used to obtain the plant extracts.

Fresh plant material was first finely shredded by hand and a sample used to work out loss on drying. The plant parts were then dispensed with 43% m/m (60% v/v EtOH) alcohol and aq. distillation, respectively. To the shredded plant material, not less than half the amount of mass of alcohol 86% was added and stored in a well closed container at a temperature not

exceeding 20°C. The amount of alcohol 86% required for the plant material was calculated. The amount of alcohol that had been used was subtracted and the remaining amount added to the mixture (Appendixes 6.1 and 6.2).

The mixture was left to stand for not less than 10 days at a temperature not exceeding 20°C, and swirled in the bottles, before being expressed and filtered using mutton cloth and Whatman No. 1 filter paper. The volumes were recorded and made to volume of either 50% EtOH or distilled water (Appendixes 7 and 8).

3.4.1.2 Method B: Hot water-based extracts using *O. basilicum* and *O. sanctum*

Fresh *O. basilicum* leaves and flowers were used to prepare water-based extract following a modified method as per Sivaranjani and Meenakshisundaram (2013). The leaves and flowers were harvested in the morning (07H00) and cleaned by dusting any contaminants or removing any diseased parts, weighed and shredded into fine pieces in a glass beaker. Then, 10 g of the fine plant parts were boiled (60°C) in distilled water (100 ml) for 30 mins. The extracts were left to stand at room temperature for 24 hours. Finally, the extracts were filtered through Whatman No. 1 filter paper. The filtrate was collected and transferred to pre-weighed centrifuge tubes and stored at 4ºC until freeze drying. This method was repeated using *O. sanctum* leaf and flower parts.

3.4.1.3 Method C: Ethanol-based extracts using *O. basilicum* and *O. sanctum*

This method is based on Ahmad and Beg (2001). Ethanol-based extracts were prepared using leaf and flower parts that were harvested early morning (07H00). The leaves and flowers were weighed, and 10 g each of leaves and flowers were cleaned and shredded in a glass beaker. To the respective plant parts 100 ml of 60% and 70% EtOH solution was added and left to stand for 24 hours. The extract was filtered into a conical flask using Whatman No. 1 filter paper. The extracts were stored at 4ºC until further use (Ahmad and Beg 2001).

3.4.1.4 Method D: Hot water vs cold water-based extracts using *O. sanctum*

Test samples were prepared to follow a modified method by Khogare and Lokhande (2011), involving a 3 day extraction period. Fresh leaves of *O. sanctum* (100 g) were placed in boiled distilled water at 100°C (10 ml) and cold water at 4°C (10 ml). The extracts were filtered

through a mutton cloth and then Whatman No. 1 filter paper and made up to 100 ml. The extracts were stored at 4ºC until further use.

3.4.2 Evaporation and freeze drying

The solvents of all samples were allowed to evaporate using a rotary evaporator (Heidolph Rotavac, Germany) at a temperature of 40°C-50°C until a semi solid sticky mass was obtained. The samples were placed in a freezer to a minimum temperature of -40°C to -70°C overnight. The extract was finally freeze dried by using a freeze-dryer (Virtis freeze dryer, USA). The aq. extracts were freeze dried at a low temperature to reduce the dehydration of bioactive natural products (Jones and Kinghorn 2005) and ethanol removed from the ethanolic extracts using the rotary evaporator then freeze dried. Once the process was completed all the test samples were checked for complete drying. The lyophilised/dried product was weighed. The extraction yield was calculated as the percentage of the weight of the crude extract from the raw material. Extraction yielded (%) = (Weight of the freeze dried extract / Weight of the original sample) X 100. Dried extracts were reconstituted in distilled water at 2 mg/ml and stored at 4ºC in a dark container.

3.4.3 GC-MS analysis of *O. basilicum* and *O. sanctum* leaves and flowers

The chemical composition of the leaf and flower aq. and ethanol extracts of *O. basilicum* and *O. sanctum* (L.) was determined via GC-MS analysis using Shimadzu Japan, GC-2010 Plus with GC-MS-QP2010SE equipped with a split/splitless capillary injection port. The capillary column used was a GL Sciences InertCap 5MS/Sil (30 mm length, 0.25 mm I.D., 0.25 µm film thickness), Helium (He) was used as a carrier gas, velocity of the gas 30.0 cm/sec, injector temperature 250°C and injector volume 1.00 µl. The oven temperature and ramping volume per time interval was expressed as the ovens initial temperature at 60°C, without holding the temperature was then ramped at 10°C/min to a final temperature of 280°C and held at 280°C for 10 min. The MS zone set temperatures include ion source temperature at 200°C and interface temperature at 250°C.

The chemical composition of the essential oils isolated from *O. sanctum* and *O. basilicum* were effectively quantified by GC-MS analysis (Kothari *et al.* 2004; Saha *et al.* 2012). The volatile components from *Ocimum* sp. were identified by comparing their retention time of the GC chromatograph with those of literature (Joshi *et al.* 2011). Interpretation of mass spectra of GC-MS was conducted using the database of National Institute Standard and

Technology (NIST) having more than 62,000 patterns. The spectrum of the known component was compared with the spectrum of the known components stored in the NIST library attached to the GC-MS instrument. The name, molecular weight and structure of the components of the test materials were ascertained. To draw the chemical structures and schemes, ChemDraw Ultra® (chemical structure drawing standard) was used, CambridgeSoft Corporation version 7.0.1 2002.

3.4.4 Synthesis of bimetallic (Au-Ag) Nps using *O. basilicum* aq. leaf and flower extract

This method is based on Sheny *et al.* (2011). The plant leaves and flowers were cleaned in deionised water. The leaf and flower broth were prepared by taking 10 g of finely shredded leaves and flowers in an Erlenmeyer flask with 100 ml of deionised water and boiling the mixtures for 10 min, followed by cooling. Briefly, 2 ml of each plant extract was added drop wise (total 10 ml) to 30 ml of 1 mM silver nitrate ($AgNO_3$), and vigorously stirred with the aid of magnetic stirrer, until the first colour change (brown solution) that indicated the reduction of Ag^+ ions after a few minutes. Then, 2 mM chloroauric acid solution (30 ml) was added, in small aliquots of 5 ml at various timed intervals. The reduction of Au^{3+} was revealed after 10 min as shown by the stable light violet colour of the solution at room temperature (Shankar *et al.* 2004). The formation of bimetallic Au-Ag Nps was monitored for 36 hours. UV-Vis Spectra were recorded as a function of the reaction time. Scheme 1 illustrates the bio-reduction mechanism and formation of bimetallic (Au-Ag) Nps from *O. basilicum* (leaves and flowers).

3.4.5 Synthesis of AgNps using *O. basilicum*, *O. sanctum* and in combination aq. leaf extract

This method is based on Sivaranjani and Meenakshisundaram (2013). The *O. basilicum* and *O. sanctum* leaf extracts were prepared by taking 10 g of washed and finely cut leaves in an Erlenmeyer flask in combination with 100 ml of deionised water; the mixture was boiled for 10 min and cooled. Then, 2 ml of the leaf broth was added drop wise (total 10 ml) to 45 ml of 1 mM aq. silver nitrate solution and vigorously stirred with the aid of magnetic stirrer, until the first colour change (brown solution) that indicated the reduction of Ag^+ ions after a few minutes. The formation of AgNps was monitored for 36 hours using a UV-Vis spectrophotometer. The method was repeated in combination (10 ml *O. sanctum* + 10 ml *O.*

basilicum) to obtain the extract from the above mentioned standard conditions to test the synergistic effect. Scheme 1 illustrates the bio-reduction mechanism and formation of AgNps from a combination of *O. basilicum* and *O. sanctum* leaf extracts.

3.4.6 Characterisation tests

The AgNps and bimetallic (Au-Ag) Nps were characterised using UV-Vis spectrophotometer (Varian Cary-50 UV spectrophotometer, USA) linked to a TCC-240A Shimadzu heating vessel temperature controlled cell holders between 200 nm – 800 nm, using a small aliquot of the sample diluted with distilled water (Sivaranjani and Meenakshisundaram 2013). This technique is vital for the purpose of previewing the formation and stability of the Nps over a fixed duration of time. A consecutive time frame/UV-Spec range of: 12-hours-24 hours-36 hours interval between the reduction of pure Au^{3+} and Ag^{+} ions, plus an added interval at 28 hours was used for AgNps formation using two plant extracts in combination, to confirm their synergistic effect and peak formation. The graphs were represented using software OriginPro 8 SRO v8.0725, USA (B725). To obtain the particle size and shape, 1 µl of the AgNps and bimetallic (Au-Ag) Nps samples were placed on formvar coated grids which were air dried and then viewed at 100 kV to conduct the transmission electron microscopy (JEOL 1010 TEM using a Megaview III camera and iTEM software) studies. The nanoparticle size distribution was determined by using *ImageJ* software and the resultant data were plotted in histograms expressed as means ± SD and plotted using OriginPro. TEM is always the first method used to determine the size and size distribution of nanoparticle samples. Once a representative group of images was obtained, the next task was to count as many particles as possible, ideally a few thousand, so that good statistics on the size and size distribution could be obtained (Woehrle *et al.* 2006).

For the particles' images and elemental analysis, the AgNps and bimetallic (Au-Ag) Nps colloidal suspensions were freeze dried. Percent yields for *O. sanctum* of bimetallic Nps leaf extract was 9.3% and of flower extract was 9.4%, and for AgNps the percentage yield was 4.2%. The percentage yield for *O. basilicum* AgNps extract was 2.4% and the combination extract was 2.75%. The samples were prepared by fixing the powder particles of microscope holders, using conducting carbon tape and subjected to Carl Zeiss, model EVO HD 15 Scanning Electron Microscope, Germany with EDX detector, Oxford Instruments, UK. The software was SmartSEM and Aztec. FT-IR analysis is used to characterise the nature of capping ligands that stabilise Nps formed by the bio-reduction process. FT-IR spectra were

recorded for the crude aq. leaf and flower extract prepared in Method 3.4.4 and 3.4.5, bimetallic Nps and AgNps with Bruker Alpha FT-IR spectrophotometer, graphs were structured using OriginPro. Differential Light Scattering *Malvern Zetasizer Nano ZS* (Malvern Instruments Ltd., UK) Merck 2423 instrument was used to measure the nanoparticle size and zeta potential. Differential Light Scattering measurement is described as the mean size of the particles of the sample that is obtained along with the correlation between the number of particles of a specific size versus the size of the Nps (Singhal *et al.* 2011); as a result negatively charged Nps prove evidence that the particles dispersed in the medium are stable (Kotakadi *et al.* 2014).

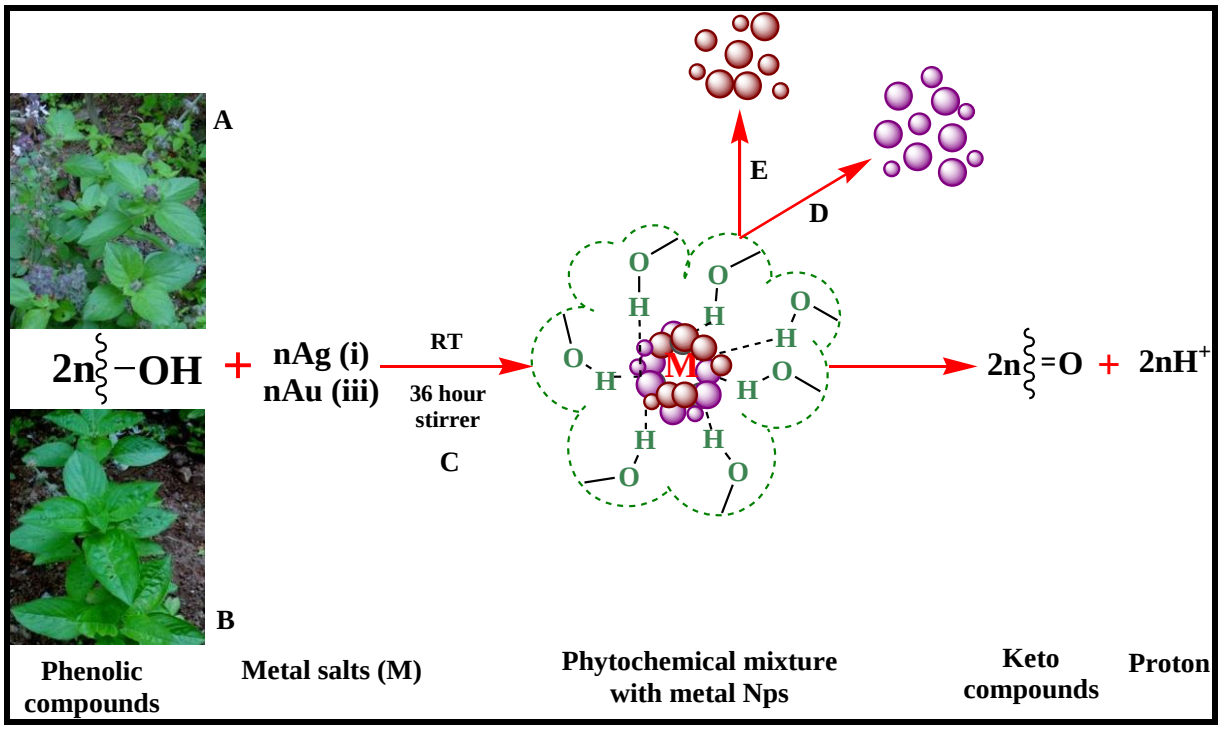

Scheme 1: Synthesis of bimetallic (Au-Ag) Nps and AgNps from phenolic rich plants such as *O. sanctum* and *O. basilicum*

Key: (A) O. sanctum (L.); (B) O. basilicum (L.); (C) Reduction reaction; (D) nAu (0) and nAg (0) (bimetallic (Au-Ag) nanoparticles); (E) nAg (0) (silver nanoparticles); RT = Room temperature; M = Metal salts

3.4.7 *In vitro* antimicrobial screening

3.4.7.1 Bacterial sensitivity testing (Agar diffusion method)

The method is based on Sivaranjani and Meenakshisundaram (2013). Mueller Hinton agar was streaked with suitable well mixed overnight nutrient broth cultures of each microorganism (*S. aureus* ATCC 25923, *E. coli* ATCC 26922, *P. aeruginosa* ATCC 27853,

Salmonella sp. UKQC 9990 and *B. subtilis* ATCC 6051) at $1x10^6$ colony forming units (CFU) per millilitre, by streaking evenly on to the surface of the medium with a sterile cotton swab to allow for even growth. Wells were cut out from the agar plates using a sterile bore (Sivaranjani and Meenakshisundaram 2013). They were filled with 30 µl for each sample using a sterile micropipette in respective wells allowing a 10 min diffusion time. Gentamycin and vancomycin discs, 1 mM $AgNO_3$ and distilled water were used as controls (refer to preparation methods and quality controls in Appendix 9.1). The plates were incubated at 37°C for 24 hours. After the incubation period, the plates were examined for any clearing zones around the walls and/or discs. The zones of inhibition were measured in mm using a ruler and compared to the controls. This experiment was carried out six times for confirmation and statistical analysis. The results were read in the presence or absence of a zone of inhibition.

3.4.7.2 Determination of the Minimum Inhibitory Concentration (MIC) and Minimum Bactericidal Concentration (MBC)

This method is based on Nsele (2012). Nutrient broth (2 ml) was aseptically transferred to 5 ml glass test tubes (eight tubes in total). For each sample that showed inhibition determined in the agar diffusion method 2 ml of the sample (AgNps synthesised from *O. sanctum* and *O. basilicum* singly and in combination) was added to the first tube in the series. It was mixed by vortex mixers and 2 ml pipetted and transferred to the next tube, the process was repeated until the eighth tube from which 2 ml was discarded. This double dilution process resulted in 2 ml of sample in each test tube. The dilutions were as follows: 1:2; 1:4; 1:8; 1:16; 1:32; 1:64; 1:128: and 1:256. Each tube was inoculated with 100 µl of each bacterial suspension of the five different bacteria. The suspensions were the same as those used for the screening test outlined in 3.4.7.1 and made to a 0.5 McFarland turbidity standard. They were incubated at 37ºC for 24 hours. Water was used as a control. The MIC was regarded as the lowest concentration of the extract that did not allow any visible growth. The results were compared with the 0.5 McFarland standards. The water control was included with each extract tested. No visible turbidity was regarded as no growth. The MBC was determined by taking the tubes from the various dilutions that showed no visible turbidity after 24 hours and streaking it on fresh blood agar plates. The plates were incubated at 37ºC for 24 hours and examined for growth. The MBC was regarded as the lowest concentration of the extracts that prevented

the growth of any bacteria colonising on a solid medium. Each sample was repeated six times with each bacterium.

3.4.7.3 Statistical assessment

The statistical analysis of data was expressed as means ± SEM. Statistical analysis was performed using the Wilcoxon Signed Ranks and Mann-Whitney test, parameters set for a two-tailed analysis of 95% Confidence interval. Data were statistically analysed by GraphPad Prism® 5.03 for Windows (GraphPad Software, USA) and considered statistically significant when $p \leq 0.05$.

3.4.8 *In vitro* antidiabetic screening

3.4.8.1 α-amylase inhibitory test

The α-amylase (Type Vi-B from porcine pancreas) inhibitory activity was investigated by time-dependent manner as described by Ali *et al.* (2006) with slight modifications. Briefly, 120 µl of the test samples (2.0 mg/ml and 3.0 mg/ml), 480 µl of distilled water and 1200 µl of potato starch (0.5% w/v prepared in 20 mM phosphate buffer) were mixed, 600 µl α-amylase (0.05 g of α-amylase prepared in 100 ml ice-cold distilled water) was added to start the reaction and incubated at 25ºC for 3 min. After every min, 200 µl was removed from the reaction mixture and added into a tube containing 100 µl of DNS (Dinitrosalicylic acid) colour reagent (96 mM 3,5-DNS, 12g sodium potassium tartrate in 8 ml of 2 M NaOH). The reaction mixture was heated for 15 min at 85ºC. After cooling to room temperature, 900 µl of distilled water was added to the mixture and mixed thoroughly. The absorbance value was recorded at 540 nm (UV spectrophotometer) against the blank. The blank contained 600 µl of distilled water instead of enzyme solution and for the control, test samples was replaced with 120 µl of distilled water and therefore represented maximum enzymatic activity. For t = 0 min, a separate experiment was performed, by adding the samples to the DNS solution immediately after addition of enzyme (Appendix 9.2). The test was performed in triplicate. From the maltose standard curve (0-2% w/v Appendix 9.3.1), the amount of maltose generated in the samples was calculated (Bernfeld 1955). For calculating the percentage inhibition, the following equations were used. First, the net absorbance (A) using equation (1) due to maltose generated was calculated. Second, from the net absorbance obtained, the percentage (w/v) of maltose generated was calculated from the equation (2) obtained from the

equation in the maltose standard calibration curve; α-amylase inhibitors result in less maltose produced and the absorbance value hence is decreased. Finally, the percentage inhibition was calculated at t = 3 min using equations (3) and 50% inhibition or higher was taken as significant ($p < 0.05$).

Equation (1) Absorbance (A) at 540 nm control or plant extract = A_{540nm} Test – A_{540nm} Blank

Equation (2) % Reaction = $\frac{\text{Mean maltose in sample}}{\text{Mean maltose in control}} \times 100$

Equation (3) % Inhibition = 100 - % Reaction

In addition, α-amylase inhibition ($I_{\alpha\text{-Amylase}}$) was assessed in a dose-dependent manner (Aujla *et al.* 2012). Briefly, 1 ml α-amylase (0.5 unit/ml) prepared in 20 mM phosphate buffers (pH 6.9) was pre-incubated for 30 mins with 1 ml samples (0.0002-2 mg/ml). The reaction was started by the addition of 1 ml potato starch (0.5% w/v, prepared by dissolving in 100 ml distilled water). The reaction mixture was incubated at 25ºC for 30 mins. Finally, the catalytic reaction terminated with the addition of 1 ml DNS reagent. The reaction mixture was heated for 15 mins at 85ºC in a water bath. The tubes were cooled to room temperature and diluted with 9 ml distilled water. Individual blanks were prepared for correcting the background absorbance; DNS colour reagent was added before the addition of starch solution and placed into the water bath. For the control incubations all procedures were again the same except that the plant extracts was replaced by 1 ml distilled water. The absorbance value was recorded at 540 nm. Antidiabetic medicine acarbose in concentrations of 0.016-1.0 mg/ml (Sinha and Kumar 2012) was used as positive control (Appendix 9.4). The test was performed in triplicate and the mean absorbance was used to calculate percentage of α-amylase inhibition, the following equations were used:

Equation (4) $I_{\alpha\text{-Amylase}}$ % = $\frac{(\Delta A540 \text{ nm Control} - \Delta A540 \text{ nm Sample})}{\Delta A540 \text{ nm Control}} \times 100$

Equation (5) $\Delta A_{\text{Control}} = A_{\text{Test}} - A_{\text{Blank}}$

Equation (6) $\Delta A_{\text{Sample}} = A_{\text{Test}} - A_{\text{Blank}}$

3.4.8.2 α-glucosidase inhibitory test

The α-glucosidase inhibitory test ($I_{\alpha\text{-Glucosidase}}$) was performed according to Nguyen *et al.* (2011). Briefly, 0.1 ml of 0.5 unit/ml α-glucosidase from *B. stearothermophilus* prepared in

ice-cold distilled water were pre-incubated with 0.1 ml of test samples (0.2 mg/ml and 0.3 mg/ml) for 5 mins. Then, 0.1 ml of the substrate pNPG 3 mM which was prepared in 0.01 M phosphate buffers (pH 6.9) was added to start the reaction. After further incubation at 37ºC for 30 mins, the reaction was stopped by adding 1.5 ml of 0.1 M sodium carbonates. Individual blanks were prepared for correcting the background absorbance; buffer was added instead of the enzyme. For control incubation all procedures were again the same except that the plant extracts were replaced by the buffer. Antidiabetic medicine acarbose in concentrations of 0.00001 mg/ml - 1.0 mg/ml was used as positive control (Appendix 9.5). Enzymatic activity was quantified by measuring the absorbance at 405 nm. For calculating the percentage of α-glucosidase enzyme inhibition, the following equations were used:

Equation (7) $I_{\alpha\text{-Glucosidase}}\ \% = \frac{(\Delta A405\ \text{nm Control} - \Delta A405\ \text{nm Sample})}{\Delta A405\ \text{nm Control}} \times 100$

Equation (8) $\Delta A_{\text{Control}} = A_{\text{Test}} - A_{\text{Blank}}$

Equation (9) $\Delta A_{\text{Sample}} = A_{\text{Test}} - A_{\text{Blank}}$

3.4.8.3 IC_{50} values of active herbal/Nps extracts

The potency of herbal extracts as inhibitors of enzyme catalytic activities of both porcine α-amylase and *B. stearothermophilus* α-glucosidase was assessed in terms of their IC_{50} values (inhibitor concentration that reduces enzyme activity by 50%) according to the methods described by Cheng and Prusoff (1973) and Mogale *et al.* (2011b). Briefly, aliquots of α-amylase (1 ml) and α-glucosidase (0.1 ml) enzymes were preincubated with increasing concentrations of the herbal/Nps extracts and acarbose (0.00001 mg/ml to 1.0 mg/ml). Catalytic reactions were started, terminated and enzyme activities determined as aforementioned. The activity of fractions and compounds was assessed by plotting percentage inhibition against a range of concentrations and determining the inhibitory concentration at 50% (IC_{50}) by interpolation of a cubic spline dose-response curve using GraphPad Prism® 5.03 software.

3.4.8.4 Mode of inhibition of α-amylase and α-glucosidase activity

Mode of inhibition of the samples of α-amylase activity was determined according to adapted methods (Ali *et al.* 2006; Mogale *et al.* 2011b). Briefly, 250 µl of the extract (*O. sanctum* and *O. basilicum* 70% EtOH crude extract, bimetallic Nps (2.5 mg/ml) and AgNps (3.0 mg/ml)

was pre-incubated with 250 µl of α-amylase from porcine (0.05 g in 100 ml) for 15 mins at 25ºC in one set of tubes. In the other set of tubes α-amylase was pre-incubated with 250 µl of phosphate buffer, pH 6.9. Thereafter, 250 µl of potato starch was added at increasing concentrations (0.15-5.0 mg/ml) to both sets of reaction mixtures to start the reaction. The mixture was then incubated for 20 mins at 25ºC, and boiled at 85ºC for 5 mins after addition of 500 µl of DNS to stop the reaction. The amount of reducing sugars released was determined spectrophotometrically using a maltose standard curve and converted to reaction rates (velocities) according to the reaction rate formula, equation (10).

Inhibition modes against *B. stearothermophilus* α-glucosidase were determined according to the method described above for α-amylase activity with modification. Briefly, fixed amounts of α-glucosidase were incubated with increasing concentrations of p-nitrophenyl α-D glucopyranoside (pNPG) as a substrate from 2 to 10 mM) at 37ºC for 20 mins, in the absence and presence of the herbal extracts (2.5 mg/ml). Reactions were terminated and absorption measurements carried out as aforementioned. The amount of p-nitrophenol released was measured spectrophotometrically at 405 nm using a pNPG standard curve (Appendix 9.3.2) and converted to reaction rates (velocities) according to the reaction rate formula, equation (10).

Equation (10) Reaction rate (v) ($mg.ml^{-1}.s^{-1}$) = $\frac{\text{Amount of product liberated (mg.ml}-1)}{1200\ (s)}$

A double reciprocal plot (1/v versus 1/[S]) where v is reaction velocity and [S] is substrate concentration was plotted. The mode of inhibition of the samples of α-amylase and α-glucosidase activity was determined by analysis of the double reciprocal (Lineweaver-Burk) plot using Michaelis-Menten kinetics (Lineweaver and Burk 1934) calculated from GraphPad Prism® software.

3.4.8.5 Statistical assessment

The statistical analysis of data was expressed as means ± SEM and performed using One-way and Two-way analysis of variance (ANOVA) to calculate the statistical significance with statistical parameters set for Bonferroni multiple comparisons and a 95% Confidence interval. For the descriptive study, data were statistically analysed by GraphPad Prism® 5.03 for Windows (GraphPad Software, USA) and considered statistically significant when $p \leq 0.05$ and response higher than the control considered as potentially effective.

CHAPTER 4 : RESULTS

4.1 GC-MS analysis of *O. basilicum* leaf and flower aq. and EtOH extracts

The chemical composition of the leaf and flower aq. and EtOH extracts from *O. basilicum* constituents were identified after comparison of the results from this study with those available in the computer library (NIST) attached to the GC-MS instrument and reported in Appendix 22-23. No hit compounds were obtained from *O. basilicum* flower extract, but they were further elucidated in the FT-IR assay (Figure 13).

Using GC-MS analyses the organic compounds identified as constituents of *O. basilicum* leaf essential oils were: cyclohexanol; menthol; hexanedioic acid/adipic acid; 3,7,11,15-tetramethyl-2-hexadecen-1-ol; 13-methyl-14-pentadecene-1,13-diol and terpenes such as squalene and phytol. There were more chemical constituents identified in the EtOH leaf extracts than the aq. leaf extract (Tables 2 and 3). Some of the compounds detected in this study were consistent with those in previous studies in which chemical components were isolated using various organic solvent extractions (Lee *et al.* 2005).

Table 2: GC-MS report of the chemical constituents present in *O. basilicum* aq. leaf extract

Peak no.	Compound	MF	MW (g/mol)	RT (min)	Area (%)
1	Hexanedioic acid, Adipic acid, Diisooctyl adipate, Bis(6-methylheptyl) hexanedioate	$C_{22}H_{42}O_4$	370	21.412	100
2	2-ethylhexyl pentadecyl ester	$C_{29}H_{56}O_4$	468	21.412	100
3	2-ethylhexyl tetradecyl ester	$C_{28}H_{54}O_4$	454	21.412	100

Key: MF = Molecular Formula; MW = Molecular Weight; RT = Retention time

Table 3: GC-MS report of the chemical constituents present in *O. basilicum* EtOH leaf extract

Peak no.	Compound	MF	MW (g/mol)	RT (min)	Area (%)
1	3,7,11,15-Tetramethyl-2-hexadecen-1-ol	$C_{20}H_{40}O$	296	16.251	15.01
2	Phytol acetate	$C_{22}H_{42}O_2$	338	16.251	15.01
3	Pentadecanal	$C_{15}H_{30}O$	226	16.251	15.01
4	Oxirane, 1,2-Epoxyoctadecane	$C_{18}H_{36}O$	268	16.251	15.01

5	Hexadecanal, Palmitaldehyde	$C_{16}H_{32}O$	240	16.251	15.01
6	Phytol	$C_{20}H_{40}O$	296	19.002	34.31
7	Cyclohexanol, 5-methyl-2-(1-methylethyl)-, (1S,2R,5R)-(+)-, Menthol	$C_{10}H_{20}O$	156	19.002	34.31
8	13-Methyl-14-pentadecene-1,13-diol	$C_{16}H_{32}O_2$	256	19.002	34.31
9	Squalene	$C_{30}H_50$	410	25.688	10.88
10	Eicosane	$C_{20}H_{42}$	282	30.752	17.88
11	2-methylhexacosane	$C_{27}H_{56}$	380	30.752	17.88
12	Tetratetracontane	$C_{44}H_{90}$	618	30.752	17.88
13	Hexatriacontane	$C_{36}H_{74}$	506	30.752	17.88
14	Pentadecane, 8-n-Hexylpentadecane	$C_{21}H_{44}$	296	30.752	17.88

Key: MF = Molecular Formula; MW = Molecular Weight; RT = Retention time

4.2 Characterisation tests of the bimetallic (Au-Ag) Nps synthesised from *O. basilicum* leaf and flower aq. extracts

4.2.1 UV-Visible studies

A well-defined absorption peak was obtained at 557 nm from the bimetallic (Au-Ag) Nps particles synthesised from the leaf extract and 534 nm from the flower extract, exhibited by the consequent colour change due to the progressive addition of small aliquots of chloroauric acid solution. The colour change from brown to a violet colour which appeared rapidly within 10 mins and confirmed the synthesis of bimetallic (Au-Ag) Nps (Figures 6 and 7). Bimetallic Nps synthesised from *O. basilicum* leaf and flowers extracts show the Surface Plasmon Resonance (SPR) band of approximately ~500 nm due to the higher concentration of Au used compared to the usual UV-Vis spectra for Ag at ~400 nm (Dong *et al.* 2013). The SPR band is much stronger for Au and Ag nanoparticles than other noble metals (see Figures 8 and 9). The SPR band intensity and wavelength are affected by the particle size, metal type, shape, structure, composition and the dielectric constant of the surrounding medium. Increasing particle size shifts the SPR wavelength and also increases the intensity; therefore, for particles larger than 100 nm the band broadening occurs due to the dominant contributions from higher order electron oscillations (Huang and El-Sayed 2010).

The effect of reaction time (Tables 4 and 5) on formation of bimetallic Nps was also analysed, indicating an increase in peak absorbance as a function of time (Appendix 10). The interaction of Nps with biomolecules of *O. basilicum* leaf and flower extracts showed intense peaks thus indicating the reduction of $Au^{3+} \rightarrow Au^0$ (gold oxidation state) and $Ag^+ \rightarrow Ag^0$

(silver oxidation state). Therefore, *O. basilicum* aq. leaf and flower extracts can be used as a natural reducing agent. Strictly pursuing Sheny *et al.* (2011), the results obtained in the present study for the facile green synthesis of bimetallic (Au-Ag) Nps could have occurred in a similar fashion.

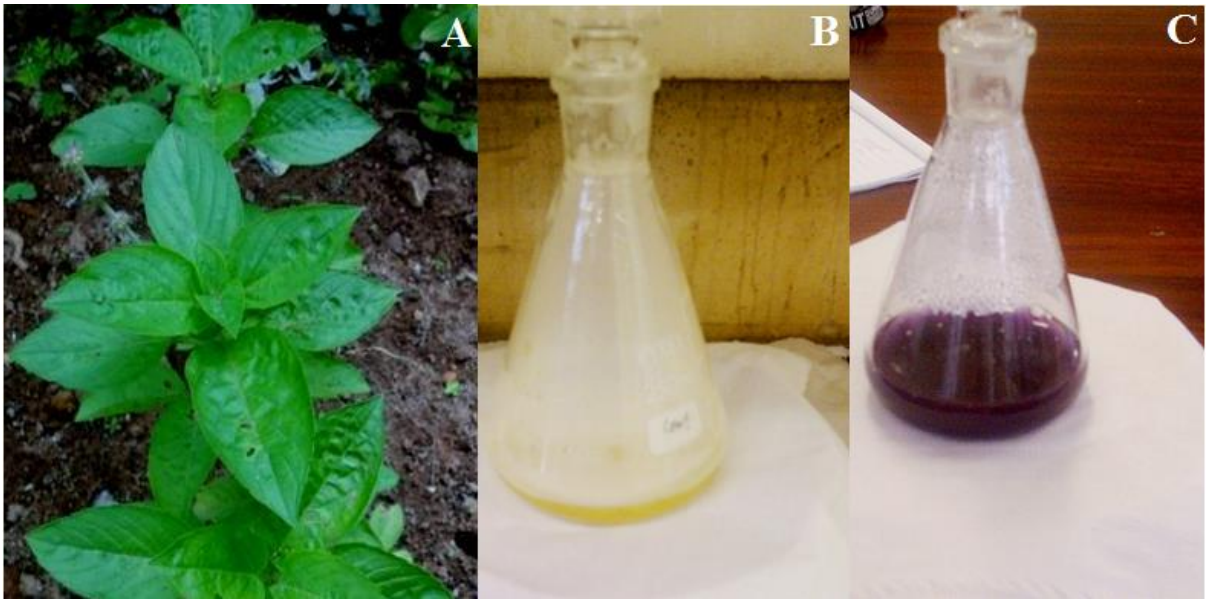

Figure 6: (A) *O. basilicum* leaves used in the study (B) Picture of aq. solution of 1 mM $AgNO_3$ mixed with *O. basilicum* leaf extract (C) Deep violet colour after the addition of 2 mM $HAuCl_4 \cdot 3H_2O$

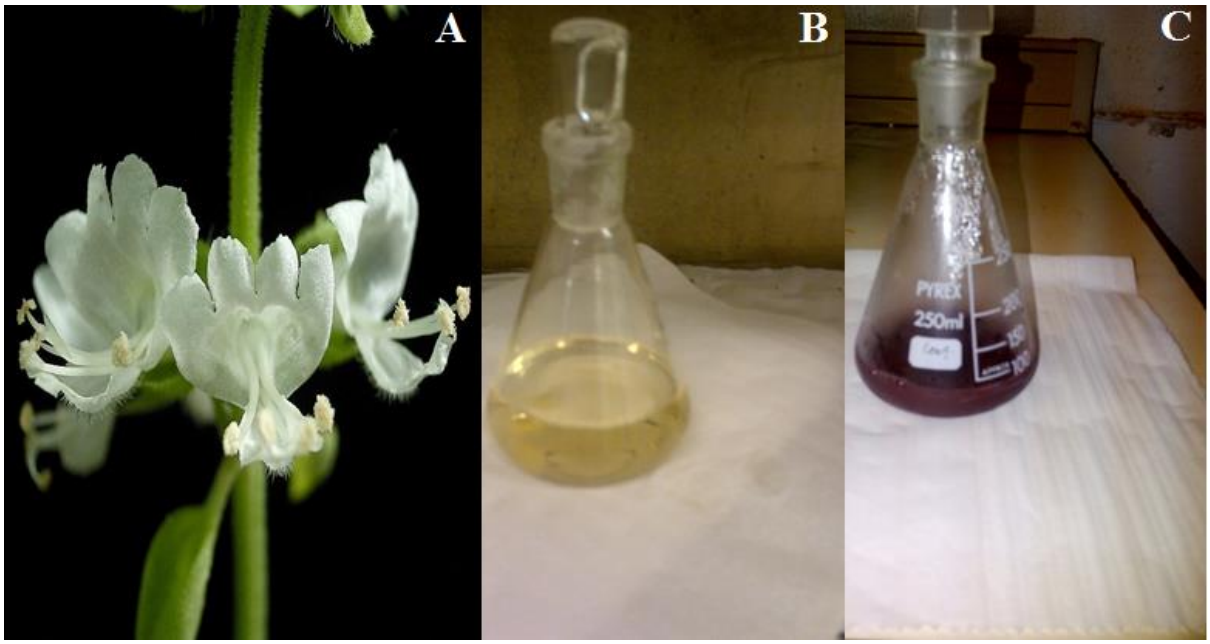

Figure 7: (A) *O. basilicum* flowers used in the study (Vincentz 2007) (B) Picture of aq. solution of 1 mM $AgNO_3$ with *O. basilicum* flower extract (C) Deep violet colour after the addition of 2 mM $HAuCl_4 \cdot 3H_2O$

Table 4: Peak wavelength and absorbance at different timed intervals for bimetallic (Au-Ag) Nps synthesised using *O. basilicum* aq. leaf extract

Intervals	Peak wavelength (300-700 nm)	Absorbance
Day 1: after 12 hours	553.0	0.652
Day 2 after 24 hours	551.0	0.683
Day 3 after 36 hours	557.0	0.792

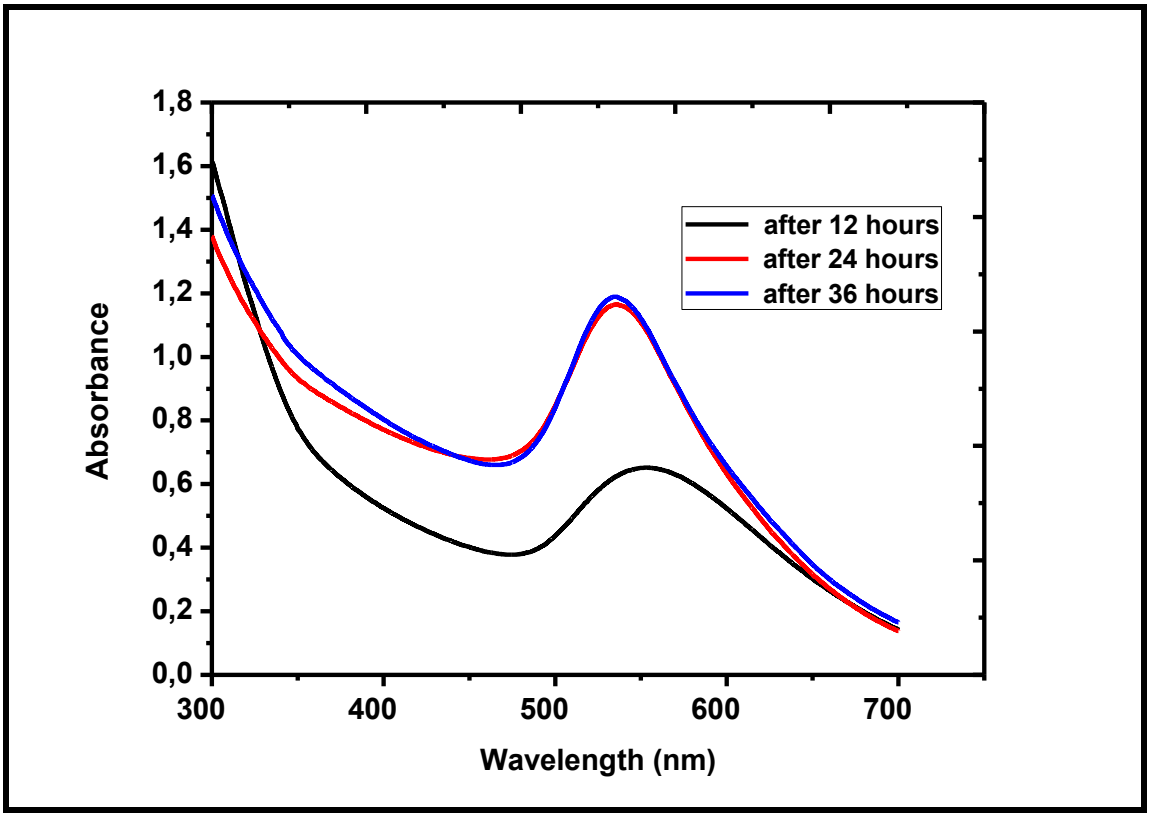

Figure 8: UV-Visible absorption spectra of bimetallic (Au-Ag) Nps synthesised using *O. basilicum* aq. leaf extract at different reaction times

Table 5: Peak wavelength and absorbance at different timed intervals for bimetallic (Au-Ag) Nps synthesised using *O. basilicum* aq. flower extract

Intervals	Peak wavelength (300-700 nm)	Absorbance
Day 1: after 12 hours	541.0	0.387
Day 2 after 24 hours	536.0	1.166
Day 3 after 36 hours	534.5	1.189

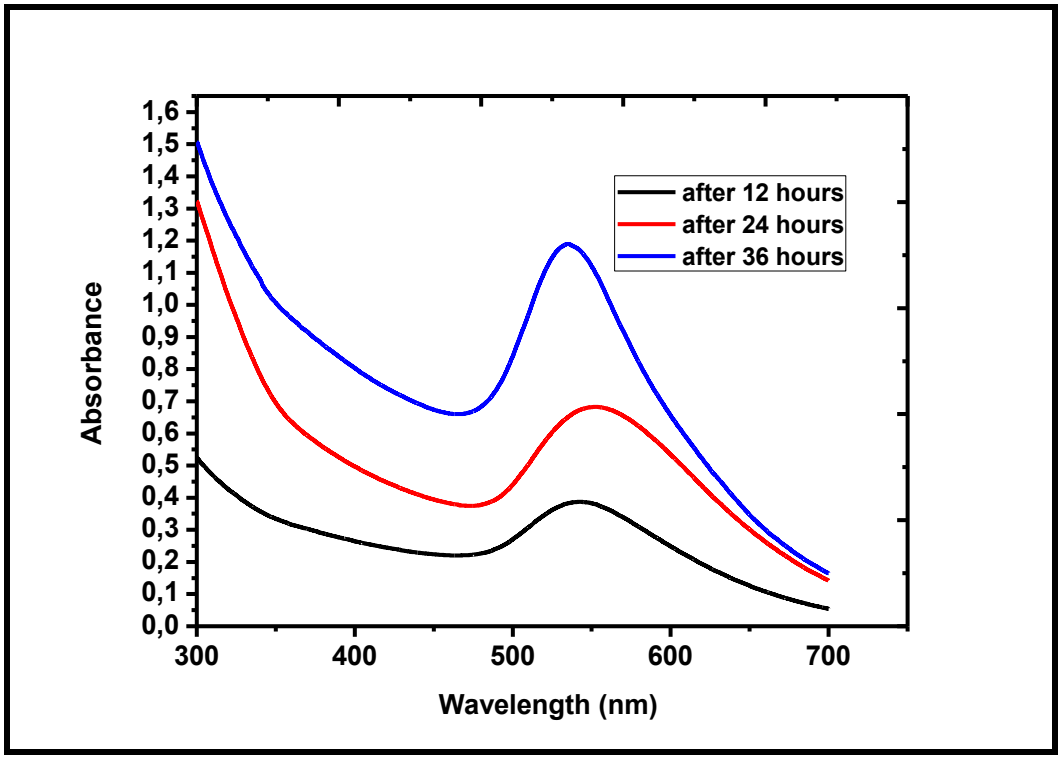

Figure 9: UV-Visible absorption spectra of bimetallic (Au-Ag) Nps synthesised using *O. basilicum* aq. flower extracts at different reaction times

4.2.2 TEM analysis

The results obtained from the TEM monograph indicated that the size and shape properties of the bimetallic (Au-Ag) Nps were predominantly monodispersed with a diameter range of 9-35 nm (leaf extract) and 2-36 nm (flower extract). Representative TEM images (Appendix 12-13 (A)) show that most of the particles are predominantly spherically shaped. The images also indicate alloy bimetallic (Au-Ag) Nps that formed AgNps first and then subsequently due to the addition of chloroauric acid solution formed AuNps; the rationale for adding Au was to facilitate further stability and for the principle of reducing toxicity of the alloyed bimetallic Nps. Previous studies reveal TEM images which show electron density banding indicated by a dark gold core and a light silver shell that confirms Au core-Ag shells Nps, suggesting the presence of alloy bimetallic (Au-Ag) Nps (Sheny *et al.* 2011; Kumari *et al.* 2015). These observations are in agreement with the UV-Vis spectrum obtained in the present study showing variation in plasmon bands (Huang and El-Sayed 2010) (see Figure 8 and 9).

The figures contained in Appendix 12-13 (B) show the particle size distribution histogram with a size of 21 nm ± 11.53 nm for the bimetallic (Au-Ag) Nps formed from the leaf extract

and 25 nm ± 9.63 nm for the bimetallic (Au-Ag) Nps formed from the flower extract. These results show that it is possible to prepare stable Au-Ag bimetallic alloy Nps of a size range that is less than 25 nm by varying the ratio of $AgNO_3$, $HAuCl_4$ and aq. *O. basilicum* leaf and flower extracts.

4.2.3 SEM-EDX analysis

The elemental composition of the powdered samples (bimetallic Au-Ag Nps synthesised from *O. basilicum* (leaf and flower extracts) were determined using SEM equipped with an EDX detector. The SEM micrograph of the synthesised bimetallic Nps using 10% *O. basilicum* leaf and flower extract reveal polydispersed bimetallic Nps with varied sizes. The crystalline nature of the bimetallic Nps and nanosize was confirmed by SEM and the EDX pattern. The SEM image showed relatively spherical shaped Nps formed in the diameter range of 100 nm (see Figures 10 and11 (A)). A few agglomerated Nps were also observed in some places therefore indicating possible sedimentation at a later stage (Sivaranjani and Meenakshisundaram 2013). Often, nanoparticle aggregation is based on assumptions about the nanoparticles interaction potential (intermolecular and electron force interactions between particles present within the metal nanoparticles and phytochemical mixture). Therefore, it is necessary to understand the sedimentation of aggregated/agglomerated Nps for a rational design of synthesis with well-controlled properties (Pranami 2009), particularly, the effects on the extrinsic (or dynamic) physiochemical properties of Nps in aq. solutions (e.g., hydrodynamic size, aggregation, agglomeration, sedimentation, and dissolution of Nps) (Park *et al.* 2013).

The energy dispersive X-ray analysis (EDX) shown in Figures 10 and 11 (B) revealed signals in the gold and silver region at five different spectra for both the leaf and flower extracts thus confirming the formation of bimetallic (Au-Ag) Nps. There were also spectral signals for oxygen (O) that indicated that extracellular organic moieties (originating from *O. basilicum* leaf and flower extracts) were adsorbed on the surface or in the vicinity of the metallic Nps or may have originated from the biomolecules that were bound to the surface of the bimetallic (Au-Ag) Nps. Peaks of sulphur (S), phosphorus (P) and nitrogen (N) correspond to the protein capping over the bimetallic (Au-Ag) Nps. However, certain elements may emanate from artefacts during sample preparation. Furthermore, peaks of carbon (C) originate from the grid used.

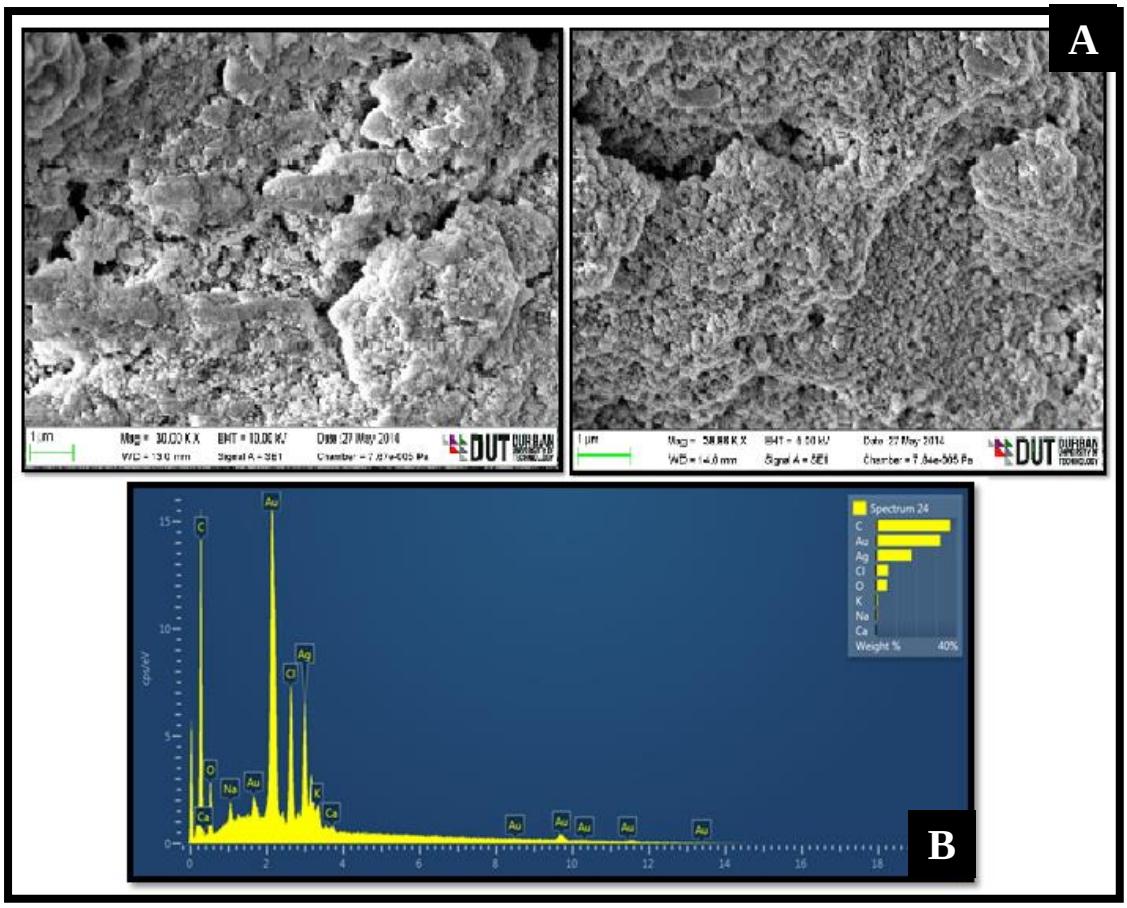

Figure 10: (A) SEM with EDX image of bimetallic (Au-Ag) Nps synthesised using *O. basilicum* leaf extract and (B) EDX showing the presence of the elements on the surface of the bimetallic (Au-Ag) Nps and confirming the presence of bimetallic (Au-Ag) Nps

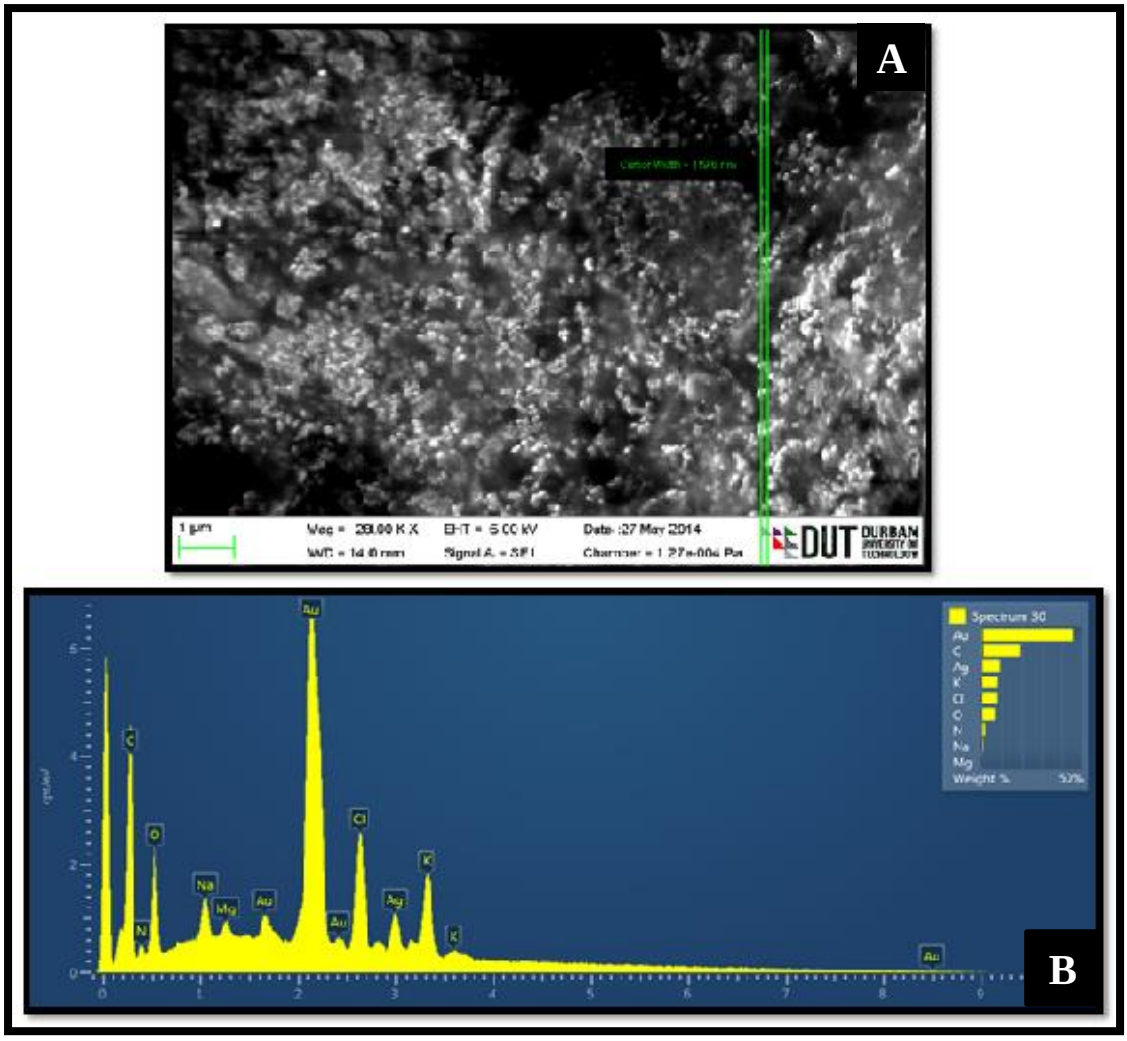

Figure 11: (A) SEM with EDX image of bimetallic (Au-Ag) Nps synthesised using *O. basilicum* flower extract and (B) EDX showing the presence of the elements on the surface of the bimetallic (Au-Ag) Nps and confirming the presence of bimetallic (Au-Ag) Nps

4.2.4 DLS and Zeta Potential analysis

Dynamic light scattering (DLS) measurement showed the size distribution of the Nps to be an average colloidal size of 73.55 nm (leaf extract) and 78.87 nm (flower extract) for the bimetallic Nps (Appendixes 17and 18 (A)) which is similar to the Nps synthesised from the leaf extract of *Melia azedarach* (Raman *et al.* 2012). Unavoidably, the particle sizes obtained from TEM, SEM-EDX and DLS analysis are slightly different due to the varying techniques used for measurement (Selva Sharma and Ilanchelian 2014). Further, the Au-Ag Nps exhibited a stable dispersion of particles evident from the zeta potential of -25.3 mV (leaf extract) and -28.4 mV (flower extract) (Appendixes 17 and 18 (B)). A zeta potential with

higher magnitude potentials (20 mV - 40 mV) and negatively charged particles indicates a stable system (Kotakadi *et al.* 2014; Selva Sharma and Ilanchelian 2014; Gengan *et al.* 2013).

4.2.5 FT-IR spectroscopy studies

FT-IR was used to identify potential biomolecules present in *O. basilicum* leaf and flower extracts, which are responsible for reducing, bio-capping and providing efficient stabilisation of Ag^{+} and Au^{3+} ions to Ag^{0} and Au^{0} (Tables 6 and 7).

The FT-IR spectra of the crude aq. extracts and bimetallic (Au-Ag) Nps derived from *O. basilicum* show a stretching frequency of 3300.21 to 3308.28 cm^{-1} for the leaf (Figure 12) and 3306.24 to 3307.96 cm^{-1} for the flower derived bimetallic (Au-Ag) Nps (Figure 14) suggesting an O-H vibration from the phenolic functional group and the possible bio-capping of silver and gold bimetallic Nps after reducing silver nitrate and chloroauric acid. Ether linkages peak at 1217 cm^{-1} (Silverstein *et al*. 2005). For the leaf derived bimetallic (Au-Ag) Nps, C-H and nitro stretch was demonstrated. Previous reports indicate the partial role of phenolic hydroxyls in the reduction mechanism by donating electrons and forming quinones that possesses a stronger ability to interact with Nps. Therefore, the secondary metabolites containing hydroxyl groups may act as capping agents and further facilitate the formation of stable metal Nps (Yallappa *et al.* 2015). Furthermore a shift from 1634.78 to 1636.25 cm^{-1} (leaf extract) and 1635.34 to 1635.32 cm^{-1} (flower extract) in the bimetallic Nps, shows a carbonyl (C=O) stretch, which may be assigned to the amide I bond or proteins which arise due to the carbonyl stretch (Silverstein *et al*. 2005), suggesting that the proteins are interacting with the bio-synthesised Nps and that their secondary structure was not affected during the reaction with Ag^{+} and Au^{3+} ions or after binding with silver and gold Nps.

Previous reports have shown the IR spectrum for pure AgNps synthesised from the aq. extract of *O. basilicum,* but the intensities and the wavelengths vary slightly to that of the crude extract (Sivaranjani and Meenakshisundaram 2013). Similarly, the IR spectra in the case of bimetallic (Au-Ag) Nps formed from the fruit juice of pomegranate show a large variation in intensity at 3420 cm^{-1} with an almost similar absorption band to that of the crude extract (Kumari *et al.* 2015). The chemical compounds identified with the present study (Table 2-3) together with previous phytochemical reports on *O. basilicum* leaf and flower extracts, suggest that polyphenols, flavonoids, terpenoids, carbohydrates (Usman *et al.* 2013), and additional biomolecules, secondary metabolites, proteins and lipids are present in the

plant leaf and flower parts, at different concentrations and may be responsible for the bio-reduction of Ag^{+} and Au^{3+} ions. Further studies are recommended to unravel the role of the biomolecules derived from *O. basilicum* leaf and flower extracts for a more detailed understanding of the bio-reduction phenomena. Scheme 1 illustrates a proposed reduction mechanism for synthesising stable bimetallic (Au-Ag) Nps from phenolic rich plants such as *O. basilicum* leaf and flower extracts. This is a proton transfer reaction whereby phenolic groups are converted to keto groups and metal salts are converted to zero (0) state metal Nps.

Table 6: FT-IR spectral data of *O. basilicum* leaf extract and bimetallic (Au-Ag) Nps

Wave number cm^{-1} aq. extract	Wave number cm^{-1} Au-Ag Nps	Bond	Functional group assignment	Group frequency cm^{-1}
3300.21	3308.28	O-H	Hydrogen bonded Alcohols, Phenols	3200-3600
-	2858	C-H	Alkanes	2850-2970
2132.31	2144.08	C≡C	Alkynes	2100-2260
1634.78	1636.25	C=C	Alkenes	1610-1680
1365.59	1369.3	NO_2	Nitro compounds	1300-1370
1217.15	1214.9	C-O	Alcohols, Ethers, Carboxylic acids, Esters	1050-1300

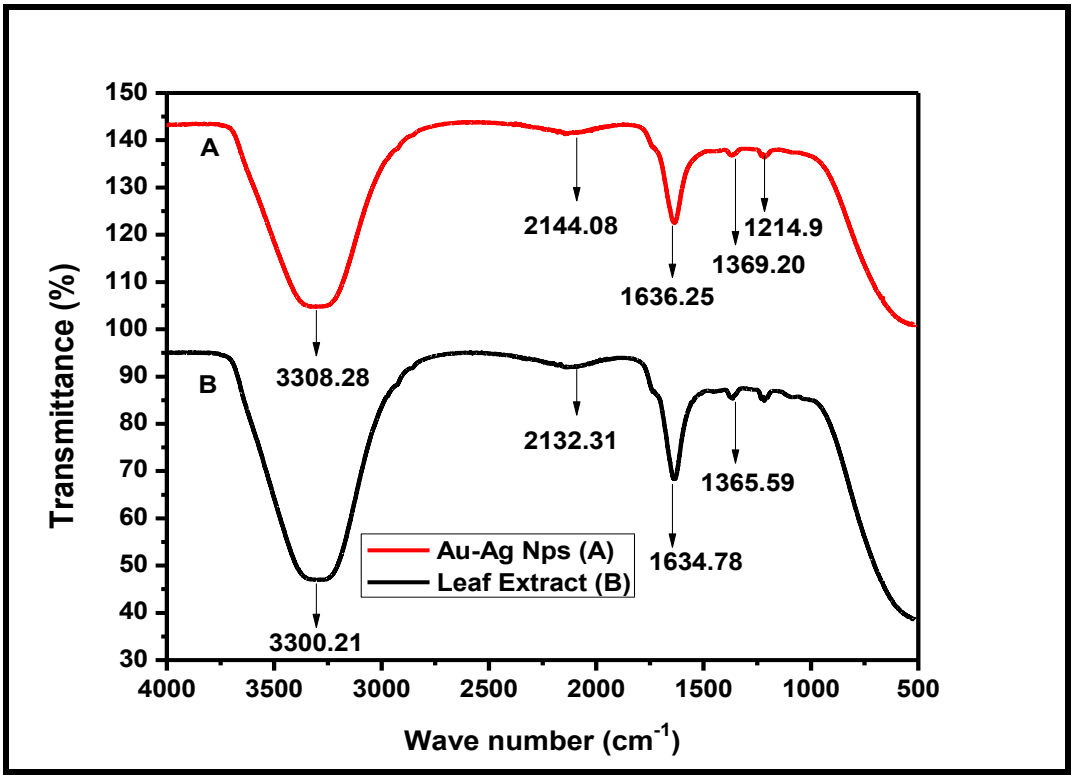

Figure 12: FT-IR spectra of (A) FT-IR Profile of bimetallic (Au-Ag) Nps synthesised using *O. basilicum* leaf extract and (B) *O. basilicum* aq. leaf extract

Table 7: FT-IR spectral data of *O. basilicum* flower extract and bimetallic (Au-Ag) Nps

Wave number cm^{-1} aq. extract	Wave number cm^{-1} Au-Ag Nps	Bond	Functional group assignment	Group frequency cm^{-1}
3306.24	3307.96	O-H	Hydrogen bonded Alcohols, Phenols	3200-3600
2133.75	2156.79	C≡C	Alkynes	2100-2260
1635.34	1635.32	C=C	Alkenes	1610-1680
1217.15	-	C-O	Alcohols, Ethers, Carboxylic acids, Esters	1050-1300

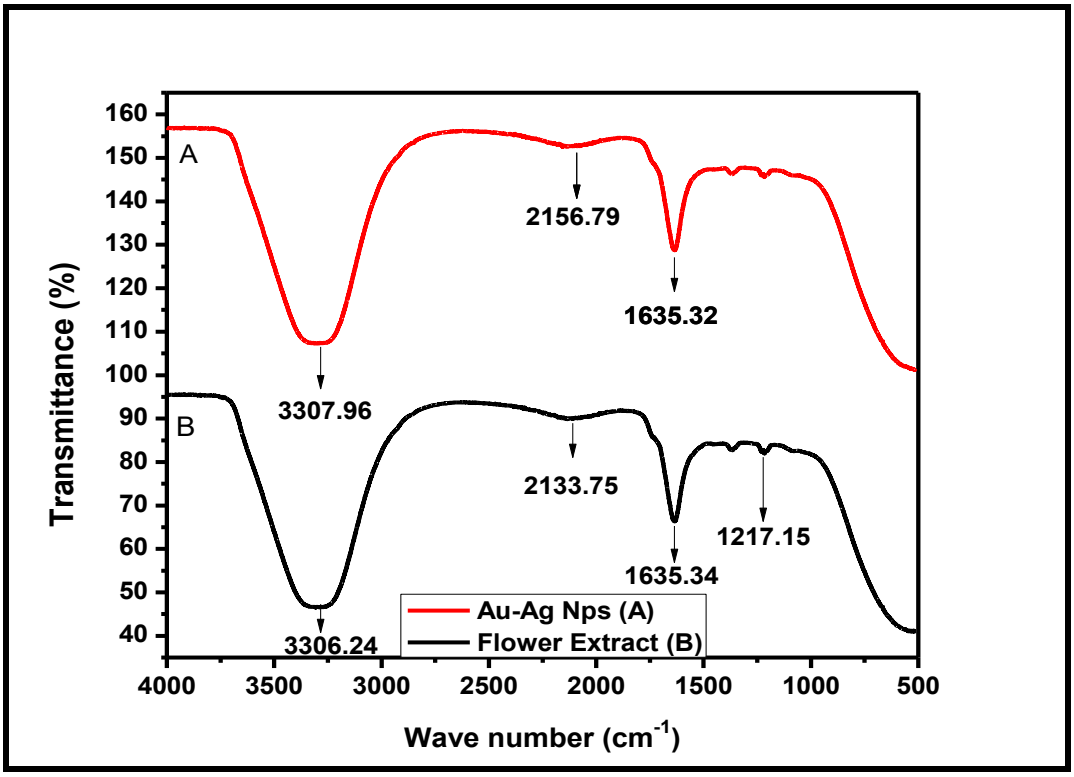

Figure 13: FT-IR spectra of (A) FT-IR Profile of bimetallic (Au-Ag) Nps synthesised using *O. basilicum* flower extract and (B) *O. basilicum* aq. flower extract

4.3 GC-MS analysis of *O. sanctum* leaf and flower aq. and EtOH extracts

The chemical composition of the leaf and flower aq. extracts of *O. basilicum* (L.) was described earlier, and the leaf and flower constituents of *O. sanctum* leaf and flower aq. extracts were identified after comparison with those available in the computer library (NIST) attached to the GC-MS instrument and reported in Appendixes 24 and 25.

The chemical compounds that were identified with *O. sanctum* leaf and flower extracts included: phenolics, terpenes (linalool, beta-terpeneol, phytol, squalene), terpenoids

(camphor), and various amine compounds as shown in Tables 8-10. The results showed variation in the main constituents present in the aq. and EtOH leaf extracts *O. sanctum*. Additionally, the EtOH extract produced more chemical constituents (Appendix 26).

Table 8: GC-MS reports of the chemical constituents present in *O. sanctum* aq. leaf extract

Peak no.	Compound	MF	MW (g/mol)	RT (min)	Area (%)
1	7,9-Di-tert-butyl-1-oxaspiro(4,5)deca-6,9-diene-2,8-dione	$C_{17}H_{24}O_3$	276	17.046	11.54
2	13-Docosenamide, Erucylamide	$C_{22}H_{43}NO$	337	25.259	88.46
	(13z)-N-([(13z)-13-Docosenoylamino]methyl)-13-docosenamide, Bis(cis-13-docosenamido)methane	$C_{45}H_{86}N_2O_2$	686	25.259	88.46
3	8-Methyl-6-nonenamide	$C_{10}H_{19}NO$	169	25.259	88.46
4	cis-11-Eicosenamide	$C_{20}H_{39}NO$	309	25.259	88.46

Key: MF = Molecular Formula; MW = Molecular Weight; RT = Retention time

Table 9: GC-MS report of the chemical constituents present in *O. sanctum* EtOH leaf extract

Peak no.	Compound Name	MF	MW (g/mol)	RT (min)	Area (%)
1	Linalool, 1,6-Octadien-3-ol, Linalyl alcohol, 2,6-Dimethyl-2,7-Ooctadien-6-ol, Cyclohexanol, cis-beta-Terpineol, 1-methyl-4-(1-methylethenyl)-, Bicyclo[3.1.0]hexan-2-ol, 5-Isopropyl-2-methylbicyclo[3.1.0]hexan-2-ol-	$C_{10}H_{18}O$	154	6.865	10.30
2	3,7-Dimethyl-1,6-nonadien-3-ol	$C_{11}H_{20}O$	168	6.865	10.30
3	Camphor, Cyclohexanone, Dihydrocarvone	$C_{10}H_{16}O$	152	7.684	3.80
4	Spirobicyclo[2.2.1]heptane-2,2'-(1',3'-dioxa-2'-oxocyclohex-5'-ene)]	$C_{14}H_{20}O_3$	236	7.684	3.80
5	Phytol acetate	$C_{22}H_{42}O_2$	338	16.247	7.79
6	3,7,11,15-Tetramethyl-2-hexadecen-1-ol	$C_{20}H_{40}O$	296	16.247	7.79
7	1,1'-Bicyclopentyl, 2-hexadecyl-, 1-Cyclopentyl-2-n-hexadecylcyclopentane	$C_{26}H_{50}$	362	16.247	7.79
8	Oxirane, 1,2-Epoxyoctadecane, cis-9-Octadecen-1-ol	$C_{18}H_{36}O$	268	16.247	7.79
9	Phytol	$C_{20}H_{40}O$	296	19.000	9.61
10	5-methyl-2-(1-methylethyl), 4-Isopropyl-1-methylcyclohexanol	$C_{10}H_{20}O$	156	19.000	9.61
11	Palmitaldehyde	$C_{26}H_{54}O_2$	398	19.000	9.61
12	Hexatriacontane	$C_{36}H_{74}$	506	24.309	24.63
13	Tetratetracontane	$C_{44}H_{90}$	618	24.309	24.63
14	Eicosane	$C_{20}H_{42}$	282	24.309	24.63
15	Tetracontane	$C_{40}H_{82}$	562	24.309	24.63
16	n-Tetratriacontane	$C_{34}H_{70}$	478	24.309	24.63

17	Squalene, 2,6,10,14,18,22-Tetracosahexaene, Supraene	$C_{30}H_{50}$	410	25.675	27.18
18	2,6,10,14,18-Pentamethyl-2,6,10,14,18-eicosapentaene	$C_{25}H_{42}$	342	25.675	27.18
19	3,7,11,15-Tetramethyl-2,6,10,14-hexadecatetraen-1-ol, trans-Geranylgeraniol	$C_{20}H_{34}O$	290	25.675	27.18
20	2-methyloctacosane	$C_{29}H_{60}$	408	30.709	7.00

Key: MF = Molecular Formula; MW = Molecular Weight; RT = Retention time

Table 10: GC-MS report of the chemical constituents present in *O. sanctum* aq. flower extract

Peak no.	Compound Name	MF	MW (g/mol)	RT (min)	Area (%)
1	Hexanedioic acid, bis(2-ethylhexyl) ester, Diisooctyl adipate, Octyl adipate	$C_{22}H_{42}O_4$	370	21.416	100
2	Adipic acid, 2-ethylhexyl pentadecyl ester	$C_{29}H_{56}O_4$	468	21.416	100
3	Adipic acid, 2-ethylhexyl tetradecyl ester	$C_{28}H_{54}O_4$	454	21.416	100

Key: MF = Molecular Formula; MW = Molecular Weight; RT = Retention time

4.4 Characterisation tests of the AgNps synthesised from *O. basilicum*, and *O. sanctum* singly and in combination

4.4.1 UV-Visible studies

The synthesis of AgNps with the various leaf extracts was successful, and confirmed by the fact that the nanometallic silver exhibited a well-defined absorption peak at 438 nm from *O. basilicum* extract, 439 nm for *O. sanctum* extract, and 433 nm from the combination extract. The consequent colour changes were observed from a light yellow to a brown colour as shown in Figures 14-16 and the absorption spectra of the AgNps are indicated in Figures 17-19. Due to excitation of the SPR, a strong absorption of electro-magnetic waves are exhibited by metal Nps in the visible range. In addition, there was an increase in intensity (12, 24, and 36 hour period) as a function of time (Tables 11-13) and a slight shift in the peak wavelength (Appendix 11). The SPR at 438 nm, 439 nm and 433 nm was broad indicating the concentration of different groups and molecules responsible for bio-capping and stabilising of Nps in the reduction process.

The interaction of Nps with biomolecules of *O. basilicum* leaf extract, *O. sanctum* leaf extract and the combination of these leaf extracts validated the reduction of Ag^+ ions to Ag^0 by the secondary plant metabolites that are in turn oxidised to other species. Even though the mechanism has not been adequately elucidated, it is components such as polyols, amines, phenolics, flavonoids and water-soluble heterocyclic compounds as well as other components

such as reducing sugars, proteins and other oxido-reductively labile metabolites present in the *O. basilicum* and *O. sanctum* leaf extracts that possess the ability to reduce Ag^{+} ions to Ag^{0}. Similar UV-Vis spectrum results have been ascertained in the case of the stabilising effect of other natural biological extracts in the formation of AgNps (Raman *et al.* 2012; Rao *et al.* 2013; Kotakadi *et al.* 2014).

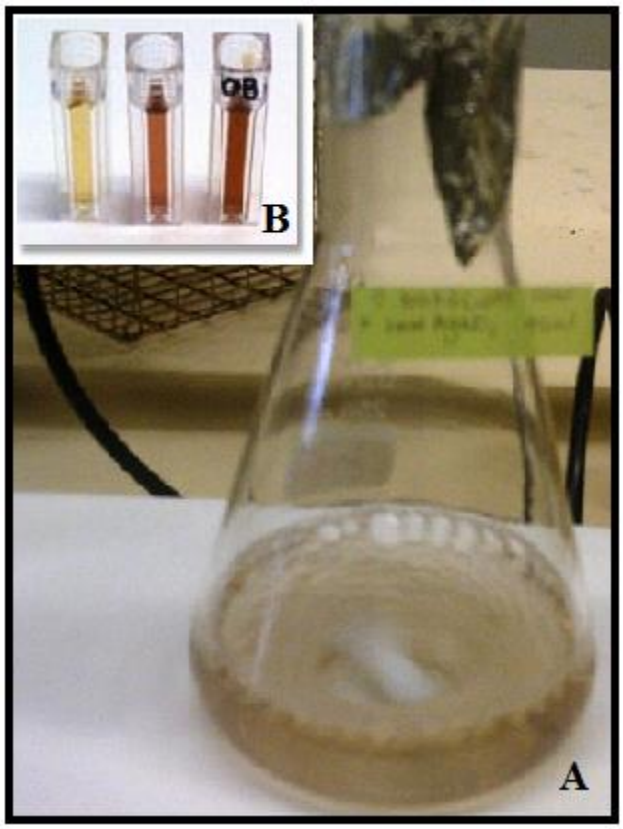

Figure 14: Progressive colour change indicating the formation of AgNps over a 36 hour period (A) *O. basilicum* extract with $AgNO_3$ aq. solution (B) from L→R AgNps formation over 12→24→36 hours

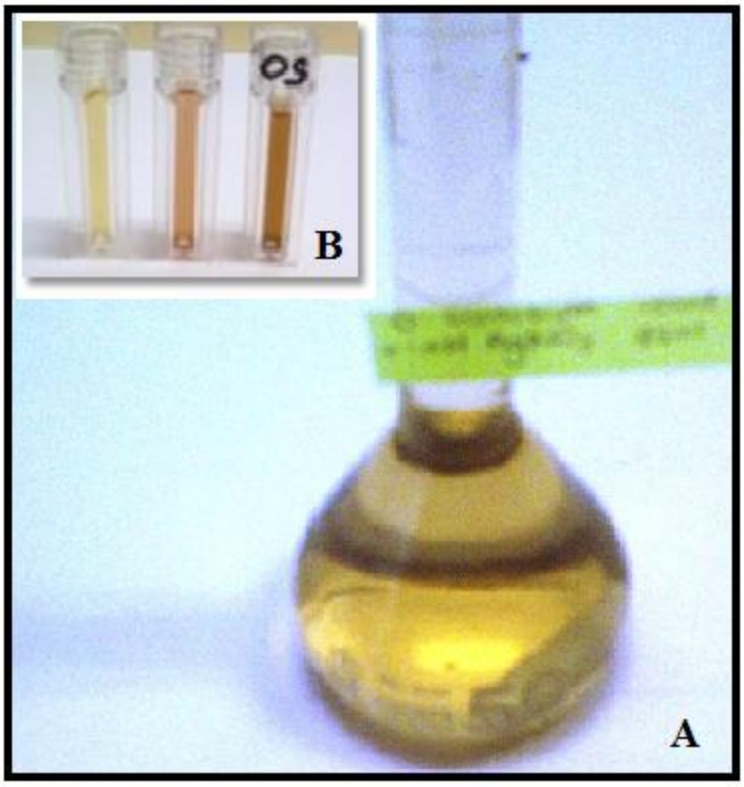

Figure 15: Progressive colour change indicating the formation of AgNps over a 36 hour period (A) *O. sanctum* extract with $AgNO_3$ aq. solution (B) from L→R AgNps formation over 12→24→36 hours

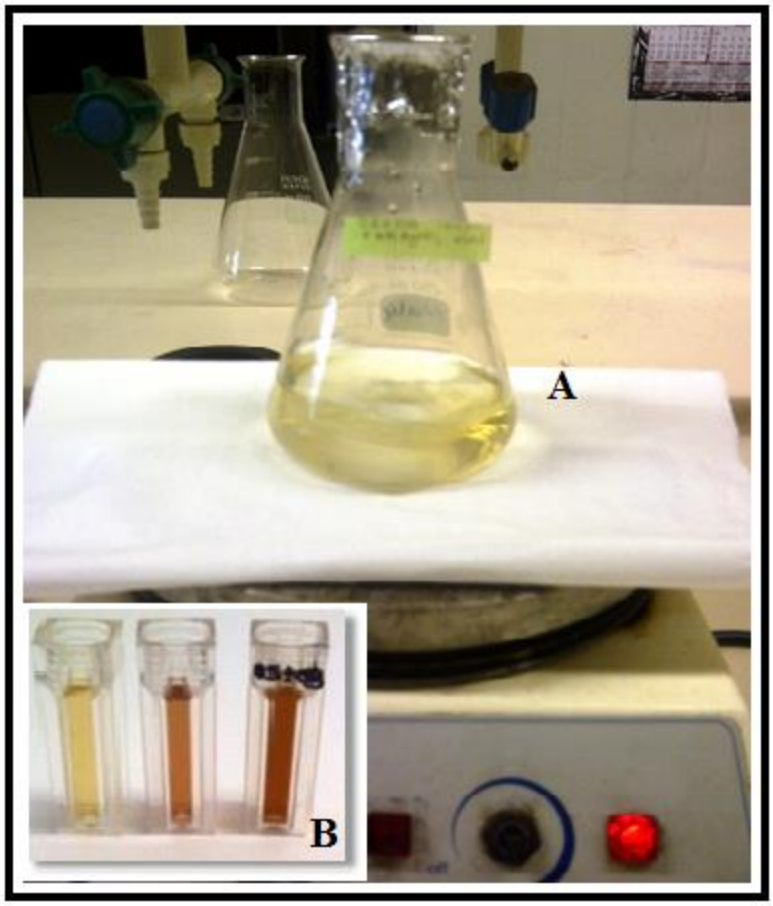

Figure 16: Progressive colour change indicating the formation of AgNps over a 36 hour period (A) *O. sanctum* + *O. basilicum* extract with $AgNO_3$ aq. solution (B) from L→R AgNps formation over 12→24→36 hours

Table 11: Peak wavelength and absorbance at different timed intervals for AgNps synthesised using aq. *O. basilicum* leaf extract

Intervals	Peak wavelength (300-700 nm)	Absorbance
Day 1: after 12 hours	436.0	1.050
Day 2 after 24 hours	436.0	1.498
Day 3 after 36 hours	438.0	1.736

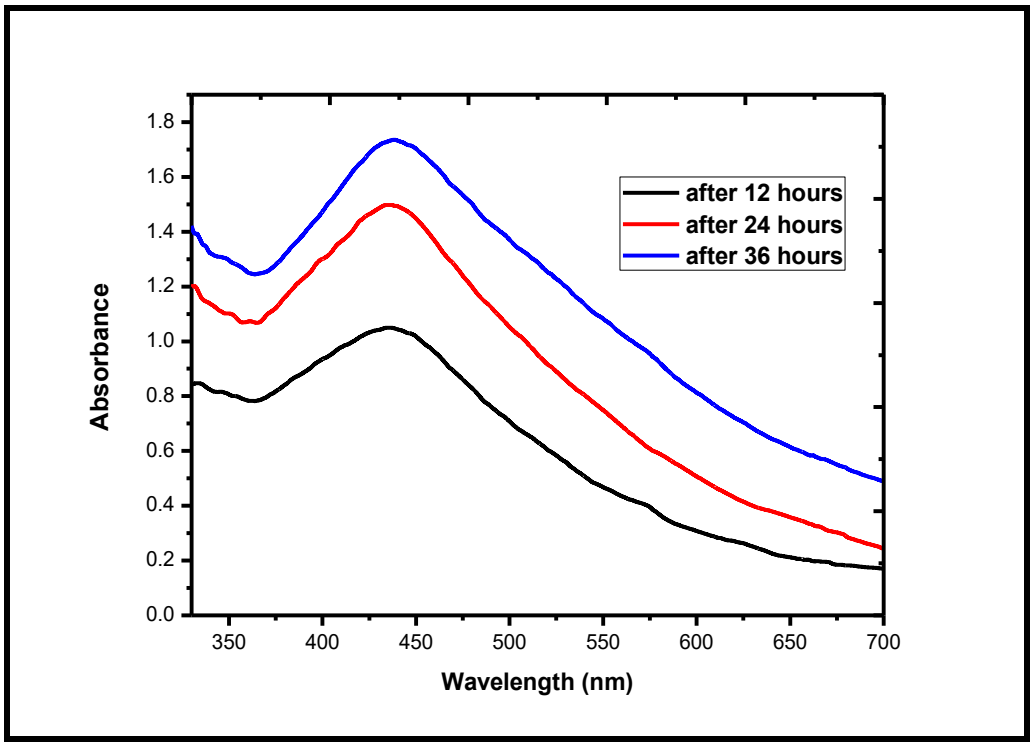

Figure 17: UV-Visible absorption spectra of AgNps synthesised using aq. *O. basilicum* leaf extract

Table 12: Peak wavelength and absorbance at different timed intervals for AgNps synthesised using aq. *O. sanctum* leaf extract

Intervals	Peak wavelength (300-700 nm)	Absorbance
Day 1: after 12 hours	444.0	0.797
Day 2 after 24 hours	444.0	0.955
Day 3 after 36 hours	439.0	1.034

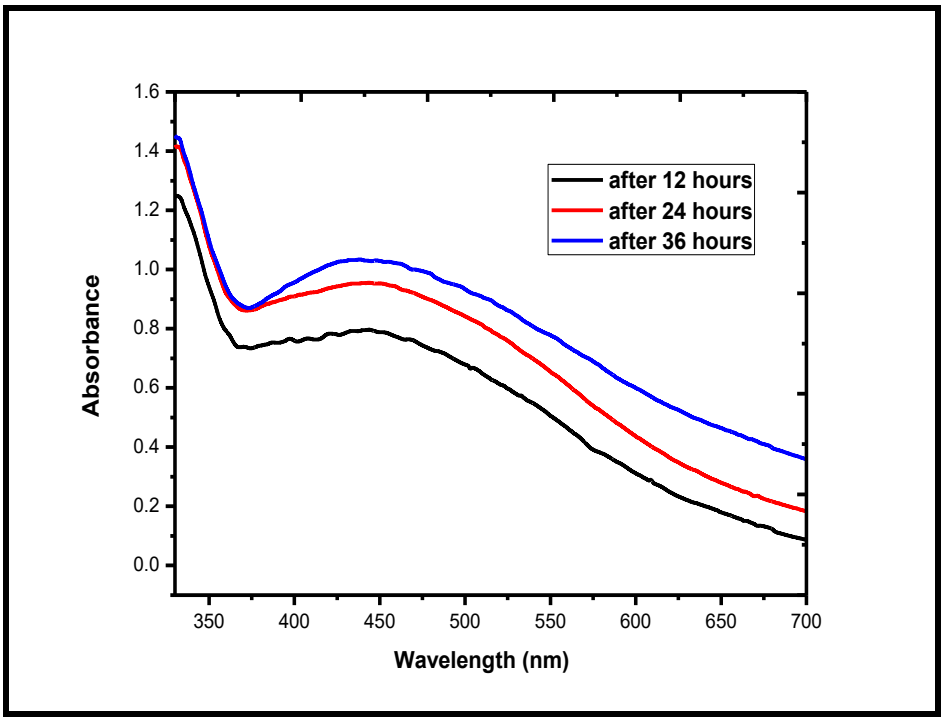

Figure 18: UV-Visible absorption spectra of AgNps synthesised using aq. *O. sanctum* leaf extract

Table 13: Peak wavelength and absorbance at different timed intervals for AgNps synthesised using aq. *O. sanctum* in combination with *O. basilicum* leaf extracts

Intervals	Peak wavelength (300-650 nm)	Absorbance
Day 1: after 12 hours	433.0	1.643
Day 2 after 24 hours	425.0	1.576
Day 2 after 28 hours	424.0	1.635
Day 3 after 36 hours	433.0	1.847

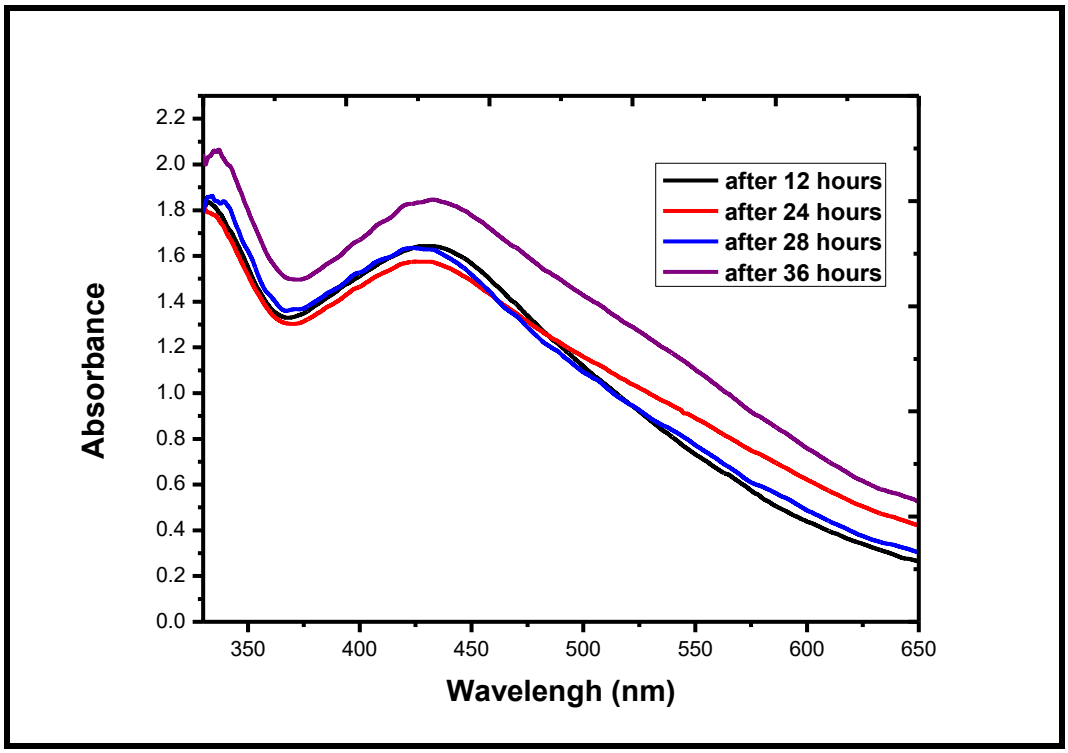

Figure 19: UV-Visible absorption spectrum of AgNps synthesised using aq. *O. sanctum* in combination with *O. basilicum* leaf extracts

4.4.2 TEM analysis

The results obtained from the TEM monograph indicated the size and shape properties of the AgNps derived from *O. sanctum*, and *O. basilicum* singly and in combination. Representative TEM images (see Appendix 14-16 (A)) indicated that the particles were predominantly spherically shaped and monodispersed. The particles exhibited a distribution of mean sizes ± SD, at a size of 17.0 ± 8.94 nm for *O. basilicum* AgNps, 15.0 ± 12.34 nm for *O. sanctum* AgNps and 17.0 ± 8.44 nm for the combination *O. sanctum* + *O. basilicum* AgNps. This observation is in agreement with the UV-Vis spectrum obtained showing variation in plasmon bands (Figure 17-19) (Huang and El-Sayed 2010). These results show that it is possible to prepare stable AgNps of size less than 17 nm by varying the ratio of $AgNO_3$, *O. sanctum*, *O. basilicum* and by using a combination of extract solutions.

4.4.3 SEM-EDX analysis

The elemental composition of powdered samples (AgNps synthesised from *O. sanctum* and *O. basilicum* singly and in combination) was determined using SEM equipped with an EDX

detector. Typical SEM images of the AgNps synthesised using 10% *O. sanctum* and *O. basilicum* singly and in combination of leaf extracts with 1 mM $AgNO_3$ at different magnification scales were obtained. The fabricated silver elements and nanosize were confirmed by SEM-EDX pattern shown in Figure 20-22 (A-B). The particle dimensions of AgNps show spherical morphology with a size range of 100 nm. The EDX pattern revealed the signals in the silver region at five different spectrums and confirmed the formation of AgNps. Spectral signals for O were observed which indicated that the extracellular organic moieties from the individual *Ocimum* sp. of leaf extract were adsorbed onto the surface or in the vicinity of the metal Nps or may have originated from the biomolecules that were bound to the surface of the AgNps. However, certain elements may have come from the artefacts formed during sample preparation. Peaks of C originate from the grid used and the peaks of S, P and N correspond to the protein capping over the AgNps.

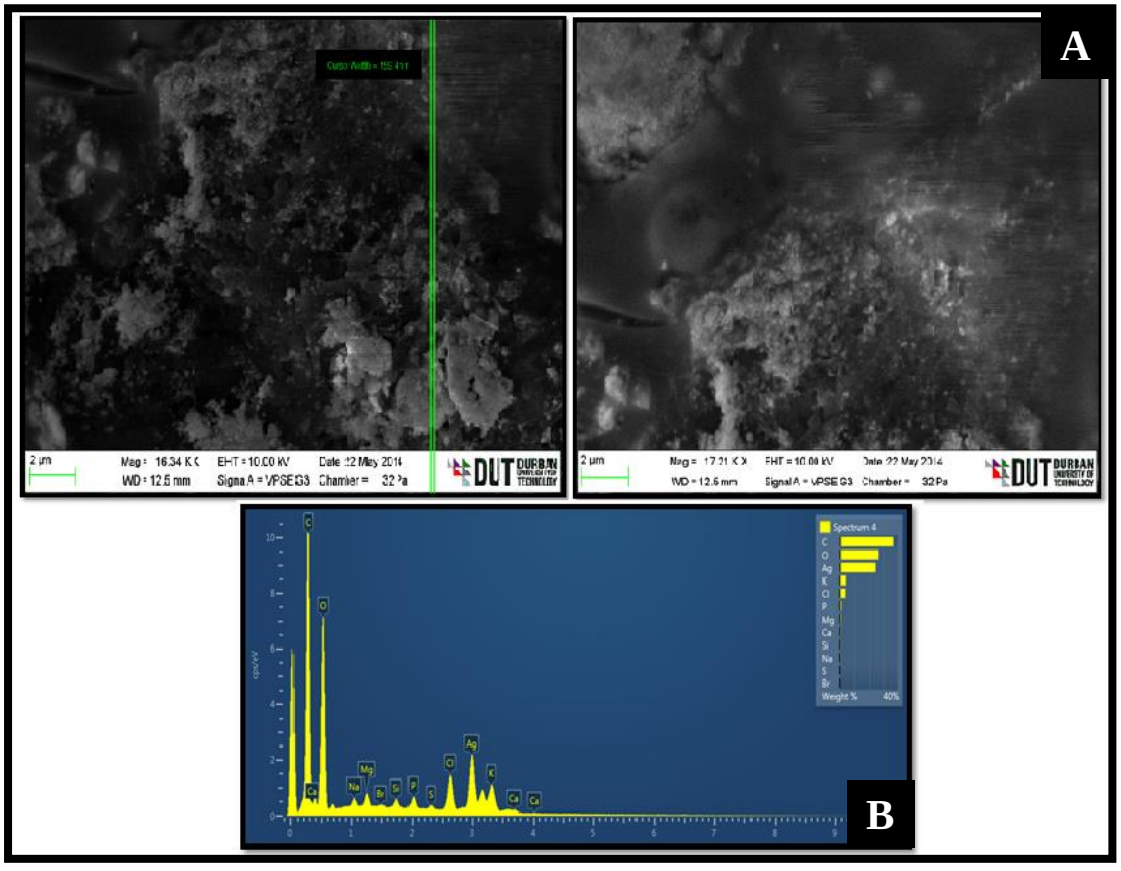

Figure 20: (A) SEM with EDX image of AgNps synthesised using *O. basilicum* leaf extract and (B) EDX show the presence of the elements on the surface of the AgNps

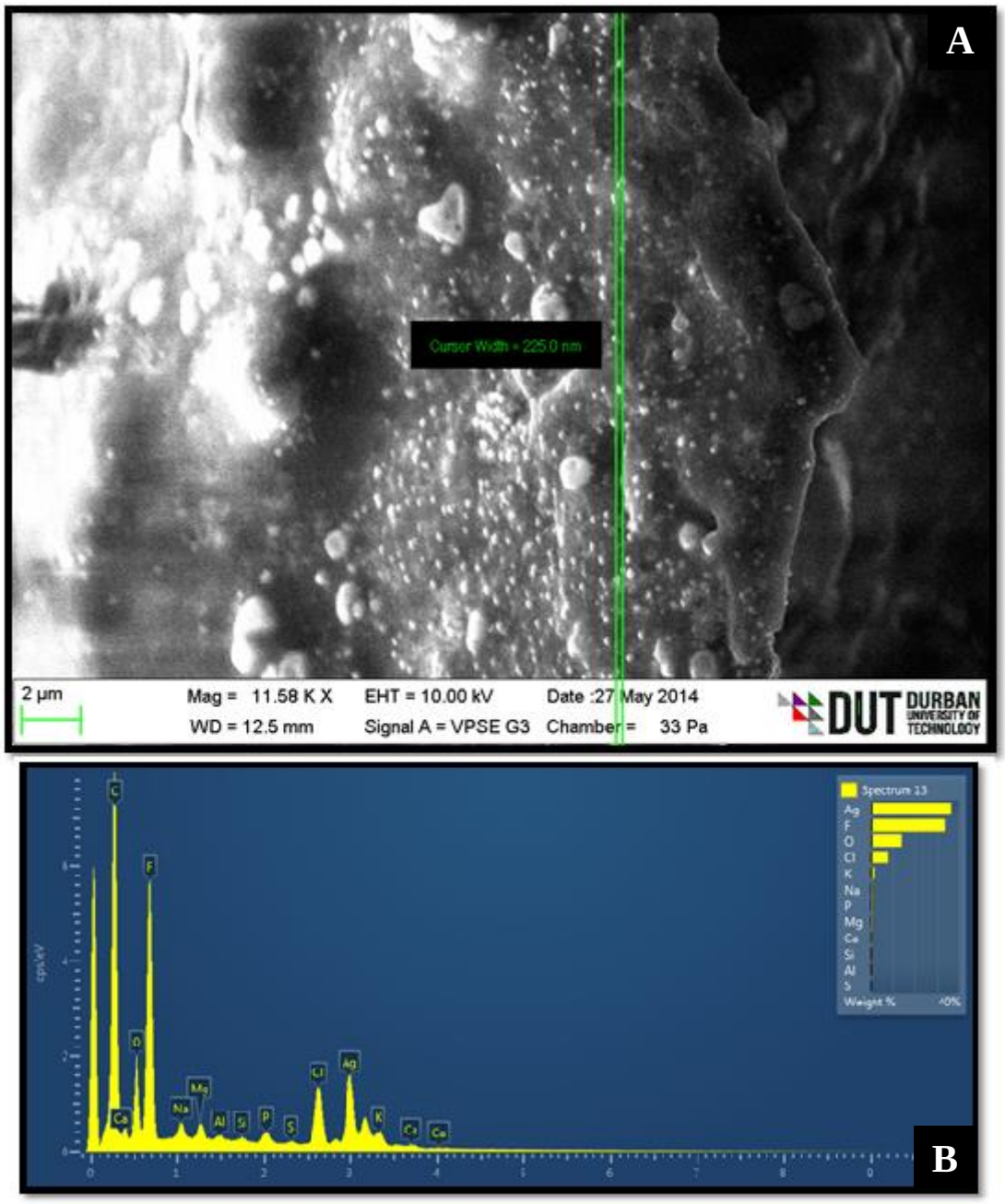

Figure 21: (A) SEM with EDX image of AgNps synthesised using *O. sanctum* leaf extract and (B) EDX show the presence of the elements on the surface of the AgNps

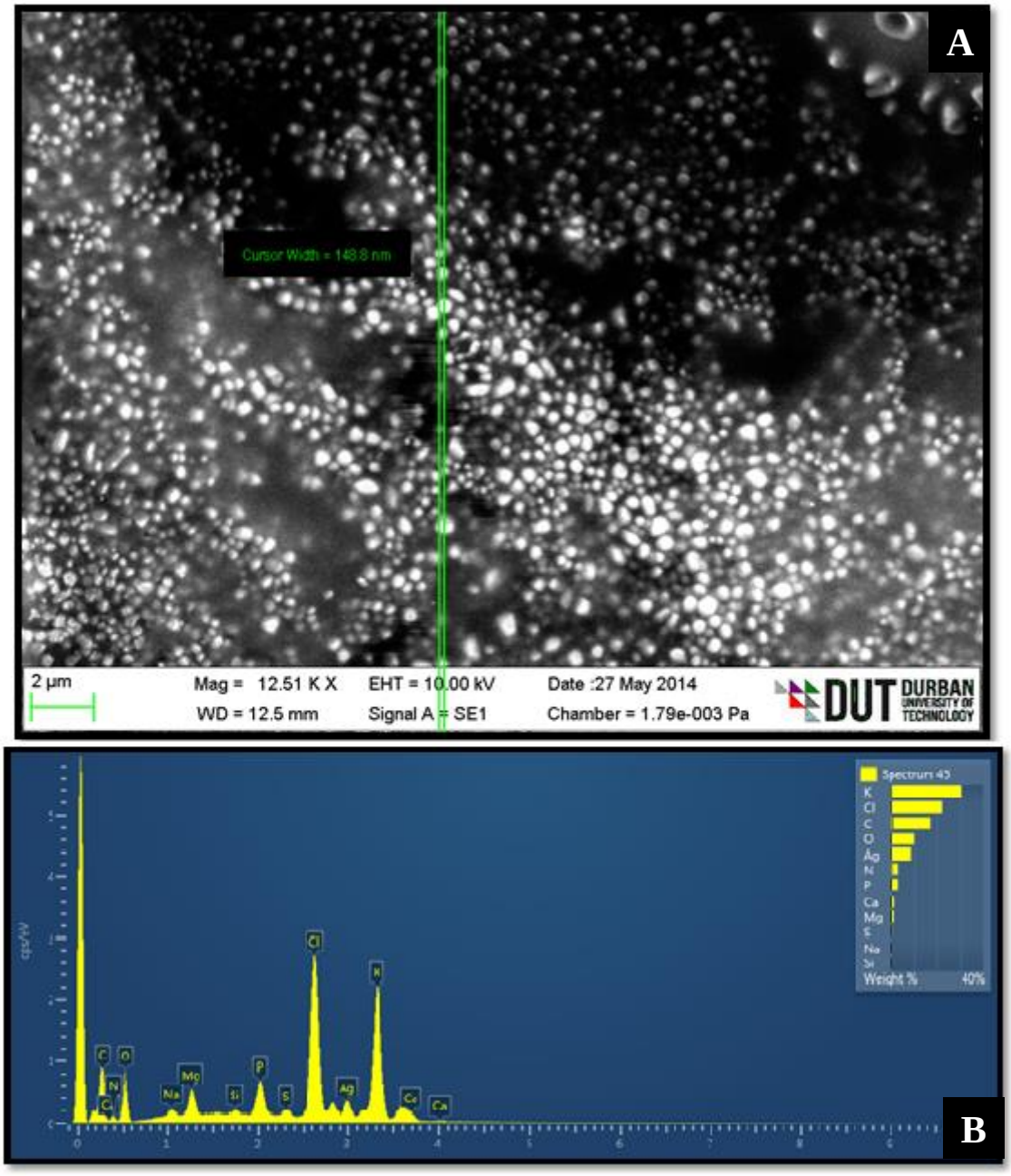

Figure 22: (A) SEM with EDX image of AgNps synthesised using *O. sanctum* + *O. basilicum* leaf extract and (B) EDX show the presence of the elements on the surface of the AgNps

4.4.4 DLS and Zeta Potential

Dynamic light scattering measurement showed the average colloidal size distribution of *O. basilicum* leaf AgNps with maximum intensity at 56.81 nm (Appendix 19 (A)). Zeta potential of *O. basilicum* leaf AgNps was stable at -19.8 mV. Dynamic light scattering measurement showed the average colloidal size distribution of *O. sanctum* leaf AgNps with maximum intensity at 467.4 nm and zeta potential analysis showed stability at -23.3 mV (Appendix 20

(A)). Dynamic light scattering measurement showed the average colloidal size distribution of the combination of *O. basilicum* leaf AgNps and *O. sanctum* leaf AgNps with maximum intensity at 155.1 nm and zeta potential analysis showed stability at -24.3 mV (Appendix 21 (A)).

The *O. basilicum* leaf extract derived AgNps shows a slightly lower magnitude. The slight decrement in the zeta potential value is ascribed to the surface charge that is due to the electrostatic interaction between phytochemicals and the negatively charged AgNps. Unavoidably, the particle size obtained from TEM, SEM-EDX and DLS analysis is different due to the varying techniques used for measurement (Selva Sharma and Ilanchelian 2014); similar observations were reported for AgNps prepared from *Melia azedarach* (Raman *et al.* 2012). However, a stable size dispersion of particles was evident from the zeta potential (Appendix 19-21 (B)); a zeta potential with higher magnitude potentials (20-40 mV) with negative charge indicates a stable system (Kotakadi *et al.* 2014; Selva Sharma and Ilanchelian 2014; Gengan *et al.* 2013).

4.4.5 FT-IR spectroscopy studies

FT-IR was used to identify any potential biomolecules present in the leaf extracts (*O. sanctum* and *O. basilicum*) which are responsible for reducing Ag^+ ions to Ag^0 (Table 14-16). FT-IR spectra (Figure 23) of the crude aq. extract and AgNps derived from *O. basilicum* showed a decrease in stretching frequency of 3300.21 cm^{-1} to 3297.12 cm^{-1} suggesting an OH functional group. Furthermore a shift from 1634.78 cm^{-1} to 1635.67 cm^{-1} is assigned to the carbonyl C=O stretch, whereas peaks at 1217 cm^{-1} can be attributed to ether linkages (Silverstein *et al*. 2005). Results for *O. sanctum* were similar to those obtained from *O. basilicum* except for a C=O bond which was identified (Figure 24). For the AgNps synthesised from the combination of extracts, the dual properties of *O. basilicum* and *O. sanctum* in combination were evident with the addition of C-H stretch (Figure 25). It is thus speculated that the conversion of C-OH biomolecules to C=O group may be responsible for the reduction of Ag^+ to Ag^0 (Ahmad *et al*. 2010). The absorption peaks at 1635.48 cm^{-1} to 1635.82 cm^{-1} for AgNps (*O. sanctum*) may be assigned to the amide I bond or proteins arising due to carbonyl stretch, suggesting that the proteins are interacting with bio-synthesised Nps and that their secondary structure was not affected during reaction to Ag^+ ions or after binding with AgNps. These IR spectroscopic studies confirmed that the carbonyl group of amino acid residues have strong binding ability with metal, therefore acting as a capping

agent surrounding the metal Np to prevent agglomeration and provide stability to the medium. Kumari *et al.* (2015) state that in the range 3250-3400 cm^{-1}, that is, the amide region, binding as well as stabilisation takes place via free amide groups present in proteinaceous substances used for synthesis. Supported by GC-MS results, N-H amide compounds were identified in the *O. sanctum* leaf extract (Appendix 26, (B)); these results confirm the presence of possible proteins acting as reducing and stabilising agents namely: Cis-11-Eicosenamide, 8-Methyl-6-nonenamide, 13-Docosenamide, (13z)-N-([(13z)-13-Docosenoylamino]methyl)-13-docosenamide. Thus, a mechanism for the biosynthesis of AgNps can be elucidated using amide compounds derived from *O. sanctum* extracts which acts as a natural reducing agent (Scheme 2).

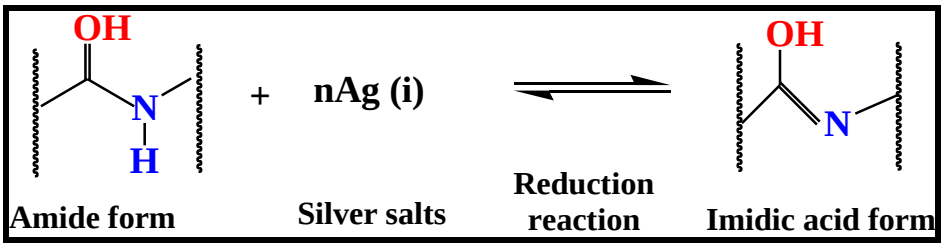

Scheme 2: Possible mechanism for biosynthesis of AgNps using amide compounds derived from *O. sanctum* extracts

Peaks at 3100-3300 cm^{-1} are assigned to O-H stretching in alcoholic and phenolic compounds; these results are similar to previous reports (Singhal *et al.* 2011). Previous reports indicate peaks of *Ocimum* sp. be more characteristic of eugenol, linalool and terpenes that are abundant in these plant extracts (Ramteke *et al.* 2013). Depending on the above observation, it can be assumed that the stabilisation and formation of AgNps is achieved by the phenolic as well as aromatic compounds present in the *O. sanctum* and *O. basilicum* leaf extracts (Scheme 1).

Table 14: FT-IR spectral data of *O. basilicum* leaf extract and AgNps

Wave number cm^{-1} aq. extract	Wave number cm^{-1} AgNps	Bond	Functional group assignment	Group frequency cm^{-1}
3300.21	3297.12	O-H	Hydrogen bonded Alcohols, Phenols	3200-3600
2132.31	2148.20	C≡C	Alkynes	2100-2260
1634.78	1635.67	C=C	Alkenes	1610-1680
1365.59	-	NO_2	Nitro compounds	1300-1370
1217.15	-	C-O	Alcohols, Ethers, Carboxylic	1050-1300

acids, Esters

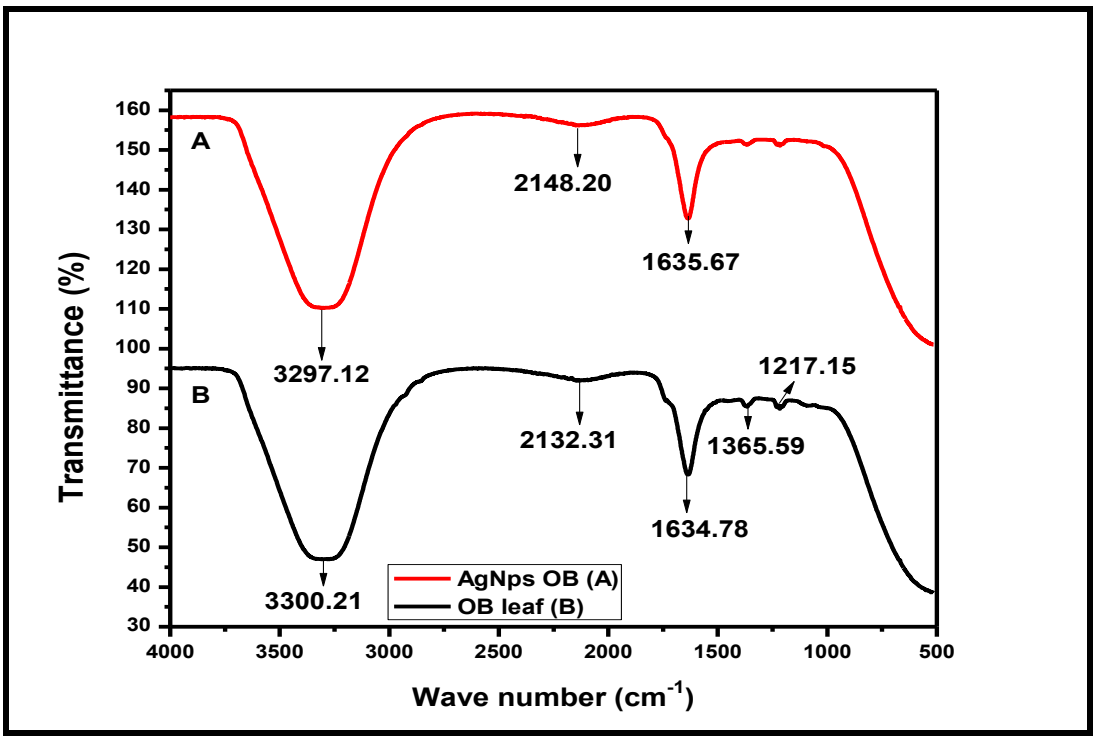

Figure 23: FT-IR spectra of (A) FT-IR Profile of AgNps synthesised using *O. basilicum* leaf extract and (B) aq. *O. basilicum* leaf extract

Table 15: FT-IR spectral data of *O. sanctum* leaf extract and AgNps

Wave number cm^{-1} aq. extract	Wave number cm^{-1} AgNps	Bond	Functional group assignment	Group frequency cm^{-1}
3307.49	3309.60	O-H	Hydrogen bonded Alcohols, Phenols	3200-3600
-	2134.59	C≡C	Alkynes	2100-2260
1635.48	1635.82	C=C	Alkenes	1610-1680
-	1740.8	C=O	Aldehydes, Ketones, Carboxylic acids, Esters	1690-1760
-	1371.9	C-H	Alkanes	1340-1470
-	1217.5	C-O	Alcohols, Ethers, Carboxylic acids, Esters	1050-1300

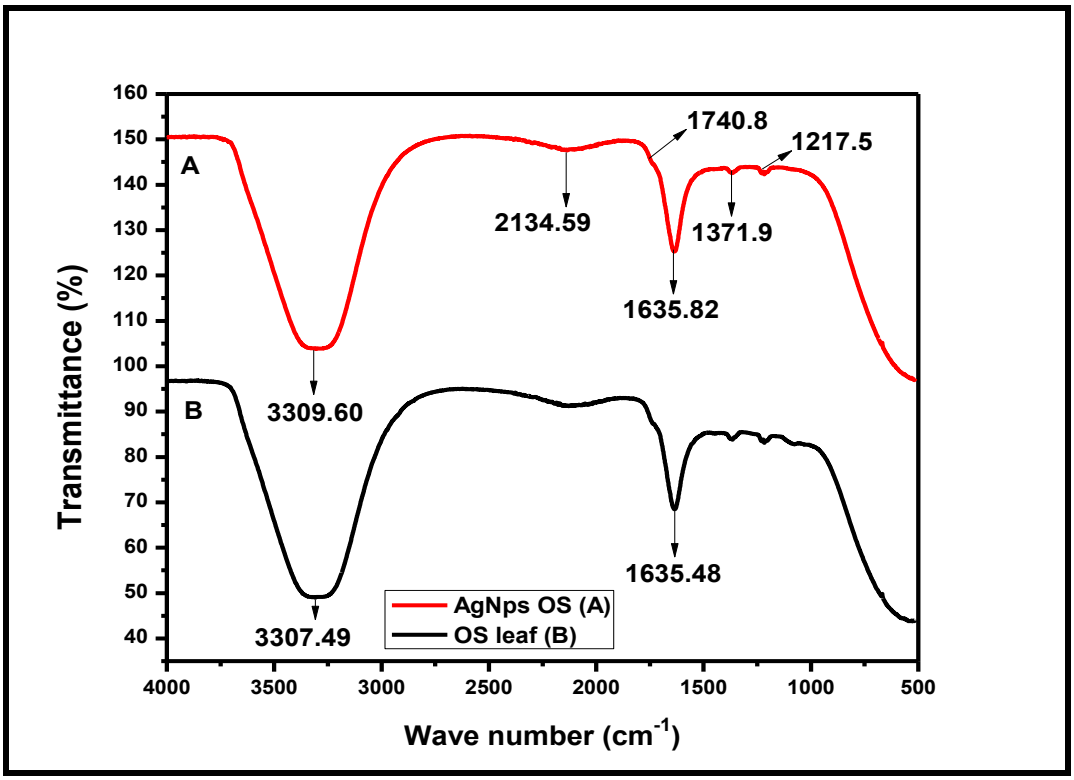

Figure 24: FT-IR spectra of (A) FT-IR Profile of AgNps synthesised using *O. sanctum* leaf extract and (B) aq. *O. sanctum* leaf extract

Table 16: FT-IR spectral data of *O. sanctum* + *O. basilicum* leaf extract and AgNps

Wave number cm^{-1} *O. basilicum* aq. extract	Wave number cm^{-1} *O. sanctum* aq. extract	Wave number cm^{-1} AgNps	Bond	Functional group assignment	Group frequency cm^{-1}
3300.21	3307.49	3307.03	O-H	Hydrogen bonded Alcohols, Phenols	3200-3600
2132.31	-	2134.64	C≡C	Alkynes	2100-2260
1634.78	1635.48	1636.29	C=C	Alkenes	1610-1680
-	-	1738.2	C=O	Aldehydes, Ketones, Carboxylic acids, Esters	1690-1760
1365.59	-	1366.6	C-H	Alkanes	1340-1470
1217.15	-	1214.9	C-O	Alcohols, Ethers, Carboxylic acids, Esters	1050-1300

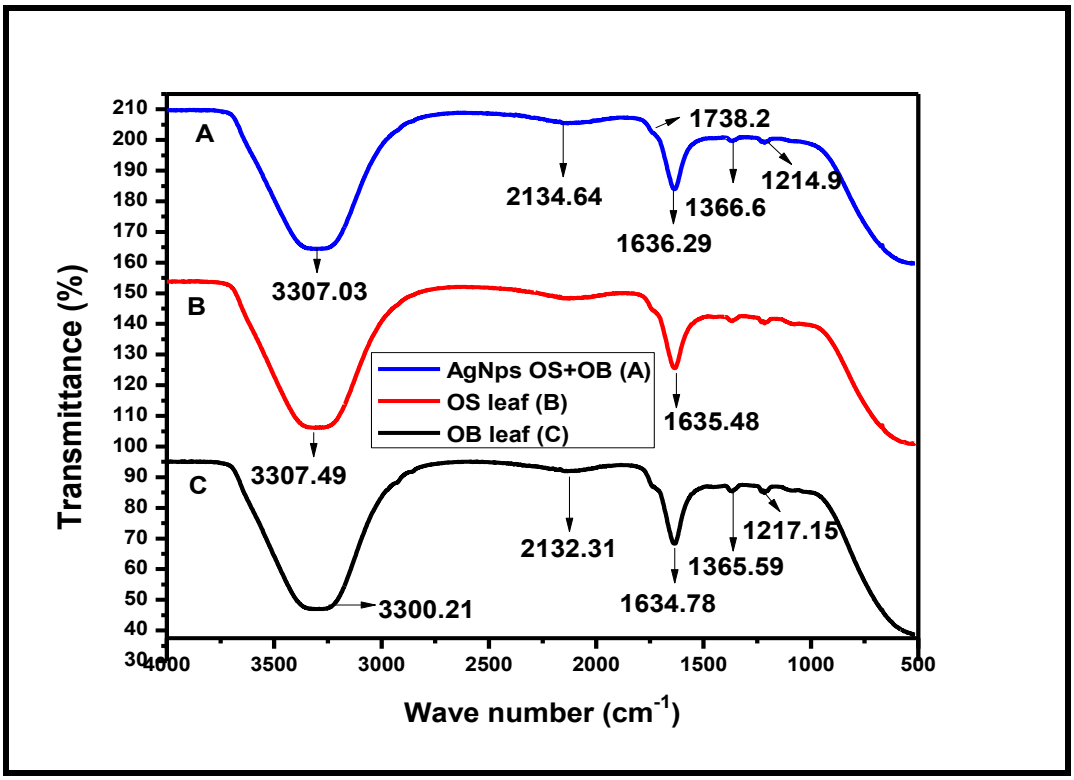

Figure 25: FT-IR spectra of (A) FT-IR Profile of AgNps synthesised using combination *O. sanctum* + *O. basilicum* leaf extract (B) aq. *O. sanctum* leaf extract and (C) aq. *O. basilicum* leaf extract

4.5 *In vitro* antibacterial sensitivity screening

The antibacterial activity of the crude *O. sanctum* and *O. basilicum* leaf and flower aq. extracts (Method 3.4.1.2), bimetallic (Au-Ag) Nps synthesised from *O. basilicum* leaf and flower aq. extracts and AgNps synthesised from a combination of *O. sanctum*, *O. basilicum* leaf aq. extracts (Method 3.4.4-3.4.5) were tested by the agar diffusion method against the following bacterial species: *B. subtilis, E. coli, P. aeruginosa, Salmonella* sp. and *S. aureus.* The radial growth of the colony upon completion of incubation was recorded and the zones of inhibition were measured in mm at 30 µl of sample. The test statistic represents the mean inhibition ± SEM and p-values less than 0.05 were considered statistically significant.

4.5.1 Antibacterial activity of bimetallic (Au-Ag) Nps

Table 17 and Tables 18-20 (significant differences highlighted in turquoise) outline the antibacterial effect of bimetallic Nps vs $AgNO_3$, antibiotics and the water control on *B. subtilis, E. coli, P. aeruginosa, Salmonella* sp. and *S. aureus.*

The antibacterial activity of the bimetallic (Au-Ag) Nps synthesised from *O. basilicum* leaf extracts were displayed against *B. subtilis*, p-value 0.014 (see Appendix 27 (A-B)).

Appendix 28 illustrates the highest significant antibacterial activity against *P. aeruginosa* (5.167 mm ± 0.167 mm) using bimetallic Nps synthesised from *O. basilicum* leaf extract, p-value 0.025 vs gentamycin see Table 18, page 88. The only and lowest inhibition was observed against *P. aeruginosa* using bimetallic Nps synthesised from the flower extract at 1.667 mm ± 0.211 mm, p-value 0.023 compared to the positive control (gentamycin).

The bimetallic Nps synthesised from the *O. basilicum* leaf extracts showed significant antibacterial activity against *E. coli* (3.333 mm ± 0.211 mm) (Appendix 29). Table 19 indicates the test statistic of the samples compared to the negative and positive controls, a significant p-value 0.014 was obtained for the bimetallic Nps compared to the positive control gentamycin (10.000 mm ± 0.000 mm).

On the other hand, bimetallic (Au-Ag) Nps synthesised from the leaf and flower extract presented no activity against *Salmonella* species. In addition, the crude *O. basilicum* leaf and flower aq. extracts exhibited no inhibitory activity against the test strains.

The antibacterial activity of the bimetallic (Au-Ag) Nps against *S. aureus* was tested for two grouping variables, at 100 µl and 200 µl bacteria per plate, respectively. The bimetallic Nps derived from the *O. basilicum* leaf extract showed inhibition against *S. aureus* at 100 µl of bacteria per plate (6.167 mm ± 0.601 mm), p-value 0.238 (Table 20) and whereas significant inhibition of bimetallic Nps derived from the flower extracts (3.500 mm ± 0.719 mm), p-value 0.026 compared to vancomycin (7.000 mm ± 0.000 mm).

The bimetallic Nps derived from the leaf extract displayed inhibition at 2.333 mm ± 0.333 mm and for the flower derived bimetallic Nps at 2.000 mm ± 0.000 mm, therefore indicate approximately halve the inhibition at 200 µl bacteria per plate (Appendix 30 and 31 (A-B)).

Table 17: Zone of inhibition (mm) for bimetallic Nps against the various bacterial test strains

Samples	*B. subtilis* [a]	*E. coli* [a]	*P. aeruginosa* [a]	*Salmonella sp.* [a]	*S. aureus* [a]	*S. aureus* [b]
Bimetallic Nps OB leaf [c]	1.000 ± 0.000	3.333 ± 0.211	5.167 ± 0.167	NI	6.167 ± 0.601	2.333 ± 0.333
Bimetallic Nps OB flower [c]	NI	NI	1.667 ± 0.211	NI	3.500 ± 0.719	1.333 ± 0.333
OB 10% aq. leaf extracts [c]	NI	NI	NI	NI	NI	NI

OB 10% aq. flower extracts [c]	NI		NI		NI		NI		NI		NI	
Control ($1 mM AgNO_3$)[c]	2.000 0.000	±	1.500 0.224	±	2.000 ± 0.000		1.667 ± 0.211		2.333 0.422	±	2.000 0.000	±
+ Control (Gentamycin 10 µg)	10.000 0.000	±	5.000 0.000	±	6.000 ± 0.000		4.000 ± 0.000		-		-	
+ Control (Vancomycin 30 µg)	-		-		-		-		7.000 0.000	±	3.000 0.000	±
- Control (Distilled water)[c]	NI		NI		NI		NI		NI		NI	

Results are expressed as mean inhibition ± SEM, N = 6; OB= O. basilicum; NI = No Inhibition
Grouping variable: 100 µl of bacteria per plate
Grouping variable: 200 µl of bacteria per plate
30 µl of sample

Table 18: Test statistic against *P. aeruginosa*

Test Statistic [a]		
	Z	Asymp. Sig. (2-tailed)
(Au-Ag) Nps (OB) flower vs (Au-Ag) Nps (OB) leaf	-2.251[b]	0.024
Control ($1 mM AgNO_3$) vs (Au-Ag) Nps (OB) leaf	-2.333[b]	0.020
+ Control (Gentamycin 10 µg) vs (Au-Ag) Nps (OB) leaf	-2.236[c]	0.025
- Control (Distilled water) vs (Au-Ag) Nps (OB) leaf	-2.333[b]	0.020
Control ($1 mM AgNO_3$) vs (Au-Ag) Nps (OB) flower	-1.414[c]	0.157
+ Control (Gentamycin 10 µg) vs (Au-Ag) Nps (OB) flower	-2.271[c]	0.023
- Control (Distilled water) vs (Au-Ag) Nps (OB) flower	-2.271[b]	0.023
+ Control (Gentamycin 10 µg) vs Control ($1 mM AgNO_3$)	-2.449[c]	0.014
- Control (Distilled water) vs Control ($1 mM AgNO_3$)	-2.449[b]	0.014
- Control (Distilled water) vs + Control (Gentamycin 10 µg)	-2.449[b]	0.014

All values < 0.05 show a significant difference in the central (median) value; OB = O. basilicum
a. Wilcoxon Signed Ranks test
b. Based on positive ranks
c. Based on negative ranks
d. The sum of negative ranks equals the sum of positive ranks

Table 19: Test statistic against *E. coli*

Test Statistic [a]		
	Z	Asymp. Sig. (2-tailed)
Control ($1 mM AgNO_3$) vs (Au-Ag) Nps (OB) leaf	-2.232[b]	0.026
+ Control (Gentamycin 10 µg) vs (Au-Ag) Nps (OB) leaf	-2.271[c]	0.023
- Control (Distilled water) vs (Au-Ag) Nps (OB) leaf	-2.271[b]	0.023
+ Control (Gentamycin 10 µg) vs Control ($1 mM AgNO_3$)	-2.251[c]	0.024
- Control (Distilled water) vs Control ($1 mM AgNO_3$)	-2.251[b]	0.024
- Control (Distilled water) vs + Control (Gentamycin 10 µg)	-2.449[b]	0.014

All values < 0.05 show a significant difference in the central (median) value; OB = O. basilicum

a. Wilcoxon Signed Ranks test
b. Based on positive ranks
c. Based on negative ranks
d. The sum of negative ranks equals the sum of positive ranks

Table 20: Test statistic against *S. aureus* at 100 µl of bacteria per plate

Test Statistic [a]		
	Z	Asymp. Sig. (2-tailed)
(Au-Ag) Nps (OB) flower vs (Au-Ag) Nps (OB) leaf	-2.226[b]	0.026
Control (1 mM $AgNO_3$) vs (Au-Ag) Nps (OB) leaf	-2.207[b]	0.027
+ Control (Vancomycin 30 µg) vs (Au-Ag) Nps (OB) leaf	-1.179[c]	0.238
- Control (Distilled water) vs (Au-Ag) Nps (OB) leaf	-2.232[b]	0.026
Control (1 mM $AgNO_3$) vs (Au-Ag) Nps (OB) flower	-1.342[b]	0.180
+ Control (Vancomycin 30 µg) vs (Au-Ag) Nps (OB) flower	-2.226[c]	0.026
- Control (Distilled water) vs (Au-Ag) Nps (OB) flower	-2.226[b]	0.026
+ Control (Vancomycin 30 µg) vs Control (1 mM $AgNO_3$)	-2.271[c]	0.023
- Control (Distilled water) vs Control (1 mM $AgNO_3$)	-2.271[b]	0.023
- Control (Distilled water) vs + Control (Vancomycin 30 µg)	-2.449[b]	0.014

All values < 0.05 show a significant difference in the central (median) value; OB = O. basilicum
a. Wilcoxon Signed Ranks test
b. Based on positive ranks
c. Based on negative ranks
d. The sum of negative ranks equals the sum of positive ranks

4.5.2 Antibacterial activity of AgNps

Table 21 and Tables 22-25 (significant differences highlighted in turquoise) outline the antibacterial effect of the various AgNps synthesised from *Ocimum* sp. leaf aq. extracts vs $AgNO_3$, antibiotics and the water control against the bacterial species *B. subtilis, E. coli, P. aeruginosa, Salmonella* sp. and *S. aureus.*

Table 21: Zone of inhibition (mm) for AgNps against the various bacterial test strains

Samples	*B. subtilis* [a]	*E. coli* [a]	*P. aeruginosa* [a]	*Salmonella* sp. [a]	*S. aureus* [a]	*S. aureus* [b]
AgNps leaf *O. sanctum* [c]	2.000 ± 0.000	6.000 ± 1.033	3.167 ± 0.601	2.000 ± 0.000	6.333 ± 1.174	2.667 ± 0.333
AgNps leaf *O. basilicum* [c]	2.000 ± 0.000	4.167 ± 0.792	2.667 ± 0.333	NI	3.667 ± 0.333	1.333 ± 0.333
AgNps leaf combination [c]	3.000 ± 0.000	1.500 ± 0.224	2.000 ± 0.365	NI	2.167 ± 0.477	1.000 ± 0.000
OS 10% aq. extracts [c]	NI	NI	NI	NI	NI	NI

OB 10% aq. extracts [c]	NI	NI	NI	NI	NI	NI
OS+OB 10% aq. extracts [c]	NI	NI	NI	NI	NI	NI
Control (1 mM $AgNO_3$) [c]	2.000 ± 0.000	1.500 ± 0.224	2.000 ± 0.000	1.667 ± 0.211	2.000 ± 1.095	2.333 ± 0.333
+ Control (Vancomycin 30 µg)	-	-	-	-	6.000 ± 0.000	3.000 ± 0.000
+ Control (Gentamycin 10 µg)	10.000 ± 0.000	5.000 ± 0.000	6.000 ± 0.000	4.000 ± 0.000	-	-
- Control (Distilled water)[c]	NI	NI	NI	NI	NI	NI

Results are expressed as mean inhibition ± SEM, N = 6; OB= O. basilicum; OS = O. sanctum; NI = No Inhibition
Grouping variable: 100 µl of bacteria per plate
Grouping variable: 200 µl of bacteria per plate
30 µl of sample

AgNps synthesised from *O. sanctum*, *O. basilicum* and in combination aq. leaf extracts displayed effective antibacterial activity against *B. subtilis*. The highest significant activity against *B. subtilis* was displayed with the AgNps derived from the combination leaf aq. extracts (*O. sanctum* + *O. basilicum*) at 3.000 mm ± 0.000 mm and p-value 0.0013 (see Appendix 32 (A-B)).

The antibacterial activity of the AgNps synthesised from *O. sanctum* leaf extract was observed against *E. coli* (6.000 mm ± 1.033 mm), p-value 0.518 (Appendix 33; Table 22), followed by significant activity against *P. aeruginosa* (3.167 mm ± 0.601 mm) (Appendix 34; Table 23), p-value 0.038 and least was noticed against *Salmonella* sp. (2.000 mm ± 0.000 mm), p-value 0.014 (Table 24).

The highest antibacterial activity was observed against *E. coli* (4.167 mm ± 0.792 mm), p-value 0.339 using AgNps synthesised from *O. basilicum* leaf extract, and the lowest was observed against *P. aeruginosa* (2.667 mm ± 0.333 mm), p-value 0.026. Furthermore, no antibacterial activity was observed against *Salmonella* sp. using AgNps derived from *O. basilicum* extract and the combination leaf aq. extracts (Appendix 35).

The antibacterial activity of the AgNps against *S. aureus* was tested for two grouping variables at 100 µl and 200 µl bacteria per plate, respectively. The AgNps extract shown

inhibition against *S. aureus* at 100 µl of bacteria per plate, the AgNps derived from *O. sanctum* leaf extracts displayed inhibition at (6.333 mm ± 1.174 mm), p-value 0.713 and significant inhibition for AgNps synthesised from *O. basilicum* leaf extract (3.667 mm ± 0.333 mm), p-value 0.026 (Table 25), whereas, combination extracts showed the lowest significant antibacterial activity compared to vancomycin (6.000 mm ± 0.000 mm), p-value 0.027. The antibacterial activity of the AgNps against the bacteria *S. aureus* at 200 µl bacteria per plate shown inhibition using AgNps synthesised from *O. sanctum* leaf extract (2.667 mm ± 0.333 mm) and for AgNps synthesised from *O. basilicum* leaf extract (1.333 mm ± 0.333 mm). The combined extracts derived AgNps shown the lowest inhibition against the bacteria *S. aureus* compared to the positive control (Appendixes 36 and 37 (A-B)).

The combination extracts AgNps displayed the lowest antimicrobial properties and the crude *Ocimum* sp. 10% aq. leaf extracts shown no inhibitory activity against the test strains.

Table 22: Test statistic against *E. coli*

Test Statistic [a]		
	Z	Asymp. Sig. (2-tailed)
OB AgNps vs OS AgNps	-2.060[b]	0.039
OS+OB AgNps vs OS AgNps	-2.226[b]	0.026
Control (1 mM $AgNO_3$) vs OS AgNps	-2.226[b]	0.026
+ Control (Gentamycin 10 µg) vs OS AgNps	-0.647[b]	0.518
- Control (Distilled water) vs OS AgNps	-2.226[b]	0.026
OS+OB AgNps vs OB AgNps	-2.333[b]	0.020
Control (1 mM $AgNO_3$) vs OB AgNps	-2.333[b]	0.020
+ Control (Gentamycin 10 µg) vs OB AgNps	-0.957[c]	0.339
- Control (Distilled water) vs OB AgNps	-2.232[b]	0.026
Control (1 mM $AgNO_3$) vs OS+OB AgNps	0.000[d]	1.000
+ Control (Gentamycin 10 µg) vs OS+OB AgNps	-2.251[c]	0.024
- Control (Distilled water) vs OS+OB AgNps	-2.251[b]	0.024
+ Control (Gentamycin 10 µg) vs (Control 1 mM $AgNO_3$)	-2.251[c]	0.024
- Control (Distilled water) vs (Control 1 mM $AgNO_3$)	-2.251[b]	0.024
- Control (Distilled water) vs + Control (Gentamycin 10 µg)	-2.449[b]	0.014

All values < 0.05 show a significant difference in the central (median) value; OB = O. basilicum; O. sanctum
a. Wilcoxon Signed Ranks test
b. Based on positive ranks
c. Based on negative ranks
d. The sum of negative ranks equals the sum of positive ranks

Table 23: Test statistic against *P. aeruginosa*

Test Statistic [a]		
	Z	Asymp. Sig. (2-tailed)
OB AgNps vs OS AgNps	-0.707[b]	0.480
OS+OB AgNps vs OS AgNps	-1.633[b]	0.102
Control (1 mM $AgNO_3$) vs OS AgNps	-1.890[b]	0.059
+ Control (Gentamycin 10 µg) vs OS AgNps	-2.070[c]	0.038
- Control (Distilled water) vs OS AgNps	-2.232[b]	0.026
OS+OB AgNps vs OB AgNps	-2.000[b]	0.046
Control (1 mM $AgNO_3$) vs OB AgNps	-1.633[b]	0.102
+ Control (Gentamycin 10 µg) vs OB AgNps	-2.232[c]	0.026
- Control (Distilled water) vs OB AgNps	-2.232[b]	0.026
Control 1 mM $AgNO_3$ vs OS+OB AgNps	0.000[d]	1.000
+ Control (Gentamycin 10 µg) vs OS+OB AgNps	-2.220[c]	0.026
- Control (Distilled water) vs OS+OB AgNps	-2.220[b]	0.026
+ Control (Gentamycin 10 µg) vs (Control 1 mM $AgNO_3$)	-2.449[c]	0.014
- Control (Distilled water) vs (Control 1 mM $AgNO_3$)	-2.449[b]	0.014
- Control (Distilled water) vs + Control (Gentamycin 10 µg)	-2.449[b]	0.014

All values < 0.05 show a significant difference in the central (median) value; OB = O. basilicum; OS = O. sanctum
a. Wilcoxon Signed Ranks test
b. Based on positive ranks
c. Based on negative ranks
d. The sum of negative ranks equals the sum of positive ranks

Table 24: Test statistic against *Salmonella* sp.

Test Statistics [a]		
	Z	Asymp. Sig. (2-tailed)
Control (1 mM $AgNO_3$) vs OS AgNps	-1.414[b]	0.157
+ Control (Gentamycin 10 µg) vs OS AgNps	-2.449[c]	0.014
- Control (Distilled water) vs OS AgNps	-2.449[b]	0.014
+ Control (Gentamycin 10 µg) vs Control (1 mM $AgNO_3$)	-2.271[c]	0.023
- Control (Distilled water) vs Control (1 mM $AgNO_3$)	-2.271[b]	0.023
- Control (Distilled water) vs + Control (Gentamycin 10 µg)	-2.449[b]	0.014

All values < 0.05 show a significant difference in the central (median) value; OS = O. sanctum
a. Wilcoxon Signed Ranks test
b. Based on positive ranks
c. Based on negative ranks

Table 25: Test statistic against *S. aureus* at 100 µl of bacteria per plate

Test Statistic [a]		
	Z	Asymp. Sig. (2-tailed)
OB AgNps vs OS AgNps	-2.214[b]	0.027

OS+OB AgNps vs OS AgNps	-2.121[b]	0.034
Control (1 mM $AgNO_3$) vs OS AgNps	-2.214[b]	0.027
+ Control (Vancomycin 30 µg) vs OS AgNps	-0.368[c]	0.713
-Control (Distilled water) vs OS AgNps	-2.214[b]	0.027
OS+OB AgNps vs OB AgNps	-1.913[b]	0.056
Control (1 mM $AgNO_3$) vs OB AgNps	-1.826[b]	0.068
+ Control Vancomycin 30 µg vs OB AgNps	-2.232[c]	0.026
-Control (Distilled water) vs OB AgNps	-2.232[b]	0.026
Control (1 mM $AgNO_3$) vs OS+OB AgNps	-0.213[b]	0.832
+ Control (Vancomycin 30 µg) vs OS+OB AgNps	-2.214[c]	0.027
-Control (distilled water) vs OS+OB AgNps	-2.214[b]	0.027
+ Control (Vancomycin 30 µg) vs (Control 1 mM $AgNO_3$)	-2.251[c]	0.024
-Control (Distilled water) vs (Control 1 mM $AgNO_3$)	-2.251[b]	0.024
-Control (Distilled water) vs + Control Vancomycin 30 µg	-2.449[b]	0.014

All values < 0.05 show a significant difference in the central (median) value; OB = O. basilicum; OS = O. sanctum
a. Wilcoxon Signed Ranks test
b. Based on positive ranks
c. Based on negative ranks
d. The sum of negative ranks equals the sum of positive ranks

4.5.3 Results of MIC and MBC

All the samples were subjected to the Minimum Inhibitory Concentration (MIC) and Minimum Bactericidal Concentration (MBC) tests. However, focus was directed at the AgNps synthesised from *O. sanctum* and *O. basilicum* singly and in combination that displayed the highest inhibition against the various test strains.

4.5.3.1 *Salmonella* sp.

The MIC and MBC for a 1 in 2 dilution for *O. sanctum* leaf synthesised AgNps against *Salmonella* sp. was 66.67% no growth (x 4 plates) and 33.33% growth when compared to the 100% growth for the water control. The MIC and MBC for 1 in 4 dilution *O. sanctum* leaf synthesised AgNps against *Salmonella* sp. was 50% no growth (x 3 plates), and 50% growth when compared to the 100% growth for the water control, p-value summary 0.045. This is presented in Figure 26.

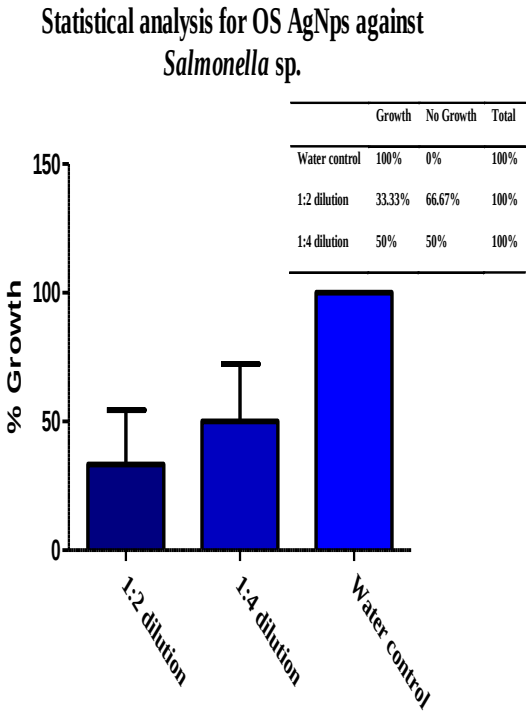

Figure 26: Statistical analysis of results for *O. sanctum* derived AgNps against *Salmonella* sp. vs water control; *N* = 6; OS = *O. sanctum*

4.5.3.2 *S. aureus*

The MIC and MBC for a 1 in 2 dilution *O. sanctum* aq. leaf synthesised AgNps against *S. aureus* sp. were 100% no growth (x 6 plates) and 0% growth when compared to the 100% growth for the water control. *O. basilicum* leaf synthesised AgNps against *S. aureus* was 83.33% no growth (x 5 plates) and 16.67% growth; and combination extracts (*O. sanctum* + *O. basilicum*) synthesised AgNps represented 50% no growth (x 3 plates) and 50% growth when compared to 100% growth for the water control, p-value 0.0003. This is presented in Figure 27.

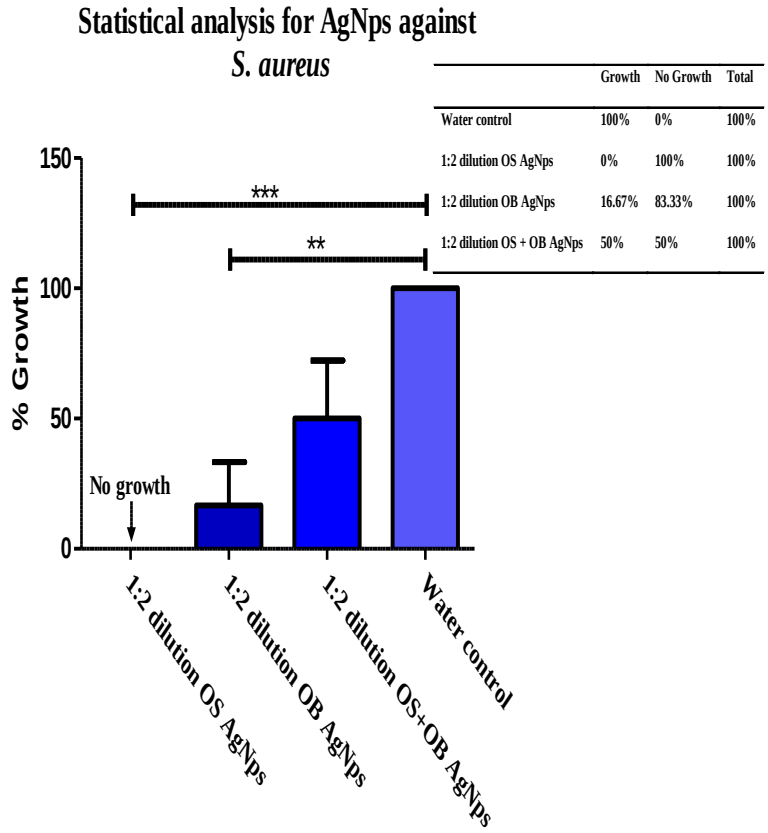

Figure 27: Statistical analysis of results for the various *Ocimum* sp. derived AgNps against *S. aureus* vs water control; *N* = 6; p-value < 0.01, p-value summary **; p-value < 0.0001, p-value summary *; OS = *O. sanctum*; OB = *O. basilicum***

4.6 *In vitro* Antidiabetic screening

In vitro inhibitory effect of the crude extracts (aq. and ethanol), bimetallic (Au-Ag) Nps and AgNps synthesised from *Ocimum* sp. were assessed using α-amylase (from porcine) and *B. stearothermophilus* α-glucosidase enzymes as models and, subsequently compared to the standard reference drug acarbose. The percentage yields of the crude extracts obtained for the antidiabetic analysis are shown in Table 26.

Table 26: Percentage yields of *O. sanctum* and *O. basilicum* extracts

Method	Plant	Extractant	% yield
A:	*O. sanctum* leaf	Water	3.2
	O. sanctum whole	Water	4.7
	O. sanctum flower	60% EtOH	0.6
	O. basilicum leaf	60% EtOH	0.9
	O. basilicum leaf	Water	5.1

B:	*O. sanctum* leaf	Water	1.3
	O. sanctum flower	Water	2.9
	O. basilicum leaf	Water	6.0
	O. basilicum flower	Water	2.9
C:	*O. sanctum* leaf	60% EtOH	9.5
	O. sanctum flower	60% EtOH	2.9
	O. sanctum leaf	70% EtOH	5.3
	O. basilicum leaf	60% EtOH	2.2
	O. basilicum flower	60% EtOH	1.3
	O. basilicum leaf	70% EtOH	3.5
D:	*O. sanctum* leaf	Hot water	3.2
	O. sanctum flower	Hot water	1.8
	O. sanctum leaf	Cold water	2.3
	O. sanctum flower	Cold water	1.5

Key: A = 3.4.1.1; B = 3.4.1.2; C = 3.4.1.3; D = 3.4.1.4

4.6.1 *In vitro* α-amylase inhibitory effect of crude *O. basilicum* extracts

The *in vitro* α-amylase inhibitory study demonstrated that the crude *O. basilicum* extracts (aq. 60% and ethanol 70%) inhibited α-amylase (derived from porcine) in terms of the time-dependent method (t = 3 min) at 2.0 mg/ml as shown in Table 27. The results obtained at t = 0 min, t = 1 min, and t = 2 min were not reported due to their low inhibition.

All crude *O. basilicum* extracts demonstrated greater inhibition compared to the standard control, acarbose. The *O. basilicum* ethanol flower and aq. leaf extracts demonstrated significant inhibitory activity at 61.73% ± 6.37%, p-value 0.011 and 61.23% ± 5.24%, p-value 0.007, respectively. The *O. basilicum* ethanol leaf extract demonstrated the lowest inhibitory activity at 55.13% ± 9.17%, p-value 0.027 against α-amylase from the extracts. There was no statistical difference between the α-amylase inhibitory activities of the crude *O. basilicum* extracts compared to acarbose.

Table 27: Inhibitory action of crude *O. basilicum* extracts leaf and flower on α-amylase activity

Samples	*In vitro* α-amylase Inhibition % (± SEM) at the concentration of 2.0 mg/ml	p-value
Acarbose	49.7 ± 3.18	0.004 **
Aq. dist. (flower)	58.03 ± 4.43	0.006 **
Aq. dist. (leaf)	61.23 ± 5.24	0.007 **
60% EtOH (flower)	61.73 ± 6.37	0.011 *
60% EtOH (leaf)	55.13 ± 9.17	0.027 *
70% EtOH (leaf)	55.81 ± 7.86	0.019 *

*Results expressed as % mean ± SEM; N = 3; time-dependent method t = 3 min at a concentration of 2 mg/ml; p-value < 0.05, p-value summary *; p-value < 0.01, p-value summary ***

4.6.2 *In vitro* α-amylase inhibitory effect of crude *O. sanctum* extracts

In vitro α-amylase inhibitory study of crude *O. sanctum* extracts (aq. 60% and ethanol 70%) demonstrated inhibition of α-amylase in terms of the time-dependent method (t = 3 min) at 2.0 mg/ml as shown in Table 28. The results obtained at t = 0 min, t = 1 min, and t = 2 min were not reported due to their low inhibition.

The *O. sanctum* EtOH 60% leaf extracts demonstrated the greatest inhibitory activity (66.33% ± 4.26%, p-value 0.004) and was significantly different compared to acarbose, p-value 0.003. The aq. *O. sanctum* flower extracts demonstrated the lowest zone of inhibitory activity (58.03% ± 4.43%, p-value 0.006) against α-amylase. All the crude *O. sanctum* extracts demonstrated greater zones of inhibition than the standard control, acarbose (see Figure 28). There was no statistical difference between the α-amylase inhibitory activities of the crude *O. sanctum* extracts compared to acarbose.

Table 28: Inhibitory action of crude *O. sanctum* leaf and flower extracts on α-amylase activity

Samples	*In vitro* α-amylase Inhibition % (± SEM) at the concentration of 2.0 mg/ml	p-value
Acarbose	49.93 ± 2.93	0.003 **
Aq. dist. (flower)	58.03 ± 4.43	0.006 **
Aq. dist. (leaf)	61.23 ± 5.24	0.007 **
60% EtOH (flower)	61.73 ± 5.07	0.011 *
60% EtOH (leaf)	66.33 ± 4.26 *	0.004 **
70% EtOH (leaf)	64.14 ± 13.47	0.018 *

*Results expressed as % mean ± SEM.; N = 3; time-dependent method t = 3 min at a concentration of 2.0 mg/ml; p-value (two-tailed) < 0.05, p-value summary * vs control; p-value < 0.05, p-value summary *; p-value < 0.01, p-value summary ***

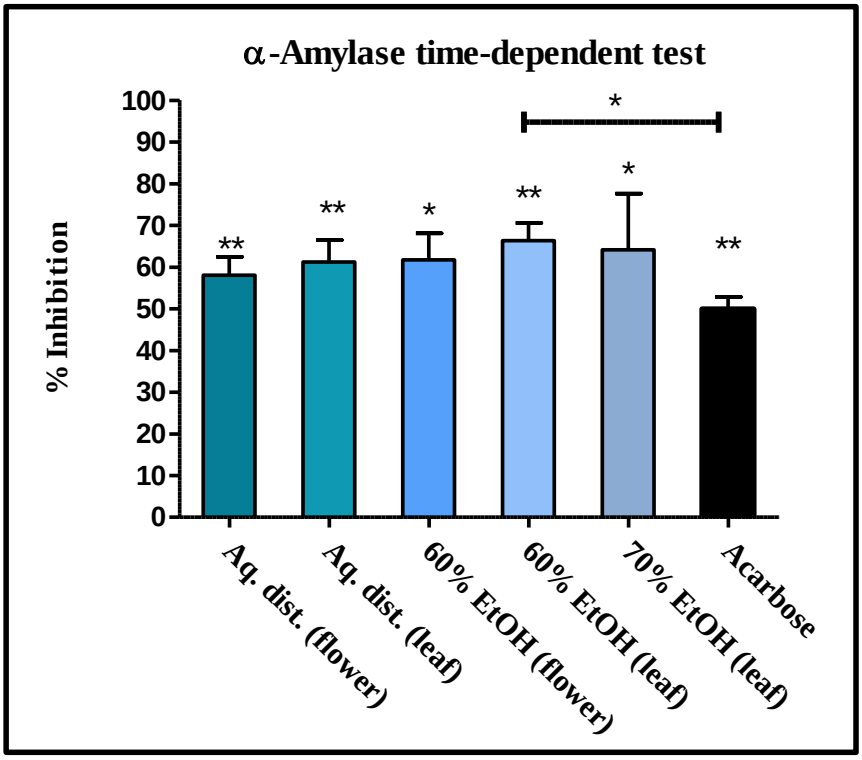

Figure 28: Inhibitory action of crude *O. sanctum* leaf and flower extracts on α-amylase activity; p-value < 0.05, p-value summary * vs control (acarbose)

4.6.3 *In vitro* α-amylase inhibitory effect of bimetallic (Au-Ag) Nps

The *in vitro* α-amylase inhibitory studies demonstrated that the bimetallic (Au-Ag) Nps derived from *O. basilicum* extracts inhibited α-amylase in terms of the time-dependent method (t = 3 min) at 2.0 mg/ml as shown in Table 29. The results obtained at t = 0 min, t = 1 min, and t = 2 min were not reported due to their low inhibition.

The bimetallic (Au-Ag) Nps synthesised from *O. basilicum* leaf extracts demonstrated inhibitory activity at 69.67% ± 3.42%, p-value < 0.0001 was significantly greater than acarbose 48.27% ± 1.79%, p-value 0.0002. The bimetallic (Au-Ag) Nps derived from the flower extract also showed significant inhibition at 60.57% ± 3.15%, p-value 0.006 (see Figure 29).

Table 29: Inhibitory action of bimetallic (Au-Ag) Nps on α-amylase activity

Samples	*In vitro* α-amylase Inhibition % (± SEM) at the concentration of 2.0 mg/ml	p-value
Acarbose	48.27 ± 1.79	< 0.0001 ***
(Au-Ag) Nps OB (leaf)	69.97 ± 3.42 ***	< 0.0001 ***

(Au-Ag) Nps OB (flower)	60.57 ± 3.15 *	< 0.0001 ***

*Results expressed as mean ± SEM.; N = 3; * p-value (two-tailed) < 0.05, p-value summary *; p-value < 0.0001, p-value summary *** vs control; OB = O. basilicum*

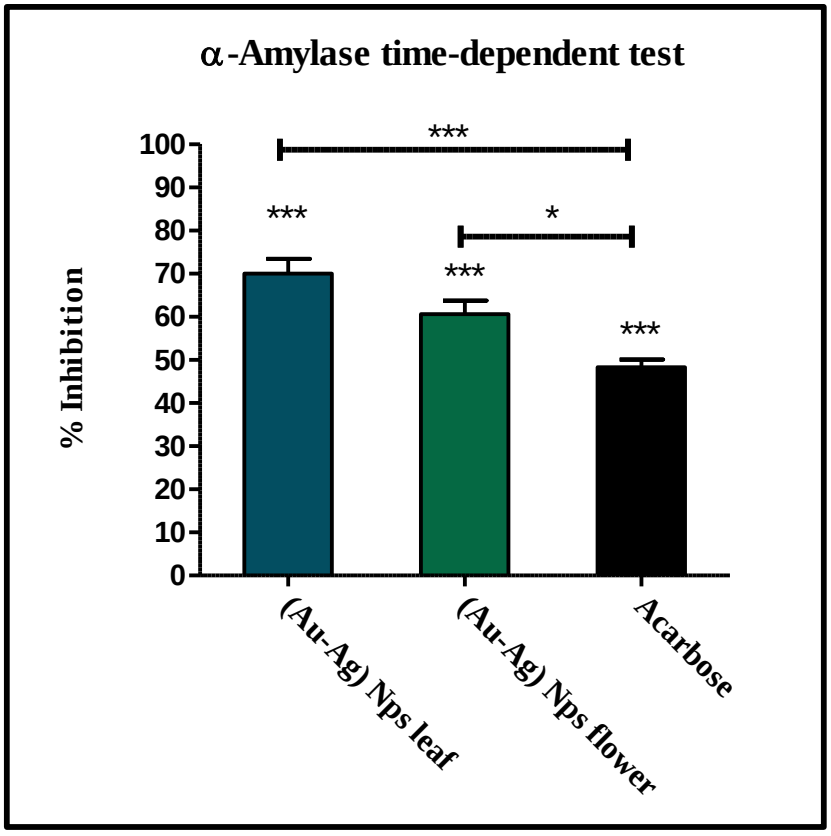

Figure 29: Inhibitory action of bimetallic (Au-Ag) Nps synthesised from the leaf and flower extracts on α-amylase activity; p-value < 0.05, p-value summary * vs control (acarbose)

4.6.4 *In vitro* α-amylase inhibitory effect of AgNps

In vitro α-amylase inhibitory studies demonstrated that the AgNps derived from *O. basilicum* and *O. sanctum* leaf aq. extracts inhibited α-amylase activity in terms of the time-dependent (t = 3 min) method at a higher concentration of 3.0 mg/ml as shown in Table 30. The results obtained at t = 0 min, t = 1 min, and t = 2 min were not reported due to their low inhibition.

The AgNps synthesised from the combination of extracts (*O. sanctum* + *O. basilicum*) demonstrated significant inhibitory activity against α-amylase at 54.94% ± 6.56%, p-value 0.014. The AgNps synthesised from *O. sanctum* extracts demonstrated significant inhibitory activity at 59% ± 3.72%, p-value 0.016 compared to acarbose (see Figure 30).

Table 30: Inhibitory action of AgNps on α-amylase activity

Samples	*In vitro* α-amylase Inhibition % (± SEM) at the concentration of 3.0 mg/ml	p-value
Acarbose	48.27 ± 1.79	< 0.0001 ***
AgNps OS	59.57 ± 3.72 *	0.004 **
AgNps OB	59.79 ± 6.91	0.013 *
AgNps OS+OB	54.94 ± 6.56	0.014 *

*Results expressed as mean ± SEM; N = 3; p < 0.05, p-value summary * vs control; OS = O. sanctum; OB = O. basilicum*

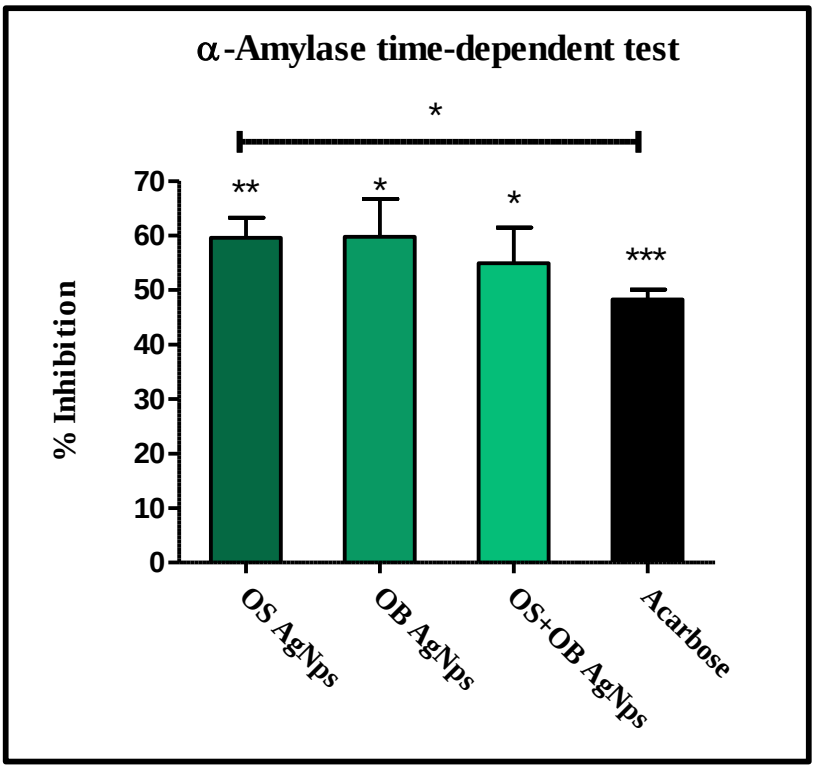

Figure 30: Inhibitory action of AgNps synthesised from the various *Ocimum* sp. aq. leaf extracts on α-amylase activity; p-value < 0.05, p-value summary * vs control (acarbose)

4.6.5 *In vitro* α-amylase inhibition dose-dependent method (*O. sanctum* and *O. basilicum* crude extracts)

The dose-dependent method shows the α-amylase inhibitory effect of all extracts and Nps and that there was an increased percentage inhibition with an increase in their concentration (Appendixes 38-40).

The concentration of the extract (inhibitor) required for 50% of inhibition (IC_{50}) for all the crude extracts were determined from corresponding dose-response curves of percentage inhibition versus inhibitor concentration and compared to acarbose, a known inhibitor of α-amylase. In the dose-response from acarbose that was dissolved in distilled water in the concentration range of 0.016-1 mg/ml, the IC_{50} value 0.022 mg/ml was obtained, and was in accordance with previous research (Deutschländera *et al.* 2009).

The lowest IC_{50} value obtained was with *O. basilicum* leaf extracts prepared in 70% EtOH which appeared to be a good inhibitor of α-amylase compared to acarbose (see Table 31). The extracts, *O. sanctum* leaf extracts prepared over 3 days in cold water, *O. sanctum* EtOH 70% leaf extract and *O. sanctum* EtOH 60% leaf extracts, displayed lower IC_{50} (IC_{50} values almost identical) than acarbose. The inhibitory effect of *O. sanctum* and *O. basilicum* flower extracts inhibitory activity were not greater than 50% therefore, were not subjected to further testing (Appendix 40).

Table 31: Inhibitory effect (IC_{50}) of crude *Ocimum* sp. extracts and acarbose on α-amylase at various concentrations

IC_{50} values of crude extracts and acarbose on α-amylase * 0.003-3.0 mg/ml; ** 0.002-2.0 mg/ml; ¥ 0.181-5.8 mg/ml	
Samples	IC_{50} (mg/ml)
Acarbose	0.022
OB EtOH 60% leaf **	0.033
OS EtOH 60% leaf **	0.021
OS Aq. leaf **	0.028
OB Aq. leaf **	0.029
OB EtOH 70% leaf *	0.009
OS EtOH 70% leaf *	0.017
OS-3 day hot water leaf *	0.027
OS-3 day cold water leaf *	0.019
OB EtOH 60% flower ¥	NI
OS EtOH 60% flower ¥	NI

Results expressed as a % mean ± SEM, N = 2; Key: OB = O. basilicum; OS = O. sanctum; NI = No Inhibition

4.6.6 *In vitro* α-amylase inhibition dose-dependent method for bimetallic (Au-Ag) Nps and AgNps

The bimetallic (Au-Ag) Nps synthesised from leaf and flower aq. extracts showed inhibition against α-amylase at a dose as low as 0.0002 mg/ml as reported in Appendix 41. The bimetallic Nps synthesised from the leaf aq. extract displayed a lower IC_{50} than the bimetallic Nps synthesised from the flower aq. extract (Table 32).

The AgNps synthesised from *O. sanctum* and *O. basilicum* aq. leaf extracts displayed inhibition against α-amylase at a dose range of 0.05 mg/ml - 1.6 mg/ml, however the *O. basilicum* derived AgNps shows inhibition higher than acarbose (IC_{50} 0.022 mg/ml), indicated by the lower IC_{50} value 0.016 mg/ml (Appendix 42).

Table 32: Inhibitory effect (IC_{50}) of bimetallic Nps and AgNps extracts and acarbose on α-amylase at various concentrations

IC_{50} values of bimetallic Nps, AgNps and acarbose on α-amylase * 0.0002-2.0 mg/ml; ** 0.05-1.6 mg/ml	
Samples	IC_{50} (mg/ml)
Acarbose	0.022
(Au-Ag) Nps OB (leaf) *	0.130
(Au-Ag) Nps OB (flower) *	0.196
AgNps OS **	0.070
AgNps OB **	0.016
AgNps OS+OB **	0.169

Results expressed as a % mean ± SEM, N = 3; Key: OB = O. basilicum; OS = O. sanctum; NI = No Inhibition

4.6.7 Mode of inhibition of bimetallic (Au-Ag) Nps and AgNps on α-amylase activity

The mode of inhibition of the crude *O. basilicum* extract and bimetallic (Au-Ag) Nps synthesised from the leaf and flower extracts (2.5 mg/ml) on the activity of α-amylase was determined by means of Lineweaver-Burk plot (double reciprocal) analysis of data according to Michaelis-Menten kinetics.

As shown in Figure 31, the mode of inhibition of bimetallic (Au-Ag) Nps synthesised from *O. basilicum* leaf extract on α-amylase activity appeared to be uncompetitive (K_m is decreased and V_{max} is decreased).

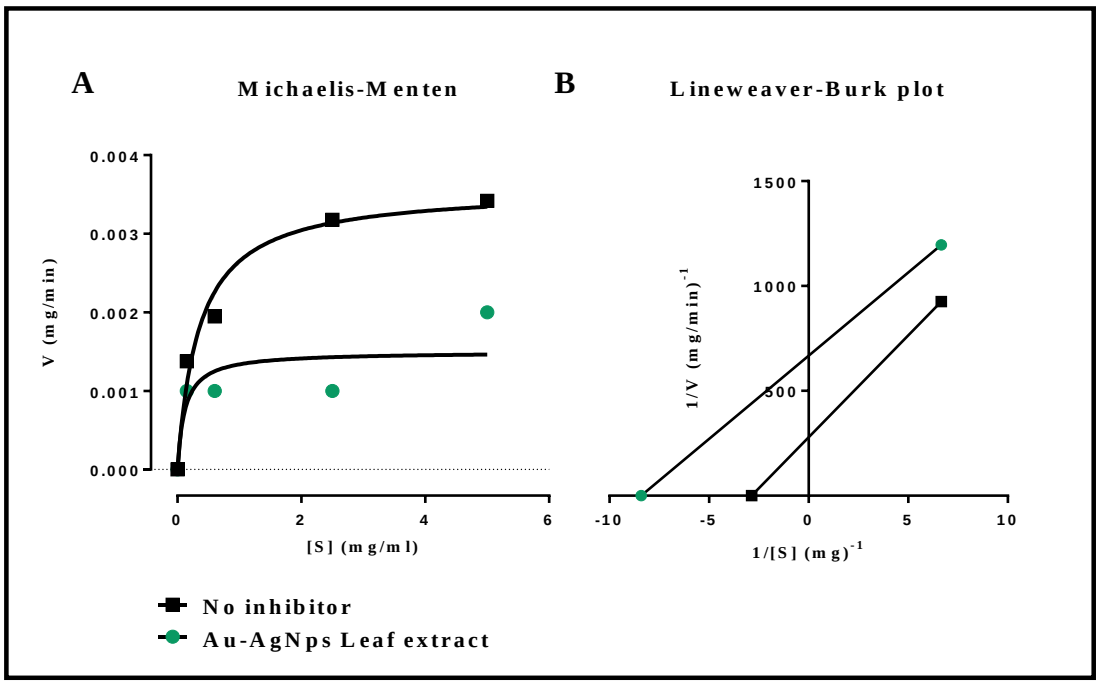

Figure 31: (A) Michaelis-Menten and (B) Lineweaver-Burk plot of the activity of α-amylase in the absence or presence of the bimetallic (Au-Ag) Nps synthesised from *O. basilicum* leaf extract

As shown in Figure 32 the mode of inhibition of bimetallic (Au-Ag) Nps synthesised from *O. basilicum* aq. flower extracts on α-amylase activity displayed non-competitive inhibition (K_m no effect whereas V_{max} is decreased).

The mode of inhibition of the AgNps synthesised from the various *Ocimum* sp. aq. leaf extracts (3.0 mg/ml) on the activity of α-amylase was determined by means of Lineweaver-Burk plot (double reciprocal) analysis of data according to Michaelis-Menten kinetics. As shown in Figure 33, the mode of inhibition of AgNps synthesised from *O. sanctum* aq. leaf extract on α-amylase activity displayed competitive inhibition (K_m is increased, whereas V_{max} remain the same). Furthermore, the mode of inhibition of AgNps synthesised from *O. basilicum* aq. leaf extract on α-amylase activity shows uncompetitive inhibition (K_m is decreased and V_{max} is decreased), identical to the result obtained from bimetallic (Au-Ag) Nps synthesised from *O. basilicum* leaf extract (Figure 31).

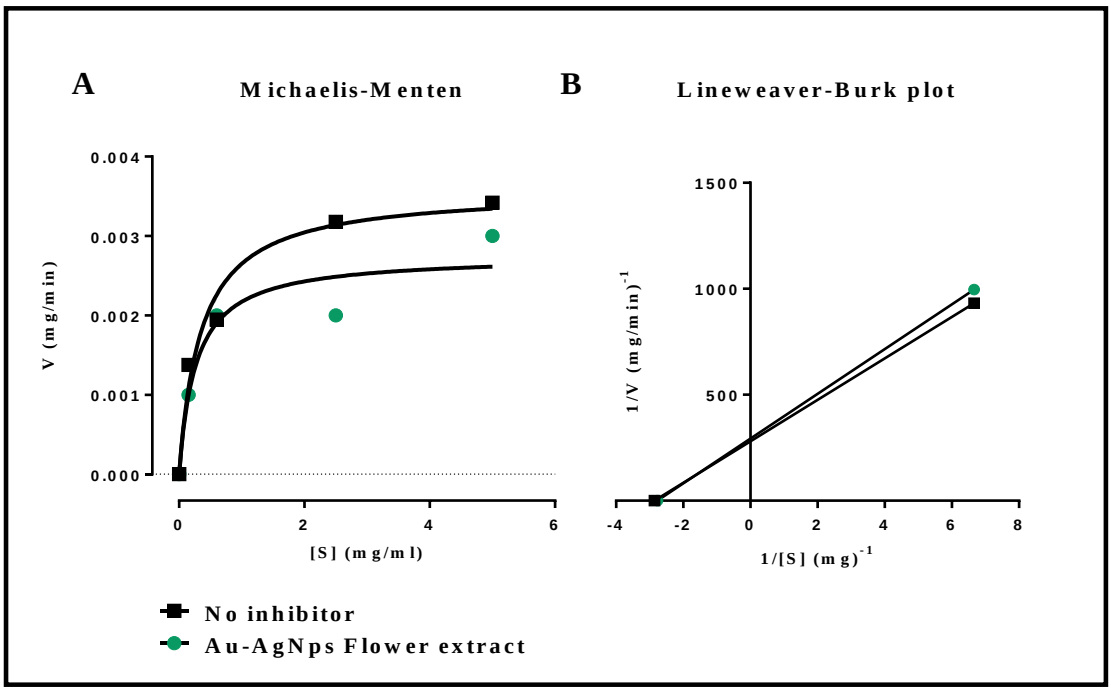

Figure 32: (A) Michaelis-Menten and (B) Lineweaver-Burk plot of the activity of α-amylase in the absence or presence of the bimetallic (Au-Ag) Nps synthesised from *O. basilicum* flower extract

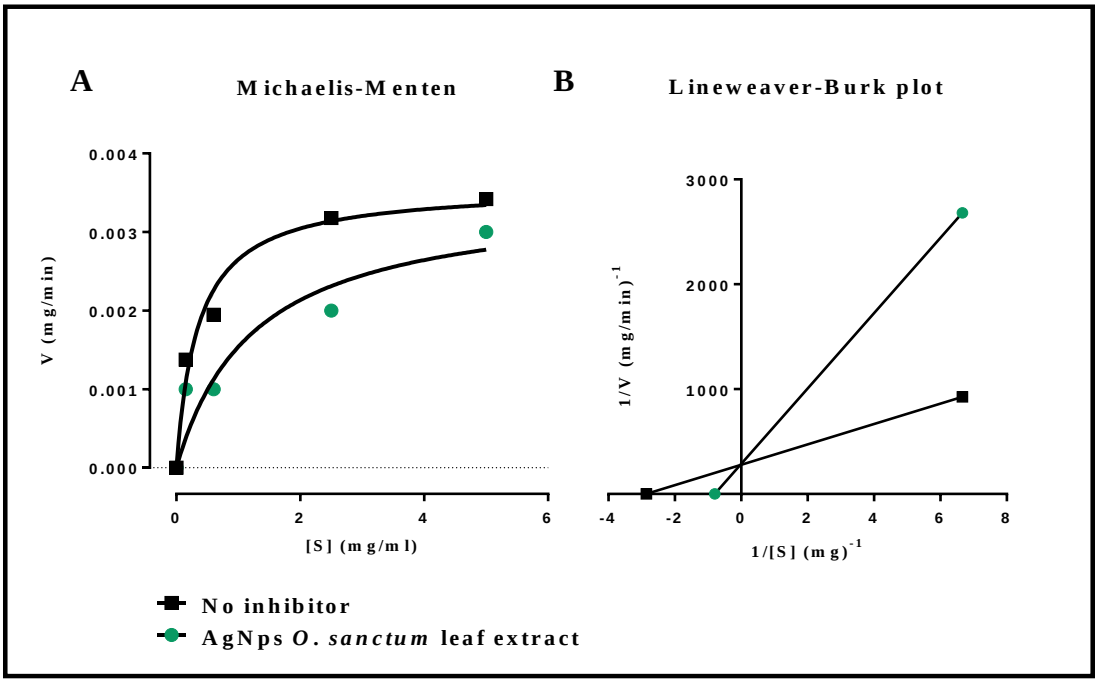

Figure 33: (A) Michaelis-Menten and (B) Lineweaver-Burk plot of the activity of α-amylase in the absence or presence of the AgNps synthesised from *O. sanctum* aq. leaf extract

4.6.8 *In vitro* α-glucosidase inhibitory effect of crude *O. basilicum* leaf and flower extracts

The inhibitory activities of *O. basilicum* crude aq. and ethanol extracts were tested for their *in vitro* activity against *Bacillus stearothermophilus* α-glucosidase. The percentage inhibition obtained at a single dose demonstrated inhibition lower than that of acarbose as indicated in Table 33.

The *O. basilicum* leaf 70% EtOH crude extracts demonstrated the highest percentage inhibition against *B. stearothermophilus* α-glucosidase activity (69.89% ± 6.871%); followed by the 60% EtOH crude extracts (50.50% ± 3.594%).

The *O. basilicum* aq. leaf extracts displayed statistically the lowest inhibitory activity (34.75% ± 3.705%) against *B. stearothermophilus* α-glucosidase compared to acarbose, p-value 0.044 (Figure 34). The inhibitory activity of the flower extracts were not greater than 50%, thus were not subjected to further testing.

Table 33: Inhibitory action of crude *O. basilicum* leaf extracts and acarbose on α-glucosidase activity

Samples	*In vitro* α-glucosidase Inhibition % (± SEM) at 0.3 mg/ml	p-value
Acarbose	73.75 ± 12.86	0.0023
70% EtOH	69.89 ± 6.871	< 0.0001
Aq. dist.	34.75 ± 3.705 *	0.0026
60% EtOH	50.50 ± 3.594	0.0008

*Results expressed as mean ± SEM; N = 6; Aq. dist. = Aqueous distillation; p < 0.05, p-value summary * vs control*

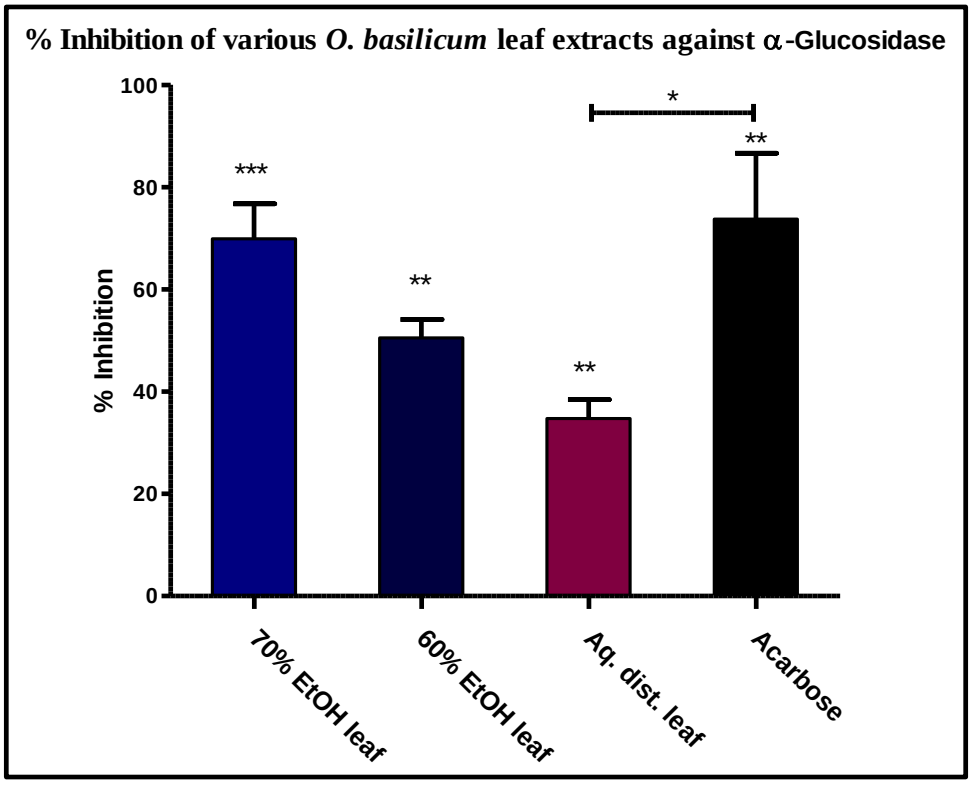

Figure 34: Inhibitory activities of various crude *O. basilicum* leaf extracts at concentration 0.3 mg/ml for 60% EtOH; Aq. dist.; 70% EtOH and 1 mg/ml acarbose, tested for their hypoglycaemic activity; p-value < 0.05, p-value summary * vs control (acarbose)

The IC_{50} values from the tested *O. basilicum* EtOH (60%, 70%) and aq. dist. leaf extracts (which demonstrated α-glucosidase inhibitory activities during the screening) as well as the IC_{50} of acarbose against *B. stearothermophilus* α-glucosidase were determined from corresponding dose-response curves of percentage inhibition versus inhibitor concentration and are summarised in Table 34. The *O. basilicum* 60% EtOH crude extracts demonstrated inhibition at very low dosages, IC_{50} of 0.002 mg/ml almost identical to that of acarbose. The 70% EtOH extracts also demonstrated a good IC_{50} of 0.007 mg/ml which was slightly higher than acarbose. Both extracts proved to be good inhibitors of α-glucosidase at a 0.0003-0.3 mg/ml dose-response. However, the aq. dist. extract shown a very high IC_{50} of 10.55 mg/ml (Appendix 43).

Table 34: Inhibitory effect (IC_{50}) of crude *O. basilicum* leaf extracts on α-glucosidase; IC_{50} concentration of inhibitor to inhibit 50% of its activity

Inhibitory effects of OB extracts 0.0003-0.3 mg/ml and acarbose on α-glucosidase activity	
Samples	IC_{50} (mg/ml)

Acarbose	0.001
70% EtOH	0.007
Aq. dist.	10.55
60% EtOH	0.002

Results expressed as a % mean ± SEM, N = 2; Key: OB = O. basilicum

4.6.9 *In vitro* α-glucosidase inhibitory effect of crude *O. sanctum* leaf and flower extracts

The inhibitory activities of crude *O. sanctum* aq. and ethanolic extracts were tested for their *in vitro* antidiabetic activity using a *B. stearothermophilus* α-glucosidase enzyme model. The percentage inhibition obtained at a single dose demonstrated lower inhibition than that of acarbose as indicated in Table 35. *O. sanctum* EtOH (70%) leaf extracts demonstrated the highest percentage inhibition against *B. stearothermophilus* α-glucosidase activity (66.00% ± 7.800%), followed by aq. dist. hot water extract (62.25% ± 11.25%). The aq. dist. (cold water) leaf extract from *O. sanctum* extract displayed statistically the lowest inhibitory activity (32.00% ± 5.45%) against *B. stearothermophilus* α-glucosidase compared to acarbose (1 mg/ml), p-value 0.0037.

Table 35: Inhibitory action of crude *O. sanctum* extracts on α-glucosidase activity

Samples	*In vitro* α-glucosidase Inhibition % (± SEM) at *0.2 mg/ml, **0.3 mg/ml, and $^{¥}$0.5 mg/ml	p-value
Acarbose	73.75 ± 12.86	0.0023
70% EtOH leaf **	66.00 ± 7.80	0.0035
60% EtOH leaf *	49.50 ± 2.18	0.0002
Aq. dist. whole plant $^{¥}$	52.25 ± 10.38	0.0151
Aq. dist. (hot d.H_2O)**	62.25 ± 11.25	0.0116
Aq. dist. (cold d.H_2O)**	32.00 ± 5.45 *	0.0098
Aq. dist. flower extract*	48.25 ± 4.46	0.0017

*Results expressed as mean ± SEM; N = 6; p < 0.05, Aq. dist. = Aqueous distillation; d.H_20 = distilled water; p-value summary * vs control*

IC_{50} values of the *O. sanctum* EtOH (60%, 70%) and aq. dist. leaf extracts (which displayed α-glucosidase inhibitory activities during screening) as well as the IC_{50} of acarbose against *B. stearothermophilus* α-glucosidase were determined from corresponding dose-response curves of percentage inhibition versus inhibitor concentration and are summarised in Table 36. The

lowest IC_{50} was obtained with *O. sanctum* aq. dist. (hot water) extract at 0.089 mg/ml, which, therefore, may display good inhibitory activity at a higher dosage (Appendix 44).

Table 36: Inhibitory effect (IC_{50}) of crude *O. sanctum* extracts on α-glucosidase; IC_{50} concentration of inhibitor to inhibit 50% of its activity

Inhibitory effects of OS extracts and acarbose on α-glucosidase [a]	
Samples	IC_{50} (mg/ml)
Acarbose	0.001
70% EtOH leaf	0.288
60% EtOH leaf	2.566
Aq. dist. whole plant	0.472
Aq. dist. (hot d.H_2O)	0.089
Aq. dist. flower extract	1.894

Results expressed as a % mean ± SEM, N = 2; Key: OS = O. sanctum; Aq. dist. = Aqueous distillation; d.H_20 = distilled water; [a] = The inhibitory activity of OS extracts on α-glucosidase was determined at various concentrations (mg/ml): Acarbose (0.00001-1.0); 70% EtOH (0.0003-0.3); 60% EtOH leaf, GHP method, filtered (0.0002-0.2); Aq. dist. whole plant, GHP method (0.0005-0.5); Aq. dist., hot d.H_2O (0.0003-0.3); Aq. dist. flower extract (0.0002-0.2)

4.6.10 *In vitro* α-glucosidase inhibitory effect of bimetallic (Au-Ag) Nps and AgNps

Inhibitory activities of bimetallic (Au-Ag) Nps (synthesised from *O. basilicum* leaf and flower aq. extracts) and AgNps (synthesised from *O. sanctum* and *O. basilicum* singly and in combination aq. leaf extracts) were tested for their hypoglycaemic activity as a single dose and dose-response at various concentrations at 0.0002 mg/ml - 0.2 mg/ml and 0.0003 mg/ml - 3.0 mg/ml respectively, against *B. stearothermophilus* α-glucosidase.

As shown in Table 37 the bimetallic Nps synthesised from the aq. flower extract demonstrated the highest percentage inhibition against *B. stearothermophilus* α-glucosidase activity at 85.77% ± 5.82%, followed by inhibition from bimetallic Nps synthesised from the aq. leaf extract at 78.62% ± 12.65%. The AgNps leaf extract synthesised from *O. sanctum* aq. leaf extract (89.31% ± 5.319%) and *O. basilicum* aq. leaf extract (79.74% ± 9.51%) also showed higher inhibition compared to control acarbose. However, AgNps synthesised from the combination of extracts (*O. sanctum* + *O. basilicum*) displayed statistically the lowest inhibitory activity at 29.03% ± 15.92% against *B. stearothermophilus* α-glucosidase compared to acarbose, p-value 0.011 (see Figure 35).

Table 37: Inhibitory action of bimetallic (Au-Ag) Nps and AgNps on α-glucosidase activity

Samples	*In vitro* α-glucosidase	p-value

	inhibition % (± SEM) at the concentration of * 0.2 mg/ml, ª 0.3 mg/ml	
Acarbose	73.75 ± 12.86	0.0023
(Au-Ag) Nps OB (leaf) *	78.62 ± 12.65	0.0249
(Au-Ag) Nps OB (flower) *	85.77 ± 5.82	0.0001
AgNps OB ª	79.74 ± 9.51	0.0139
AgNps OS ª	89.31 ± 5.32 *	< 0.0001
AgNps OS+OB ª	29.03 ± 15.92 *	-

Results expressed as mean ± SEM; N = 6; OB = O. basilicum; OS = O. sanctum; p < 0.05 and < 0.01 vs control

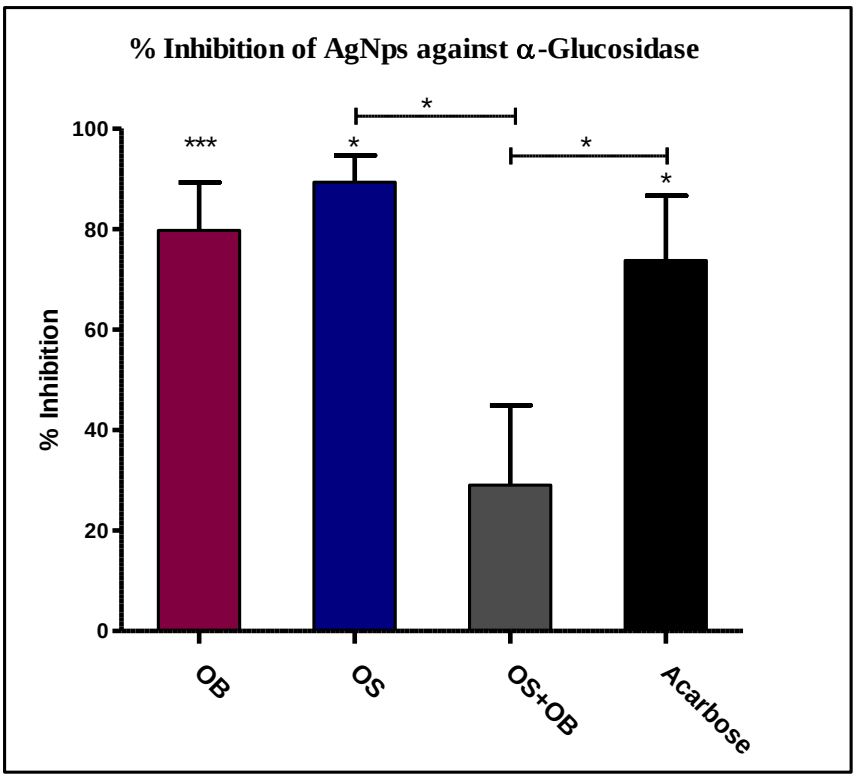

Figure 35: Inhibitory activities of AgNps synthesized from various *Ocimum* sp. extracts at concentration of 0.3 mg/ml and 1 mg/ml acarbose, tested for their hypoglycaemic activity; p-value < 0.05, p-value summary * vs control (acarbose)

The IC_{50} values of bimetallic Nps synthesised from *O. basilicum* leaf and flower aq. extracts and AgNps synthesised from various *Ocimum* sp. extracts (which displayed α-glucosidase inhibitory activities during screening) and the IC_{50} of acarbose against *B. stearothermophilus* α-glucosidase were determined from corresponding dose-response curves of percentage inhibition versus inhibitor concentration and are summarised in Table 38.

Bimetallic (Au-Ag) Nps synthesised from the leaf and flower extracts and AgNps synthesised from *O. sanctum* aq. leaf extracts appeared to be good inhibitors at various concentrations and were similar to that of the reference drug, acarbose (no significant difference between the calculated IC_{50} values) (Appendix 45-46).

Table 38: Inhibitory effect (IC_{50}) of bimetallic (Au-Ag) Nps and AgNps extracts on α-glucosidase; IC_{50} concentration of inhibitor to inhibit 50% of its activity

Inhibitory effects of bimetallic Nps, AgNps, and acarbose on α-glucosidase [a]	
Samples	IC_{50} (mg/ml)
Acarbose	0.001
(Au-Ag) Nps OB (leaf)	0.004
(Au-Ag) Nps OB (flower)	0.001
AgNps OB	1.533
AgNps OS	0.009
AgNps OS+OB	NI

Results expressed as a % mean ± SEM, N = 3; Key: OS = O. sanctum; OB = O. basilicum; [a] = Inhibitory activity of bimetallic Nps and AgNps on α-glucosidase was determined with various concentrations: bimetallic (Au-Ag) Nps at (0.0002-0.2 mg/ml) and for leaf and flower, respectively and AgNps OB, OS and OS+OB at a concentration (0.0003-3.0 mg/ml)

4.6.11 Mode of inhibition of bimetallic (Au-Ag) Nps, AgNps and their respective crude extracts on α-glucosidase activity

Mode of inhibition of the *O. basilicum* crude extracts, bimetallic (Au-Ag) Nps synthesised from the leaf and flower extracts (2.5 mg/ml) and AgNps (3.0 mg/ml) on the activity of α-glucosidase was determined by means of Lineweaver-Burk plot (double reciprocal) analysis of data according to Michaelis-Menten kinetics.

As shown in Figure 36, the mode of inhibition of bimetallic (Au-Ag) Nps synthesised from *O. basilicum* leaf extract on α-glucosidase was found to be competitive (K_m is increased whereas V_{max} remain the same). Furthermore, Figure 37 illustrates the mode of inhibition of bimetallic Nps synthesised from *O. basilicum* flower extracts on α-glucosidase and displayed uncompetitive inhibition (K_m is decreased and V_{max} is decreased).

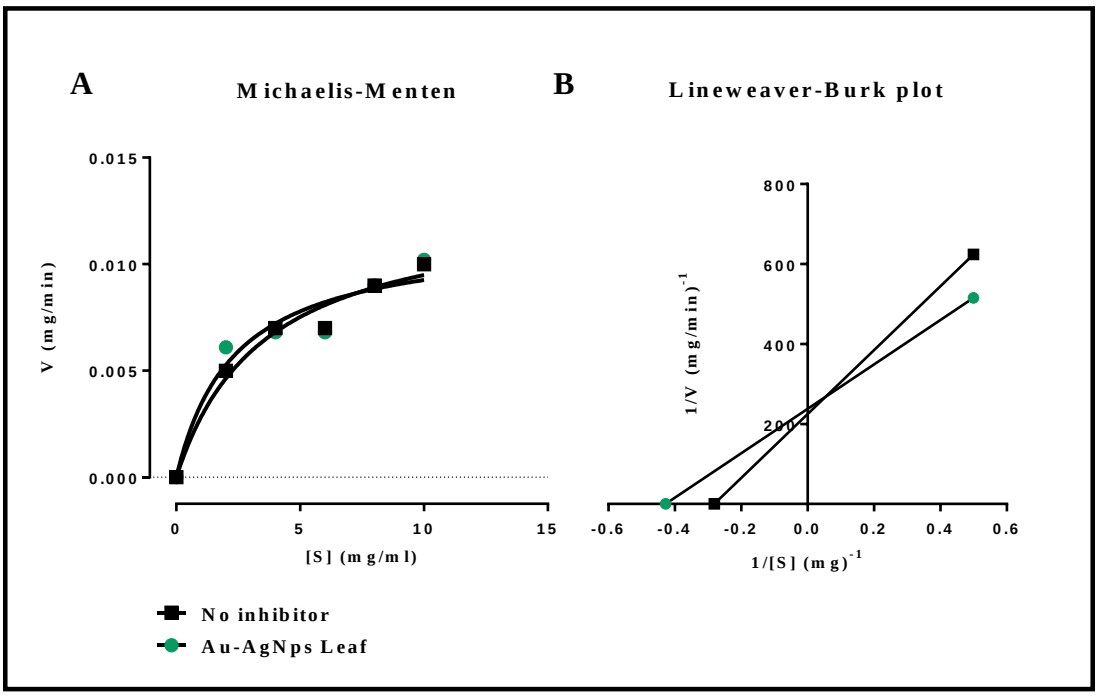

Figure 36: (A) Michaelis-Menten and (B) Lineweaver-Burk plot of the activity of α-glucosidase in the absence or presence of the bimetallic (Au-Ag) Nps synthesised from *O. basilicum* leaf extract

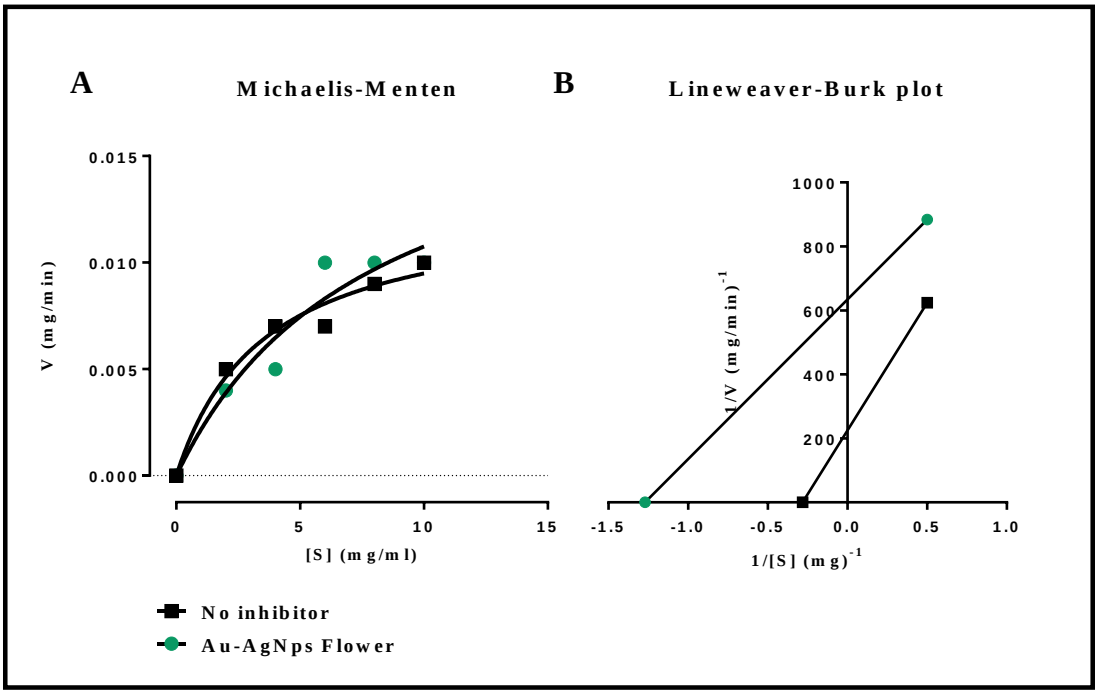

Figure 37: (A) Michaelis-Menten and (B) Lineweaver-Burk plot of the activity of α-glucosidase in the absence or presence of the bimetallic (Au-Ag) Nps synthesised from *O. basilicum* flower extract

The mode of inhibition for the AgNps synthesised from *O. sanctum* aq. leaf extract displayed inhibition in a competitive manner against α-glucosidase activity (K_m is increased whereas

V_{max} remain the same); notably, for the AgNps synthesised from *O. basilicum* aq. leaf extracts against α-glucosidase activity, inhibition also appeared to be in a competitive manner (Figures 38 and 39.

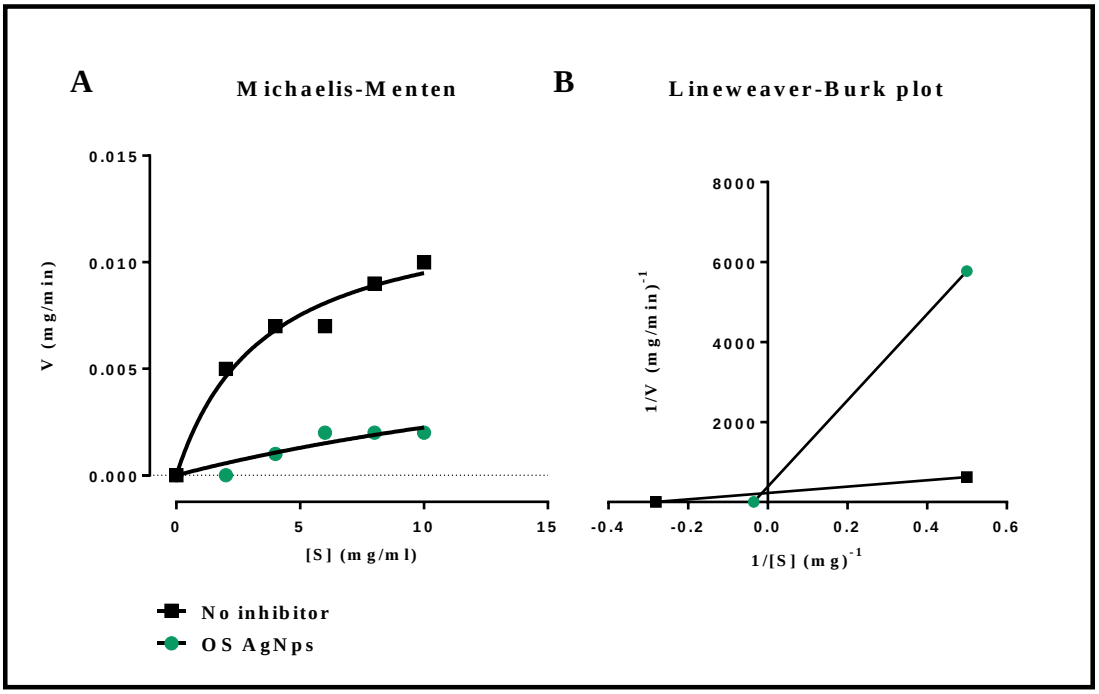

Figure 38: (A) Michaelis-Menten and (B) Lineweaver-Burk plot of the activity of α-glucosidase in the absence or presence of the AgNps synthesised from *O. sanctum* leaf extract

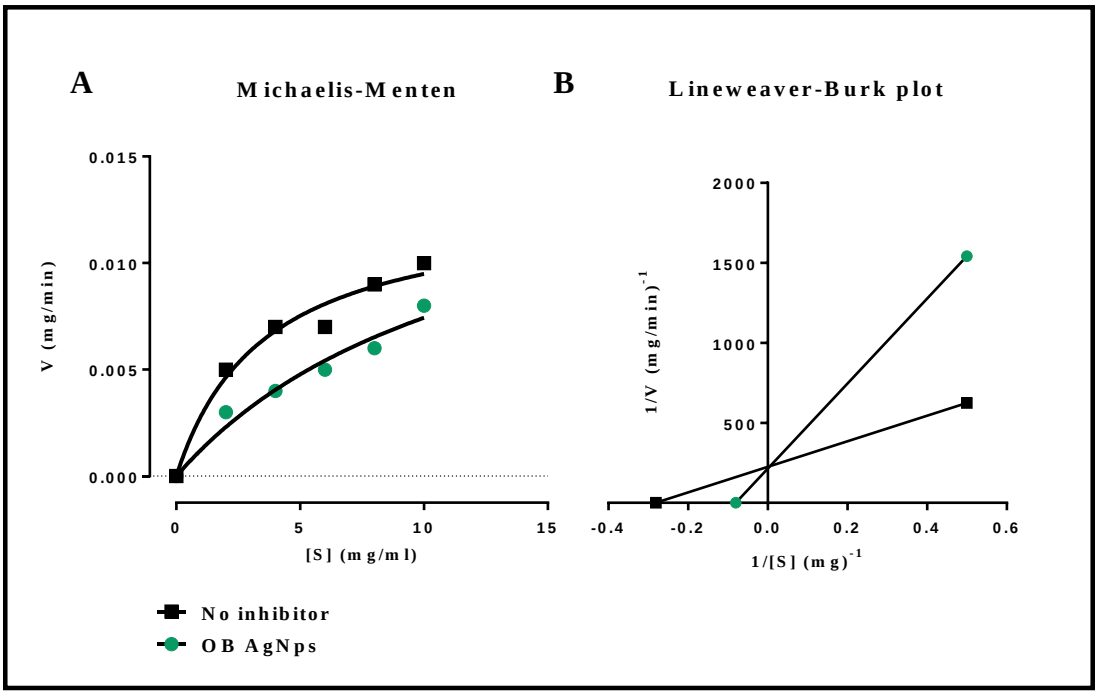

Figure 39: (A) Michaelis-Menten and (B) Lineweaver-Burk plot of the activity of α-glucosidase in the absence or presence of the AgNps synthesised from *O. basilicum* leaf extract

The crude *O. basilicum* and *O. sanctum* 70% EtOH leaf extracts displayed high inhibition against α-glucosidase (see Tables 32 and 34) so were used to determine their modes of inhibition. The crude *O. sanctum* 70% EtOH extracts was found to be a close competitive inhibitor (K_m is increased whereas V_{max} remain the same) (Figure 40). Moreover, the crude *O. basilicum* EtOH (70%) extract displayed inhibition in an uncompetitive manner against α-glucosidase activity (K_m is decreased and V_{max} is decreased) (see Figure 41).

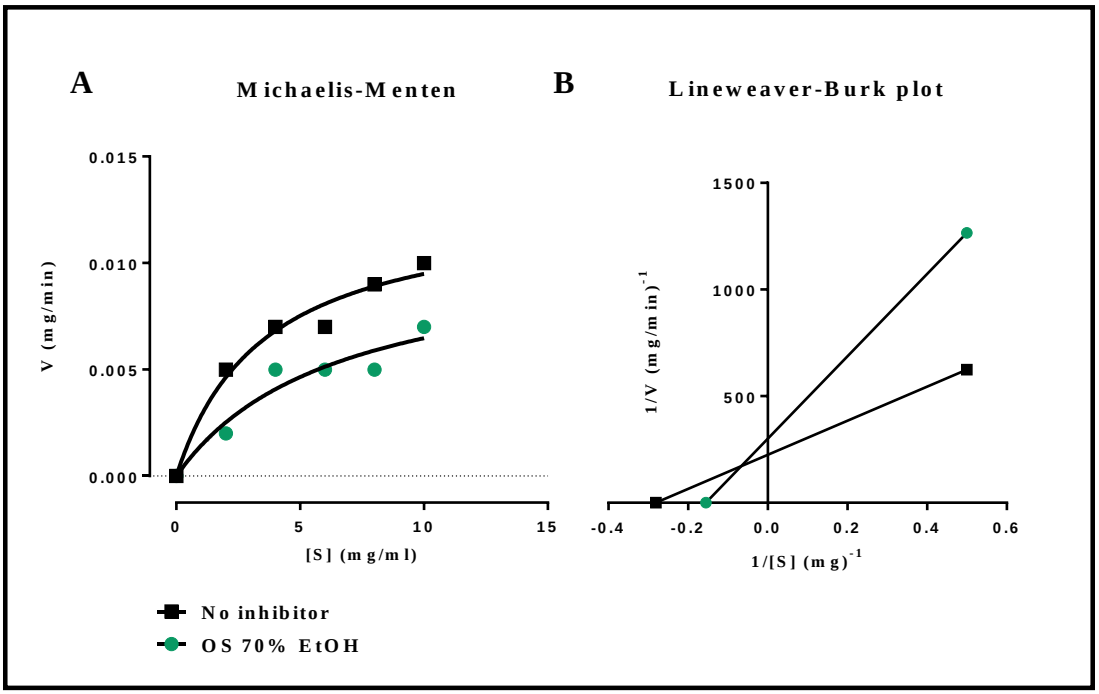

Figure 40: (A) Michaelis-Menten and (B) Lineweaver-Burk plot of the activity of α-glucosidase in the absence or presence of the crude *O. sanctum* EtOH (70%) leaf extract

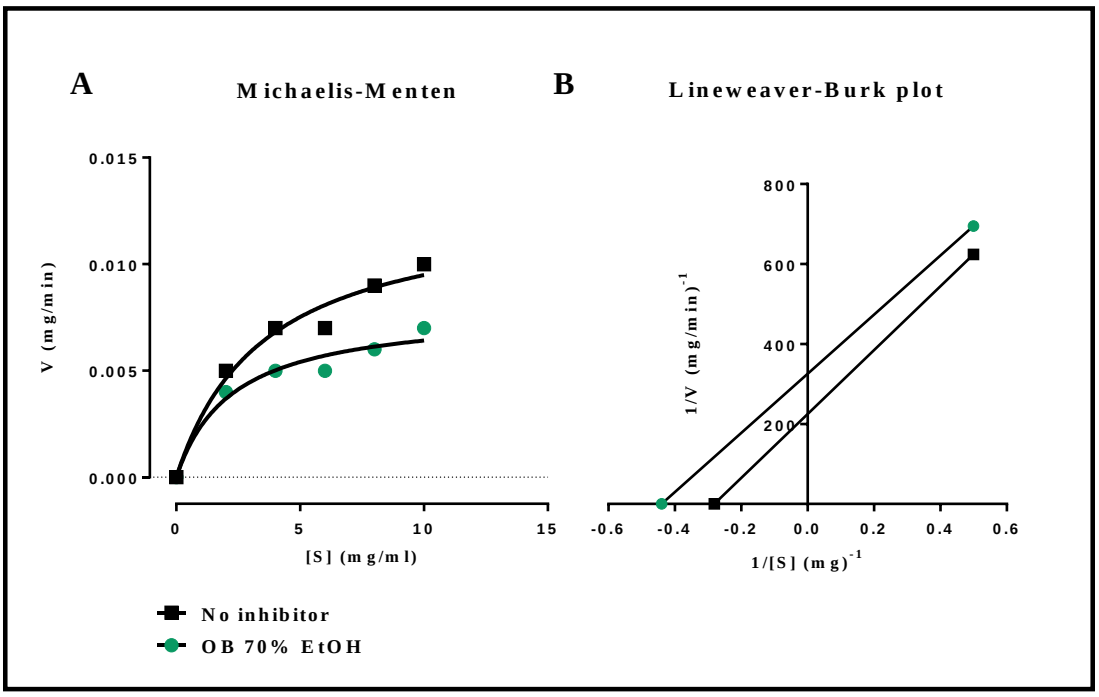

Figure 41: (A) Michaelis-Menten and (B) Lineweaver-Burk plot of the activity of α-glucosidase in the absence or presence of the crude *O. basilicum* EtOH (70%) leaf extract

CHAPTER 5 : DISCUSSION

5.1 Extraction and phytochemical profiles of *O. basilicum* and *O. sanctum*

Plant extracts for traditional remedies to treat certain diseases are more likely to contain biologically active compounds of medicinal interest (Hannan *et al.* 2006; Tchoumbougnang *et al.* 2006; Singh *et al.* 2012). Medicinal plants contain a variety of phytochemical compounds with different polarities and hence different solubility properties (Devendran and Balasubramanian 2011; Lee *et al*. 2005). The most popular herbal remedies prepared by traditional practitioners are aq. based extracts for the treatment of various ailments (van Huyssteen 2007) whereas the majority of published research report the use of two or more polar and non-polar solvents for the extraction of bioactive compounds from medicinal plants (Benny and Adithan 2000; Hannan *et al.* 2006; Govender 2011; Joshi *et al.* 2011; Mogale *et al.* 2011).

In the present study, water and ethanol were selected to extract bioactive compounds from the leaves and flowers of *O. basilicum* and *O. sanctum*. In general, ethanol is known to extract high polar compounds such as flavonoids, tannins and glycosides. On the other hand, water is known to extract carbohydrates, amino acids, polypeptides, phenolic acids, phenylpropanoids, flavonoids, glycosides and alkaloids (Bruneton, 1999).

In two phytochemical investigations into the *O. basilicum* leaf plant examination, the presence of tannins, steroids, terpenoids, flavonoids and cardiac glycosides were identified (El-Beshbishy and Bahashwan 2012; Usman *et al.* 2013). Jaiganesh *et al.* (2012) observe that the findings regarding chemical compounds from *O. basilicum* leaf extracts have varied over time (history) and location, with earlier phytochemical studies in India revealing the presence of squalene; phenol,2-methoxy-4-(1-propenyl)-[Isoeugenol]; caryophyllene oxide; nonadecane; decane,2,9-dimethyl-; linolenic acid, ethyl ester and hexadecanoic acid ethyl ester as the main constituents. Plants grown in north central Nigeria showed a higher consistency of linalool; 1,8-cineole; borneol; eugenol and α-caryophyllene (Usman *et al.* 2013). Some of the phytochemicals present in *O. basilicum* are believed to be responsible for blood glucose lowering and antimicrobial effects (El-Beshbishy and Bahashwan 2012; Duthie

et al. 2000). The phytochemical screening for the current study indicated the presence of phenols and terpenes in the *O. basilicum* EtOH leaf extracts (Table 3) whereas, polyphenols, flavonoids, terpenoids, esters and carbohydrates were present in the aq. leaf and flower extracts (Figure 12-13). The presence of terpenes and phenolic compounds in *O. basilicum* EtOH and aq. extract are in agreement with the results of previous studies (Usman *et al.* 2013). Some examples of terpenoids include methanol and camphor (monoterpenes) which are reported to be active against bacteria (Rotblatt and Zimet 2002). In addition, *O. basilicum* aq. extracts are rich in phenolics and flavonoids which are known to exhibit antioxidant potential (Lee *et al.* 2005).

Although essential oils in different *Ocimum* sp. remain variable, prevalent components are phenylpropanoids and monoterpenes (Rahman *et al*. 2011). *O. basilicum* contains primarily phenoyl derivatives, such as eugenol, methyleugenol, chavicol, estragole, methyl-cinnamate and are often combined with various amounts of linalool (Labra *et al.* 2004). Others, including *O. sanctum* contains primarily eugenol, camphor, linalool, phytol, carvacrol, caryophyllene, decylaldehyde, nerol, α-pinene, α-selinene, cirsilineol, cirsimartin, isothymusin, isothymosin and tannins or flavanoids such as luteolin, orientin, vicenin; triterpenoids such as ursolic acid and fixed oils such as palmitic, stearic, oleic, linoleic, linolenic acids (Kelm *et al*. 2000). In previous phytochemical studies, several compounds have been demonstrated to be responsible for the hypoglycaemic and antimicrobial effects of *O. sanctum* (Chopra *et al.* 1992; Govind and Madhuri 2010; Joshi *et al.* 2011) including leaf and stem extracts rich in alkaloids, tannins (Sudha *et al*. 2011; Joshi *et al*. 2011), glycosides, saponins, terpenoids, triterpenoids, steroids (Joshi *et al*. 2011), flavonoids (Sudha *et al*. 2011), ascorbic acid, carotene, polyphenols, fatty acids and sitosterol, sugars (xylose and polysaccharides), pectins, sesquiterpene and monoterpenes which all display antidiabetic and antimicrobial potential (Kelm *et al*. 2000). In particular, linalool was identified as the most active constituent of *O. sanctum* aq. extract to display prominent antioxidant activity (Khan *et al.* 2010; Hussain *et al.* 2008).

In the current study, amide compounds were identified in *O. sanctum* leaf aq. extract namely, cis-11-eicosenamide, 8-methyl-6-nonenamide, 13-docosenamide, (13z)-n-([(13z)-13-docosenoylamino] methyl)-13-docosenamide. In the *O. sanctum* EtOH leaf extracts, linalool, camphor, phytol acetate, squalene and palmitaldehyde were identified. The bioactive compounds identified from *O. sanctum* the leaf and flower extract were consistent with those

previously published in which chemical components were isolated using various types of organic solvent extraction (Kothari *et al.* 2004).

In accordance with previous studies *O. basilicum* and *O. sanctum* variability in chemical composition of the current study is dependent on the selection of extractant, extraction techniques (Eloff 1998), climatic and geographical conditions of the parent plant (Saha *et al.* 2013; Carović-Stanko *et al.* 2011). Furthermore, from a comparative perspective, the crude extract composition of *O. sanctum* appears to be different from *O. basilicum*, similar to previous studies (Vani *et al.* 2009). As a result the biological activity and characterisation of the synthesised bimetallic (Au-Ag) Nps and AgNps from the respective plants appeared to be remarkably different, which is further discussed.

5.2 Synthesis and characterisation of bimetallic (Au-Ag) Nps and AgNps synthesised from various *Ocimum* sp. aq. leaf and flower extracts

Nanobiotechnology is an important field of study, especially in countries such as South Africa that give high priority to its biodiversity of plants (Gengan *et al.* 2013). The advances in phyto-nanotechnology have allowed the medicinal properties of *O. sanctum* and *O. basilicum* to be further enhanced due to the rich source of bioactive molecules or secondary metabolites that contribute to plants' unique capacity for metal tolerance. To overcome the problem of toxicity in synthesis, $AgNO_3$ and chloroauric acid solution were prepared in water. Water is a highly polar solvent which is suitable for extraction of highly polar compounds, particularly reducing agents (with high polar functional groups such as amine and OH groups) and not so suitable for extraction of lower polar hydrocarbons. For noble metal Nps, the metal salts and reducing agents are, in general, water-soluble, which is ideal for synthesising water-soluble particles. Additionally, aqueous synthesis is preferable as it is straightforward, homogenous and more "green" (Sathishkumar *et al.* 2009). Previous reports suggest that important phytochemicals such as proteins, amino acids, vitamins, polysaccharides, polyphenols, terpenoids and organic acids present within specific plants sustain and potentiate the formation of Nps, thus enhancing medicinal applications thereafter (Mallikarjuna *et al.* 2011).

The current study is the first time the formation of alloyed bimetallic (Au-Ag) Nps has been studied using *O. basilicum* leaf and flower aq. extracts as the reducing, stabilising and bio-capping agents. The reduction of Ag^{+} was instantaneous and Au^{3+} was revealed after 10 mins

as shown by a stable light violet colour at room temperature suggesting a higher reaction rate than chemical methods previously used in the synthesis of Ag/Pd Nps (Adekoya *et al.* 2014). The consequent colour change from brown to a violet colour confirmed the synthesis of alloyed bimetallic (Au-Ag) Nps (Figures 6 and7).The reaction was monitored by UV-Vis spectroscopy at different time intervals (12 h, 24 h and 36 h). A well-defined absorption peak was obtained at 557 nm from the leaf extract and 534 nm from the flower extract as exhibited by the nanometallic Au-Ag particles. A similar increase in SPR intensity and a decrease in SPR width was reported by Amendola *et al.* (2010). Since the reported synthesis of Au-Ag Nps involves the slow addition of *O. basilicum* extract, it was expected that continuous formation of Au-Ag Nps would occur throughout this process. The sigmoidal nature of the reaction time plot suggests the formation of Nps in the reaction path (Figures 8 and 9). However, the increase in absorbance from 300 nm to 700 nm with peaks indicates that formation of Au-Ag Nps occurred early in the reaction. Similar UV-Vis spectra results have been ascertained in the case of the plasmonic properties and stabilising effects of natural biological extracts in formation of bimetallic (Au-Ag) Nps (Sheny *et al.* 2011; Shankar *et al.* 2004; Kumari *et al.* 2015). Many of the proposed mechanisms of Nps formation, including those of Noruzi (2015) indicate that Nps is formed by a combination of growth processes or mechanisms (McKenzie 2009). Therefore, for greater efficiency of the reaction, a higher concentration of *O. basilicum* aq. leaf or flower extract may facilitate the reduction of Au and Ag precursors in a shorter time-scale. The result from EDX analysis indicated a series of peaks at several areas in the spectra of Au and Ag elements in the colloidal suspension of *O. basilicum* leaf and flower derived Nps (Figures 10-11 (B)), thus providing evidence to demonstrate that the Nps are bimetallic. From the EDX, the metallic silver nanocrystals showed a typical optical absorption peak at 2.983 keV due to SPR and line energies for gold at 9.712 keV, therefore confirming the reduction states of $Ag^{+} \rightarrow Ag^{0}$ and $Au^{3+} \rightarrow Au^{0}$. In some cases, the formation of alloy-type Au/Ag bimetallic Nps have been characterised successfully using EDX analysis (Menezes *et al.* 2012; Castro-Longoria *et al.* 2011).

Most green synthesis protocols look at synthesising AgNps exclusively with a view to their antimicrobial medicinal value. In the current study colloidal AgNps were synthesised combining the inherent properties of silver and a phytochemical mixture made up of various *Ocimum* sp. aq. leaf extracts, with a view to enhanced antidiabetic application. A promising result of the synergistic inhibitory activity of the combination of *O. sanctum* + *O. basilicum* (methanol, hexane and hydro-distillate) extracts was previously demonstrated for an α-

amylase enzyme model (Khair-ul-Bariyah *et al.* 2012), therefore a study on the effect AgNps synthesised from the combined extracts was warranted. Additionally, in view of the observed differences in the GC-MS analysis of *O. sanctum* and *O. basilicum* leaf extract, a study involving the characterisation analysis of the synthesised Nps was also justified.

Although there are several physical, chemical and biological methods for synthesis of colloidal AgNps prepared from plant extracts as reducing agents, the current study reports the antidiabetic and antibacterial efficacy of AgNps derived from *O. basilicum* and *O. sanctum* singly and in combination (*O. sanctum* + *O. basilicum*) aq. leaf extracts. The reduction of silver nitrate led to the formation of AgNps within a few minutes at room temperature, suggesting a higher reaction rate than with high thermal energy or chemical methods (e.g., $NaBH_4$, sodium citrate) which are conventionally used for synthesis (Wang *et al.* 2005; Zhang *et al.* 2010).

In this work, AgNps synthesised from *O. basilicum* extract has more intensity and sharper plasmonic resonance (Figure 17) than AgNps derived from *O. sanctum* extract (Figure 18). Figure 19 shows a small overlap between SPR in the particles, this is due to the different dielectric properties and to the electromagnetic interactions between particles (stabilising molecules) in close proximity that may induce significant broadening of the bands for the AgNps derived from *O. sanctum* aq. leaf extract and the combination of aq. leaf extracts. These results demonstrated that the SPR is affected by the effect of shape, size, structure and assembly of AgNps (Table 39) (Amendola *et al.* 2010).

Table 39: Effect of particle (AgNps) assembly

Samples	Peak wavelength (nm)	Maximum size (nm)	Shape
AgNps OB	438	17 ± 8.94	spherical
AgNps OS	439	15 ± 12.34	spherical
AgNps OB + OS	433	17 ± 8.44	spherical

Key: OB = O. basilicum; OS = O. sanctum

Previous reports indicate the size properties of AgNps derived by green chemistry methods are dependent on the concentration of plant extract and the silver metal ions (Dubey *et al.* 2010). In this study the size properties of the combined *O. sanctum* + *O. basilicum* extracts appeared to decrease with an increase in leaf extract concentration. This findings was supported by the findings regarding surface morphology (Appendix 16 (B)) and the stability of the derived AgNps at -24.3 mV in the zeta potential analysis (Appendix 21 (B)). Many reports have proposed that surface active molecules can stabilise the Nps and the reaction

against the metal ions is possibly facilitated by reducing sugars and/or terpenoids (Song and Kim 2009).

Nanobiotechnology provides an avenue for understanding of living plant cells and molecular level interactions of phytochemicals for more efficient synthesis of metal Nps. The green synthesis of Nps using plant extracts is highly advantageous as medicinal plants such as *O. basilicum* and *O. sanctum* contain an orchestra of chemical compounds that work together in a dynamic way as they act synergistically to allow active compound bioavailability to produce maximal therapeutic efficiency that is less toxic. The interaction of Nps with biomolecules of *Ocimum* sp. leaf extracts validated the reduction of Ag^{+} ions to Ag^{0} and Au^{3+} to Au^{0} by the secondary plant metabolites that are oxidised to other species. Although phytochemical analysis in different *Ocimum* sp. shows variability, common components such as phenylpropanoids, monoterpenes (Labra *et al.* 2004) and other phenol derivatives can act as natural reducing agents.

Organic molecules such as carotenoids, vitamins, minerals, amino acids, sterols, glycosides, alkaloids, flavonoids, terpenes and phenolics can also act as metal surface active molecules responsible for the stability and the formation of alloy bimetallic (Au-Ag) Nps and AgNps (Huang *et al.* 2007; Bakkali *et al.* 2008). FT-IR in combination with GC-MS confirmed that phenolic (Appendix 23) and amine functional groups (Appendix 26 (A-B)) adhered to the surface of the nanoparticles. This is important in order to achieve the consistency of synthesis of bimetallic (Au-Ag) Nps using *O. basilicum* aq. leaf and flower extracts, and the synthesis of AgNps using various *Ocimum* sp. aq. leaf extracts.

5.3 *In vitro* antibacterial activity of aq. *Ocimum* sp. extracts, bimetallic (Au-Ag) Nps and AgNps

Extracts derived from *Ocimum* sp. have been used traditionally and commercially for their profound antibacterial and antifungal properties, specifically *O. sanctum* (Singhal *et al.* 2011) and *O. basilicum* (Jaiganesh *et al.* 2012). The diverse chemical composition presented within *Ocimum* sp. and being rich sources of phenolic (-OH) compounds contribute to the medicinal properties of these plants. Compounds with antimicrobial value include phenols, terpenoids, flavonoids, carbohydrates, tannins and quinones (Nsele 2012). In the current study, the green synthesis of bimetallic and AgNps capped with these important phytochemicals contribute to the enhanced properties of the phytochemical mixture. This is especially significant in the

battle to overcome antimicrobial resistance while at the same time increasing the beneficial outcomes and lowering toxicity to humans (Lokina *et al.* 2014).

In the present study, vancomycin (30 µg) was used as a positive control for the Gram positive bacterial species *S. aureus* and gentamycin (10 µg) was used as the positive control for the Gram negative bacterial species *E. coli*, *P. aeruginosa*, *Salmonella* sp. and *B. subtilis*. The crude 10% aq. *O. sanctum* and *O. basilicum* extracts showed no inhibition possibly due to the low concentration of the aq. solution (see Tables 17 and 21). The intermolecular interactions of the *O. basilicum* and *O. sanctum* aq. leaf and flower extract may have lost functionality when interacting with the outer and inner proteins on the surface of the bacterial cells, as found with *B. subtilis*, *E. coli*, *P. aeruginosa*, *Salmonella* sp. and *S. aureus*. It is important to take into consideration that, besides the outer and inner cell wall, other mechanisms are involved in the functioning of bacteria such as enzymes, proteins, cytoplasm, nuclei and other biomolecules that may have negatively influenced the inhibitory action of the crude extracts or controls (Losasso *et al.* 2014).

Bimetallic (Au-Ag) Nps synthesised from *O. basilicum* leaf extracts and AgNps synthesised from *O. sanctum* displayed significant antibacterial properties against the test strains compared to the individual aq. crude extracts. The highest antibacterial activity was observed with bimetallic (Au-Ag) Nps (derived from *O. basilicum* aq. leaf extract) against *S. aureus* (6.167 mm ± 0.601 mm), *P. aeruginosa* (5.167mm ± 0.167 mm), followed by *E. coli* (3.333 mm ± 0.211 mm). Previous studies have demonstrated that various AgNps synthesised from *Ocimum* sp. displayed significant antibacterial potency. AgNps synthesised from *O. sanctum* aq. leaf extract displayed the highest inhibition against *E. coli* (6.000 mm ± 1.033 mm) and *S. aureus* (6.333 mm ± 1.174 mm). Similar results were obtained from *O. sanctum* AgNps synthesised by the green route which were found to be highly toxic to clinically isolated bacterial and fungal species (Rout *et al.* 2012).

Previous research in the green mediated synthesis of AgNps and AuNps displayed similar activity against *P. aeruginosa* (Amirulhusni *et al.* 2012), *S. aureus* (Rai *et al.* 2010; Jagtap and Bapat 2013), *E. coli* (Rai *et al.* 2010; Vijayan *et al.* 2014), *Bacillus* sp. and *Salmonella* sp. (Krishnamoorthy and Jayalakshmi 2012), so it is evident that many plants that exhibit natural reducing properties when used to synthesise Nps may produce enhanced antibacterial activity (Jagtap and Bapat 2013).

A distinct inhibitory effect was observed from AgNps derived from *O. basilicum* and AgNps derived from the combination of extracts (*O. sanctum* + *O. basilicum*) against Gram negative *Salmonella* sp., compared to against *E. coli* and *P. aeruginosa* (Table 21). The AgNps synthesised from *O. basilicum* alone and in combination indicated different physiochemical properties which is mainly due to the various plant molecules capping the surface of the metal Np, confirmed via GC-MS (Tables 2 and 3, and 8-10) and FT-IR (Figures 23 and 25). The variety of plant molecules may induce varied chemical forms, toxicity mechanisms, size of particles and surface areas, with specific shapes and dimensional range playing a prominent role in their biological activity (Losasso *et al.* 2014). Gram negative bacteria consist of chemical components in the cell wall structure (lipopolysaccharide or lipoproteins), antigens, virulence factors and varied genomes that contribute to its pathogenicity, as is the case in *E. coli*, *P. aeruginosa* and *Salmonella* sp. In the present study, different antibacterial activities were observed in relation to *E. coli* and *P. aeruginosa* compared to *Salmonella* sp. which may be due to the interaction with the AgNps capped with the phytochemicals derived from *O. basilicum* and the combined extracts (*O. sanctum* + *O. basilicum*), resulting in a failed attempt to destabilise *Salmonella* sp. outer membrane barrier components such as lipopolysaccharide or the inner membrane. Therefore, examination of the dose dependent effect of AgNps (in the size range of < 15 nm) on Gram negative bacteria is recommended for further studies.

The surface functionalities of AgNps derived from the combined aq. leaf extracts (*O. sanctum* + *O. basilicum*) may also explain the lack of permeation into the bacterial cell which would have led to cell death. The zeta potential analysis presented the stability of the AgNps synthesised from *O. sanctum* + *O. basilicum* at -24.3 mV. This value indicates that AgNps carry a negative charge which can easily interact with positively charged protein molecules present in the bacterial cell membranes but not so easily Gram negative charged bacteria (Sondi and Salopek-Sondi, 2004). The present study indicates that intermolecular interactions by the two distinct plants may have lost functionality when interacting with the outer and inner proteins on the surface of the bacterial cells as in the case of *Salmonella* sp. It is also important to take into consideration that, besides the outer and inner cell wall, other mechanisms are also involved in the functioning of bacteria such as, enzymes, proteins cytoplasm, nuclei and other biomolecules that may have negatively influenced the inhibitory action of the AgNps.

The antimicrobial activity of silver colloid Nps are well known, due to their small sizes and high surface to volume ratios which enhance the interaction with microbes to carry out greater antimicrobial activities (Morones *et al.* 2005). The small sizes of the Nps play a central role in the interaction with and penetration into bacterial cells and exhibit higher antibacterial activity than particles larger than the bacterial cells. The colloidal silver particles, with variable sizes (17 nm, 15 nm and 17 nm) (Appendix 14-16), synthesised from *O. basilicum* and *O. sanctum* singly and in combination, demonstrated higher particle penetration with smaller size. The antibacterial activity was thus particle size dependent.

Previous studies indicate that the bactericidal properties of the most exploited AgNps can be explained by the release of reactive and charged silver ions from particles (Rout *et al.* 2012), causing bacterial cells damage in two ways. Firstly by adhering to the bacterial cell wall causing disruption in cell wall permeability and cellular respiration (Singhal *et al.* 2011), and secondly by causing damage through interaction with phosphorus and sulphur containing compounds such as deoxyribonucleic acid (DNA) and proteins (Krishnamoorthy and Jayalakshmi 2012). In view of these facts the bactericidal properties of the bimetallic and AgNps in the current study may have due to these factors.

AgNps derived from *O. sanctum* aq. leaf extract displayed better overall antibacterial activity against all the bacterial sp. compared to bimetallic Nps (*O. basilicum* aq. leaf). It demonstrated activity against Gram negative and Gram positive bacteria with the exception of *Salmonella* sp. The bimetallic (Au-Ag) Nps (*O. basilicum* aq. flower) failed to display antibacterial activity against *E. coli*, *B. subtillis* and *Salmonella* sp. The antibacterial properties of AgNps (reactive silver particles) and bimetallic (Au-Ag) Nps (silver particles + gold particles) may result in destruction of Gram negative and Gram positive bacteria based on the charge they carry and the variation in microbial cell wall composition (Mubarak *et al.* 2011).

The concept of synergy strives to investigate the mechanisms of interaction between herbal ingredients and synthetic drugs, based on their pharmacokinetics or pharmacodynamics (Rai *et al.* 2012). Ironically, the sceptical stance adopted by many scientists regarding plant polypharmacy is contradicted by the common medical practice of combining synthetic drugs with medicinal plants to treat a wide range of serious diseases like cancer (chemotherapy) (Nikolaeva-Glomb and Galabov 2004), HIV/AIDS, TB, malaria, diabetes, hypertension (McIntyre 2012). Several synergistic antibiotic mediated syntheses have been researched for

their antimicrobial coatings and favorable effects thereof provide new choices for treatment of infectious diseases such as MRSA etc. (Rai *et al.* 2010; Grace and Pandian 2007; Sondi and Salopek-Sondi 2004; Zhao *et al*. 2011; Li *et al*. 2005; Fayaz *et al.* 2010; Dar *et al.* 2013; Huh and Kwon 2011). This research is particularly important due to the growing issue of multi-drug resistance (Ahmad and Beg 2001). Combination therapy using nanomaterials can attain the same or greater therapeutic effect with fewer deleterious side effects when a single drug is no longer effective (McIntyre 2012). Clearly, bio-capping metal Nps with the functional groups of *Ocimum* sp. proved to be beneficial to minimise the dose needed for total antibacterial reduction of *P. aeruginosa*, *E. coli*, *Salmonella* sp. and *S. aureus*.

5.4 *In vitro* inhibitory effects of *Ocimum* sp. crude extracts, bimetallic (Au-Ag) Nps and AgNps on α-amylase and α-glucosidase activity

Control of PPHG is an important strategy and a relevant therapeutic approach to the management of diabetes, specifically Type 2 diabetes mellitus (Nguyen *et al.* 2011; Elya *et al.* 2012). The enzyme activity of human pancreatic α-amylase and α-glucosidase in the small intestine correlates to an increase in postprandial glucose levels (Sudha *et al.* 2011). After a mixed carbohydrate diet pancreatic α-amylase catalyses the initial step in hydrolysis of starch to a mixture of smaller oligosaccharides consisting of maltose, maltotriose and a number of α-(l-6) and α-(1-4) oligoglucans that are ultimately converted to monosaccharides by α-glucosidase and further degraded to glucose (Sudha *et al.* 2011). Liberated glucose is absorbed by the gut, enters the bloodstream and results in high blood glucose levels (PPHG) (Nickavar and Yousefian 2009). Thus, the inhibition of α-amylase (Funke and Melzig 2006) and the inhibition of α-glucosidase (Subramanian *et al.* 2008) have been targeted as potential avenues for modulation of PPHG in diabetic patients, through mild inhibition of the enzymatic breakdown of complex carbohydrates thereby decreasing meal-derived glucose absorption (McCue *et al.* 2005) so that glucose levels in the blood can more easily return to normal limits.

The results obtained in this study are consistent with previous research confirming the hypoglycaemic properties of crude *O. basilicum* (El-Beshbishy and Bahashwan 2012) and *O. sanctum* extracts (Chattopadhyay 1993) using a variety of extraction techniques. Both plants (*O. basilicum* and *O. sanctum*) exhibited higher inhibitory activity at a lower concentration (Tables 27 and 28) towards the enzymes than many other plants reported in previous studies. Further evidence in support of this statement was revealed in an *in vitro* model investigating

the inhibitory effect of α-amylase enzyme at a concentration of 36.0 mg/ml (*A. akaka*, 67.48% ± 0.26%; *A. ampeloprasum* subsp. *iranicum*, 48.36% ± 0.35%; *A. sativum*, 54.96% ± 0.40%; *A. hirtifolium*, 33.29% ± 0.35%) (Nickavar and Yousefian 2009; Mukherjee *et al.* 2006). In another *in vitro* study involving the inhibitory effect of α-glucosidase enzyme at a concentration of 0.1 mg/ml the extract *C. zeylanicum* demonstrated 38.46% ± 0.00% inhibition (Nair *et al.* 2013).

In comparison, first time *in vitro* hypoglycaemic assessment of bimetallic and AgNps derived from *Ocimum* sp. indicate possible enhanced activity by varying the doses, and displayed greater biological activity than their crude extracts and acarbose (Tables 29, 30 and 38). The increased activity results from the Nps high surface areas to volume ratios that may be correlated to the increased surface area phenomenon (promotes electron transfer reaction) and may increase the pharmacokinetics from a biological point of view. Further *in vivo* pharmacokinetic studies are encouraged.

The properties of *Ocimum* sp. have long been investigated by means of phytochemical tests, particularly *O. sanctum* (Kothari *et al.* 2004; Tchoumbougnang *et al.* 2006), and *O. basilicum* (Dev *et al* 2011). Thus, it is anticipated that certain plant phytochemicals such as phenolics (McCue and Shetty 2004), flavonoids and other important bioactive compounds which have previously been highlighted (Benalla *et al.* 2010; Lokina *et al.* 2014) were present in the phytochemical mixture with the metal Nps and contributed to the inhibition of α-amylase and α-glucosidase enzymes. The results are very encouraging and the plants *O. sanctum* and *O. basilicum* can be further explored for these lines to develop an appropriate herbal formula to inhibit α-amylase and α-glucosidase enzymes to decrease blood glucose levels in diabetic patients at a lower dosage than acarbose without the associated gastrointestinal effects or abdominal discomfort (Bhat *et al.* 2011; Sudha *et al.* 2011). Such formulae may be explored for their ability to delay other chronic complications associated with diabetes such as cardiovascular disease.

In the present study, the inhibition mode of isolated compounds from α-amylase and α-glucosidase was analysed from the data derived from enzyme assays containing different concentrations of pNPG, ranging from 2 mM to 10 mM in different extracts/Nps. The data indicated that both bimetallic (Au-Ag) Nps synthesised from *O. basilicum* aq. leaf extract and AgNps synthesised from *O. basilicum* aq. leaf extract showed uncompetitive inhibition against α-amylase. The enzyme kinetics reveals that some of the α-amylase inhibitory

components in bimetallic (Au-Ag) Nps and AgNps bind only to the enzyme-substrate complex and may distort the active site. Bimetallic Nps synthesised from the flower extract on α-amylase appeared to be non-competitive (Figure 32), similar to the mode of inhibition of acarbose which can be mixed non-competitive on α-amylase activity as shown in previous studies (Koukiekolo *et al.* 2001).

The inhibitory effect of AgNps synthesised from *O. sanctum* on α-amylase activity was found to be competitive (K_m is increased, whereas V_{max} remain the same). These findings indicate that some of the α-amylase inhibitory components in AgNps derived from *O. sanctum* aq. extract may be structural analogues of the substrates that compete for binding at the active site of α-amylase. The mode of inhibition of bimetallic (Au-Ag) Nps synthesised from *O. basilicum* leaf extracts displayed competitive inhibition of α-glucosidase activity. The crude *O. sanctum* extracts from also displayed close competitive inhibition of α-glucosidase activity, indicating that the bimetallic Nps as well as the crude extracts may be structural analogues of the substrates that compete for binding at the active site of the α-glucosidase enzyme. The mode of inhibition of α-glucosidase activity by crude *O. basilicum* (leaf extract) and bimetallic Nps synthesised from *O. basilicum* flower extracts was demonstrated to be uncompetitive while the mode of inhibition of *O. sanctum* and *O. basilicum* derived AgNps was shown to be competitive. This study has demonstrated that the α-glucosidase inhibitory effects of bimetallic Nps and AgNps synthesised from *O. sanctum* and *O. basilicum* is similar to the inhibitory effects of the standard α-amylase and α-glucosidase inhibitor, acarbose, which competitively and reversibly inhibits α-glucosidase enzymes from the intestine and the pancreas (Kim *et al.* 1999) (Figure 42). Furthermore, the different inhibition kinetics of these Nps and extracts may be due to structural differences formed by the origins of the enzymes (Kim *et al.* 2005).

O. basilicum and *O. sanctum* are the two most important medicinal herbs of the family Lamiaceae (Khair-ul-Bariyah *et al*. 2012). On their own members of this family have been shown to possess notable inhibitory α-amylase and α-glucosidase potential, but in the form of silver and bimetallic (Au-Ag) Nps they have proven to possess dual antidiabetic and antimicrobial properties. Thus, phytonanotherapy can find more effective applications for treating diabetic patients. This phytochemical mixture can be included as a dietary supplement to treat associated diabetic induced infections as well as to inhibit hydrolysis of starch into di- and monosaccharides providing dual relief to diabetic patients.

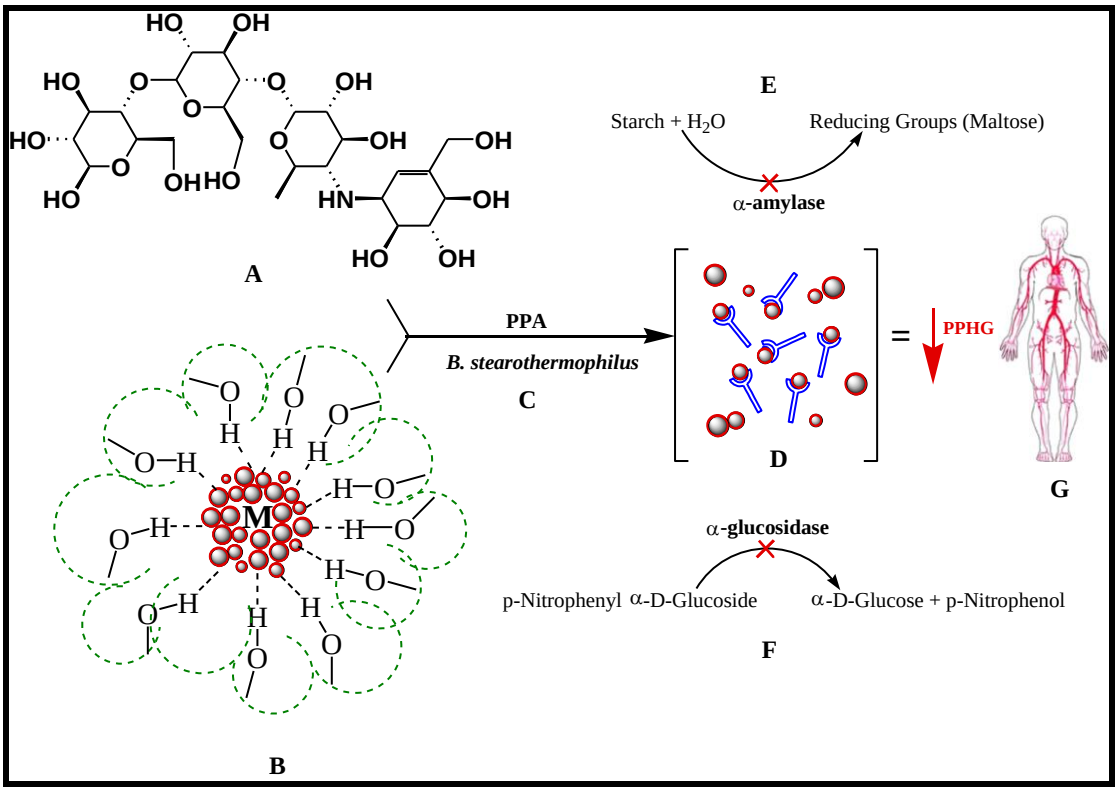

Figure 42: Proposed MOA of silver and bimetallic Nps using *in vitro* catalytic activity of α-amylase and α-glucosidase as a means of evaluation, for modulation of PPHG (Janecek 1994); (A) Acarbose; (B) Phytochemical mixture with Metal Nps (capped with phenolic groups); (C) Catalytic hydrolysis reaction using *in vitro* α-amylase (derived from porcine) and *B. stearothermophilus* as models; (D) Metal-Np-Enzyme composite; (E) Hydrolysis of α-amylase adapted from Bernfeld (1955); (F) Hydrolysis of α-glucosidase adapted from Bernfield (1955); (G) Decrease in PPHG

CHAPTER 6 : CONCLUSION

In conclusion, it is appropriate to assess the extent to which the objectives have been achieved. This project was based on the well-established observation that diabetic patients are very likely to suffer from long-term complications such as bacterial infections and CVDs, and despite years of research, there is still no ideal drug to cure this disease. Diabetic patients are usually treated with contemporary Western medicine over long periods of time and unpleasant side effects have been reported. In recent years, research in phytonanotherapy has emerged with the potential of fewer side effects and are therefore being considered suitable for long-term treatment for various chronic diseases.

The primary focus of this study was to extract various phytochemical compounds of medicinal importance from *O. basilicum* and *O. sanctum* leaf and flower plant parts. Four such methods of preparation, consisting of aq. and ethanol extracts, were utilised in the development process. In the present project, a phytochemical profile was established for the aq. and ethanol extracts from both plants via the GC-MS analysis. Bioactive compounds such as phenolic constituents (menthol), terpenes (linalool), terpenoids (camphor) and various amine compounds (cis-11-eicosenamide) were identified. It would be of great interest to purify and characterise novel compounds from *Ocimum* sp. with potential antidiabetic and antibacterial activity.

The secondary objective was to synthesise bimetallic (Au-Ag) Nps using *O. basilicum* leaf and flower aq. leaf and flower extracts and synthesise AgNps using various *Ocimum* sp. aq. leaf extracts exclusively and in combination, at room temperature. *O. basilicum* and *O. sanctum* extracts can be efficiently used in the synthesis of silver and alloyed bimetallic (silver-gold) Nps via a simple, rapid, non-toxic and eco-friendly green chemistry route. The Nps formation was characterised by spectroscopic techniques such as UV-Vis spectroscopy and the size, morphology and elemental analysis were confirmed by TEM, SEM-EDX and DLS. The stability of the Nps was confirmed by zeta potential. Finally, information gained from the FT-IR combined with that gained from GC-MS identified the biomolecules responsible for the bio-reduction and bio-capping of Nps.

The *in vitro* effects of the plant extracts and Nps on the bacterial species *B. subtilis*, *E. coli*, *P. aeruginosa*, *Salmonella* sp. and *S. aureus* demonstrated that bimetallic and AgNps may be used to target Gram negative and Gram positive induced infections, which are a major problem for diabetic patients with peripheral neuropathy.

Intensive literature reviews have revealed the mechanism by which Gram negative and Gram positive bacterial species may be inhibited by AgNps or bimetallic Nps, namely by disruption of the bacterial cell wall and destruction of bacterial cell DNA; the current study indicated that AgNps and bimetallic Nps antibacterial activity may also be dependent on specific size, shape, charge and the phytochemicals bio-capping the surface of the metal Np.

The most noteworthy result from the *in vitro* antidiabetic study was the ability of the *Ocimum* sp. aq. and ethanol extracts to favour inhibition of diabetic related carbohydrate metabolising enzymes α-amylase and α-glucosidase. This confirms previous literature reports. Moreover, the bio-derived metallic nanoparticles have shown enhanced inhibitory enzymatic activity (on both enzymes) that showed greater inhibitory effects than a standard synthetic inhibitor (acarbose). This outcome prompted the investigation into the mode of inhibition of the various extracts and Nps, another facet important to enzymatic analysis and kinetics.

These favourable results provide impetus for further *in vivo* studies. The use of traditional herbal remedies prepared from various *Ocimum* sp. and phyto-synthesised AgNps and bimetallic (Au-Ag) Nps are unknown and not easily accepted by Western practitioners. Therefore, further scientific and clinical investigations are required before such regimens are implemented.

CHAPTER 7 : RECOMMENDATIONS

The key contribution of this study has been to demonstrate the biosynthesis of silver and bimetallic Nps derived from two *Ocimum* sp. which produced positive enzymatic inhibition. In antidiabetic studies, it is postulated that plants or herbs traditionally used to decrease glucose concentrations in diabetic patients could theoretically precipitate hypoglycaemia if taken in combination with common conventional drugs (Miller 1998). Yet, numerous studies contradict this point (Rai *et al.* 2012), indicating a positive interaction between plants and antidiabetic drugs such as glibenclamide; however, negative drug-herb interactions do need to be considered (Sharma and Kar 2014; Kudolo 2001) (Appendix 47). Therefore, further tests to evaluate the effects of improved antidiabetic controls using conventional drugs and new delivery systems such as phytonanotherapy are necessary. In addition to this, their effect *in vivo* would be expected to be modified by the presence of other enzymes, absorption through the GIT, GIT movement and other physiological processes. Therefore, the actual *in vivo* pharmacological consequence of α-amylase and α-glucosidase inhibition by phyto-synthesised Nps needs to be further characterised.

With respect to understanding the synergistic activity of synthesised Nps in antimicrobial testing, the synergistic activity of cefaclor (second generation drug) (Rai *et al.* 2010) and various aminoglycosidic antibiotics such as streptomycin, gentamycin and neomycin in combination with reduced gold Nps as carrier molecules display potent antimicrobial activity against both Gram positive (*S. aureus*) and Gram negative (*E. coli* and *P. aeruginosa*) bacteria as compared to the individual drug or gold Nps. Thus, future attempts must also be targeted at understanding the role silver and bimetallic (Au-Ag) Nps derived from *Ocimum* sp. can play in the human body as they may also find application to improve drug delivery systems of existing antibiotics or facilitate the transport of antibiotics to the cell surface.

In the current study, a positive synergistic combination was achieved between *O. basilicum* and *O. sanctum*, mediated by stable AgNps, which displayed antibacterial activity and enzymatic inhibition in the antidiabetic screening. Further investigation to isolate the main chemical compounds from each plant for enhanced activity would be another avenue of interest in future studies.

In addition, the potential for reducing oxidative damage leading to diabetic complications using AgNps and bimetallic (Au-Ag) Nps specifically derived from phenolic rich plants such as *Ocimum* sp. is significant, and should be investigated. It is important to note the findings obtained in this *in vitro* study is substrate and condition specific and cannot necessarily be extrapolated to the clinical situation. Nevertheless, the results indicate that it is worthwhile to conduct studies to find out the efficacy, longevity and toxicity of this phytonanotherapeutic formulation. This may result in the discovery of a cheaper and more beneficial form of therapy for diabetes and its associated long-term complications.

REFERENCES

Adekoya, J.A., Dare, E.O., Mesubi, M.A., Nejo, A.A., Swart, H.C., Revaprasadu, N. 2014. Synthesis of polyol based Ag/Pd nanocomposites for applications in catalysis. *Results in Physics*, 4: 12-19.

Amendola, V., Bakr, O.M., Stellacci, F. 2010. A study of the surface plasmon resonance of silver nanoparticles by the discrete dipole approximation method: effect of shape, size, structure, and assembly. *Plasmonics*, 5(1): 85-97.

Adwan, G., Abu-Shanab, B., Adwan, K. 2010. Antibacterial activities of some plant extracts alone and in combination with different antimicrobials against multidrug-resistant *Pseudomonas aeruginosa* strains. *Asian Pacific Journal of Tropical Medicine*, 3(4): 266-269.

Afolayan, A.J., Sunmonu, T.O. 2010. *In vivo* studies on antidiabetic plants used in South African herbal medicine. *Journal of Clinical Biochemistry and Nutrition*, 47(2): 98-106.

Agoreyo, F.O., Agoreyo, B.O., Onuorah, M.N. 2006. Effect of aqueous extracts of *Hibiscus sabdariffa* and *Zingiber officinale* on blood cholesterol and glucose levels of rats. *Phytotheraphy Research*, 20(9): 764-772.

Agrawal, P., Rai, V., Singh, R. B. 1996. Randomized placebo controlled, single blind trial of holy basil leaves in patients with non-insulin dependent diabetes mellitus. *International Journal of Clinical Pharmacology and Therapeutics*, 34(9): 406-409.

Ahmad, I., Beg, A.Z. 2001. Antimicrobial and phytochemical studies on 45 Indian medicinal plants against multidrug resistant human pathogens. *Journal of Ethnopharmacology*, 74(2): 113-123.

Ahmad, N., Sharmab, S., Alama, M.K., Singh, V.N., Shamsid, S.F., Mehtac, B.R., Fatmae, A. 2010. Rapid synthesis of silver nanoparticles using dried medicinal plant of basil. *Colloids and Surfaces B: Biointerfaces*, 81(1): 81-86.

Akkarachiyasit, S., Charoenlertkul, P., Yibchok-Anun, S., Adisakwattana, S. 2010. Inhibitory activities of cyanidin and its glycosides and synergistic effect with acarbose against intestinal α-glucosidase and pancreatic α-amylase. *International Journal of Molecular Sciences*, 11(9): 3387-3396.

Ali, H., Houghton, P.J., Soumyanath, A. 2006. α-amylase inhibitory activity of some Malaysian plants used to treat diabetes with particular reference to *Phyllanthus amarus*. *Elservier Journal of Ethnopharmacology*, 107(3): 449-455.

Al-Omaria, I.L., Afifib, F.U., Salhaba, A.S. 2012. Therapeutic effect and possible herb drug interactions of ginger (*Zingiber officinale* Roscoe, Zingiberaceae) crude extract with glibenclamide and insulin. *Pharmacognosy Communications*, 2(1): 12-20.

Amirulhusni, A.N., Palanisamy, N.K., Mohd-Zain, Z., Ping, L.J., Durairaj, R. 2012. Antibacterial effect of silver nanoparticles on multidrug resistant *Pseudomonas aeruginosa*. *World Academy of Science, Engineering and Technology*, 6: 210-213.

Anand, K., Gengan, R.M., Phulukdaree, A., Chuturgoon, A. 2015. Agroforestry waste *Moringa oleifera* petals mediated green synthesis of gold nanoparticles and their anticancer and catalytic activity. *Journal of Industrial and Engineering Chemistry*, 21, 1105-1111.

Arunachalam, K.D., Annamalai, S.K., Hari, S. 2013. One-step green synthesis and characterization of leaf extract mediated biocompatible silver and gold nanoparticles from *Memecylon umbellatum*. *International Journal of Nanomedicine*, 8(1): 1307-1315.

Aujla, M.I., Ahmed, D., Khair-Ul-Bariyah, S. 2012. Comparative analysis of *Ocimum basilicum* and *Ocimum sanctum*: Extraction Techniques and Urease and alpha-Amylase inhibition. *Pakistan Journal of Chemistry*, 2(3): 134-141.

Badole, S.L., Patel, N.M., Thakurdesai, P.A., Bodhankar, S.L. 2008. Interaction of aqueous extract of *Pleurotus pulmonarius* (Fr.) Quel-Champ. with glyburide in alloxan induced diabetic mice. *Evidence-based Complementary and Alternative Medicine*, 5(2): 159-164.

Bhakta, T., Banerjee, S., Mandal, S.C., Maity, T.K., Saha, B.P., Pal, M. 2001. Heptoprotective activity of *Cassia fistula* leaf extract. *Phytomedicine*, 8(3): 220-224.

Barathmanikanth, S., Kalishwaralal, K., Sriram, M., Pandian, S.B.R.K., Youn, H., Eom, S., Gurunathan, S. 2010. Antioxidant effect of gold nanoparticles restrains hyperglycaemic conditions in diabetic mice. *Journal of Nanobiotechnology*, 8(1): 1-15.

Barnes, J., Anderson, L.A., Phillipson, J.D. 2007. *Herbal medicines: a guide for healthcare professionals*. Grayslake, IL: Pharmaceutical Press.

Bastaki, S. 2005. Review: diabetes mellitus and its treatment. *International Journal Diabetes and Metabolism*, 13(3): 111-134.

Bauman, R. 2007. *Microbiology with diseases by taxonomy*. 2nd ed. San Francisco, USA: Pearson Benjamin Cummings.

Baynes, K.C.R. 2006. Introduction to diabetes. In: Soumyanath, A. (ed), *Traditional medicines for modern times: antidiabetic plants.* Boca Raton, FL: CRC Taylor & Francis.

Benalla, W., Bellahcen, S., Bnouham, M. 2010. Antidiabetic medicinal plants as a source of alpha Glucosidase inhibitors. *Current Diabetes Reviews*, 6(4): 247-254.

Benny, K.A., Adithan, C. 2000. Review of endocrine pharmacology. *Indian Journal of Pharmacology*, 32: 67-80.

Bernfeld, P. 1955. *Methods in Enzymology 1*. Available: <http://www.sigmaaldrich.com/technical-documents/protocols/biology/enzymatic-assay-of-a-amylase.html> (Accessed 04/11/2012).

Bhargava, K.P., Singh, N. 1981. Anti-stress activity of *Ocimum sanctum* Linn. *Indian Journal of Medical Research*, 73: 443-451.

Bhat, M., Zinjarde, S.S., Bhargava, S.Y., Kumar, A.R., Joshi, B.N. 2011. Antidiabetic indian plants: A good source of potent amylase inhibitors. *Evidence-Based Complementary and Alternative Medicine*, 2011: 1-7.

Bhowmik, A., Khan, L.A., Akhter, M., Rokeya, B. 2009. Studies on the antidiabetic effects of *Mangifera indica* stem-barks and leaves on nondiabetic, type 1 and type 2 diabetic model rats. *Bangladesh Journal Pharmacology*, 4(4): 110-114.

Bilal, A., Jahan, N., Ahmed, A., Bilal, S.N., Habib, S., Hajra, S. 2012. Phytochemical and Pharmacological studies on *Ocimum basilicum* Linn - a review. *International Journal of Current Research and Review*, 4(23): 73-83.

Bruneton, J. 1999. *Pharmacognosy, phytochemistry and medicinal plants*. Andover, U.K.: Intercept.

Bunyapraphatsara, N., Yongchaiyudha, S., Rungpitarangsi, V., Chokechaijaroenporn, O. 1996. Antidiabetic activity of *Aloe vera* L. juice II. Clinical trial in diabetes mellitus patients in combination with glibenclamide. *Phytomedicine*, 3: 245-248.

Cappuccino, J.G., Sherman, N. 1992. *Microbiology*: *a laboratory manual.* 3rd ed. New York, NY: Benjamin Cummings.

Carović-Stanko, K., Liber, Z., Politeo, O., Strikić, F., Kolak, I., Milos, M., Satovic, Z. 2011. Molecular and chemical characterization of the most widespread *Ocimum* species. *Plant Systematics and Evolution*, 294(3-4): 253-262.

Castro-Longoria, E., Vilchis-Nestor, A.R., Avalos-Borja, M. 2011. Biosynthesis of silver, gold and bimetallic nanoparticles using the filamentous fungus *Neurospora crassa*. *Colloids Surfaces B Biointerfaces*, 83(1): 42-48.

Chadwick, W.A., Roux, S., van de Venter, M., Louw, J., Oelofsen, W. 2007. Antidiabetic effects of *Sutherlandia frutescens* in wistar rats fed a diabetogenic diet. *Journal of Ethnopharmacology*, 109(1): 121-127.

Chattopadhyay, R.R. 1993. Hypoglycaemic effect of *Ocimum sanctum* leaf extract in normal and streptozotocin diabetic rats. *Indian Journal of Experimental Biology*, 31(11): 891-893.

Cheng, Y., Prusoff, W.H. 1973. Relationship between the inhibition constant (KI) and the concentration of inhibitor which causes 50 percent inhibition (I50) of an enzymatic reaction. *Biochemistry and Pharmacology*, 22(23): 3099-3108.

Chiha, M., Njeim, M., Chedrawy, E.G. 2012. Diabetes and coronary heart disease: a risk factor for the global epidemic. *International Journal of Hypertension*, Epub Oct 18.

Chopra, R.N., Nayer, S.L., Chopra, I.C. 1992. *Glossary of Indian medicinal plants*. 3rd ed. New Delhi: Council of Scientific and Industrial Research.

Clinical and Laboratory Standards Institute 2007. *Performance standards for antimicrobial susceptibility testing; seventeenth informational supplement*. Available: <http://www.microbiolab-bg.com/CLSI.pdf > (Accessed 01/11/2014).

Daisy, P., Saipriya, K. 2012. Biochemical analysis of *Cassia fistula* aqueous extract and phytochemically synthesised gold nanoparticles as hypoglycaemic treatment for diabetes mellitus. *International Journal of Nanomedicine*, 7: 1189-1202.

Dar, M.A., Ingle, A., Rai, M. 2013. Enhanced antimicrobial activity of silver nanoparticles synthesized by *Cryphonectria* sp. evaluated singly and in combination with antibiotics. *Nanomedicine: Nanotechnology, Biology and Medicine*, 9(1): 105-110.

Dev, N., Das, A.K., Hossain, M.A., Rahman, S.M.M. 2011. Chemical compositions of different extracts of *Ocimum basilicum* leaves. *Journal of Scientific Research*, 3: 197-206.

Devendran, G., Balasubramanian, U. 2011. Qualitative phytochemical screening and GC-MS analysis of *Ocimum sanctum* L. leaves. *Asian Journal of Plant Science and Research*, 1(4): 44-48.

Deutschländera, M., van de Venter, M., Roux, S., Louw, J., Lall, N. 2009. Hypoglycaemic activity of four plant extracts traditionally used in South Africa. *Journal of Ethnopharmacology*, 124(3): 1-6.

Dineshkumar, B., Mitra, A., Manjunatha, M. 2010. A comparative study of alpha amylase inhibitory activities of common antidiabetic plants at Kharagpur 1 block. *International Journal of Green Pharmacy*, 4(2): 115-121.

Dong, P., Lin, Y., Deng, J., Di, J. 2013. Ultrathin gold-shell coated silver nanoparticles onto a glass platform for improvement of plasmonic sensors. *ACS Applied Materials and Interfaces*, 5(7): 2392-2399.

Dorman, H., Deans, S. 2000. Antimicrobial agents from plants: antibacterial activity of plant volatile oils. *Journal of applied microbiology*, 88(2): 308-316.

Dubey, S.P., Lahtinen, M., Sillanp, M. 2010. Tansy fruit mediated greener synthesis of silver and gold nanoparticles. *Process Biochemistry*, 45(7): 1065-1071.

Durai, P., Chinnasamy, A., Gajendran, B., Ramar, M., Pappu, S., Kasivelu, G., Thirunavukkarasu, A. 2014. Synthesis and characterization of silver nanoparticles using crystal compound of sodium para-hydroxybenzoate tetrahydrate isolated from *Vitex negundo* L. leaves and its apoptotic effect on human colon cancer cell lines. *European Journal of Medicinal Chemistry*, 84: 90-99.

Duthie, G.G., Duthie, S.J. Kyle, J.A. 2000. Plant polyphenols in cancer and heart disease: implications as nutritional antioxidants. *Nutrition Research Reviews*, 13(1): 79-106.

Eidia, A., Eidib, M., Esmaeillia, E. 2006. Antidiabetic effect of garlic (*Allium sativum* L.) in normal and streptozotocin-induced diabetic rats. *Phytomedicine*, 13: 624-629.

El-Beshbishy, H., Bahashwan, S. 2012. Hypoglycaemic effect of basil (*Ocimum basilicum*) aqueous extract is mediated through inhibition of α-glucosidase and α-amylase activities: an *in vitro* study. *Toxicology and Industrial Health*, 28(1): 42-50.

Eloff, J.N., 1998. Which extractant should be used for the screening and isolation of antimicrobial components from plants? *Journal of Ethnopharmacology*, 60(1): 1-8.

Elya, B., Basah, K., Mun'im, A., Yuliastuti, W., Bangun, A., Septiana, E.K. 2012. Screening of α-glucosidase inhibitory activity from some plants of Apocynaceae, Clusiaceae, Euphorbiaceae, and Rubiaceae. *Journal of Biomedicine and Biotechnology*, Article ID 281078.

Eyo, J.E., Ozougwu, J.C., Echi, P.C. 2011. Hypoglycaemic effect of *Allium cepa*, *Allium sativum*, and *Zinziber officinal* aqueous extract of alloxan-induced diabetic rattus novergicus. *Medical Journal of IslamicWorld Academy of Sciences*, 19(3): 121-126.

Fang, Y.Y. 2011. *In vitro* drug-herb interaction potential of African medicinal plant products used by Type II diabetics. Masters, Nelson Mandela Metropoloitan University. 02/11/2011.

Fayaz, A.M., Balaji, K., Girilal, M., Yadav, R., Kalaichelvan, P.T., Venketesan, R. 2010. Biogenic synthesis of silver nanoparticles and their synergistic effect with antibiotics: a study against Gram positive and Gram negative bacteria. *Nanomedicine: Nanotechnology, Biology and Medicine*, 6(1): 103-109.

Funke, I., Melzig, M.F. 2006. Traditionally used plants in diabetes therapy- phytotherapeutics as inhibitors of α-amylase activity. *Revista Brasileira de Farmacognosia*, 16(1): 1-5.

Gan, S.K., Yuen, R.W., Welborn, T.A. 1999. *Hyperlipidaemia in diabetes*. Available: <http://www.australianprescriber.com/magazine/22/3/67/9/> (Accessed 12/06/2013).

Ganesh, K.V., Dinesh Gokavarapu, S., Rajeswari, A., Stalin Dhas, T., Karthick, V., Kapadia, Z., Shrestha, T., Barathy, I.A., Roy, A., Sinha, S. 2011. Facile green synthesis of gold nanoparticles using leaf extract of antidiabetic potent *Cassia auriculata*. *Colloids and Surfaces B: Biointerfaces*, 87(1): 159-163.

Gengan, R.M., Anand, K., Phulukdaree, A., Chuturgoon, A. 2013. A549 lung cell line activity of bio-synthesised silver nanoparticles using *Albizia adianthifolia* leaf. *Colloids and surfaces. B, Biointerfaces*, 105, 87-91.

Gephardt, P., Murray, R.G.E., Costilow, R.N., Nester, E.W., Wood, W.A., Krieg, N.R. Phillips, G.B. 1884. *Manual methods for general bacteriology*. Washington, D.C.: ASM Press.

German Homoeopathic Pharmacopoeia. 2005. *German homoeopathic pharmacopoeia: GHP*. Stuttgart: Medpharm Scientific Publ..

Gondwe, M., Kamadyaapa, D.R., Tufts, M., Chuturgoon, A.A., Musabayane, C.T. 2008. *Sclerocarya birrea* [(A. Rich.) Hochst.] [Anacardiaceae] stem-bark ethanolic extract (SBE) modulates blood glucose, glomerular filtration rate (GFR) and mean arterial blood pressure (MAP) of STZ-induced diabetic rats. *Phytomedicine*, 15(9): 699-709.

Govender, S. 2011. A comparison of the effectiveness of two homoeopathic dosage forms of *Momordica charantia* in the treatment of type 2 diabetes mellitus in patients on Metformin. MTech, Durban University of Technology. 02/02/2013.

Govind, P., Madhuri, S. 2010. Pharmacological activities of *Ocimum sanctum* (Tulsi): a review. *International Journal of Pharmaceutical Sciences Review and Research*, 5(1): 61-66.

Grace, A.N., Pandian, K. 2007. Antibacterial efficacy of aminoglycosidic antibiotics protected gold nanoparticles: a brief study. *Colloids and Surfaces A: Physicochemical and Engineering Aspects*, 297(1): 63-70.

Grover, J.K., Yadav, S., Vats, V. 2002. Medicinal plants of India with antidiabetic potential. *Journal of Ethnopharmacology*, 81(1), 81-100.

Guariguata, L., Whiting, D.R., Hambleton, I., Beagley, J., Linnenkamp, U., Shaw, J.E. 2014. Global estimates of diabetes prevalence for 2013 and projections for 2035. *Diabetes Research and Clinical Practice*. 103(2): 137-149.

Gupta, A., Gupta, R, Lal, B. 2001. Effect of *Trigonella foenumgraecum* (Fenugreek) seeds on glycaemic control and insulin resistance in type 2 diabetes mellitus: a double blind placebo controlled study. *Journal of Association of Physicians of India*, 49: 1057-1061.

Gurib-Fakim, A. 2006. Medicinal plants: Traditions of yesterday and drugs of tomorrow. *Molecular Aspects of Medicine*, 27(1): 1-93.

Hackl, E., Zechmeister-Boltenstern, S., Bodrossy, L., Sessitsch, A. 2004. Comparison of diversities and compositions of bacterial populations inhabiting natural forest soils. *Applied and Environmental Microbiology*, 70, 5057-5065.

Hall, V., Thomsen, R.W., Henriksen, O., Lohse, N. 2011. Diabetes in sub-Saharan Africa 1999-2011: epidemiology and public health implications. a systematic review. *BMC Public Health*, 11, 564-564.

Hamdan, I.I., Afifi, F., Taha, M.O. 2004. *In vitro* alpha-amylase inhibitory effect of some clinically-used drugs. *Department of Pharmaceutical Sciences*, 59(10), 799-801.

Hamdan, I.I., Afifi, F.U. 2004. Studies on the *in vitro* and *in vivo* hypoglycaemic activities of some medicinal plants used in treatment of diabetes in Jordanian traditional medicine. *Journal of Ethnopharmacology*, 93(1): 117-121.

Hannan, J.M., Marenah, L., Ali, L., Rokeya, B., Flatt, P.R., Abdel-Wahab. Y.H. 2006. *Ocimum sanctum* leaf extracts stimulate insulin secretion from perfused pancreas, isolated islets and clonal pancreatic beta-cells. *Journal of Endocrinology*, 189(1): 127-136.

Harborne, J.B. 1998. *Phytochemical methods: a guide to modern techniques of plant analysis*. New York: Chapman and Hall.

Harisaranraj, R., Prasitha, R., Saravana Babu, S., Suresh, K. 2008. Analysis of inter-species relationships of *Ocimum* species using RAPD Markers. *Ethnobotanical Leaflets*, 12, 609-613.

Honeyman, A., Friedman, H., Bendinelli, M. 2001. *Staphylococcus aureus Infection and Disease*. New York: Kluwer Academic / Plenum Publishers.

Houghton, P., Raman, A. 1998. *Laboratory handbook for the fractionation of natural extracts*. Boston, MA: Springer.

Huang, X., El-Sayed, M.A. 2010. Gold nanoparticles: optical properties and implementations in cancer diagnosis and photothermal therapy. *Journal of Advanced Research*, 1(1): 13-28.

Huang, J., Li, Q., Sun, D., Lu, Y., Su, Y., Yang, X., Wang, H., Wang, Y., Shao, W., Ning, H., Hong, J., Chen, C. 2007. Biosynthesis of silver and gold nanoparticles by novel sundried *Cinnamommum camphora* leaf. *Nanotechnology*, 18: 104.

Huh, A.J., Kwon, Y.J. 2011. Nanoantibiotics: a new paradigm for treating infectious diseases using nanomaterials in the antibiotics resistant era. *Journal of Controlled Release*, 156(2): 128-145.

Iravani, S. 2011. Green synthesis of metal nanoparticles using plants. *Green Chemistry*, 13(10), 2638-2650.

Ishikawa, A., Yamashita, H., Hiemori, M., Inagaki, E., Kimoto, M., Okamoto, M., Tsuji, H., Memon, A.N., Mohammadi, A., Natori, Y. 2007. Characterization of inhibitors of postprandial hyperglycaemia from the leaves of *Nerium indicum*. *Journal of Nutritional Science and Vitaminology*, 53: 16-173.

Ismail, M.Y.M. 2009. Clinical evaluation of antidiabetic activity of *Trigonella* seeds and *Aegle marmelos* leaves. *World Applied Sciences Journal*, 7(10): 1231-1234.

Jagtap, U.M., Bapat, V.A. 2013. Green synthesis of silver nanoparticles using *Artocarpus heterophyllus* Lam. seed extract and its antibacterial activity. *Industrial Crops and Products*, 46: 123-137.

Jaiganesh, K.P., Baskar, N., Ramasamy, N., Arunachalam, G. 2012. Phytochemical and Antimicrobial Screening of *Ocimum basilicum*, Linn. *Journal of Scientific Research in Pharmacy*, 1(3): 102-106.

Janecek, S. 1994. Sequence similarities and evolutionary relationships of microbial, plant and animal α-amylases. *European Journal of Biochemistry*, 224(2): 519-524.

Jarald, E., Joshi, S.B. Jain, D.C. 2008. Diabetes vs herbal medicines. *Iranian Journal of Pharmacology and Therapeutics*, 7(1): 97-106.

Jayapriya, E., Lalitha, P. 2013. Synthesis of silver nanoparticles using leaf aqueous extract of *Ocimum basilicum*. *International Journal of Chemtech Research*, 5: 2985-2992.

Jones, W.P., Kinghorn, A.D. 2005. Natural product isolation: extraction of plant secondary metabolites. *Methods in Biotechnology*, 20: 323-351.

Joshi, B., Sah, G.P., Basnet, B.B., Bhatt, M.R., Sharma, D., Subedi, K., Pandey, J., Malla, R. 2011. Phytochemical extraction and antimicrobial properties of different medicinal plants: *Ocimum sanctum* (Tulsi), *Eugenia caryophyllata* (Clove), *Achyranthes bidentata* (Datiwan) and *Azadirachta indica* (Neem). *Journal of Microbiology and Antimicrobials*, 3(1): 1-7.

Jung, B., Matzke, M., Stoltefuss, J. 1996. *Handbook of experimental pharmacology: Oral antidiabetics*. Berlin: Springer.

Kadian, R., Parle, M. 2012. Therapeutic potential and phytopharmacology of Tulsi. *International Journal of Pharmacy and Life Sciences*, 3(7): 1858-1867.

Kaleem, M., Sarmad, H., Bano, B. 2005. Protective effects of *Piper nigrum* and *Vinca rosea* in alloxan-induced diabetic rats. *Indian Journal Physiology and Pharmacology*, 49(1): 65-71.

Karlowsky, Draghi, D.C., Jones, M.E., Thornsberry, C., Friedland, I.R. Sahm, D.F. 2003. Surveillance for antimicrobial susceptibility among clinical isolates of *Pseudomonas aeruginosa* and *Acinetobacter baumannii* from hospitalised patients in the United States, 1998 to 2001. *Antimicrobial Agents and Chemotherapy*, 47(5): 1681-1688.

Karthikeyan, K., Gunasekaran, P., Ramamurthy, N., Govindasamy, S. 1999. Anticancer activity of *Ocimum sanctum*. *Pharmaceutical Biology*, 37(4): 285-290.

Katzung, B.G., Masters, S.B., Trevor, A.J. 2009. *Basic and clinical pharmacology*. New York: The McGraw-Hill Companies.

Kavishankar, G.B., Lakshmidevi, N., Murthy, S.M., Prakash, H.S., Niranjana, S.R. 2011. Diabetes and medicinal plants - A Review. *International Journal of Pharmacy and Biomedical Sciences*, 2(3): 65-80.

Kaya, I., Yiğit, N., Benli, M. 2008. Antimicrobial activity of various extracts of *Ocimum basilicum* L. and observation of the inhibition effect on bacterial cells by use of Scanning Electron Microscopy. *African Journal of Traditional, Complementary and Alternative Medicines*, 5(4): 363-369.

Kelm, M., Nair, M., Strasburg, G., Dewitt, D. 2000. Antioxidant and cyclooxygenase inhibitory phenolic compounds from *Ocimum sanctum* Linn. *Phytomedicine*, 7(1): 7-13.

Khair-Ul-Bariyah, S., Ahmed, D., Ikram Aujla, M. 2012. Comparative analysis of *Ocimum basilicum* and *Ocimum sanctum*: extraction techniques and urease and alpha-amylase inhibition. *Pakistan Journal of Chemistry*, 2(3): 1-8.

Khan, M.R.I., Islam, M.A., Hossain, M.S., Asadujjaman, M., Waheda, M.I.I., Rahman, B.M., Anisuzzaman, A.S.M., Shaheen, S.M., Ahmeda, M. 2010. Antidiabetic effects of the different fractions of ethanolic extracts of *Ocimum sanctum* in normal and alloxan-induced diabetic rats. *Journal of Scientific Research*, 2(1): 158-168.

Khogare, D.T., Lokhande, S.M. 2011. Effect of Tulasi (*Ocimum sanctum*) on diabetes mellitus. *Indian Streams Research Journal*, 1(2): 189-191.

Kil, I.S., Lee, J.H., Shin, A.H., Park, J.W. 2004. Glycation-induced inactivation of NADP +-dependent isocitrate dehydrogenase: implications for diabetes and ageing. *Free Radical Biology and Medicine*, 37: 1765-1778.

Kim, M.J., Lee, S.B., Lee, H.S., Lee, S.Y., Baek, J.S., Kim, D., Moon, T.W., Robyt, J.F., Park, K.H. 1999. Comparative study of the inhibition of α-glucosidase, α-amylase, and cyclomaltodextrin glucanosyltransferase by acarbose, isoacarbose, and acarviosine glucose. *Archives of Biochemistry and Biophysics*, 371(2): 277-283.

Kim, Y.M., Jeong, Y.K., Wang, M.H., Lee, W.Y., Rhee, H.I. 2005. Inhibitory effect of pine extract on α-glucosidase activity and postprandial hyperglycemia. *Nutrition*, 21(6): 756-761.

Kotakadi, V.S., Gaddam, S.A., Rao, Y.S., Prasad, T.N.V.K.V., Reddy, A.V., Sai Gopal, D.V.R. 2014. Biofabrication of silver nanoparticles using *Andrographis paniculata*. *European Journal of Medicinal Chemistry*, 73: 135-140.

Kothari, S.K., Bhattacharya, A.K., Ramesh, S. 2004. Essential oil yield and quality of methyl eugenol rich *Ocimum tenuiflorum* L.f. (syn. *O. sanctum* L.) grown in south India as influenced by method of harvest. *Journal of Chromatography A*, 1054(1-2): 67-72.

Koukiekolo, R., Desseaux, V., Moreau, Y., Marchis-Mouren, G., Santimone, M. 2001. Mechanism of porcine pancreatic α-amylase. *European Journal of Biochemistry*, 268(3): 841-848.

Krishnamoorthy, P., Jayalakshmi, T. 2012. Preparation, characterization and synthesis of silver nanoparticles by using *Phyllanthusniruri* for the antimicrobial activity and cytotoxic effects. *Journal of Chemical and Pharmaceutical Research*, 4(11): 4783-4794.

Kudolo, G.B. 2001. The effect of 3-month ingestion of *Ginkgo biloba* extract (EGb 761) on pancreatic β-cell function in response to glucose loading in individuals with non-insulin dependent diabetes mellitus. *Journal of Clinical Pharmacology*, 41: 600-611.

Kuldeep, K.T., Singh, A.K., Kumar, R., Gupta, V., Tripathi, K. 2013. *Ocimum sanctum* Linn: A Review on phytopharmacology and therapeutic potential of Tulsi. *International Journal of Pharmaceutical and Pytopharmacological Research*, 3(2): 148-151.

Kumari, M.M., Jacob, J., Philip, D. 2015. Green synthesis and applications of Au–Ag bimetallic nanoparticles. *Spectrochimica Acta Part A: Molecular and Biomolecular Spectroscopy*, 137: 185-192.

Kuyvenhoven, J.P., Meinders, A.E. 1999. Oxidative stress and diabetes mellitus: pathogenesis of long-term complications. *European Journal of Internal Medicine*, 10(1): 9-19.

Labra, M., Miele, M., Ledda, B., Grassi, F., Mazzei, M., Sala, F. 2004. Morphological characterization, essential oil composition and DNA genotyping of *Ocimum basilicum* L. cultivars. *Plant Science*, 167(4): 725-731.

Lal, V.K., Gupta, P.P., Tripathi, P., Pandey, A. 2011. Interaction of *Momordica charantia* fruit juice with glibenclamide in streptozotocin induced diabetic rats. *Pharmacology Online*, 3: 853-857.

Larkin, J.G., Frier, B.M., Ireland, J.T. 1985. Diabetes mellitus and infection. *Postgraduate Medical Journal*, 61(713): 233-237.

Lebovit, H. 1998. Alpha glucosidase inhibitors as agents in the treatment of diabetes. *Diabetes Review*, 6(2): 132-145.

Lee, J.H., Lee, S.R. 1994. Some physiological activity of phenolic substances in plant foods. *Korean Journal of Food Science and Technology*, 26: 317-323.

Lee, S.J., Umano, K., Shibamoto, T., Lee, K.G. 2005. Identification of volatile components in Basil (*Ocimum basilicum* L.) and thyme leaves (*Thymus vulgaris* L.) and their antioxidant properties. *Food Chemistry*, 91(1): 131-137.

Lewis, E., South-Paul, J., Matheny, S. (eds). 2010. *Current diagnosis and treatment in family medicine*.New York, NY: McGraw Hill.

Li, P., Li, J., Wu, C., Wu, Q., Li, J. 2005. Synergistic antibacterial effects of β-lactam antibiotic combined with silver nanoparticles. *Nanotechnology*, 16(9): 1912.

Lineweaver, H., Burk, D. 1934. The determination of enzyme dissociation constants. *Journal American Chemical Society*, 56(3): 658-666.

Liu, Y., Wang, M.W. 2008. Botanical drugs: challenges and opportunities-contribution to Linnaeus memorial symposium. *Life Sciences*, 82(9): 445-449.

Lokesh, D., Amit, S.D. 2006. Diabetes mellitus: its possible pharmacological evaluation techniques and naturotherapy. *International Journal Green Pharmacology*, 1: 15-28.

Lokina, S., Stephen, A., Kaviyarasan, V., Arulvasu, C., Narayanan, V. 2014. Cytotoxicity and antimicrobial activities of green synthesised silver nanoparticles. *European Journal of Medicinal Chemistry*, 76: 256-263.

Losasso, C., Belluco, S., Cibin, V., Zavagnin, P., Mičetić, I., Gallocchio, F., Zanella, M., Bregoli, L., Biancotto, G., Ricci, A. 2014. Antibacterial activity of silver nanoparticles: sensitivity of different *Salmonella* serovars. *Frontiers in microbiology*, 5: 1-9.

Maduna, P.M.H. 2006. The role of traditional medicine in the treatment of diabetes mellitus. *Continuing Medical Education*, 24(10): 574-577.

Mahomed, I.M., Ojewole, J.A. 2004. Analgesic, antiinflammatory and antidiabetic properties of *Harpagophytum procumbens* DC (Pedaliaceae) secondary root aqueous extract. *Phytotherapy Research*, 18(12): 982-989.

Mahomed, I.M., Ojewole, J.A.O. 2003. Hypoglycaemic effect of *Hypoxis hemerocallidea corm* (African potato) aqueous extract in rats. *Methods and Findings Experimental and Clinical Pharmacology*, 25(8): 617-623.

Mallikarjuna, K., Narasimha, G., Dillipa, G.R., Praveen, B., Shreedhar, B., Sree Lakshmi, C., Reddy, B.V.S., Deva Prasad Raju, B. 2011. Green Synthesis of silver nanoparticles using *Ocimum* leaf extract and their characterization. *Digest Journal of Nanomaterials and Biostructures*, 6(1): 181-186.

Manila, T.N., Mary Shoba Das, C., Gayathri Devi, S. 2012. *In vitro* antidiabetic properties of the fruits and leaves of *Terminalia bellirica*. *Journal of Natural Sciences Research*, 2(9): 54-62.

Martin, K.W., Ernst, E. 2004. Herbal medicines for treatment of fungal infections: a systematic review of controlled clinical trials. *Mycoses*, 47: 87-92.

McCarthy, M., Maher, D., Ly, A., Ndip, A. 2010. Developing the agenda for European Union collaboration on non-communicable diseases research in Sub-Saharan Africa. *Health research policy and systems / BioMed Central*, 8: 13-13.

McFarland, J. 1907. Nephelometer: An instrument for estimating the number of bacteria in suspension used for calculating the opsonic index for vaccines. *Journal of the American Medical Association*, 14: 1176-1178.

McCue, P., Kwon, Y.I., Shetty, K. 2005. Anti-amylase, anti-glucosidase and anti-angiotensin I-converting enzyme potential of selected foods. *Journal of Food Biochemistry*, 29: 278-294.

McCue, P.P., Shetty, K. 2004. Inhibitory effects of rosmarinic acid extracts on porcine pancreatic amylase *in vitro*. *Asia Pacific Journal Clinical Nutrition*, 13(1): 101-106.

Mckenzie, L.C. 2009. Mechanistic Insights on Nanoparticle Formation: Investigation of Reaction Pathways and Development of Controlled Syntheses for Triphenylphosphine-stabilised Undecagold (Doctorate). Philosophiae Doctor, University of Oregon, USA. 02/09/2015.

McIntyre, M. 2012. *Synergy - a key herbal concept*. Available: <http://www.anh-europe.org/files/Michael_McIntyre_Synergy_in_1000_words.pdf> (Accessed 05/10/2012).

Miller, L.G. 1998. Herbal medicinals: selected clinical considerations focusing on known or potential drug-herb interactions. *Archives of Internal Medicine*, 158(2): 2200-2211.

Menezes, W.G., Zielasek, V., Dzhardimalieva, G.I., Pomogailo, S.I., Thiel, K., Wöhrle, D., Hartwig, A., Bäumer, M. 2012. Synthesis of stable Au/Ag bimetallic nanoparticles encapsulated by diblock copolymer micelles. *Nanoscale*, 4: 1658-1664.

Mizuno, C.S., Chittiboyina, A.G., Kurtz, T.W., Pershadsingh, H.A. Avery, M.A.2008. Type 2 diabetes and oral antihyperglycemic drugs. *Current Medicinal Chemistry*, 15(1): 61-74.

Mogale, M.A., Lebelo, S.L., Shai, L.J., Eloff, J.N. 2011a. *Aloe arborescens* aqueous gel extract alters the activities of key hepatic enzymes and blood concentration of triglycerides, glucose and insulin in alloxan-induced diabetic rats. *African Journal of Biotechnology*, 10(20), 4242-4248.

Mogale, M.A., Lebelo, S.L., Thovhogi, N., De Freitas, A.N., Shai, L.J. 2011b. α-Amylase and α-glucosidase inhibitory effects of *Sclerocarya birrea* [(A. Rich.) Hochst.] subspecies caffra (Sond) Kokwaro (Anacardiaceae) stem-bark extracts. *Afican Journal of Biotechnology*, 10(66): 15033-15039.

Mohammadi, J., Naik, P.R. 2008. Evaluation of hypoglycaemic effect of *Morus alba* in an animal model. *Indian Journal of Pharmacology*, 40(1): 15-18.

Mollentze, W.F., Levitt, N.S. 2005. Diabetes mellitus and impaired glucose tolerance in South Africa. In: Steyn, K., Fourie, J., Temple, N. eds. *Chronic diseases of lifestyle in South Africa since 1995 to 2005*. Cape Town: Medical Research Council, 109-121.

Momoh, S., Yusuf, O.W., Adamu, M.M., Agwu, C.O.C., Atanu, F.O. 2011. Evaluation of the phytochemical composition and hypoglycaemic activity of methanolic leaves extract of *Costus afer* in albino rats. *British Journal of Pharmaceutical Research,* 1(1): 1-8.

Mondal, S., Bijay, R., Miranda, R.B., Sushil, C. 2009. The science behind sacredness of Tulsi (*Ocimum sanctum* Linn.). *Indian Journal of Physiology and Pharmacology*, 53: 291-306.

Morones, J.R., Elechiguerra, J.L., Camacho, A., Holt, K., Kouri, J.B., Ramírez, J.T., Yacaman, M.J. 2005. The bactericidal effect of silver nanoparticles. *Nanotechnology*, 16: 2346.

Mubarak, A.D., Thajuddin, N., Jeganathan, K., Gunasekaran, M. 2011. Plant extract mediated synthesis of silver and gold nanoparticles and its antibacterial activity against clinically isolated pathogens. *Colloids and Surfaces B: Biointerfaces*, 85(2): 360-365.

Mukherjee, P., Maiti, K., Mukherjee, K., Houghton, P. 2006. Leads from Indian medicinal plants with hypoglycaemic potentials. *Elsevier Journal of Ethnopharmacology*, 106(1): 1-28.

Musabayane, C.T., Mahlalela, N., Shode, F.O., Ojewole, J.A.O. 2005. Effects of *Syzygium cordatum* (Hochst.) [Myrtaceae] leaf extract on plasma glucose and hepatic glycogen in streptozotocin-induced diabetic rats. *Journal of Ethnopharmacology*, 97(3): 485-490.

Nammi, S., Boini, M., Lodagala, S., Behara, R. 2003. The juice of fresh leaves of *Catharanthus roseus* Linn. reduces blood glucose in normal and alloxan diabetic rabbits. *BMC Complementary and Alternative Medicine*, 3: 1-4.

Nair, S. S., Kavrekar, V., Mishra, A. 2013. *In vitro* studies on alpha amylase and alpha glucosidase inhibitory activities of selected plant extracts. *European Journal of Experimental Biology*, 3(1): 128-132.

National Department of Health, Medical Research Council, Council for Scientific and Industrial Research. 2006. *A model for South Africa: the National reference centre for African traditional medicines*. Available: <www.sahealthinfo.org/traditionalmeds/traditionalpart1.pdf> (Accessed 20/06/2013).

Neri, S., Calvagno, S., Leotta, C., Signorelli, S.S., Torrisi, B., Pulvirenti, D., Mauceri, B., Abate, G., Ignaccolo, L., Bordonaro, F., Cilio, D. 2005. Effects of antioxidant supplementation on postprandial oxidative stress and endothelial dysfunction: a single-blind, 15-day clinical trial

in patients with untreated type 2 diabetes, subjects with impaired glucose tolerance, and healthy controls. *Clinical Therapeutics*, 27(11): 1764-1773.

Nguyen, T.H., Um, B.H., Kim, S.M. 2011. Two unsaturated fatty acids with potent α-glucosidase inhibitory activity purified from the body wall of Sea Cucumber (*Stichopus japonicus*). *Journal of Food Science*, 76, 208-214.

Nickavar, B., Yousefian, N. 2009. Inhibitory Effects of six *Allium* species on alpha-amylase enzyme activity. *Iranian Journal of Pharmaceutical Research*, 8(1): 53-57.

Nikolaeva-Glomb, L., Galabov, A.S. 2004. Synergistic drug combinations against the *in vitro* replication of Coxsackie B1 virus. *Antiviral Research*, 62(1): 9-19.

Noruzi, M. 2015. Biosynthesis of gold nanoparticles using plant extracts. *Bioprocess and Biosystems Engineering*, 38(1): 1-14.

Nowak, J.T., Handford, A.G. 2004. *Pathophysiology concepts and applications for health care professionals*. 3rd ed. America, New York: McGraw-Hill.

Nsele, N.W. 2012. Assessment of the antibacterial activity of *Artemisia afra*, *Erythrina lysistemon* and *Psidium guajava*. MTech, Durban University of Technology. 04/11/2013.

Ojewole, J.A.O. 2002. Hypoglycaemic effect of *Clausena anisata* (Willd) Hook methanolic root extract in rats. *Elservier Journal of Ethnopharmacology*, 81(2): 231-237.

Omran, A. 1983. The epidemiologic transition theory: a preliminary update. *Journal of Tropical Paediatrics*, 29(6): 305-316.

Palatty, P.L., Shivashankara, A.R., Baliga, M.S., Jaiswal, A., Pankaj, P., Joseph, N. 2013. The Indian Medicinal Plant Aegle marmelos in the Treatment of Diabetes Mellitus: Promise and Prospects. In: Watson, R.R., Preedy, V.R. ed. *Bioactive food as dietary interventions for diabetes*. eBook. Boston: Academic Press, 519-536.

Park, M.S., Park, J., Jeon, S.K., Yoon, T.H. 2013. The effects of sedimentation and dissolution on the cytotoxicity of Ag nanoparticles. *Journal of Nanoscience and Nanotechnology*, 13(11): 7264-7270.

Peláez, F. 2006. The historical delivery of antibiotics from microbial natural products. *Biochemical pharmacology*, 71(7): 981-990.

Philip, D., Unni, C. 2011. Extracellular biosynthesis of gold and silver nanoparticles using Krishna Tulsi (*Ocimum sanctum*) leaf. *Physica E*, 43(7): 1318-1322.

Prabhakar, P.K., Doble, M. 2011. Mechanism of action of natural products used in the treatment of diabetes mellitus. *Journal of Intergrative Medicine*, 17(8): 563-574.

Pranami, G. 2009. Understanding nanoparticle aggregation. Doctor Of Philosophy, Iowa State University Ames, Iowa. 10/09/2015.

Premila, M.S., Conboy, L. 2007. Ayurvedic herbs: a clinical guide to the healing plants of traditional Indian medicine. *The Journal of Alternative and Complementary Medicine*: 13(8): 841-842.

Rahman, S., Islam, R., Kumrazzaman, M., Alam, K., Jamal, A.H.M. 2011. *Ocimum sanctum* L.: review of phytochemical and pharmacological profile. *American Journal of Drug Discovery and Development*, 2011: 1-15.

Rai, A., Eapen, C., Prasanth, V.G. 2012. Interaction of herbs and glibenclamide: a review. *International Scholarly Research Network ISRN Pharmacology*, 2012: 1-5.

Rai, A., Prabhune, A., Perry, C.C. 2010. Antibiotic mediated synthesis of gold nanoparticles with potent antimicrobial activity and their application in antimicrobial coatings. *Journal of Materials Chemistry*, 20(32): 6789-6798.

Raman, S., Kandula, M.P., Jacob, J.A., Soundararajan, K., Ramar, T., Palani, G., Muthukalingan, K., Shanmugam, A. 2012. Cytotoxic effect of green synthesised silver nanoparticles using *Melia azedarach* against *in vitro* HeLa cell lines and lymphoma mice model. *Elsevier: Process Biochemistry*, 47(2): 273-279.

Ramteke, C., Chakrabarti, T., Sarangi, B.K., Pandey, R.A. 2013. Synthesis of silver nanoparticles from the aqueous extract of leaves of *Ocimum sanctum* for enhanced antibacterial activity. *Journal of Chemistry*, 2013: 1-7.

Rang, H.P., Dale, M.M., Ritter, J.M., Moore, P.K. 2003. *Pharmacology*. Edinburgh: Churchill Livingstone.

Rao, N.K., Nammi, S. 2006. Antidiabetic and renoprotective effects of the chloroform extract of *Terminalia chebula* Retz. seeds in streptozotocin-induced diabetic rats. *BMC Complementary and Alternative Medicine*, 6: 1-6.

Rao, Y.S., Kotakadi, V.S., Prasad, T.N.V.K.V., Reddy, A.V., Gopal, D.V.R.S. 2013. Green synthesis and spectral characterization of silver nanoparticles from Lakshmi tulasi (*Ocimum sanctum*) leaf extract. *Elsevier Spectrochimica Acta Part A: Molecular and Biomolecular Spectroscopy*, 103: 156-159.

Ratner, R.E. 2001. Glycemic control in the prevention of diabetic complications. *Clinical Cornerstone*, 4(2): 24-37.

Reddy, P., Steyn, K., Saloojee, Y. 1998. The emerging epidemic of cardiovascular disease in developing countries. *Circulation*, 97: 596-601.

Reid, M.J.A., Tsima, B.M., Kirk, B. 2012. HIV and diabetes in Africa. *African Journal of Diabetes Medicine*, 20(2): 28-32.

Robert, B., Fick, J. 1993. *Pseudomonas Aeruginosa the Opportunist*. Boca Raton, FL: CRC Press, Inc.

Rotblatt, M., Zimet, I. 2002. *Evidence based herbal medicinal*. Philadelphia: Hanley and Belfus.

Rout, Y., Behera, S., Ojha, A.K., Nayak, P.L. 2012. Green synthesis of silver nanoparticles using *Ocimum sanctum* (Tulashi) and study of their antibacterial and antifungal activities. *Journal of Microbiology and Antimicrobials*, 4(6): 103-109.

Sabir, S., Anjum, A. A., Ijaz, T., Ali,M.A., Khan, M.R., Nawaz,M. 2014. Isolation and antibiotic susceptibility of *E. coli* from urinary tract infections in a tertiary care hospital. *Pakistan Journal of Medical Sciences*, 30(2): 389.

Saha, S., Dhar, T.N., Sengupta, C., Ghosh, P. 2013. Biological activities of essential oils and methanol extracts of five *Ocimum* species against pathogenic Bacteria. *Czech Journal of Food Science*, 31(2): 194-202.

Saha, S., Mukhopadhyay, M.K., Ghosh, P.D., Nath, D. 2012. Effect of methanolic leaf extract of *Ocimum basilicum* L. on benzene-induced hematotoxicity in mice. *Evidence-based Complementary and Alternative Medicine*, 2012: 1-7.

Sánchez-Borges, M., Thong, B., Blanca, M., Ensina, L., González-Díaz, S., Greenberger, P. A., Jares, E., Jee, Y.K., Kase-Tanno, L., Khan, D. 2013. Hypersensitivity reactions to non beta-lactam antimicrobial agents, a statement of the WAO special committee on drug allergy. *World Allergy Organ Journal*, 6(1): 18.

Sathishkumar, M., Sneha, K., Won, S.W., Cho, C.W., Kim, S., Yun, Y.S. 2009. *Cinnamon zeylanicum* bark extract and powder mediated green synthesis of nano-crystalline silver particles and its bactericidal activity. *Colloids and Surfaces B: Biointerfaces*, 73(2): 332-338.

Sethi, J., Sood, S., Seth, S., Talwar, A. 2004. Evaluation of hypoglycemic and antioxidant effect of *Ocimum sanctum*. *Indian Journal Clinical Biochemistry*, 19(2): 152-155.

Selva Sharma, A., Ilanchelian, M. 2014. Elucidation of photophysical changes and orientation of acridine orange dye on the surface of borate capped gold nanoparticles using multi-spectroscopic techniques. *Photochemical and Photobiological Sciences*, 13: 1741-1752.

Shankar, E.M., Mohan, V., Premalatha, G., Srinivasan, R.S., Usha, A.R. 2005. Bacterial aetiology of diabetic foot infections in South India. *European Journal of Internal Medicine*, 16(8): 567-570.

Shankar, S.S., Ahmad, A., Pasricha, R., Sastry, M., Mater, J. 2003. Bio-reduction of chloroaurate ions by geranium leaves and it endophytic fungus yields gold nanoparticles of different shapes *Chemistry*, 13: 1822-1826.

Shankar, S.S., Rai, A., Ahmad, A., Sastry, M. 2004. Rapid synthesis of Au, Ag, and bimetallic Au core–Ag shell nanoparticles using Neem (*Azadirachta indica*) leaf broth. *Journal of Colloid and Interface Science*, 275(2): 496-502.

Sharma, N., Kar, A. 2014. Combined effects *Gymnema Sylvestre* and glibenclamide on alloxan-induced diabetic mice. *International Journal of Applied Pharmaceutics*, 6(2): 11-14.

Sheny, D.S., Mathew, J., Philip, D. 2011. Phytosynthesis of Au, Ag and Au–Ag bimetallic nanoparticles using aqueous extract and dried leaf of *Anacardium occidentale*. *Spectrochimica Acta Part A: Molecular and Biomolecular Spectroscopy*, 79(1): 254-262.

Silverstein, R.M., Webster, F.X., Kiemle, D.J. 2005. *Spectrometric identification of organic compounds*. Hoboken NJ: John Wiley.

Sinha, V.R., Kumar, R.V. 2012. Utility of an oxidation reaction for the spectrophotometric determination of acarbose in controlled release tablets at various simulated gastrointestinal media. *Acta Poloniae Pharmaceutica*, 69(1): 23-32.

Singh, N., Verma, P., Pandey, B.R., Bhalla, M. 2012. Therapeutic Potential of *Ocimum sanctum* in Prevention and Treatment of Cancer and Exposure to Radiation: An Overview. *International Journal of Pharmaceutical Sciences and Drug Research*, 4(2): 97-104.

Singh, S., Majumdar, D.K., 1994. Toxicological studies of fixed oil of *Ocimum sanctum* Linn Tulsi. *New Botanist*, 21: 139.

Singh, S.S., Pandey, S.C., Srivastava, S., Gupta, V.S., Patro, B., Ghosh, A.C. 2003. Chemistry and Medicinal Properties of *Tinospora cordifolia* (Guduchi). *Indian Journal of Pharmacology*, 3: 83-91.

Singhal, G., Bhavesh, R., Kasariya, K., Sharma, A.R., Singh, R.P. 2011. Biosynthesis of silver nanoparticles using *Ocimum sanctum* (Tulsi) leaf extract and screening its antimicrobial activity. *Journal Nanoparticle Research*, 13(7): 2981-2988.

Sivaranjani, K., Meenakshisundaram, M. 2013. Biological synthesis of silver nanoparticles using *Ocimum basilicum* leaf extract and their antimicrobial activity. *International Research Journal of Pharmacy*, 4, 225-229.

Song, J.Y., Kim, B.S. 2009. Rapid biological synthesis of silver nanoparticles using plant leaf extracts. *Bioprocess Biosystem Engineering*, 32(2): 79-84.

Sondi, I., Salopek-Sondi, B. 2004. Silver nanoparticles as antimicrobial agent: a case study on *E. coli* as a model for Gram negative bacteria. *Journal of Colloid and Interface Science*, 275(1): 177-182.

Soumyanath, A. 2006. *Traditional medicines for modern times: antidiabetic plants*. Boca Raton, FL: CRC Press.

South African Medical Association. 2005. *South African Medicines Formulary (SAMF)*. University of Cape Town: Division of Clinical Pharmacology, Faculty of Health Science.

Subramania, K., Pathak, S., Hosseinkhani, H. 2012. Recent trends in diabetes treatment using nanotechnology. *Digest Journal of Nanomaterials and Biostructures*, 7(1): 85-95.

Subramanian, R., Asmawi, M.Z., Sadikun, A. 2008. *In vitro* α-glucosidase and α-amylase enzyme inhibitory effects of *Andrographis paniculata* extract and *Andrographolide*. *Acta Biochimica Polonica*, 55(2): 391-398.

Sudha, P., Zinjarde, S., Bhargava, S., Kumar, A. 2011. Potent alpha-amylase inhibitory activity of Indian Ayurvedic medicinal plants. *BMC Complementary and Alternative Medicine*, 11: 5.

Swarnalatha, L., Rachela, C., Ranjanb, S., Baradwaj, P. 2012. Evaluation of *in vitro* antidiabetic activity of *Sphaeranthus Amaranthoides* silver nanoparticles *International Journal of Nanomaterials and Biostructures*, 2(3): 25-29.

Tanko, Y., Yerima, M., Mahdi, M.A., Yaro, A.H., Mohammed, A. 2008. Hypoglycaemic activity of methanolic stem-bark of *Adansonnia digitata* extract on blood glucose levels of streptozocin-induced diabetic wistar rats. *International Journal of Applied Research in Natural Products*, 1(2): 32-36.

Tayyab, F., Smith Lal, S., Mishra, M., Kumar, U. 2012. *A review: medicinal plants and its impact on diabetes* Available: <http://www.wjpr.net/admin/article_issue/13465224997%20WJPR%20226.pdf> (Accessed 05/05/13).

Tchoumbougnang, F., Zollo, P.H.A., Avlessi, F., Alitonou, G.A., Sohounhloue, D.K., Ouamba, J.M., Tsomambet, A., Okemy-Andissa, N., Dagne, E., Agnaniet, H., Bessiere, J.M., Menut, C. 2006. Variability in the chemical compositions of the essential oils of five *Ocimum* species from tropical African area. *Journal of Essential Oil Research*, 18(2): 194-199.

Thakur, G., Mitra, A., Pal, K., Rousseau, D. 2009. Effect of flaxseed gum on reduction of blood glucose and cholesterol in Type 2 diabetic patients. *International Journal of Food Science and Nutrition*, 60(s6): 126-136.

Tortora, G.J., Funke, B.R., Case, C.L. 2007. *Microbiology: an introduction*. San Francisco: Pearson Benjamin Cummings.

Tudhope, L. 2008. The diabetic foot: protocols and current therapies. *Wound Healing Southern Africa*, 1(1): 37-39.

Udayakumar, R., Kasthurirengan, S., Mariashibu, T.S., Rajesh, M., Anbazhagan, V.R., Kim, S.C., Ganapathi, A., Choi, W.C. 2009. Hypoglycaemic and hypolipidaemic effects of *Withania Somnifera* root and leaf extracts on alloxan-induced diabetic rats. *International Journal of Molecular Science*, 10(5): 2367-2382.

Ugochukwu, N.H., Babady, N.E. 2003. Antihyperglycaemic effect of aqueous and ethanolic extracts of *Gongronema latifolium* leaves on glucose and glycogen metabolism in livers of normal and streptozotocin-induced diabetic rats. *Life Sciences*, 73(15): 1925-1938.

Usman, L.A., Ismaeel, R.O., Zubair, M.F., Saliu, B.K., Olawore, N.O., Elelu, N. 2013. Comparative studies of constituents and antibacterial activities of leaf and fruit essential oils of *Ocimium basilicum* grown in north central Nigeria. *International Journal of Chemical and Biochemical Sciences*, 3: 47-52.

van de Venter, M., Roux, S., Bungu, L.C., Louw, J., Crouch, N.R., Grace, O.M., Maharaj, V., Pillay, P., Sewnarian, P., Bhagwandin, N., Folb, P. 2008. Antidiabetic screening and scoring of 11 plants traditionally used in South Africa. *Elsevier Journal of Ethnopharmacology*, 119(1): 81-86.

van Huyssteen, M. 2007. Collaborative research with traditional African health practitioners of the Nelson Mandela Metropole; antimicrobial, anticancer and antidiabetic activities of five medicinal plants (Doctorate). Philosophiae Doctor, Nelson Mandela Metropolitan University. 04/02/2012.

Vani, S., Cheng, S., Chuah, C. 2009. Comparative study of volatile compounds from genus *Ocimum*. *American Journal of Applied Sciences*, 6(3): 523-528.

Verspohl, E.J., Bauer, K., Neddermann, E. 2005. Antidiabetic effect of *Cinnamomum cassia* and *Cinnamomum zeylanicumin in vivo* and *in vitro*. *Phytotheraphy Research*, 19(3): 203-206.

Vijayan, S.R., Santhiyagu, P., Singamuthu, M., Ahila, N.K., Jayaraman, R., Ethiraj, K. 2014. Synthesis and characterization of silver and gold nanoparticles using aqueous extract of seaweed, *Turbinaria conoides*, and their antimicrofouling activity. *The Scientific World Journal*, 2014: 1-10.

Vincentz, F. 2007. *Ocimum basilicum* Available: <http://commons.wikimedia.org/wiki/File:Ocimum_basilicum_05_ies.jpg> (Accessed 05/11/2014).

Vishnu, K.M., Murugesan, S. 2013. Biogenic silver nanoparticles by *Halymenia poryphyroides* and its *in vitro* antidiabetic efficacy. *Journal of Chemical and Pharmaceutical Research*, 5(12): 1001-1008.

Vishnu, K.M., Murugesan, S. 2014. Biological synthesis of silver nanoparticles from marine algae *Colpomenia sinuosa* and its *in vitro* antidiabetic activity. *American Journal of Bio-pharmacology, Biochemistry and Life Sciences*, 3: 1-7.

Wadkar, K.A., Magdum, C.S., Patil, S.S., Naikwade, N.S. 2007. Antidiabetic potential and Indian plants. *Journal of Herbal Medicine and Toxicology*, 2(1): 1-6.

Wang, H., Qiao, X., Chen, J., Ding, S. 2005. Preparation of silver nanoparticles by chemical reduction method. *Colloids and Surfaces A: Physicochemical and Engineering Aspects*, 256(2-3): 111-115.

World Health Organization (WHO). 2007. *WHO guidelines on good manufacturing practice (GMP) for herbal medicines*. Available: <http://apps.who.int/medicinedocs/documents/s14215e/s14215e.pdf> (Accessed 05/05/2012).

World Health Organization (WHO). 2011. *Global status report on non-communicable diseases 2010*. Available: <http://www.who.int/nmh/publications/ncd_report_full_en.pdf > (Accessed 01/10/2013).

Wild, S., Roglic, G., Green, A., Sicree, R., King, H. 2004. Global prevalence of diabetes: estimates for the year 2000 and projections for 2030. *Diabetes care*, 27(5): 1047-1053.

Woehrle, G.H., Hutchison, J.E., Ozkar, S., Finke, R.G. 2006. Analysis of nanoparticle transmission electron microscopy data using a public-domain image-processing program, image. *Turkish Journal of Chemistry*, 30(1): 1-13.

Yagi, A., Hegazy, S., Kabbash, A., Abd-El Wahab, E. 2009. Possible hypoglycaemic effect of *Aloe vera* L. high molecular weight fractions on Type 2 Diabetic patients. *Saudi Pharmaceutical Journal*, 17: 210-218.

Yallappa, S., Manjanna, J., Dhananjaya, B.L. 2015. Phytosynthesis of stable Au, Ag and Au–Ag alloy nanoparticles using *J. Sambac* leaves extract, and their enhanced antimicrobial activity in presence of organic antimicrobials. *Spectrochimica Acta Part A: Molecular and Biomolecular Spectroscopy*, 137: 236-243.

Yeh, G.Y., Eisenberg, D.M., Kaptchuk, T.K., Phillips, R.S. 2003. Systematic review of herbs and dietary supplements for glycemic control in diabetes. *Diabetes Care*, 26(4): 1277-1294.

Youn, J.Y., Park, H.Y., Cho, K.H. 2004. Antihyperglycaemic activity of *Commelina communis* L: Inhibition of α-glucosidase. *Diabetes Research and Clinical Practice*, 66: 149-155.

Zhang, Q.L., Yang, Z.M., Ding, B.J., Lan, X.Z., Guo, Y.J. 2010. Preparation of copper nanoparticles by chemical reduction method using potassium borohydride. *Transactions of Nonferrous Metals Society of China*, 20: 240-244.

Zhao, L., Wang, H., Huo, K., Cui, L., Zhang, W., Ni, H., Zhang, Y., Wu, Z., Chu, P. K. 2011. Antibacterial nano-structured titania coating incorporated with silver nanoparticles. *Biomaterials*, 32(24): 5706-5716.

Zeggwagh, N., Eddouks, M. 2007. Antihyperglycaemic and hypolipidemic effects of *Ocimum basilicum* aqueous extract in diabetic rats. *American Journal of Pharmacology and Toxicology*, 2(3): 123-129.

APPENDICES

Appendix 1: Current oral hypoglycaemic agents for diabetic patients with advantages and side effects

Agent	Mechanism	Site of action	Advantages	Side effects	References
1. Sulphonylureas Glibenclamide, Glipizide, Gliclazide, Glimepiride, Chlorpropamide	↑ β-cell insulin secretion by inhibiting the K-ATP channel	Pancreatic β-cells	Effective and inexpensive	↑ Cardiovascular risk, hypoglycaemia and ↑ weight.	Katzung *et al.* 2009
2. Biguanide Metformin	↓ Hepatic glucose production by potentiating insulin action (↓ insulin resistance)	Liver	Weight loss	Nausea, diarrhoea, hypoglycaemia occurs when combined with a sulfonylurea or insulin.	Katzung *et al.* 2009
3. Thiazolidinediones Pioglitazone Rosiglitazone	↑ muscle and adipose tissue glucose uptake by potentiating insulin action (↓ insulin resistance by activating PPAR-γ)	GI tract	Low risk	↑ Liver enzymes, liver toxicity, weight gain, oedema, mild anaemia, increased risk of cardiovascular death.	Katzung *et al.* 2009
4. Enzyme inhibitors (Alpha glucosidase) Acarbose	↓ Intestinal glucose absorption, as a result PPHG is blunted.	Adipose and muscle tissue	↓ PPHG	Diarrhoea, pain, abdominal discomfort, distension, bloating, flatulence, bacterial fermentation of undigested carbohydrates.	Bhat *et al.* 2011; Sudha *et al.* 2011
5. Meglitinides Glitinides, Repaglinide, Nateglinide	↑ β-cell insulin secretion, increase 1st phase release.	Pancreatic β-cells	Short acting and more favourable effect on β-cell survival as compared to sulfonylureas.	Weight gain, gastrointestinal disturbances, and hypersensitivity reactions (pruritus, and urticaria).	Bastaki 2005

Key: ↑ = Increase; ↓ = Decrease; PPHG = Postprandial hyperglycaemia

Appendix 2: Hypoglycaemic action of the most popular medicinal plants (A-C)

Plants and Family	Hypoglycaemic and medicinal properties
Adansonia digitata L., leaves; Bombacaceae	↓ Blood glucose level due to insulin like effect on peripheral tissues by promoting glucose uptake and metabolism or by inhibiting hepatic gluconeogenesis (Tanko *et al.* 2008).
Allium sativum L., rhizomes; Alliaceae	↓ BP and improves lipid profile, ↓ serum glucose, TG, cholesterol, urea, uric acid and, ↑ serum insulin levels (Eidia *et al.* 2006).
Aloe vera (L.) Burm.f., leaves; Liliace	↓ FBG, hepatic transaminases, plasma and liver cholesterol, TG, FFA and phospholipids. Improves plasma insulin level, restores normal levels of LDL, HDL and cholesterol, ↓ levels of hepatic phosphatidylcholine hydroperoxide and has hypocholesterimic efficacy, diminishes degenerative changes observed in kidney tissue (Yagi *et al.* 2009).
Aloe arborescen, leaves Asphodelaceae *	↓ FBG in alloxan diabetic rats but no effect in normal rats, ↓ Plasma insulin and TG levels in diabetic rats, Glucokinase and G6P activities in diabetic rats (Mogale *et al.* 2011a).
Brachylaena discolour DC., whole plant; Asteraceae *	↑ Glucose utilization in 3T3-L1 adipocytes, Chang liver and C2C12 muscle cells (van de Venter *et al.* 2008).
Casia fistula L., leaves; Caesalpiniaceae	↓ Blood glucose level in alloxan diabetic rats (Bhakta *et al.* 2001).
Catharanthus roseus (L.). G. Don; leaves; Apocynaceae	↓ Blood glucose by enhancing secretion of insulin from β-cells of Langerhans or through extra pancreatic mechanism (Nammi *et al.* 2003).
Cinnamomum cassia and *Cinnamomum zeylanicum;* leaves and bark; Lauraceae	↓ Blood glucose and elevates plasma insulin level (Verspohl *et al.* 2005).
Clausena anisata (Willd) Hook, root; Rutaceae *	Dose-dependent reduction in blood glucose levels (Ojewole 2002).
Cissampelos capensis L.f., whole plant; Menispermaceae *	↓ FBG in diabetic rats, No alteration in FBG of controls. Nontoxic to cells (van de Venter *et al.* 2008).

*Key: * = Study in SA; ↓ = Decrease; ↑ = Increase; BP = Blood pressure FBG = Fasting blood glucose; FFA = Free fatty acids; GFR = Glomerular filtration rate; HDL = High density lipoprotein; LDL = Low density lipoprotein; PPHG = Postprandial hyperglycaemia; STZ = Streptozotocin; TG = Triglycerides*

Appendix 3: Hypoglycaemic action of the most popular medicinal plants (H-P)

Plants and Family	Hypoglycaemic and medicinal properties
Harpagophytum procumbens D, root; Pedaliaceae *	Dose-dependent reduction in blood glucose levels (Mahomed and Ojewole 2004).
Hypoxis hemerocallidea (African potato); Hypoxydaceae *	Dose-dependent ↓ in FBG of normal and diabetic rats (less effective than Glibenclamide) (Mahomed and Ojewole 2003).
Linum usitatisumum L., seeds; Linaceae	↓ FBG levels, TG; reduces carbohydrate absorption from gut and clinical symptoms of diabetes associated with dyslipidaemia (Thakur *et al.* 2009).
Mangifera indica L., fruits and leaves; Anacardiaceae	Reduces glucose absorption in type 2 diabetics. Stimulates glycogenesis in liver causing reduction in blood glucose levels (Bhowmik *et al.* 2009).
Momordica balsamina L., stem and flowers; Cucurbitaceae *	Increases glucose utilization in 3T3-L1 adipocytes, Chang liver and C2C12 muscle cells (van de Venter *et al.* 2008).
Morus alba L.; leaves; Moraceae	Antiphlogistic, diuretic, expectorant and antidiabetic. ↑ β-cell number in diabetic islets. Reduces levels of glycosylated haemoglobin. ↓ TG, cholesterol and VLDL to normal levels in type IDDM patients. Restores elevated levels of blood urea (Mohammadi and Naik 2008).
Nerium oleander L., leaves; Apocynaceae	Clorogenic acid, querecetin and cathechin induced PPHG by acting as α-glucosidase inhibitors (Ishikawa *et al.* 2007).
Ocimum tenuiflorum (*O. sanctum*), leaves; Lamiaceae	↓ Blood glucose level and modulates cellular antioxidant defence system. Improves β-cell function and enhances insulin secretion. Inhibits absorption of glucose from the intestine (Sethi *et al.* 2004).
Ocimum basilicum (*O. basilicum*), leaves; Lamiaceae	↓ FBG by 21.0 mg/dL and subsequent ↓ in PPHG by 15.8 mg/dL (Agrawal *et al.* 1996).
Piper nigrum L.; seeds; Piperaceae	↓ Glucose and serum lipid levels (Kaleem *et al.* 2005).
Psidium guajava L., leaves and root; Myrtaceae *	↑ Increased glucose utilization in liver cells. Toxic to liver and muscle cells (van de Venter *et al.* 2008).

*Key: * = Study in SA; ↓ = Decrease; ↑ = Increase; BP = Blood pressure FBG = Fasting blood glucose; FFA = Free fatty acids; GFR = Glomerular filtration rate; HDL = High density lipoprotein; LDL = Low density lipoprotein; PPHG = Postprandial hyperglycaemia; STZ = Streptozotocin; TG = Triglycerides; VLDL = Very low density lipoprotein*

Appendix 4: Hypoglycaemic action of the most popular medicinal plants (P-Z)

Plants and Family	Hypoglycaemic and medicinal properties
Psidium guajava L., leaves and root; Myrtaceae *	↑ Increased glucose utilization in liver cells. Toxic to liver and muscle cells (van de Venter *et al*. 2008).
Sclerocarya birrea [(A. Rich.) Hochst.], stem-bark; Anacardiaceae *	↓ FBG and had no effect on insulin levels in STZ rats. ↑ Hepatic glycogen synthesis. ↓ plasma urea and creatinine and ↑ GFR (Gondwe *et al.* 2008).
	↓ FBG in normal and STZ- rats, inhibition of α-amylase and α-glucosidase (Mogale *et al.* 2011b).
	↑ Glucose utilization in liver and muscle cells. Toxic to liver cells (van de Venter *et al.* 2008)
Sutherlandia frutescens, leaves; Fabaceae *	Normalized insulin levels in experimental rats. ↑ Glucose uptake in muscle and adipose tissue. ↓ intestinal glucose uptake (Chadwick *et al.* 2007).
Syzygium cordatum (Hochst.), leaves; Myrtaceae *	Decreased FBG levels and increased hepatic glycogen by Musabayane *et al*. (2005)
Terminalia chebula Retz., seeds; Combretaceae	↓ Blood glucose levels by enhancing secretion of insulin from β-cells of Langerhans or through extra pancreatic mechanism. Inhibits advanced glycosylation end products, which contribute to renal damage (Rao and Nammi 2006).
Tinospora cordifolia (Willd.) Miers, root; Menispermaceae	↓ Blood glucose level through glucose metabolism. It exhibits inhibitory effect on adrenaline-induced hyperglycaemia (Singh *et al.* 2003).
Trigonella foenum-graceum L., seeds; Fabaceae	↓ PPHG level (Ismail 2009).
Vinca major L., stem, root, leaves; Apocynaceae *	↑ Glucose utilization in Chang liver, C2C12 muscle and 3T3-L1 adipocytes. Very toxic to cells (van de Venter *et al.* 2008).
Zingiber officinale Rosc., rhizomes; Zingiberaceae	↓ Plasma glucose level (Agoreyo *et al.* 2006).

*Key: * = Study in SA; ↓ = Decrease; ↑ = Increase; BP = Blood pressure FBG = Fasting blood glucose; FFA = Free fatty acids; GFR = Glomerular filtration rate; HDL = High density lipoprotein; LDL = Low density lipoprotein; PPHG = Postprandial hyperglycaemia; STZ = Streptozotocin; TG = Triglycerides*

Appendix 5: Documented natural enzyme inhibitors

Plant and family; active compound	Study design	Result	References
Commelina communis, Commelinaceae	*In vitro* α-glucosidase and *in vivo* (STZ)-induced diabetic mice.	Showed inhibitory activity of the α-glucosidase in a dose-dependent manner and alleviated hyperglycaemia caused by maltose or starch loading in normal and STZ, greater efficacy than that of acarbose.	Youn *et al.* 2004
Tamarindus indica, Fabaceae	*In vitro* α-amylase.	90% inhibitory activity against α-amylase.	Funke and Melzig 2006
Ocimum basilicum, Lamiaceae	*In vitro* α-glucosidase and α-amylase activities.	Positive antioxidant, α-glucosidase and α-amylase inhibiting activities.	El-Beshbishy and Bahashwan 2012
Azadirachta indica, Meliaceae; *Mangifera indica*, Anacardiaceae; *Murraya koenigii*, Rutaceae;	*In vitro* α-amylase activity using ethanol and petroleum ether extracts	*Mangifera indica*, *Azadirachta indica* and *Murraya koenigii* exhibited a high α-amylase activity when compared with acarbose proved effective in lowering PPHG.	Dineshkumar *et al.* 2010
Andrographis paniculata (AP), Acanthaceae and andrographolide	*In vitro* α-glucosidase activity.	Both extracts showed appreciable α-glucosidase inhibitory but, AP extract can be considered as a potential candidate for the management of type 2 diabetes.	Subramanian *et al.* 2008
Origanum vulgare, Lamiaceae; Purified Rosmarinic acid (RA) and Lemon balm	*In vitro* experiments using PPA.	RA-containing oregano extracts yielded higher than expected α-amylase inhibition than similar amount of purified RA. Suggesting that other phenolic compounds or phenolic synergies may contribute to additional α-amylase inhibitory activity.	McCue and Shetty 2004
Gongronema latifolium, Asclepiadaceae	Liver of non-diabetic and STZ diabetic rats.	Antihyperglycaemic potency, which is mediated through the activation of HK, PFK, G6PDH and inhibition of GK in the liver.	Ugochukwu and Babady 2003

Key: STZ = Streptozotocin; PPA = Porcine pancreatic α-amylase; HK = Hexokinase; PFK = Phosphofructokinase; G6PDH = Glucose-6-phosphate dehydrogenase; GK = Glucokinase; PPHG = Postprandial hyperglycaemia

Appendix 6: Formulas and calculations

6.1 Preparation of 60% and 70% ethanol that were used for preparation of the plant extracts.

Calculation: Volume (g) x % (g) = Volume (required) x % (required)

E.g. of the preparation of 60% EtOH, the same formula can be used for preparation of 70% EtOH.

A: X x 99.5% = 1000 X 60%

99.5x = 60 000

x= 603.015 ml (ROH)

B: Aq. Dist. = 1000 - 603.01507

= 396.985 ml

A+B = 1000 ml of 60% ROH

6.2 Determining loss on drying

The plant material was finely broken by hand and placed under a desiccator which removes all the water content. The desiccator was timed for 15 min and subsequently increased for one hour of 15 min intervals to check if all the water is removed from the finely shredded plant material.

$$A2 = \frac{m.T\ (kg)}{100}$$

m = mass of plant material in kg (300 g)

T = loss on drying of the sample (in per cent)

A2 = mass of ROH (ethanol 60% v/v that is equivalent to 86% m/m)

Fresh *Ocimum* sp. was weighed: 10.000 g

Final dried *Ocimum* sp.: 0.770 g

Therefore:

$$A2 = \frac{0.3 \times 93\ \%}{100}$$

= 0.279 kg Ethanol

= 279 g Ethanol or aq. distillation (water) extracts

Appendix 7: Extraction methods: GHP Method 2a (A) Loss on drying process 105ºC for 2 hours, expressed as a percentage (m/m) (B) Picture of aq. solutions prepared with *O. sanctum* leaf extract (C) Picture of an ethanolic solution prepared by *O. sanctum* leaf extract

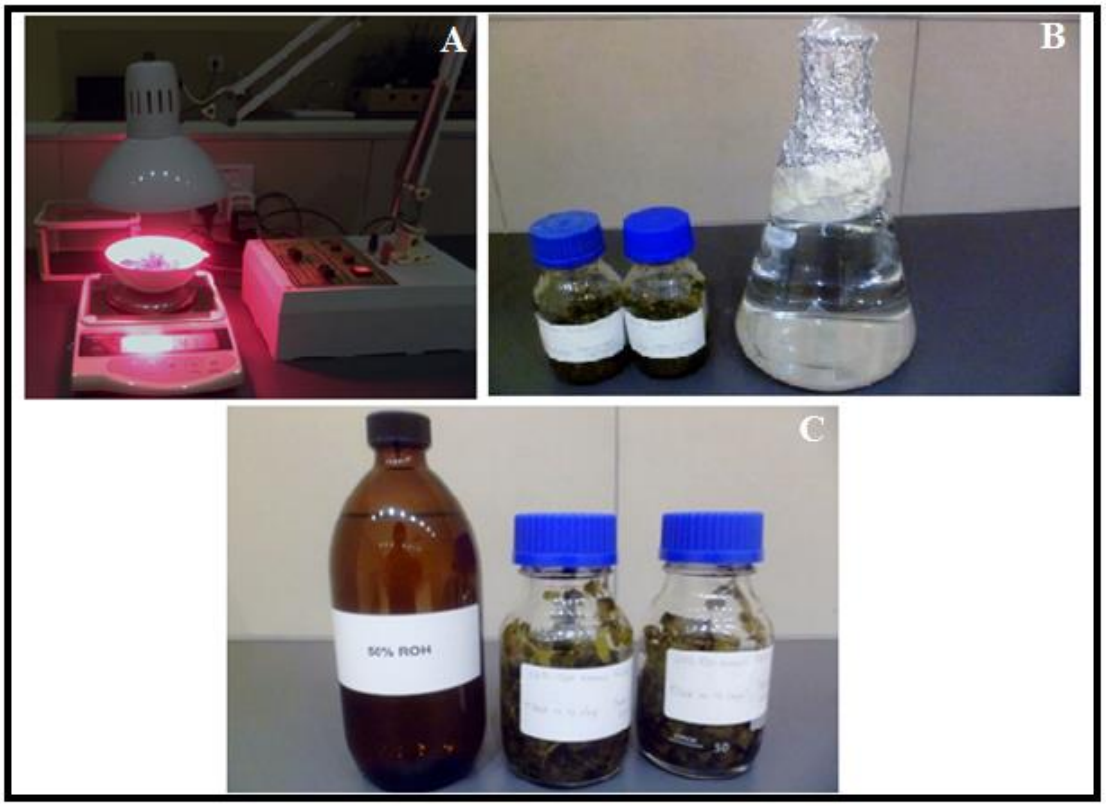

Appendix 8: Filtration method by German Homoeopathic Pharmacopoeia (2005) (A) Picture illustrating the filtration method first using mutton cloth (B) Second process of filtration using Whatman No. 1 filter paper of *Ocimum sanctum* leaf extracts

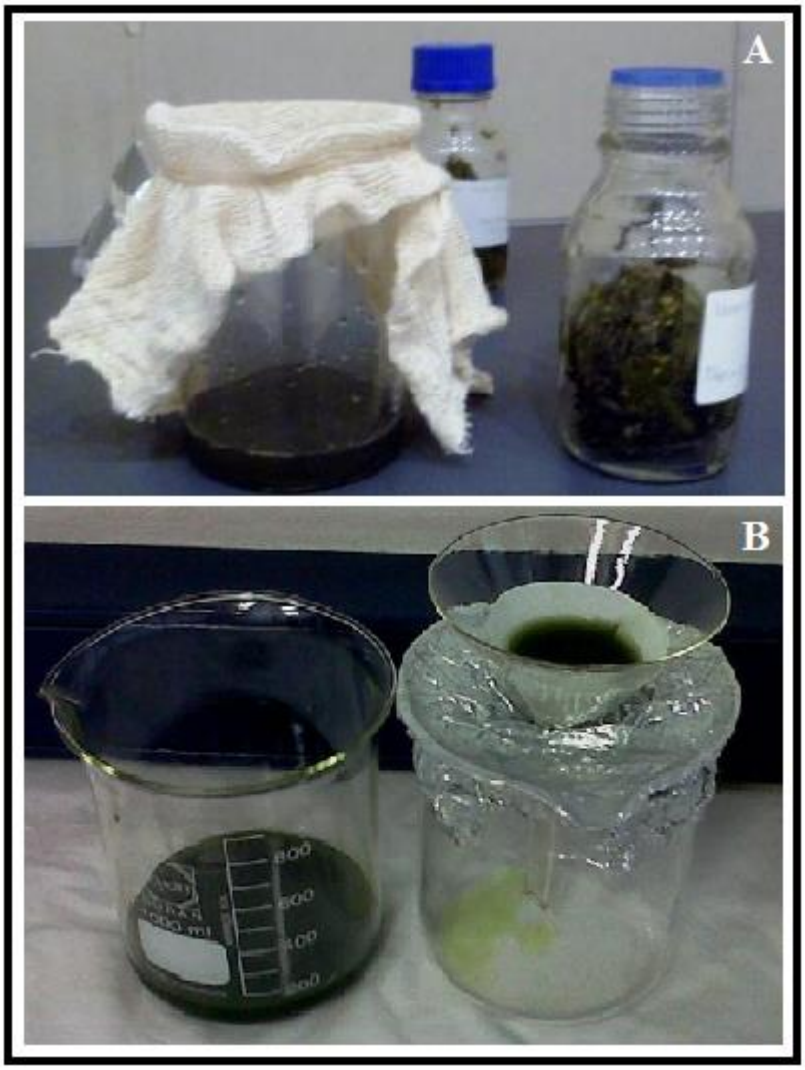

Appendix 9: Preparation of materials used for the antimicrobial and antidiabetic analysis

9.1 Preparation of distilled water control, agar, broth, inoculums, stains and controls

9.1.1 Preparation of distilled water control

Distilled water was obtained from the Department of Chemistry at the Durban University of Technology. The water was sterilised by autoclaving for 1 hour at 121°C at 15 psi pressure.

9.1.2 Preparation of Mueller Hinton Agar

Mueller Hinton Agar was prepared according to the manufacturer's instructions (Davies diagnostics, SA, 276725). Briefly, 36 g of powder was weighed into 1 L glass bottles. Sterile distilled water (autoclaved for 1 hour at 121°C at 15 psi pressure) was added to the 1 L mark with the aid of a measuring cylinder. The bottles were shaken until completely dissolved. The medium was sterilised by autoclaving for 15 min at 121°C at 15 psi pressure. Sterile molten cool (50°C) agar was poured aseptically into sterile Petri plates (15 ml each) to solidify at room temperature in sterile conditions (Laminar flow cabinet).

9.1.3 The Preparation of the Nutrient Broth

Nutrient broth Biolab (Merck, SA, 1039422), is medium suitable for cultivation of a wide range of non-fastidious microorganisms. According to the manufacturer's instructions 16 g of nutrient broth powder was weighed into a 1 L glass bottle. Sterile distilled water was added to the 1 L mark with the aid of a measuring cylinder. The broth was shaken until completely dissolved. The broth was then sterilised by autoclaving for 15 min at 121°C at 15 psi pressure. After cooling, 5 ml was dispensed to test tubes.

9.1.4 Gram stain

Identification using the Gram stain was performed to confirm the bacterial isolates (Gephardt *et al.* 1981).

Protocol:

1. Flood air-dried, heat fixed smear of cells for 1-2 minute with crystal violet staining reagent.
2. Wash the slide with the tap water for 2 seconds.
3. Flood the slide with mordant: Grams iodine and wait 1 minute.
4. Wash the slide in a general and the indirect stream of the tap water for 2 seconds.
5. Flood the slide with the decolorising agent, acetone and wait 15 seconds.
6. Flood the slide with the counterstain, safranin and wait 1-2 minute.
7. Wash the slide with the tap water and then blot dry.
8. Observe the results of the staining procedure under oil immersion using a Brightfield microscope. At completion of the Gram stain, Gram negative bacteria will stain pink/red and Gram positive bacteria will stain blue/purple.

9.1.5 Preparation of Inoculums

The following cultured bacterial strains were used: *S. aureus* ATCC 25923, *E. coli* ATCC 26922, *P. aeruginosa* ATCC 27853, *B. subtilis* ATCC 6051 and *Salmonella* sp. UKQC 9990 and were maintained by growing the organism on Blood agar and identified using the Gram stain (9.1.4).

Few colonies were picked from the overnight cultures (*S. aureus, E. coli, P. aeruginosa, B. subtilis* and *Salmonella* sp.) and were suspended in 5 ml Nutrient broth (9.1.3), swirled around and then mixed using a vortex to allow even distribution of the culture. The suspension was made up to the equivalent of 0.5 McFarland turbidity standards. McFarland standards were effectively used to perform visual comparisons of bacterial densities in water, saline or liquid growth medium (McFarland 1907). The Mueller Hinton agar was seeded with appropriate well mixed overnight nutrient broth culture of each test microorganism equivalent to a 0.5 McFarland turbidity standard (visual interpretation). In addition, 100 µl of each microorganism was placed on the Mueller Hinton plates, with the exception of *S. aureus* that also used 200 µl per plate (Cappuccino and Sherman 1992).

9.1.6 Quality Controls

Positive and negative controls were included in every plate to validate results. Sterile antibiotic discs were used, vancomycin 30 µg discs (Davies Diagnostics SA, 292041) and gentamycin 10 µg discs (Davies Diagnostics SA, 329385) were used as positive controls. Distilled water; EtOH 60% and 70% and 1 mM $AgNO_3$ were used as negative controls and the plate for each sample was repeated 6 times.

9.1.6.1 Zone Diameter Interpretative Standards for Organisms (Clinical and Laboratory Standards Institute 2007)

Antimicrobial agent	Zone diameter, nearest whole mm			
	Disk content (µg)	Resistant	Intermediate	Susceptible
Gentamycin	10	<12	13-14	>15
Vancomycin	30	<9	10-11	>12

9.2 Preparation of Buffers and reagents

9.2.1 Incubation buffer for α-amylase enzyme inhibition measurement

The buffer was made fresh and consisted of 20 mM Sodium Phosphate Buffer with 6.7 mM Sodium Chloride, pH 6.9 at 20^{o}C (Prepared in 100 ml sterile distilled water using Sodium Phosphate Monobasic Anhydrous, Sigma SA product lot no. BCBK0389V and Sodium Chloride, Sigma SA product lot no. SZBB215BV and adjusted to pH 6.9 at 20^{o}C with 1 M NaOH).

9.2.2 Incubation buffer for α-glucosidase enzyme inhibition measurement

The buffer was made up fresh and consisted of 67 mM Potassium Phosphate Buffer, pH 6.8 at 37°C (Prepared in 100 ml sterile distilled water using Potassium Phosphate Monobasic

Anhydrous, Sigma Product lot no. SZBC1790V and adjusted to pH 6.8 at 37°C with 1 M NaOH).

9.2.3 Preparation of DNS colour reagent

The reagent was prepared fresh and consisted of 20 ml of 96 mM 3, 5-dinitrosalicylic acid (Sigma, SA, MKBL2572V) and 12 g sodium potassium tartarate (Radchem, 11302) in 8 ml of 2 M sodium hydroxide (NaOH) (Minema, 29951) and gently heated until the final addition of 12 ml sterile distilled water.

9.3 Standard curves

9.3.1 Maltose

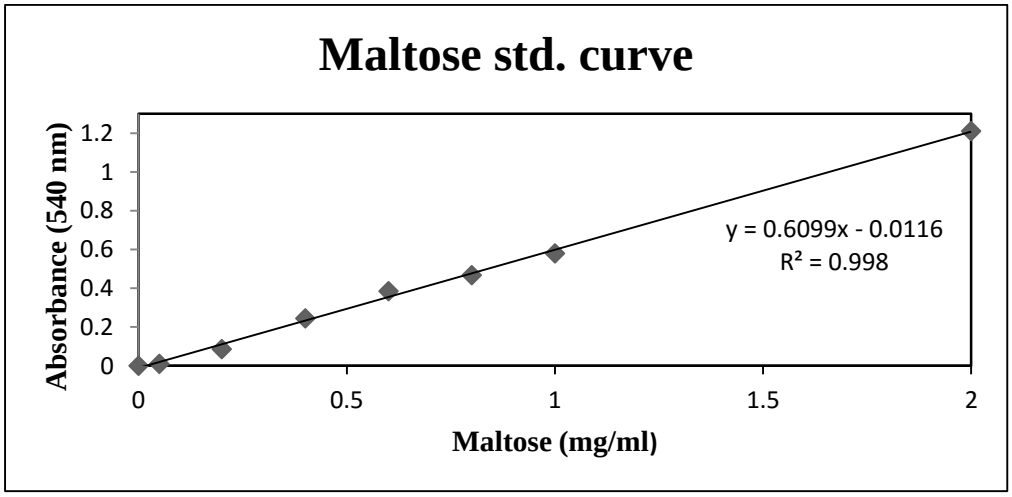

9.3.2 pNPG

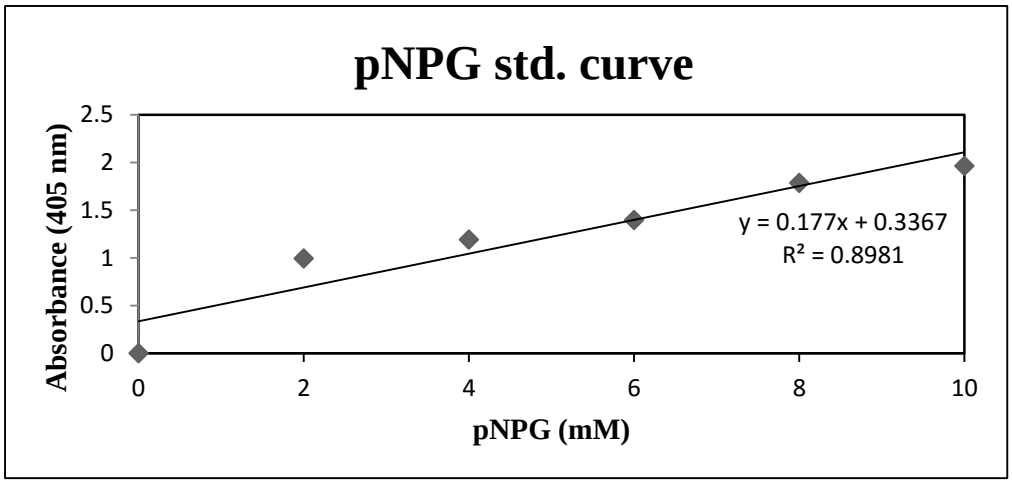

9.4 Inhibition of α-amylase by different concentrations of acarbose (standard control)

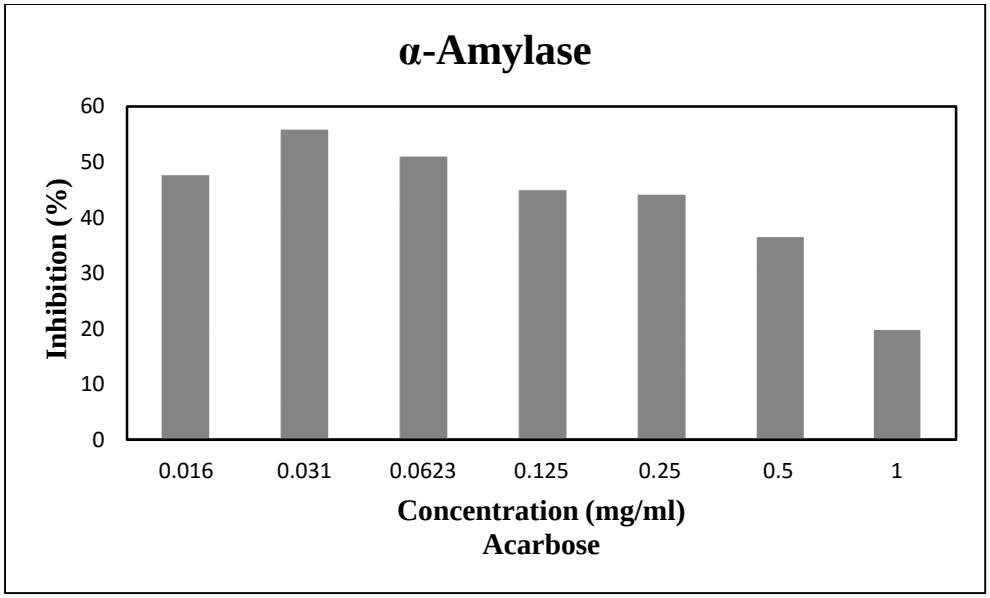

9.5 Inhibition of α-glucosidase by different concentrations of acarbose (standard control)

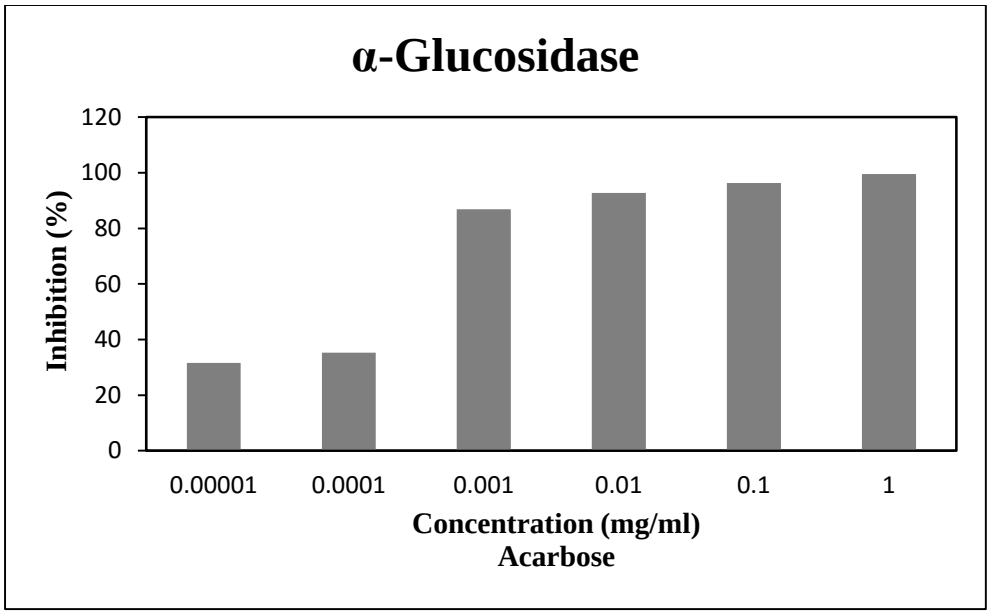

Appendix 10: Peak absorbance versus reaction time for bimetallic (Au-Ag) Nps formed using (A) *O. basilicum* flower and (B) leaf extracts, respectively

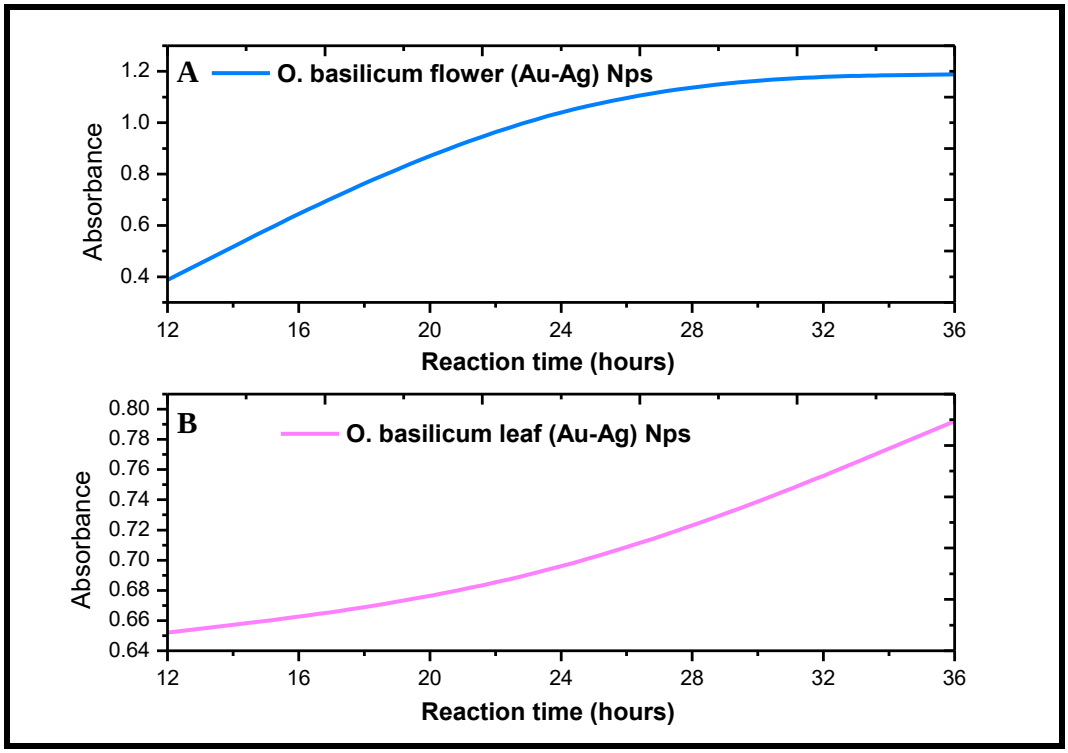

Appendix 11: Peak absorbance versus reaction time for the AgNps (A) *O. sanctum* (B) *O. basilicum* and (C) *O. sanctum* + *O. basilicum*

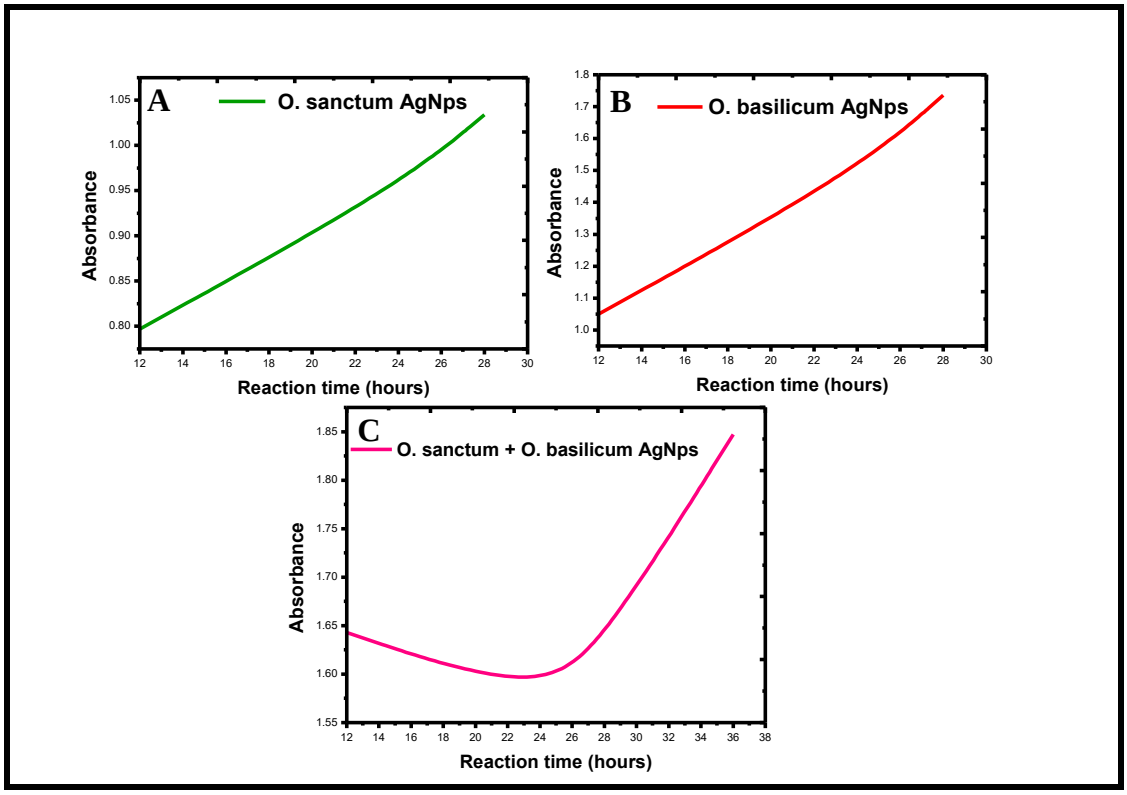

Appendix 12: (A) Representative TEM micrograph of bimetallic (Au-Ag) Nps bio-synthesised by aq. leaf extracts of *O. basilicum* (B) Histogram representation of size distribution of bimetallic (Au-Ag) Nps; mean size of 21 ± 11.53

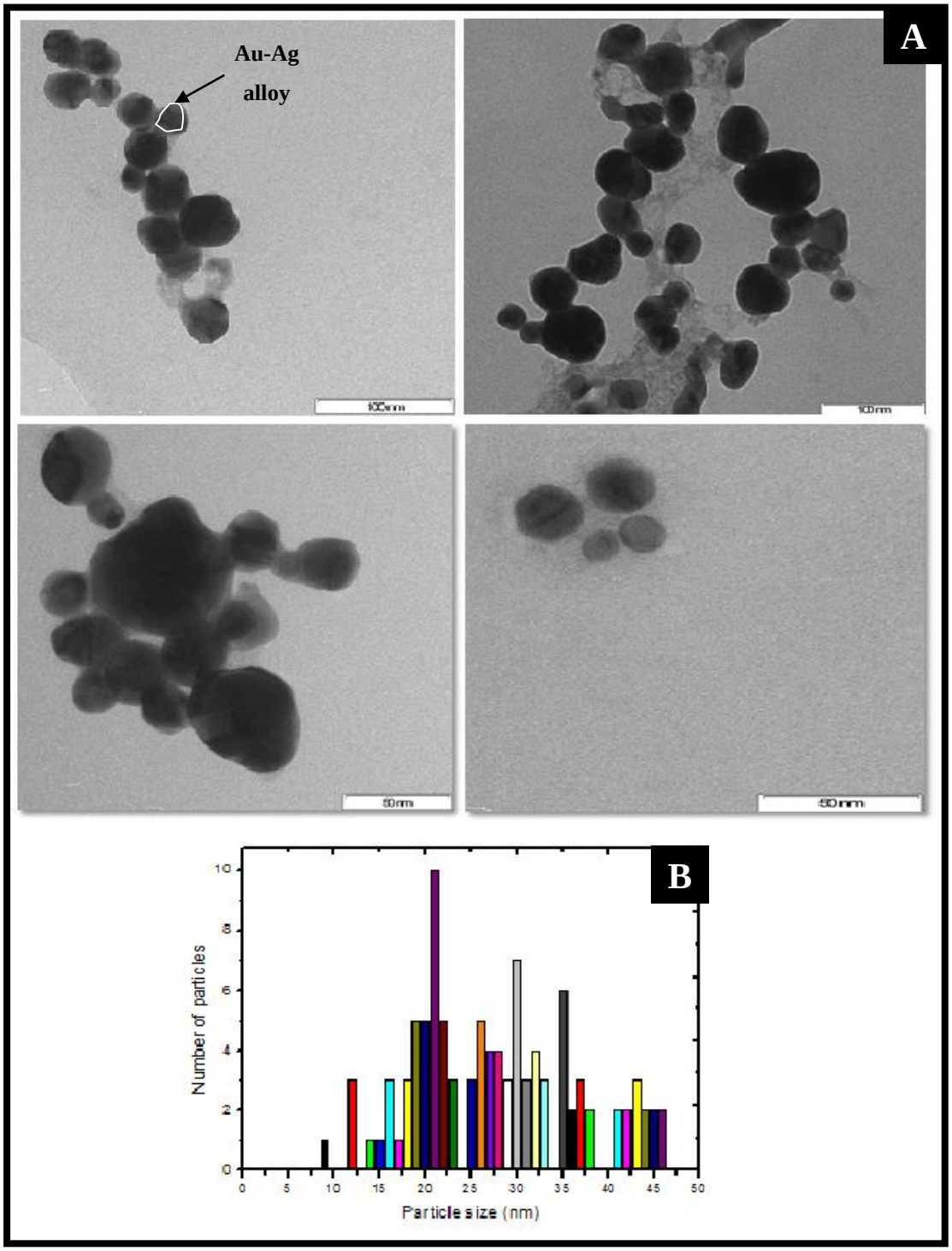

Appendix 13: (A) Representative TEM micrograph of bimetallic (Au-Ag) Nps bio-synthesised by aq. flower extracts of *O. basilicum* (B) Histogram representation of size distribution of bimetallic (Au-Ag) Nps; mean size of 25 ± 9.63

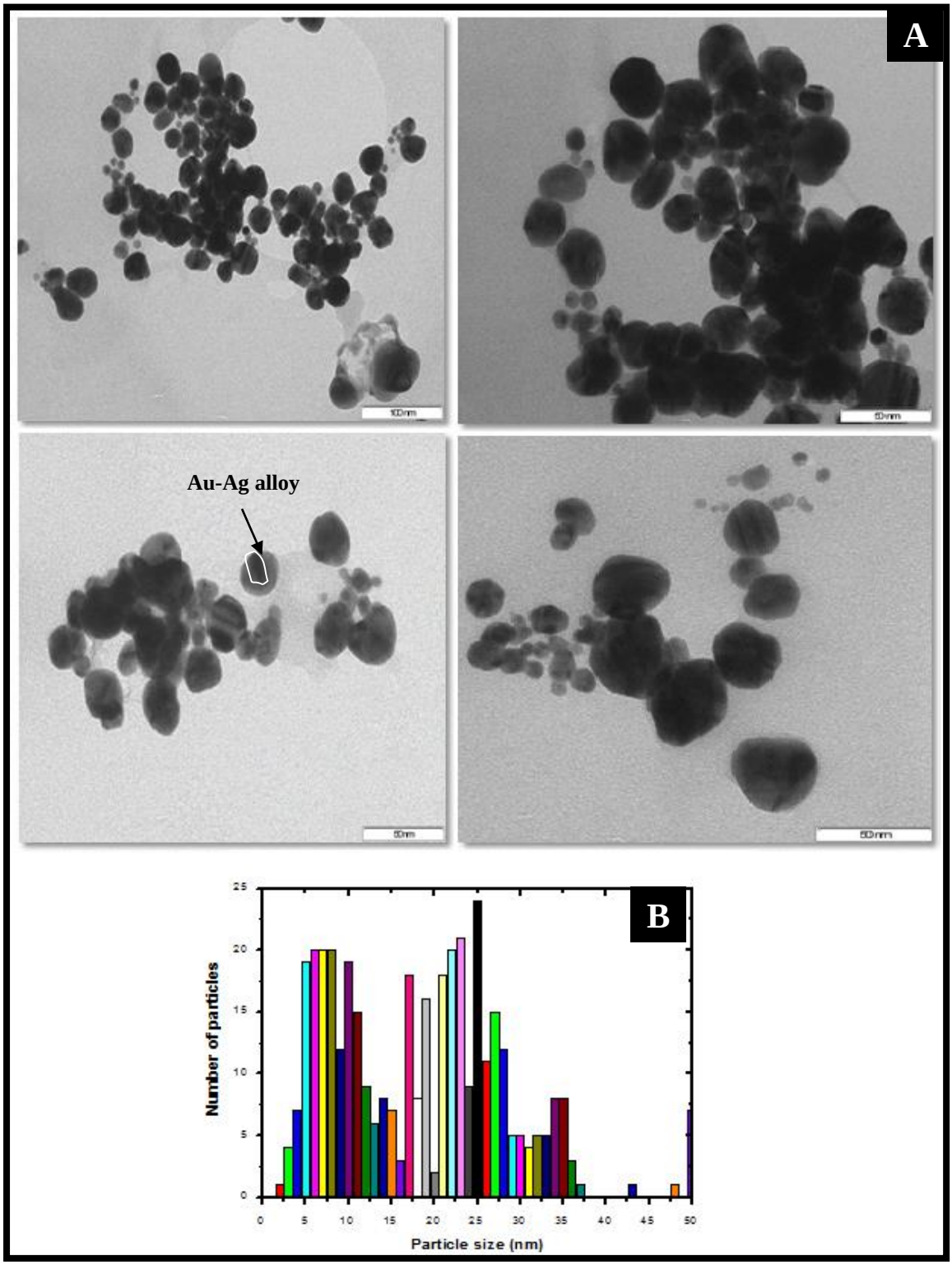

Appendix 14: (A) Representative TEM micrograph of AgNps bio-synthesised by aq. leaf extracts of *O. basilicum* (B) Histogram representation of size distribution of AgNps; mean size of 17.0 ± 8.94

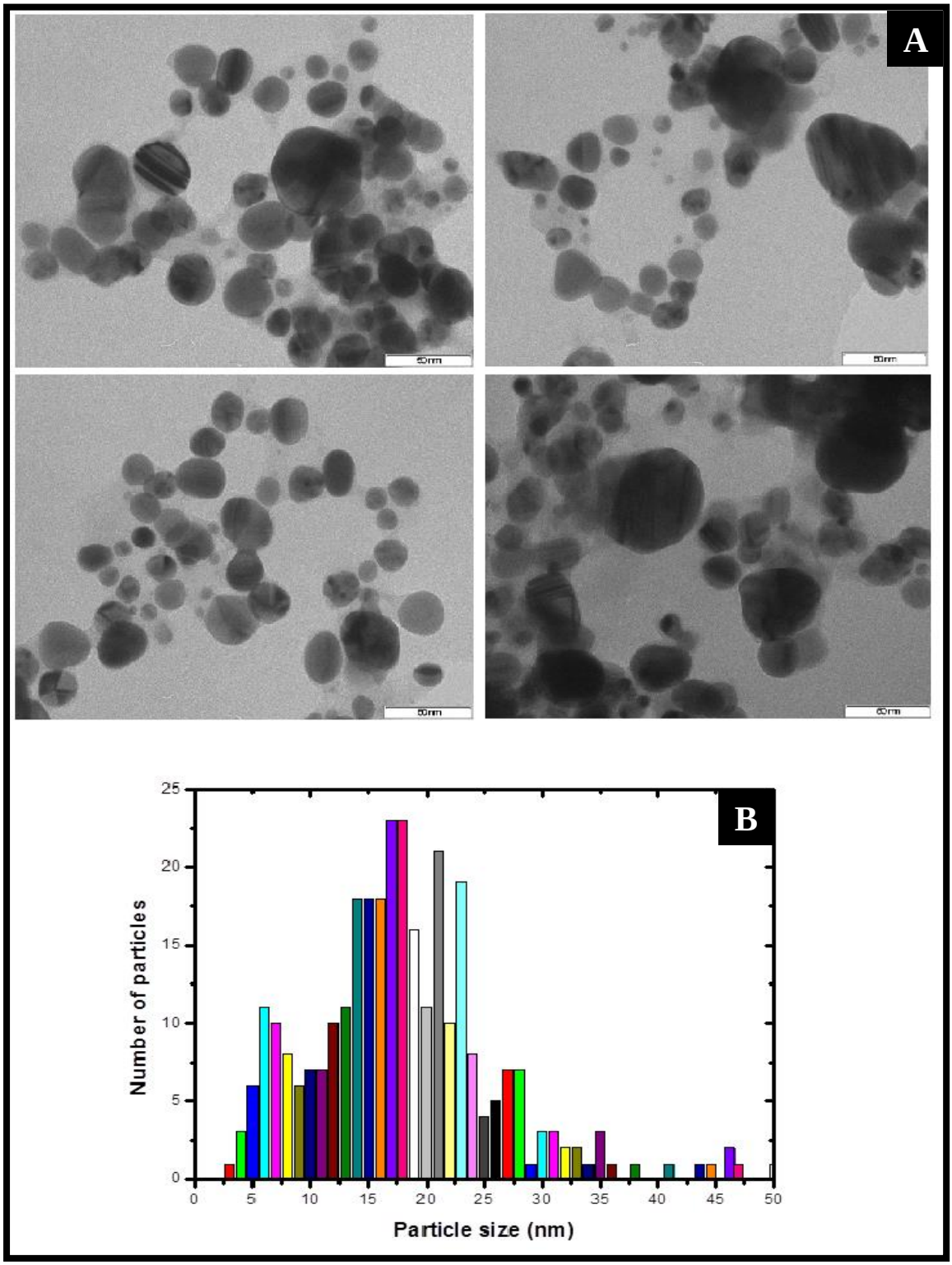

Appendix 15: (A) Representative TEM micrograph of AgNps bio-synthesised by aq. leaf extracts of *O. sanctum* (B) Histogram representation of size distribution of AgNps; mean size of 15.0 ±12.34

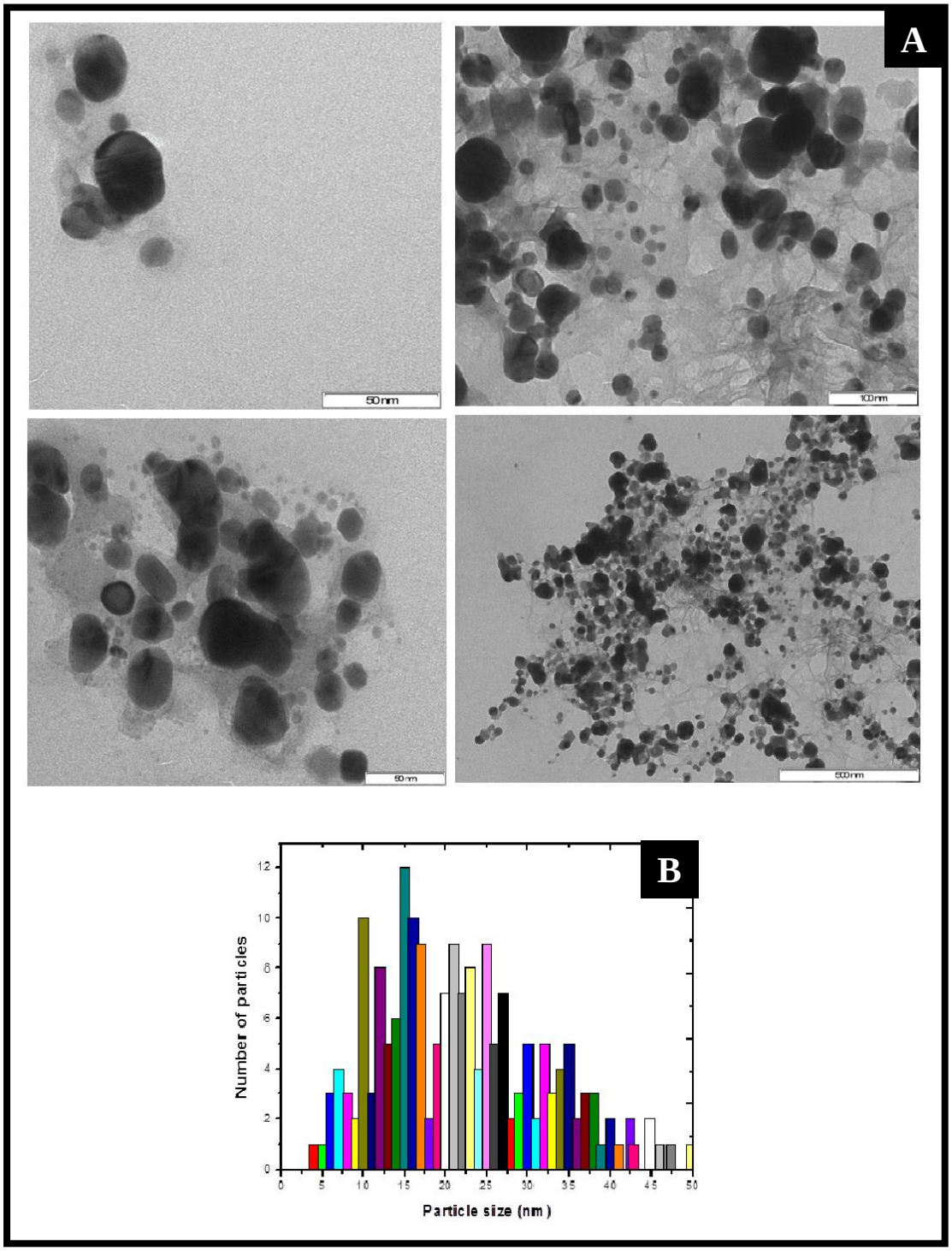

Appendix 16: (A) Representative TEM micrograph of AgNps bio-synthesised by aq. leaf extracts of *O. sanctum* + *O. basilicum* (B) Histogram representation of size distribution of AgNps; mean size of 17.0 ± 8.44

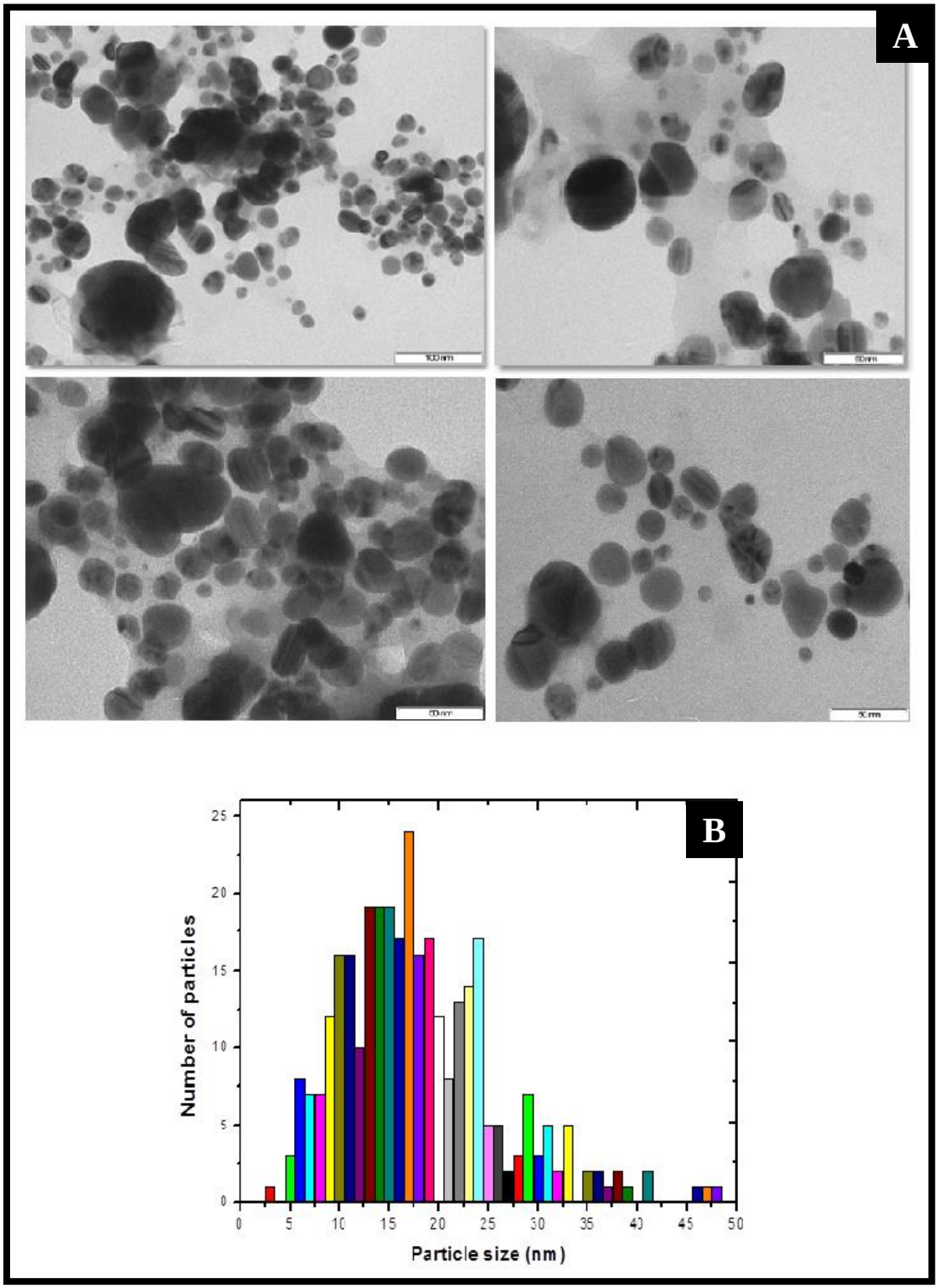

Appendix 17: DLS profile of *O. basilicum* leaf bimetallic (Au-Ag) Nps: (A) Size distribution of bimetallic (Au-Ag) Nps with maximum intensity at 73.55 nm. (B) Stability of bimetallic (Au-Ag) Nps at -25.3 mV in zeta potential analysis

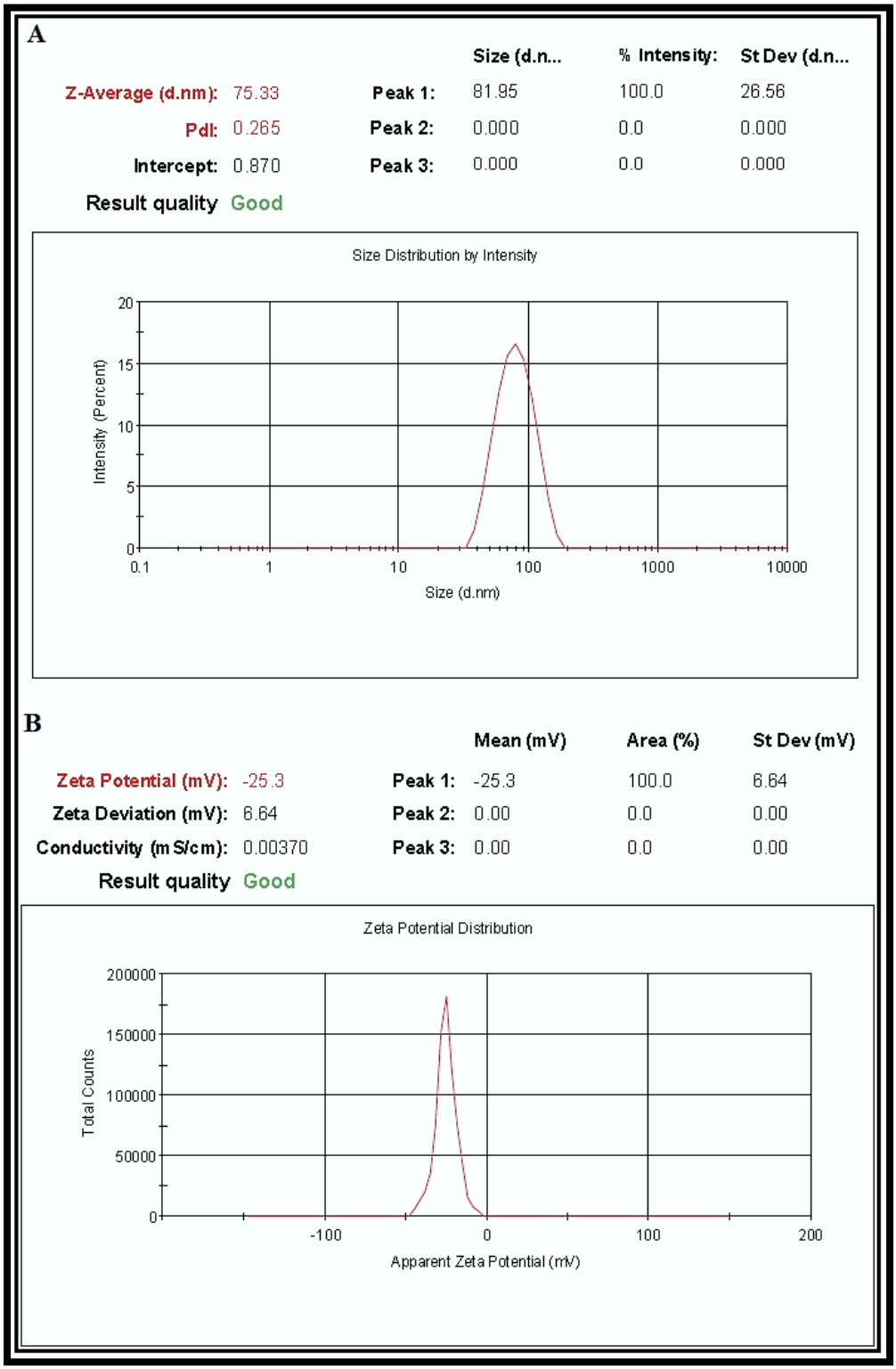

Appendix 18: DLS profile of *O. basilicum* flower bimetallic (Au-Ag) Nps: (A) Size distribution of bimetallic (Au-Ag) Nps with maximum intensity at 78.87 nm. (B) Stability of bimetallic (Au-Ag) Nps at -28.4 mV in zeta potential analysis

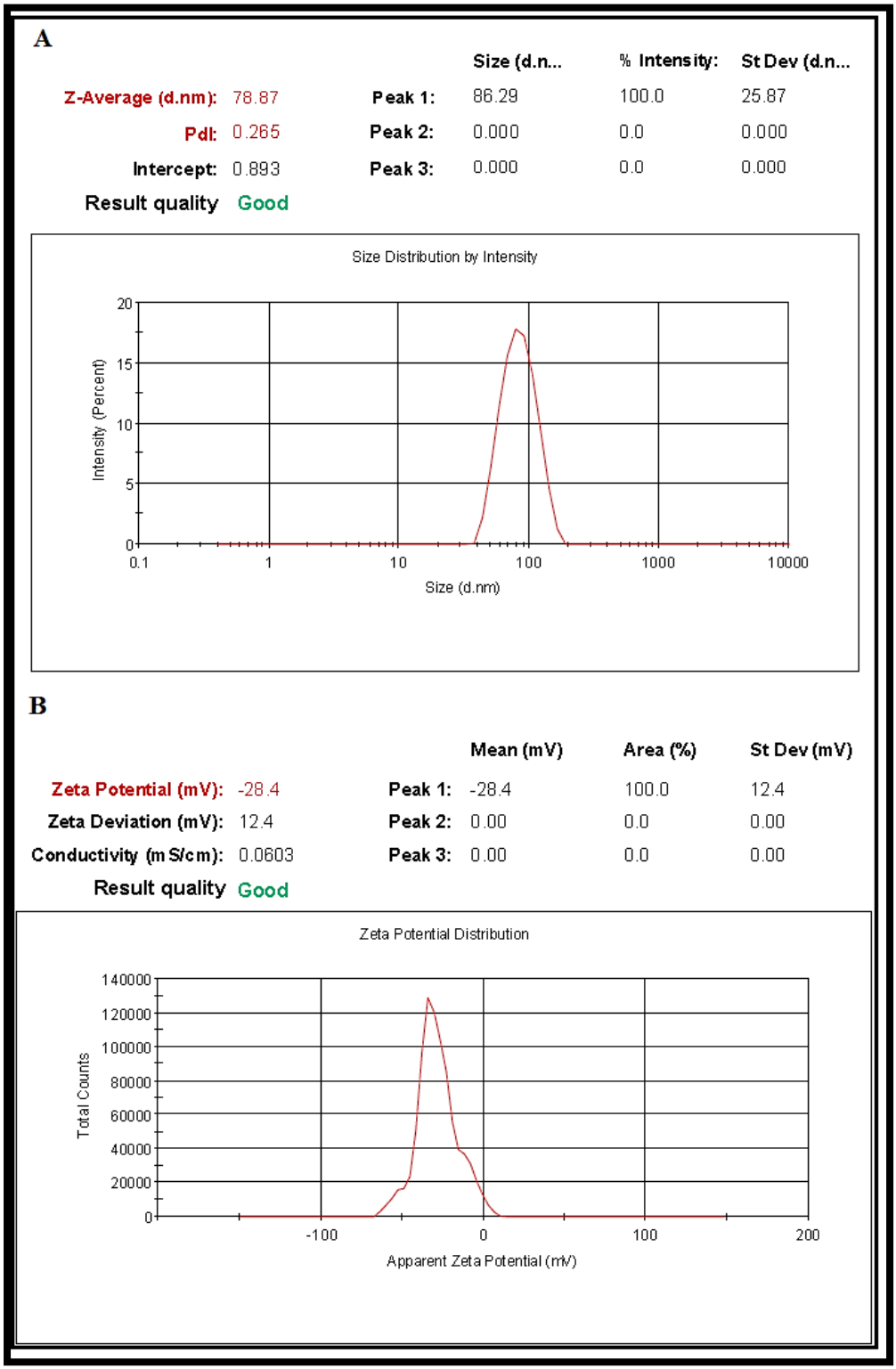

Appendix 19: DLS profile of *O. basilicum* leaf AgNps: (A) Size distribution of AgNps with maximum intensity at 56.81 nm (B) Stability of AgNps at -19.8 mV in zeta potential analysis

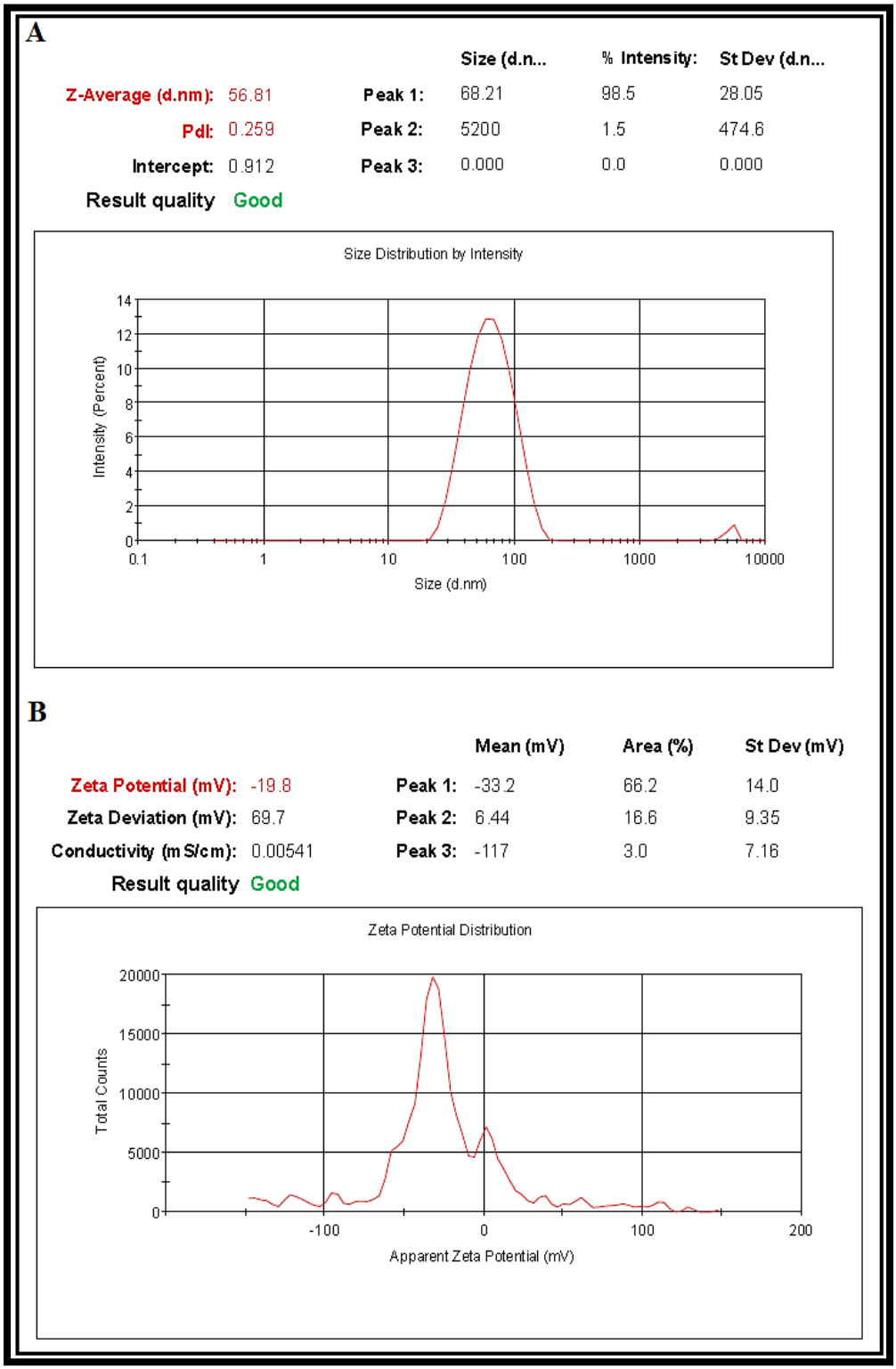

Appendix 20: DLS profile of *O. sanctum* leaf AgNps: (A) Size distribution of AgNps with maximum intensity at 467.4 nm (B) Stability of AgNps at -23.3 mV in zeta potential analysis

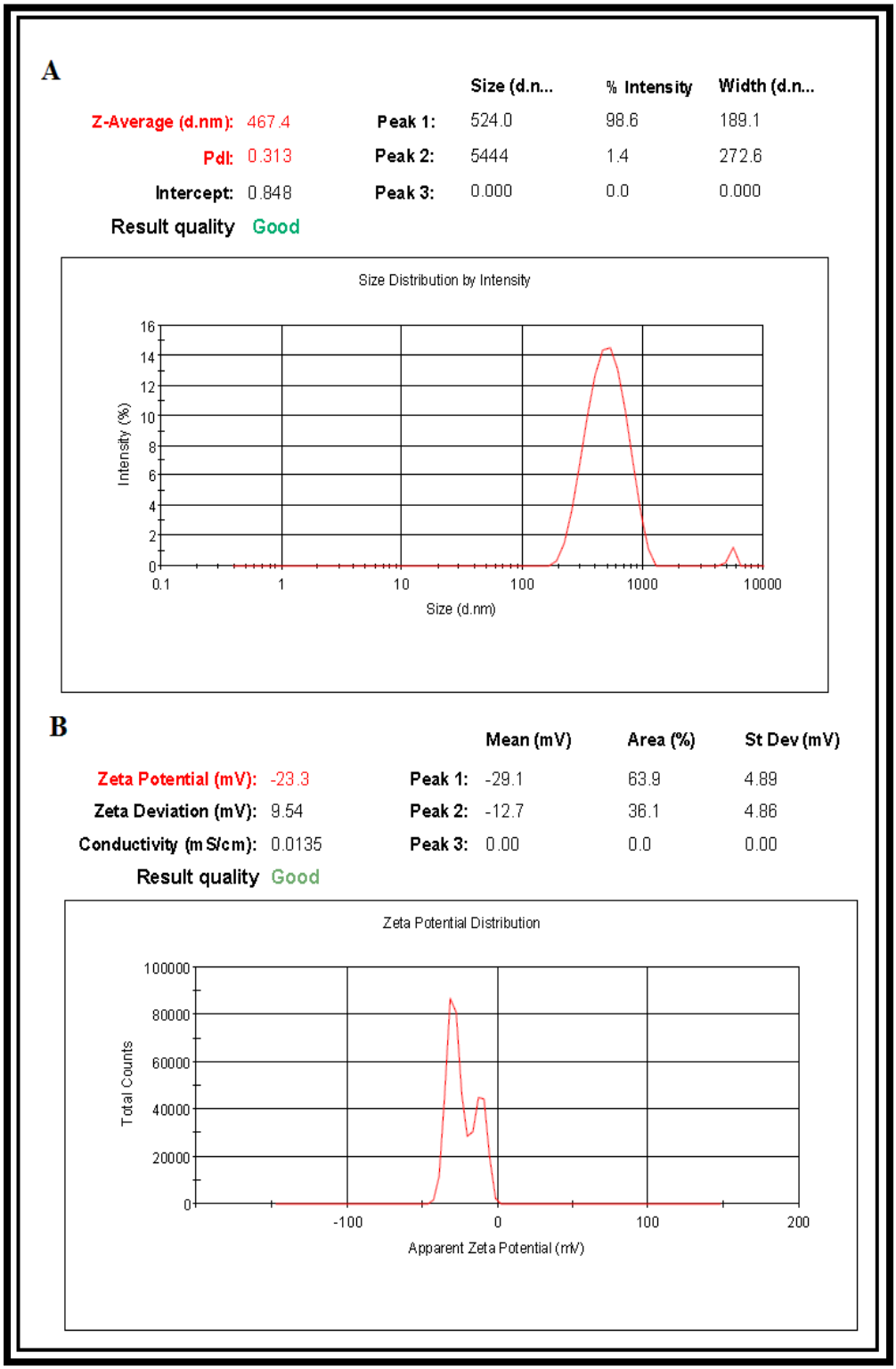

Appendix 21: DLS profile of *O. sanctum* + *O. basilicum* leaf AgNps: (A) Size distribution of AgNps with maximum intensity at 155.1 nm (B) Stability of AgNps at -24.3 mV in zeta potential analysis

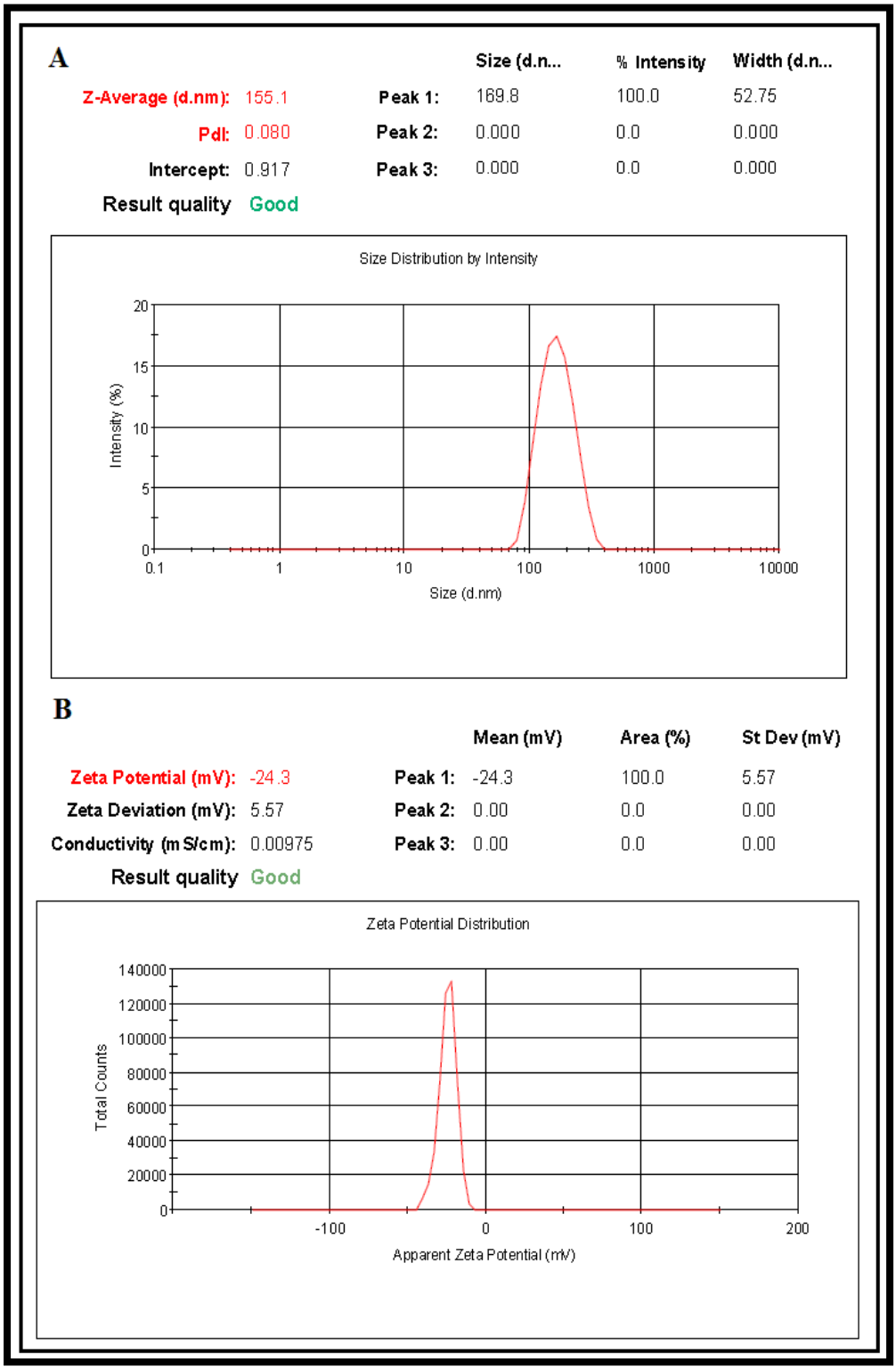

Appendix 22: GC-MS spectra indicating the chemical constituents present in *O. basilicum* (A) Flower extract (no hit compounds) (B) EtOH leaf and (C) aq. leaf extract

(A)

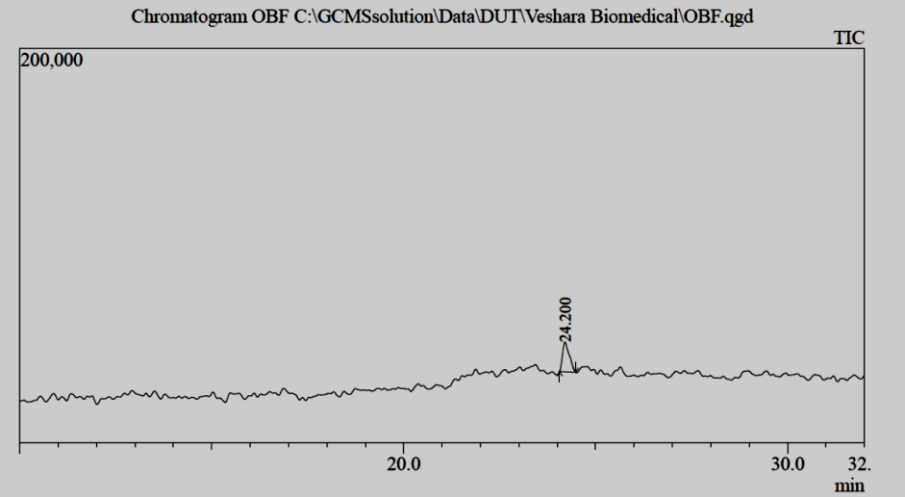

Peak Report TIC

Peak#	R.Time	I.Time	F.Time	Area	Area%	Height	Height%
1	24.200	24.060	24.480	185186	100.00	15097	100.00
				185186	100.00	15097	100.00

(B)

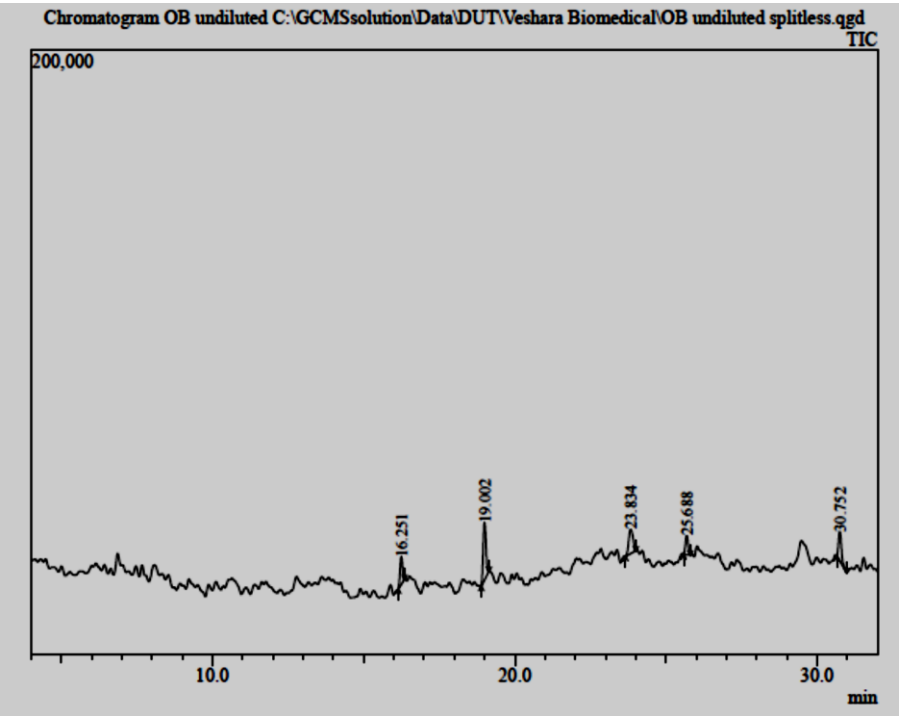

Peak Report TIC

Peak#	R.Time	I.Time	F.Time	Area	Area%	Height	eight%
1	16.251	16.145	16.355	53340	15.01	9073	17.53
2	19.002	18.890	19.145	121907	34.31	18624	35.99
3	23.834	23.660	24.005	77916	21.93	7930	15.32
4	25.688	25.580	25.805	38653	10.88	6326	12.22
5	30.752	30.650	30.980	63522	17.88	9797	18.93
				355338	100.00	51750	100.00

(C)

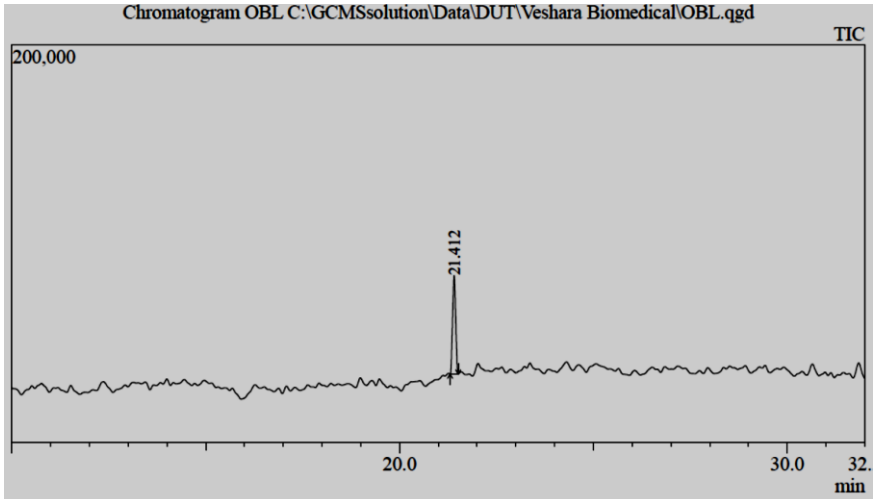

Peak Report TIC

Peak#	R.Time	I.Time	F.Time	Area	Area%	Height	Height%
1	21.412	21.305	21.515	272338	100.00	49378	100.00
				272338	100.00	49378	100.00

Appendix 23: Chemical structures of the main chemical compounds identified in *O. basilicum* leaf extract

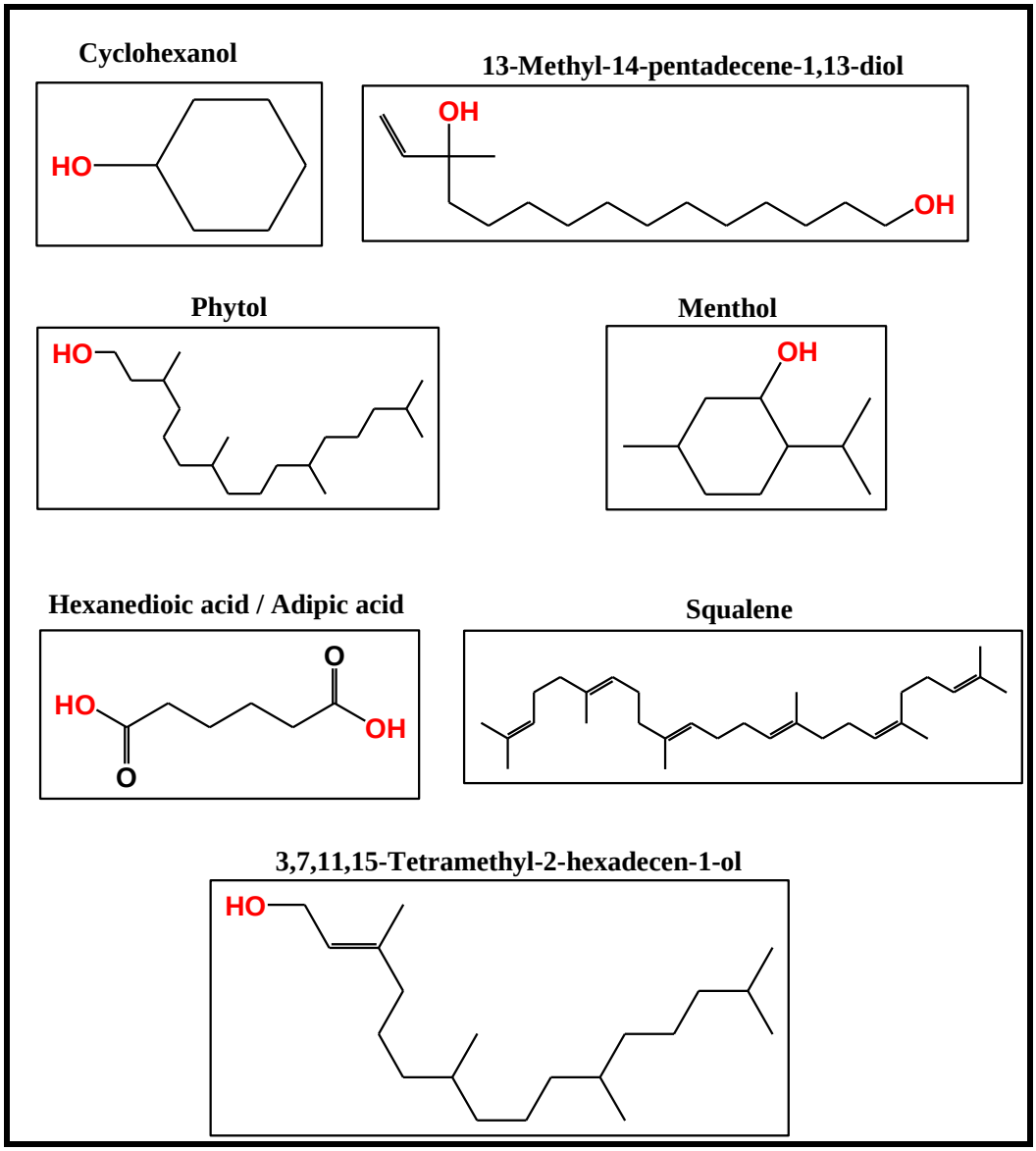

Appendix 24: GC-MS spectra indicating the chemical constituents present in *O. sanctum* (A) EtOH and (B) aq. leaf extract

(A)

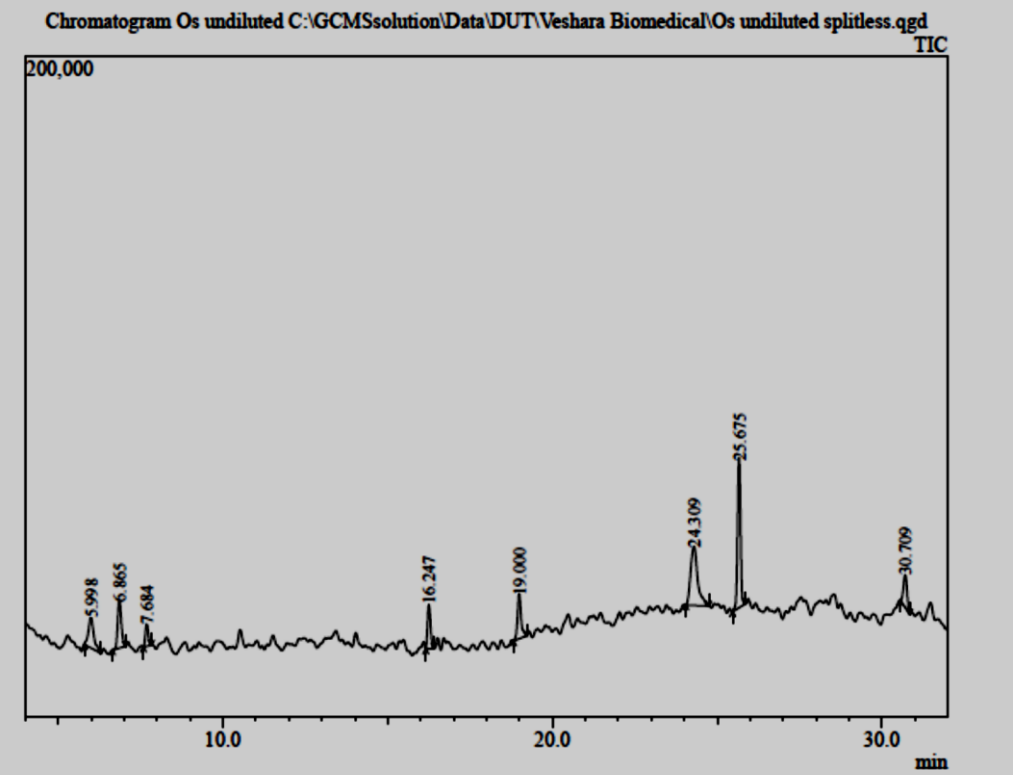

Peak Report TIC

Peak#	R.Time	I.Time	F.Time	Area	Area%	Height	eight%
1	5.998	5.795	6.295	103982	9.68	9074	7.06
2	6.865	6.645	7.045	110606	10.30	14050	10.93
3	7.684	7.585	7.825	40828	3.80	6709	5.22
4	16.247	16.155	16.410	83626	7.79	13449	10.46
5	19.000	18.820	19.220	103249	9.61	13308	10.35
6	24.309	24.045	24.745	264497	24.63	17713	13.78
7	25.675	25.470	25.870	291932	27.18	44351	34.51
8	30.709	30.555	30.845	75205	7.00	9875	7.68
				1073925	100.00	128529	100.00

(B)

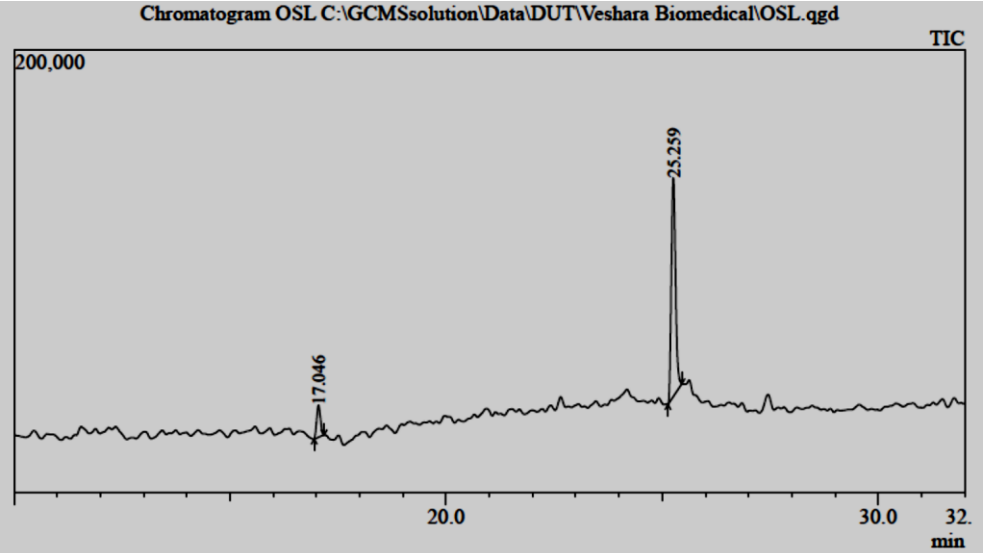

Peak Report TIC

Peak#	R.Time	I.Time	F.Time	Area	Area%	Height	Height%
1	17.046	16.945	17.175	87817	11.54	14476	12.85
2	25.259	25.135	25.455	673100	88.46	98212	87.15
				760917	100.00	112688	100.00

Appendix 25: GC-MS spectra indicating the chemical constituents present in *O. sanctum* aq. flower extract

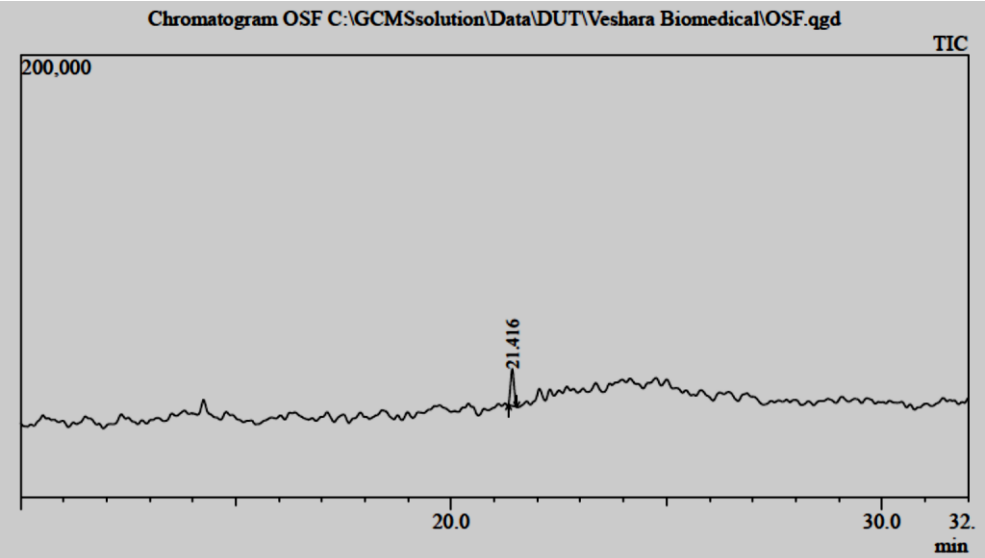

Peak Report TIC

Peak#	R.Time	I.Time	F.Time	Area	Area%	Height	Height%
1	21.416	21.330	21.520	91815	100.00	16719	100.00
				91815	100.00	16719	100.00

Appendix 26: (A) Chemical structures of the main chemical compounds identified in *O. sanctum* leaf extract (B) Amide compounds identified in *O. sanctum* leaf extract (C) Main chemical compounds identified in *O. sanctum* flower extract

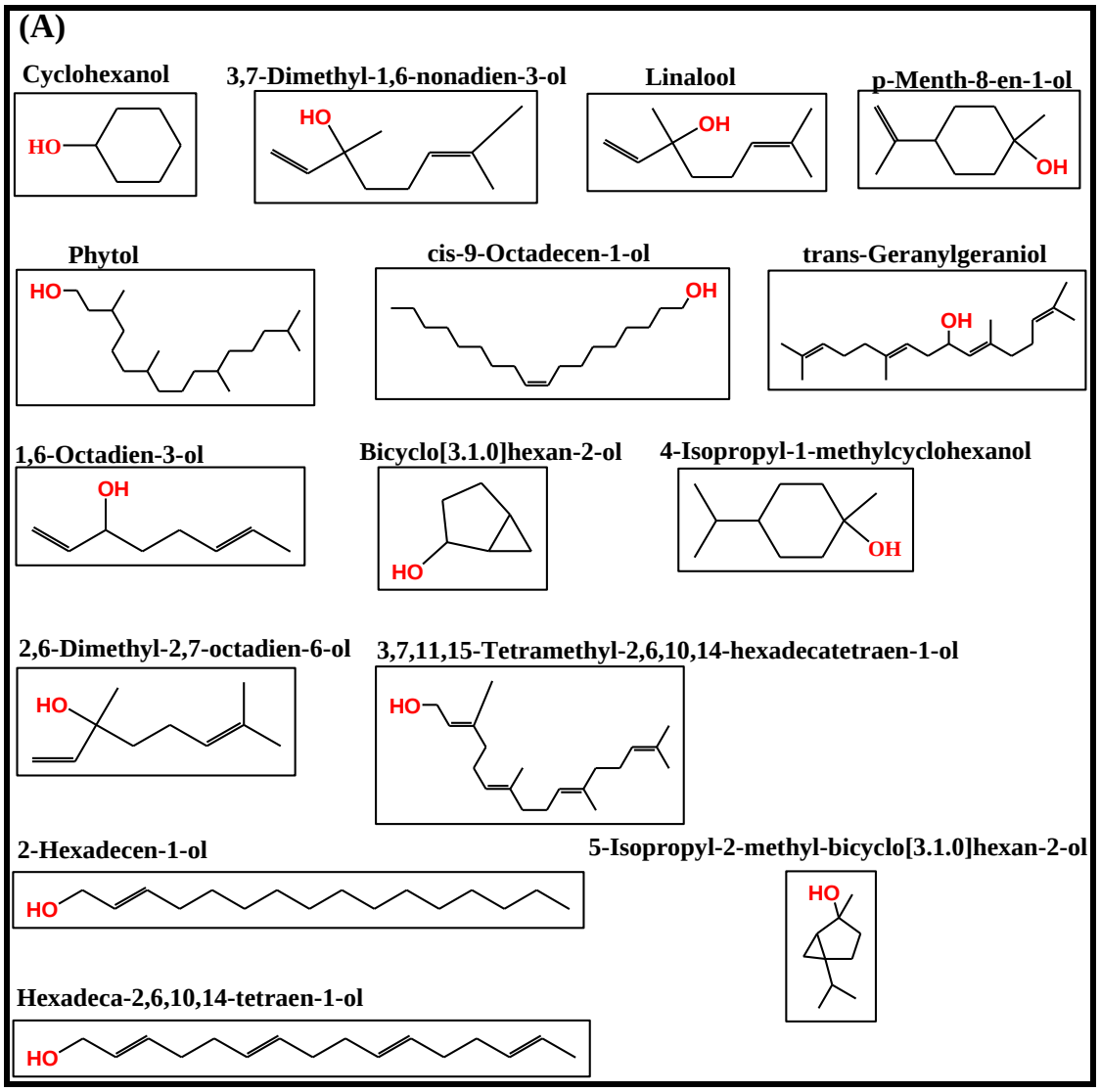

(B)

(13Z)-N-([(13Z)-13-Docosenoylamino]methyl)-13-docosenamide

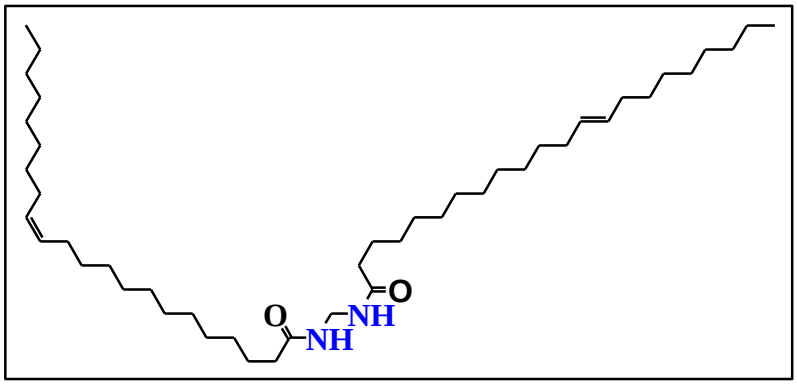

13-Docosenamide / Erucylamide

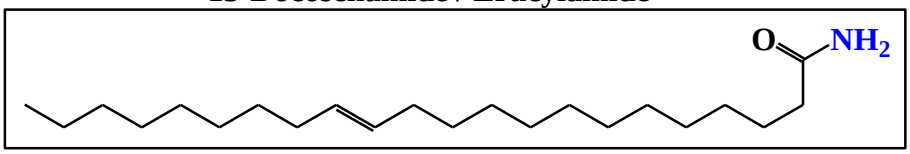

cis-11-Eicosenamide

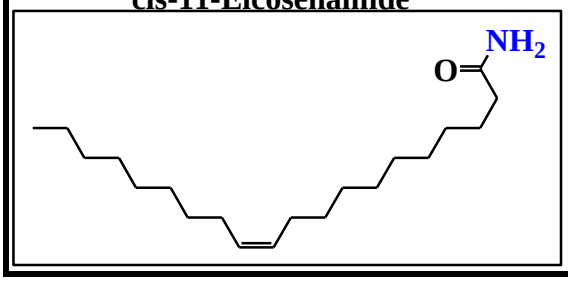

8-Methyl-6-nonenamide

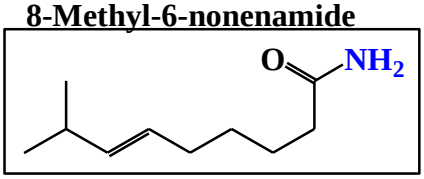

(C)

Octyl adipate

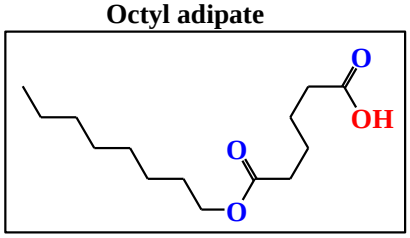

Adipic acid

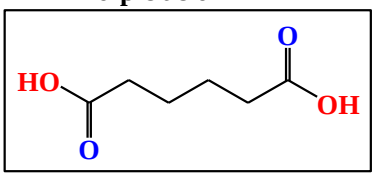

2-ethylhexyl pentadecyl

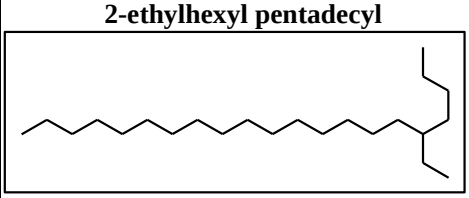

2-ethylhexyl tetradecyl

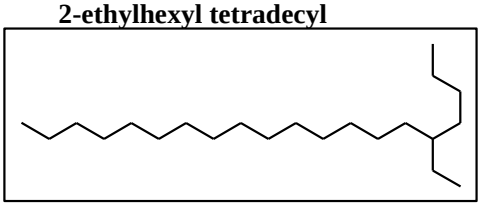

Diisooctyl adipate

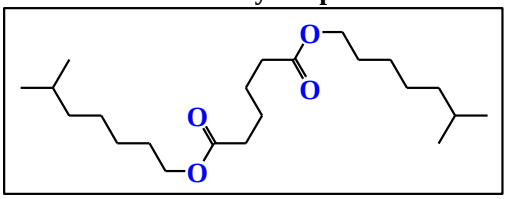

Appendix 27: Antibacterial activity of bimetallic Nps indicated by the mean inhibition (mm) against (A) *B. subtilis* and (B) Test statistic

*The mean inhibition (mm) ± SEM, N = 6 and comparisons of bimetallic (Au-Ag) Nps against all control groups. All values p < 0.05, p-value summary *; p < 0.01, p-value summary ** show a significant difference in the central (median) value; OB = O. basilicum*

(A)

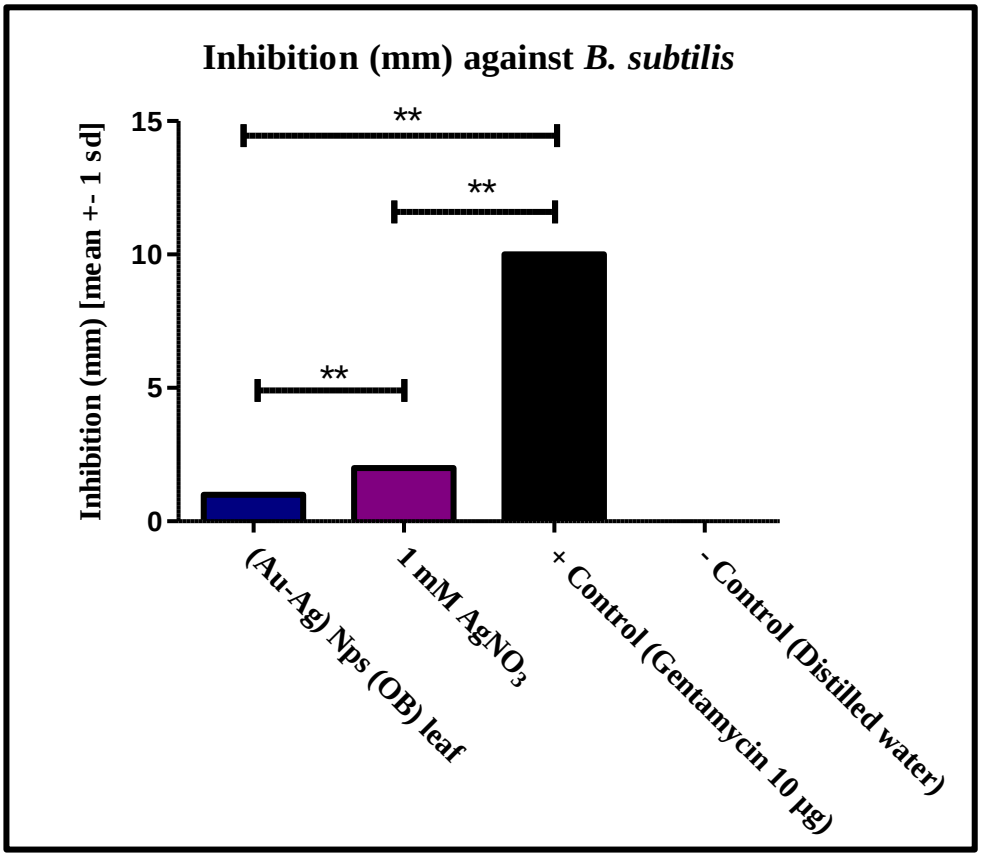

(B)

Test Statistic[a]		
	Z	Asymp. Sig. (2-tailed)
Control (1 mM $AgNO_3$) vs (Au-Ag) Nps (OB) leaf	-2.449[b]	0.014
+ Control (Gentamycin 10 µg) vs (Au-Ag) Nps (OB) leaf	-2.449[b]	0.014
- Control (Distilled water) vs (Au-Ag) Nps (OB) leaf	-2.449[c]	0.014
+ Control (Gentamycin 10 µg) vs Control (1 mM $AgNO_3$)	-2.449[b]	0.014
- Control (Distilled water) vs Control (1 mM $AgNO_3$)	-2.449[c]	0.014
- Control (Distilled water) vs + Control (Gentamycin 10 µg)	-2.449[c]	0.014

a. Wilcoxon Signed Ranks Test,
b. Based on positive ranks,
c. Based on negative ranks,

All values < 0.05 show a significant difference in the central (median) value.

Appendix 28: Antibacterial activity of bimetallic Nps indicated by the mean inhibition (mm) against *P. aeruginosa*

*The mean inhibition (mm) ± SEM, N = 6 and comparisons of bimetallic (Au-Ag) Nps against all control groups. All values with a $p < 0.05$, p-value summary * show a significant difference in the central (median) value; OB = O. basilicum*

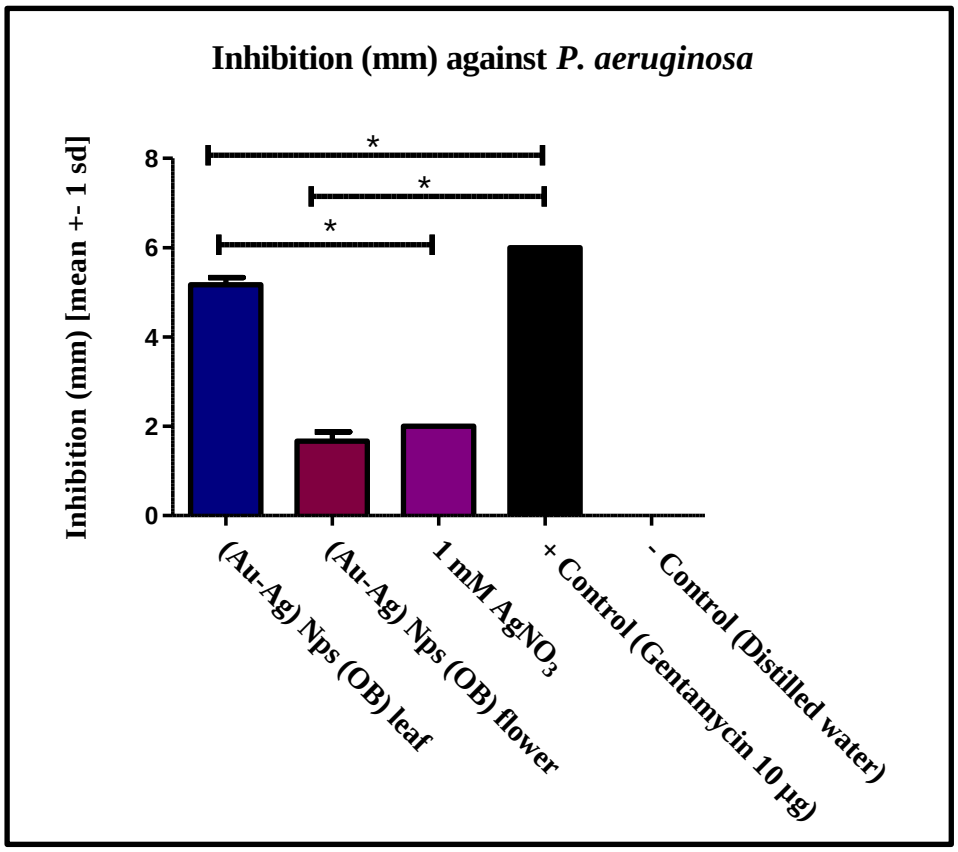

Appendix 29: Antibacterial activity of bimetallic Nps indicated by the mean inhibition (mm) against *E. coli*

*The mean inhibition (mm) ± SEM, N = 6 and comparisons of bimetallic (Au-Ag) Nps against all control groups. All values p < 0.05, p-value summary * show a significant difference in the central (median) value; OB = O. basilicum*

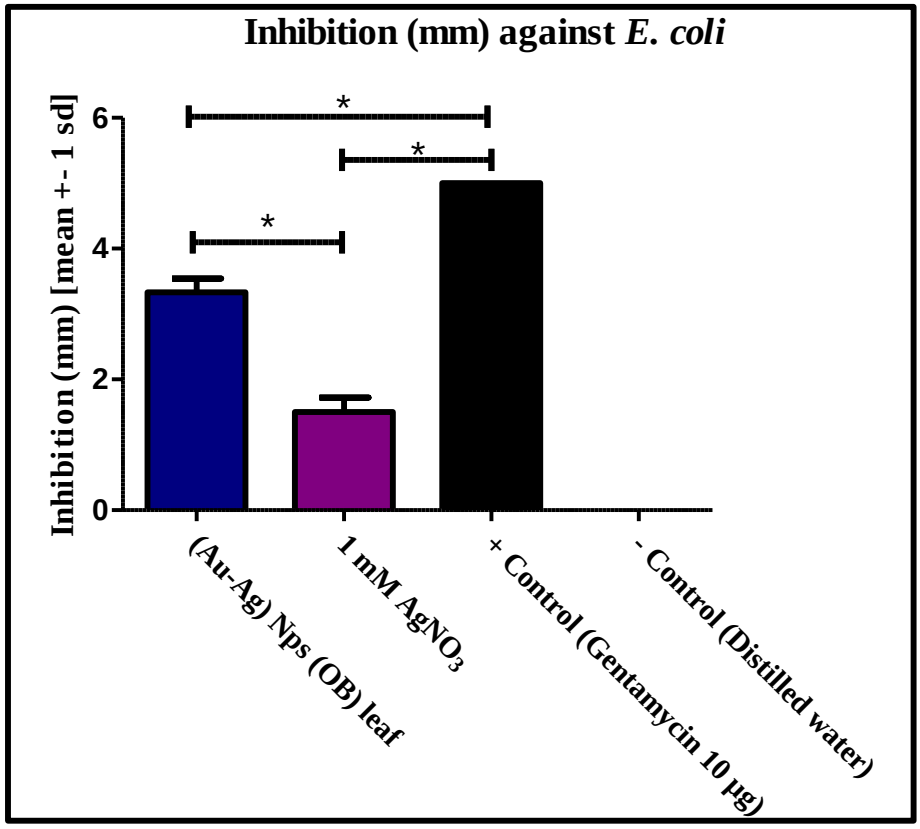

Appendix 30: Antibacterial activity of bimetallic Nps indicated by the mean inhibition (mm) against *S. aureus* at 100 µl/plate

*The mean inhibition (mm) ± SEM, N = 6 and comparisons of bimetallic (Au-Ag) Nps against all control groups. All values p < 0.05, p-value summary * show a significant difference in the central (median) value; OB = O. basilicum*

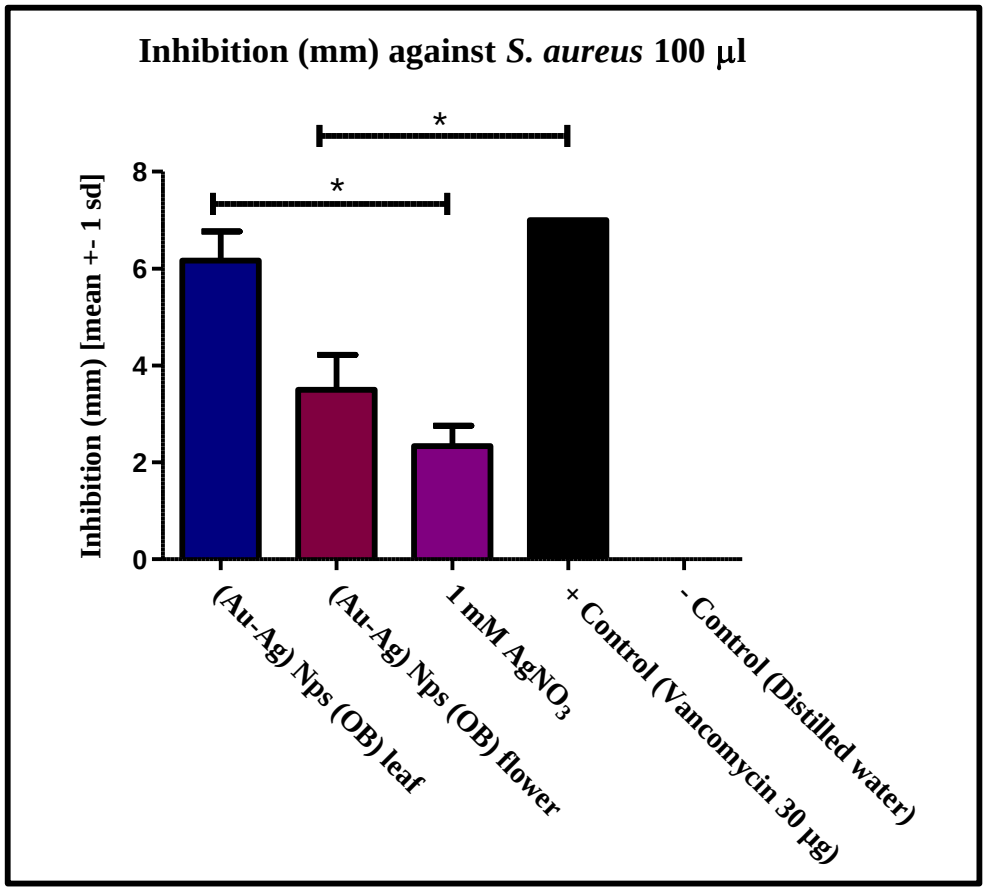

Appendix 31: Antibacterial activity of bimetallic Nps indicated by the mean inhibition (mm) against (A) *S. aureus* at 200 µl/plate and (B) Test statistic

*The mean inhibition (mm) ± SEM, N = 6 and comparisons of bimetallic (Au-Ag) Nps against all control groups. All values p < 0.05, p-value summary * show a significant difference in the central (median) value; OB = O. basilicum*

(A)

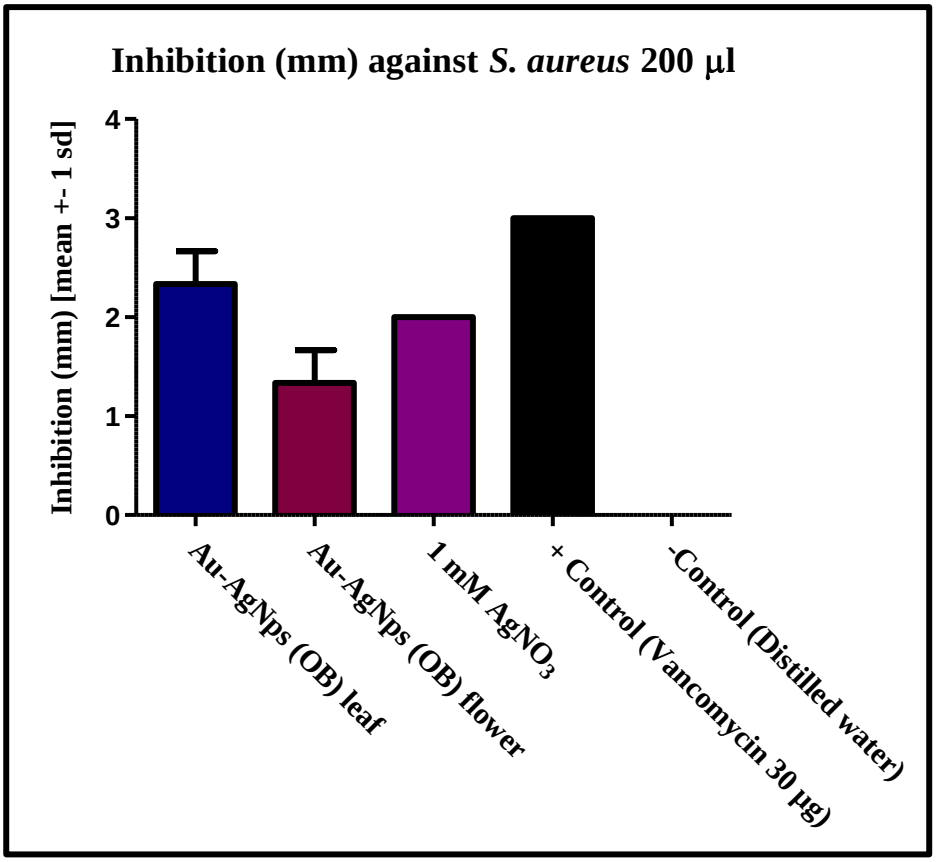

(B)

Test Statistic [a]		
	Z	Asymp. Sig. (2-tailed)
(Au-Ag) Nps (OB) flower vs (Au-Ag) Nps (OB) leaf	-1.342[b]	0.180
+ Control (Vancomycin 30 µg) vs (Au-Ag) Nps (OB) leaf	-1.414[c]	0.157
- Control (Distilled water) vs (Au-Ag) Nps (OB) leaf	-1.633[b]	0.102
+ Control (Vancomycin 30 µg) vs (Au-Ag) Nps (OB) flower	-1.633[c]	0.102
- Control (Distilled water) vs (Au-Ag) Nps (OB) flower	-1.633[b]	0.102
- Control (Distilled water) vs + Control (Vancomycin 30 µg)	-1.732[b]	0.083

a. Wilcoxon Signed Ranks Test,
b. Based on positive ranks,
c. Based on negative ranks,

All values < 0.05 show a significant difference in the central (median) value.

Appendix 32: Antibacterial activity of AgNps indicated by the mean inhibition (mm) against (A) *B. subtilis* and (B) Test statistic

*The mean inhibition (mm) ± SEM, N = 6 and comparisons of AgNps against all control groups. All values p < 0.05, p-value summary *; p < 0.01, p-value summary ** show a significant difference in the central (median) value; OS = O. sanctum, OB = O. basilicum*

(A)

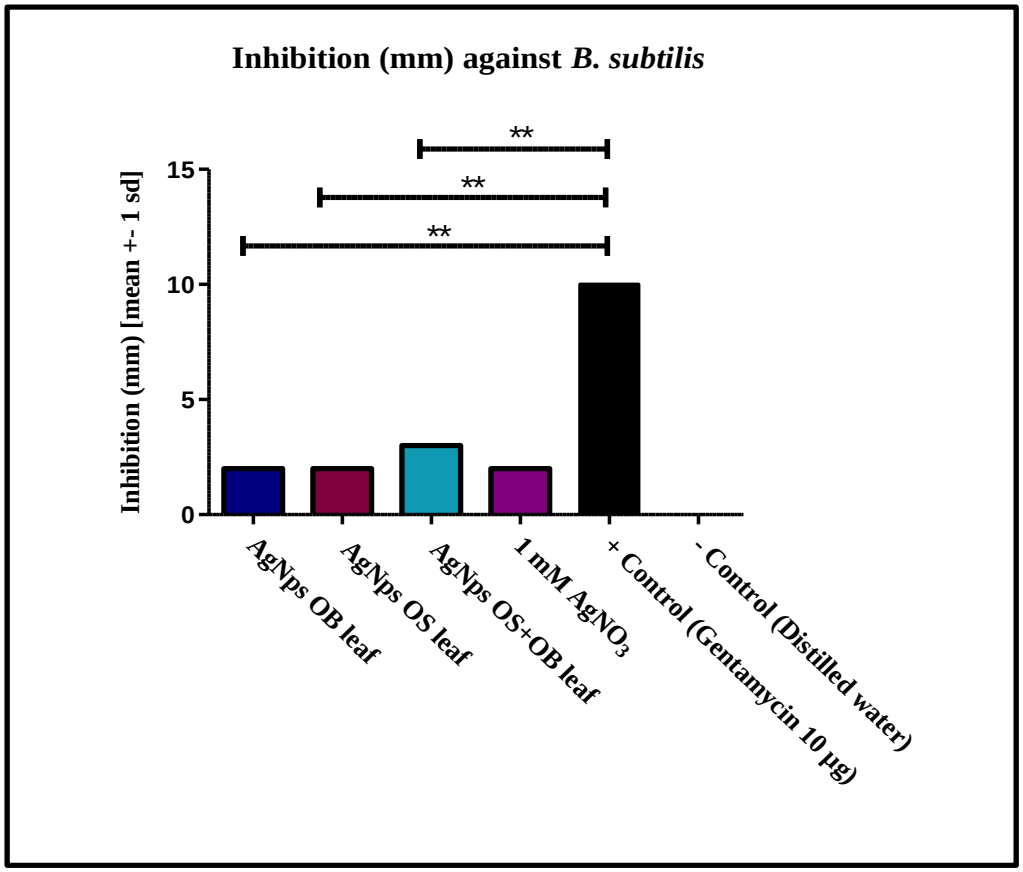

(B)

Test Statistic[a]			
	Sum of ranks	Mann-Whitney U	Asymp. Sig. (2-tailed)
OB AgNps vs OS AgNps	39, 39	18.00	<0.0001
OB AgNps vs OS+OB AgNps	21, 57	0.0	0.0013
OB AgNps vs 1 mM $AgNO_3$	39, 39	18.00	<0.0001
OB AgNps vs Gentamycin 10 µg	21, 57	0.0	0.0013
OB AgNps vs Distilled water	57, 21	0.0	0.0013
OS AgNps vs OS+OB AgNps	21, 57	0.0	0.0013
OS AgNps vs 1 mM $AgNO_3$	39, 39	18.00	<0.0001
OS AgNps vs Gentamycin 10 µg	21, 57	0.0	0.0013
OS AgNps vs Distilled water	57, 21	0.0	0.0013
OS+OB AgNps vs 1 mM $AgNO_3$	57, 21	0.0	0.0013
OS+OB AgNps vs Gentamycin 10 µg	21, 57	0.0	0.0013
OS+OB AgNps vs Distilled water	57, 21	0.0	0.0013
1 mM $AgNO_3$ vs Gentamycin 10 µg	57, 21	0.0	0.0013
1 mM $AgNO_3$ vs Distilled water	57, 21	0.0	0.0013

Grouping variable: Bacteria per plate (100 µl)

Appendix 33: Antibacterial activity of AgNps indicated by the mean inhibition (mm) against *E. coli*

*The mean inhibition (mm) ± SEM, N = 6 and comparisons of AgNps against all control groups. All values p < 0.05, p-value summary * show a significant difference in the central (median) value; OS = O. sanctum, OB = O. basilicum*

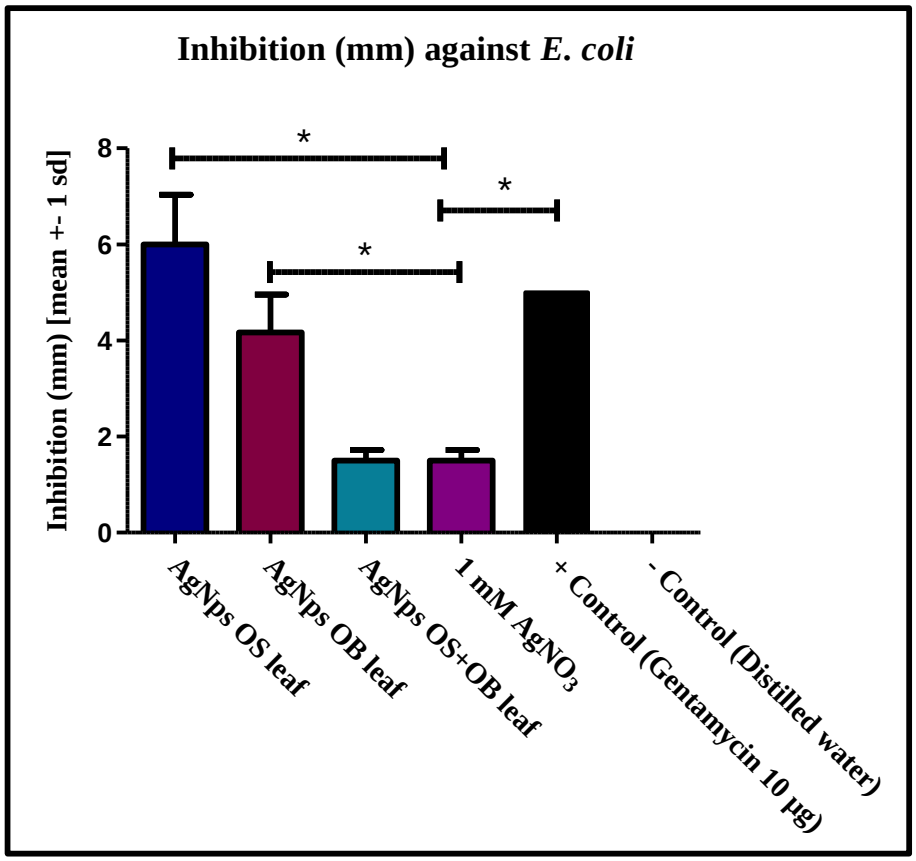

Appendix 34: Antibacterial activity of AgNps indicated by the mean inhibition (mm) against *P. aeruginosa*

*The mean inhibition (mm) ± SEM, N = 6 and comparisons of AgNps against all control groups. All values p < 0.05, p-value summary * show a significant difference in the central (median) value; OS = O. sanctum, OB = O. basilicum*

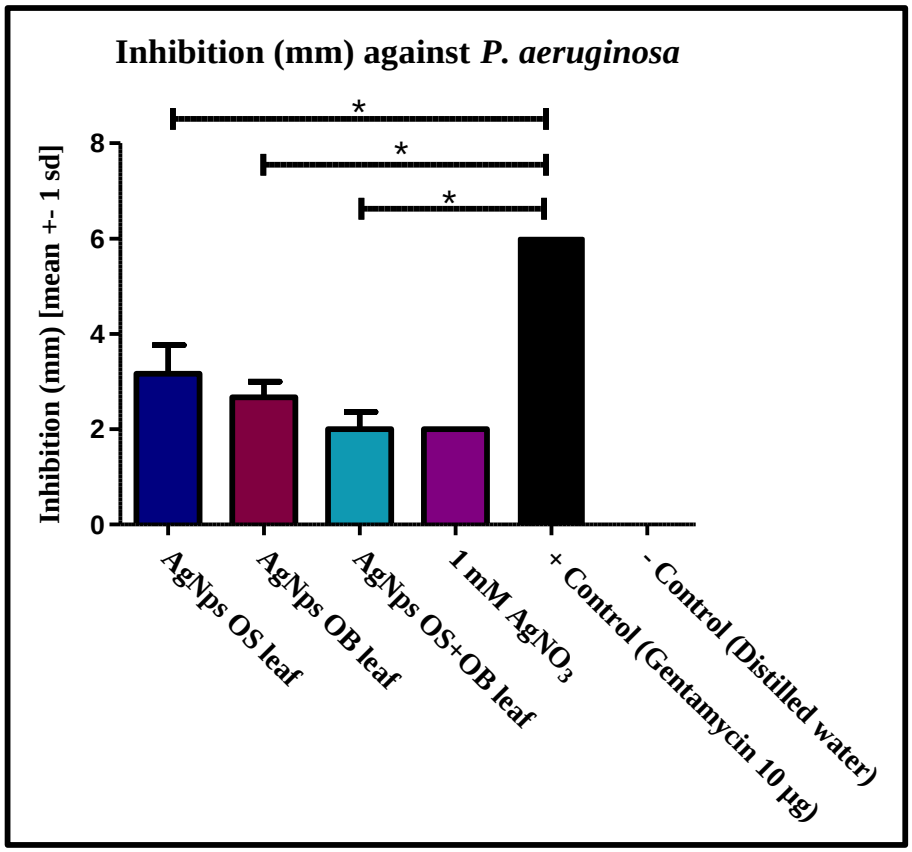

Appendix 35: Antibacterial activity of AgNps indicated by the mean inhibition (mm) against *Salmonella* sp.

*The mean inhibition (mm) ± SEM, N = 6 and comparisons of AgNps against all control groups. All values p < 0.05, p-value summary * show a significant difference in the central (median) value; OS = O. sanctum*

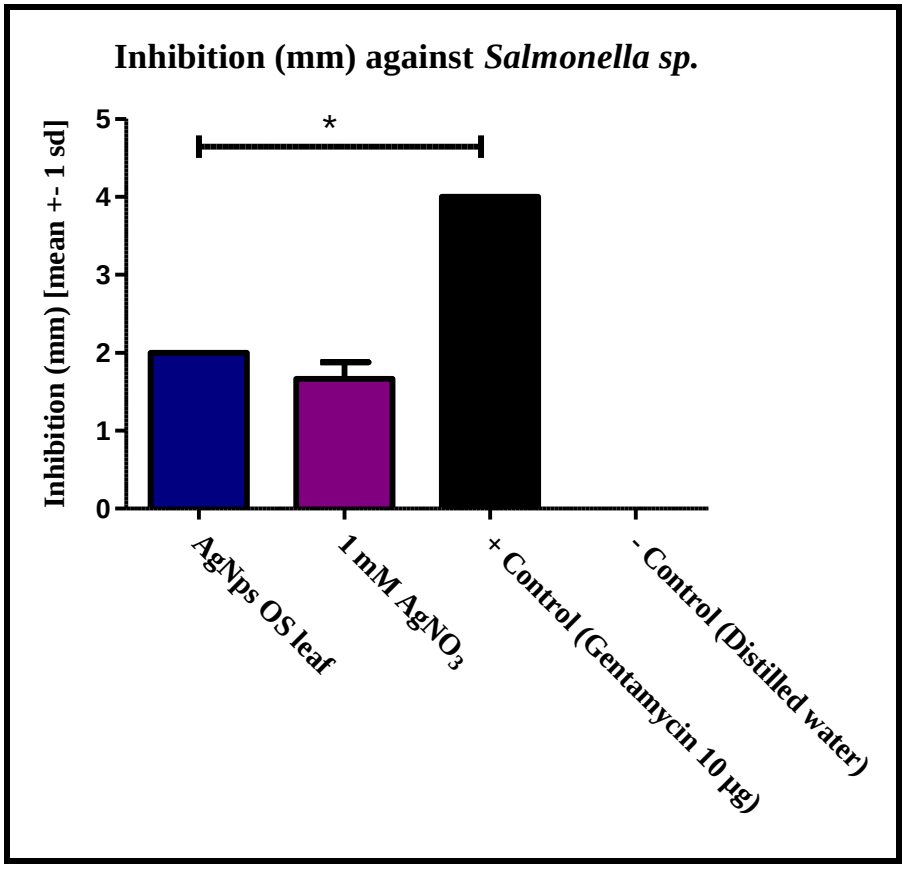

Appendix 36: Antibacterial activity of AgNps indicated by the mean inhibition (mm) against *S. aureus* at 100 µl/plate

*The mean inhibition (mm) ± SEM, N = 6 and comparisons of AgNps against all control groups. All values p < 0.05, p-value summary * show a significant difference in the central (median) value; OS = O. sanctum, OB = O. basilicum*

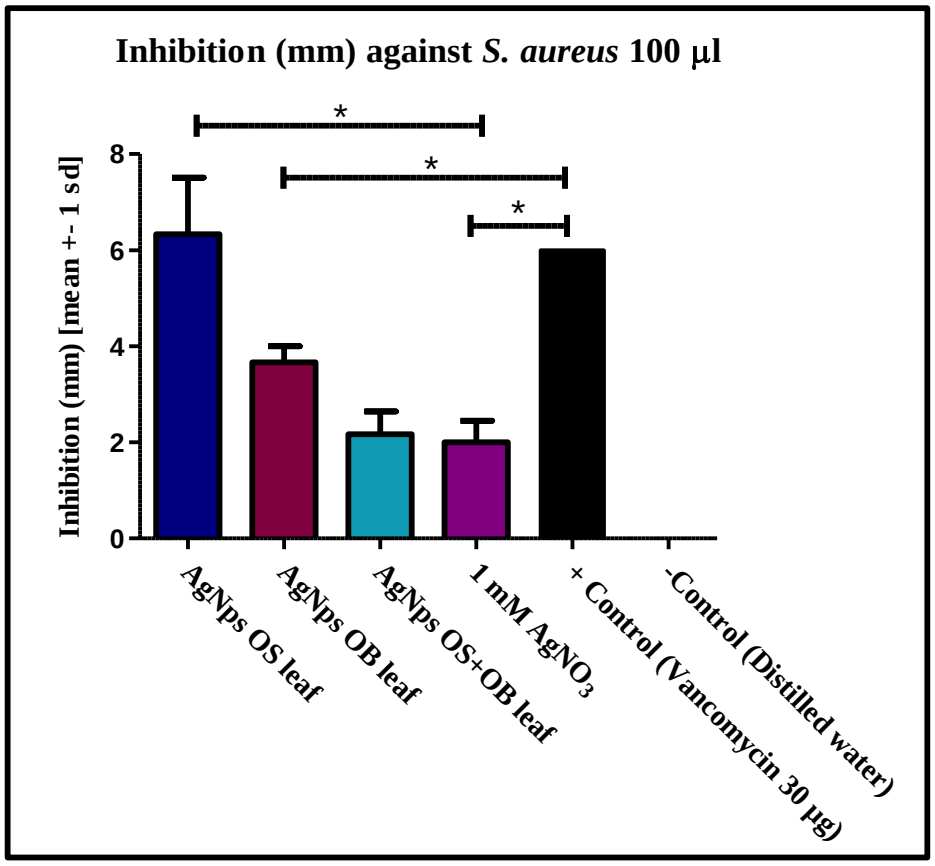

Appendix 37: Antibacterial activity of AgNps indicated by the mean inhibition (mm) against (A) *S. aureus* at 200 µl/plate and (B) Test statistic

The mean inhibition (mm) ± SEM, N = 6 and comparisons of AgNps against all groups. All values p < 0.05 show a significant difference in the central (median) value

(A)

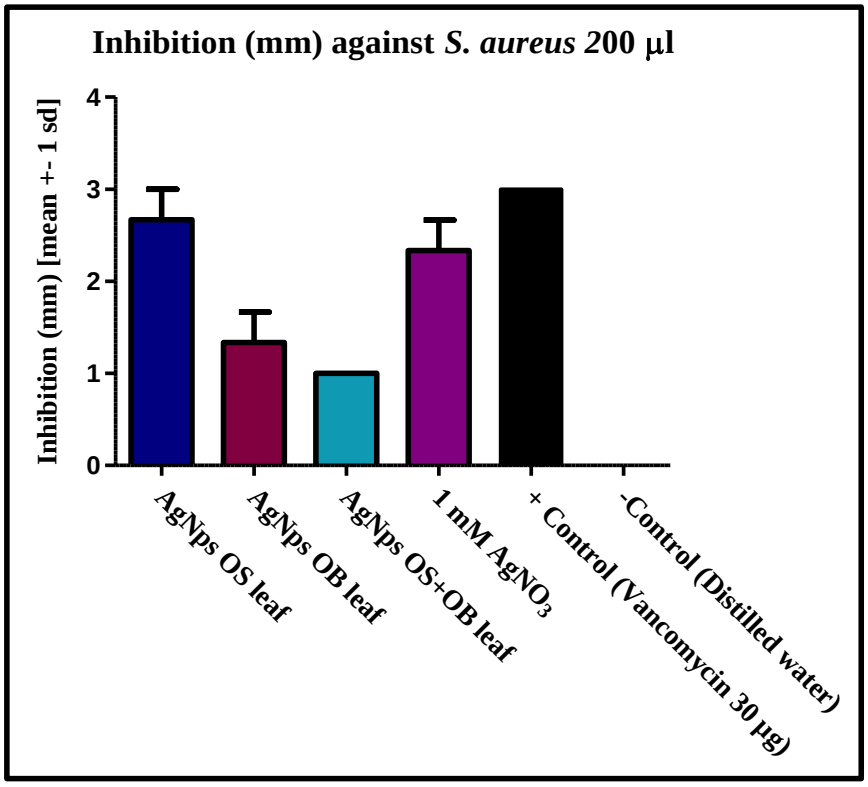

(B)

Test Statistic [a]		
	Z	Asymp. Sig. (2-tailed)
OB AgNps vs OS AgNps	-1.633[b]	0.102
OS+OB AgNps vs OS AgNps	-1.633[b]	0.102
+ Control (Vancomycin 30 µg) vs OS AgNps	-1.000[c]	0.317
-Control (Distilled water) vs OS AgNps	-1.633[b]	0.102
OS+OB AgNps vs OB AgNps	-1.000[b]	0.317
+ Control (Vancomycin 30 µg) vs OB AgNps	-1.633[c]	0.102
-Control (Distilled water) vs OB AgNps	-1.633[b]	0.102
+ Control (Vancomycin 30 µg) vs OS+OB AgNps	-1.732[c]	0.083
-Control (Distilled water) vs OS+OB AgNps	-1.732[b]	0.083
-Control (Distilled water) vs + Control (Vancomycin 30 µg)	-1.732[b]	0.083

a. Wilcoxon Signed Ranks Test,
b. Based on positive ranks,
c. Based on negative ranks,

All values < 0.05 show a significant difference in the central (median) value.

Appendix 38: Inhibitory activities on α-amylase of various crude *Ocimum* sp. extracts tested for their hypoglycaemic activity at different dose-response, in a concentration range (0.002-2 mg/ml)

Results expressed as a % mean ± SEM, N = 2; OS = O. sanctum, OB = O. basilicum; Aq. dist. = Aqueous distillation

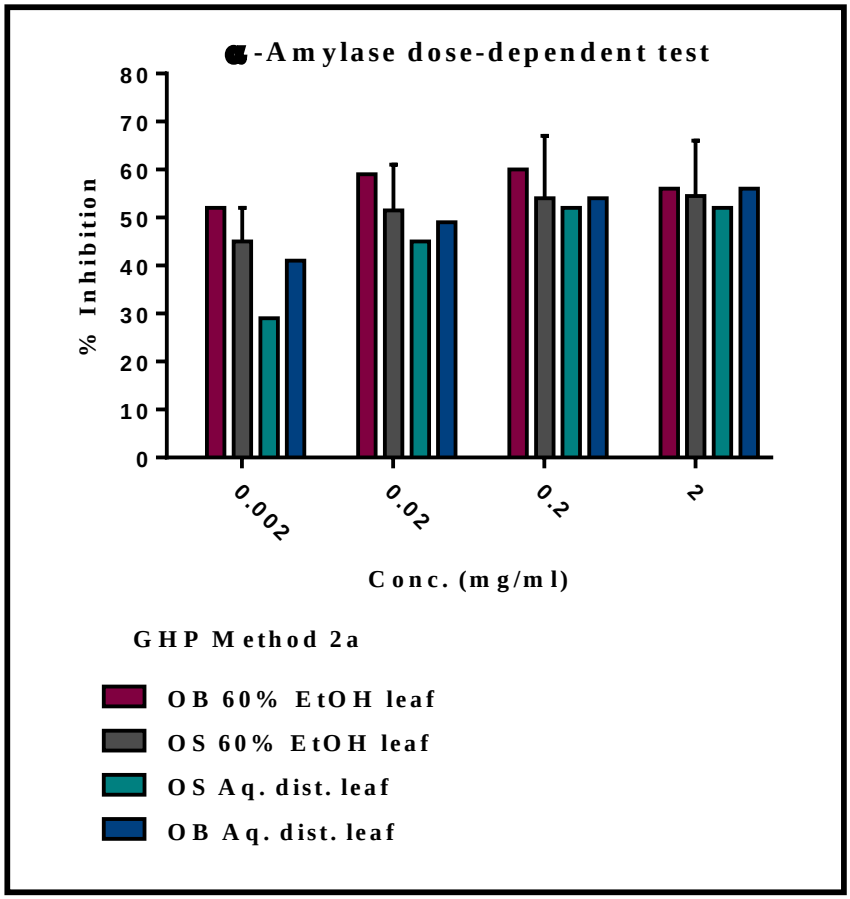

Appendix 39: Inhibitory activities on α-amylase of various crude *Ocimum* sp. extracts, tested for their hypoglycaemic activity at different dose-response, in a concentration range (0.003-3 mg/ml)

Results expressed as a % mean ± SEM, *N* = 2; OS = *O. sanctum*, OB = *O. basilicum; Aq. dist. = Aqueous distillation*

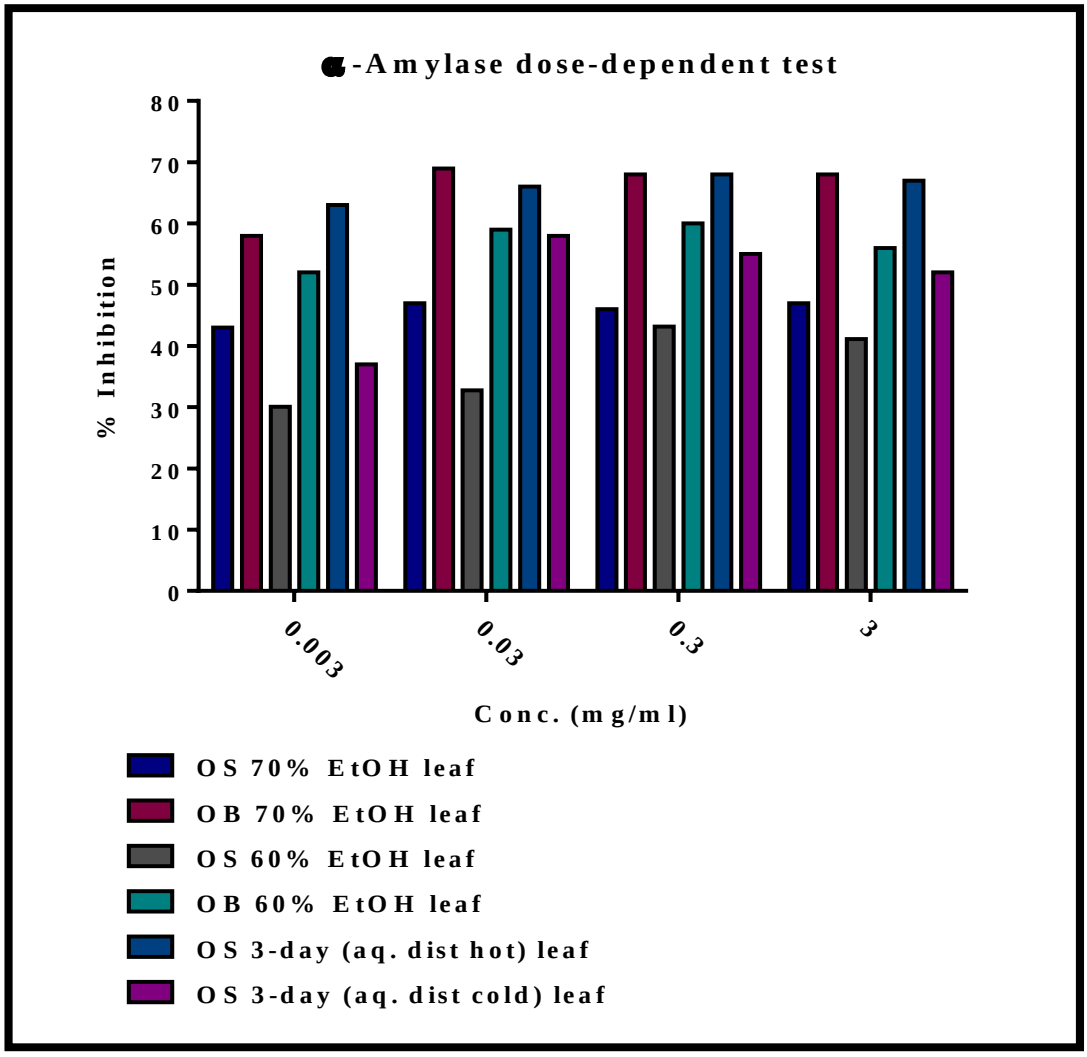

Appendix 40: Inhibitory activities on α-amylase of various crude *Ocimum* sp. flower extracts tested for their hypoglycaemic activity at different dose-response, in a concentration range (0.181-5.8 mg/ml)

Results expressed as a % mean ± SEM, N = 2; OS = O. sanctum, OB = O. basilicum

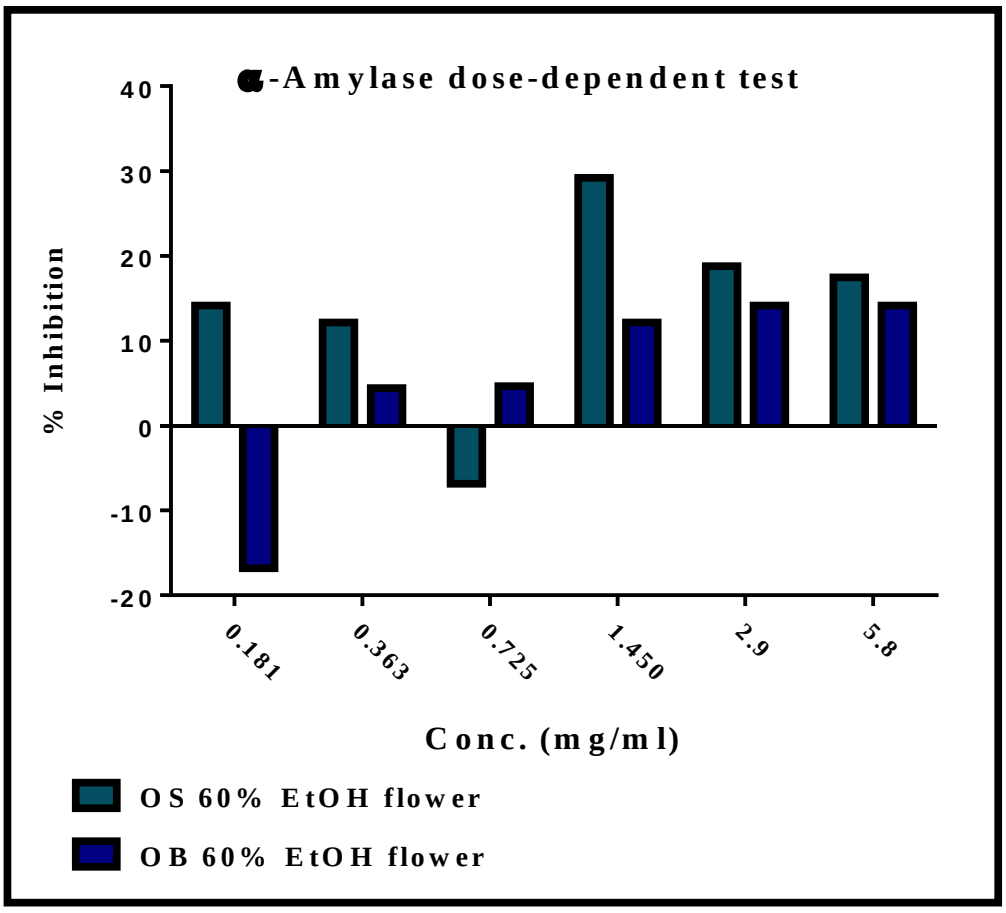

Appendix 41: Inhibitory activities on α-amylase of bimetallic (Au-Ag) Nps synthesised from *O. basilicum* for leaf and flower extracts, tested for their hypoglycaemic activity at different dose-response, in a concentration range (0.0002-2 mg/ml)

*Results expressed as a % mean ± SEM, N = 3, p-value < 0.05, p-value summary *; p-value < 0.01, p-value summary **; p-value < 0.0001, p-value summary ****

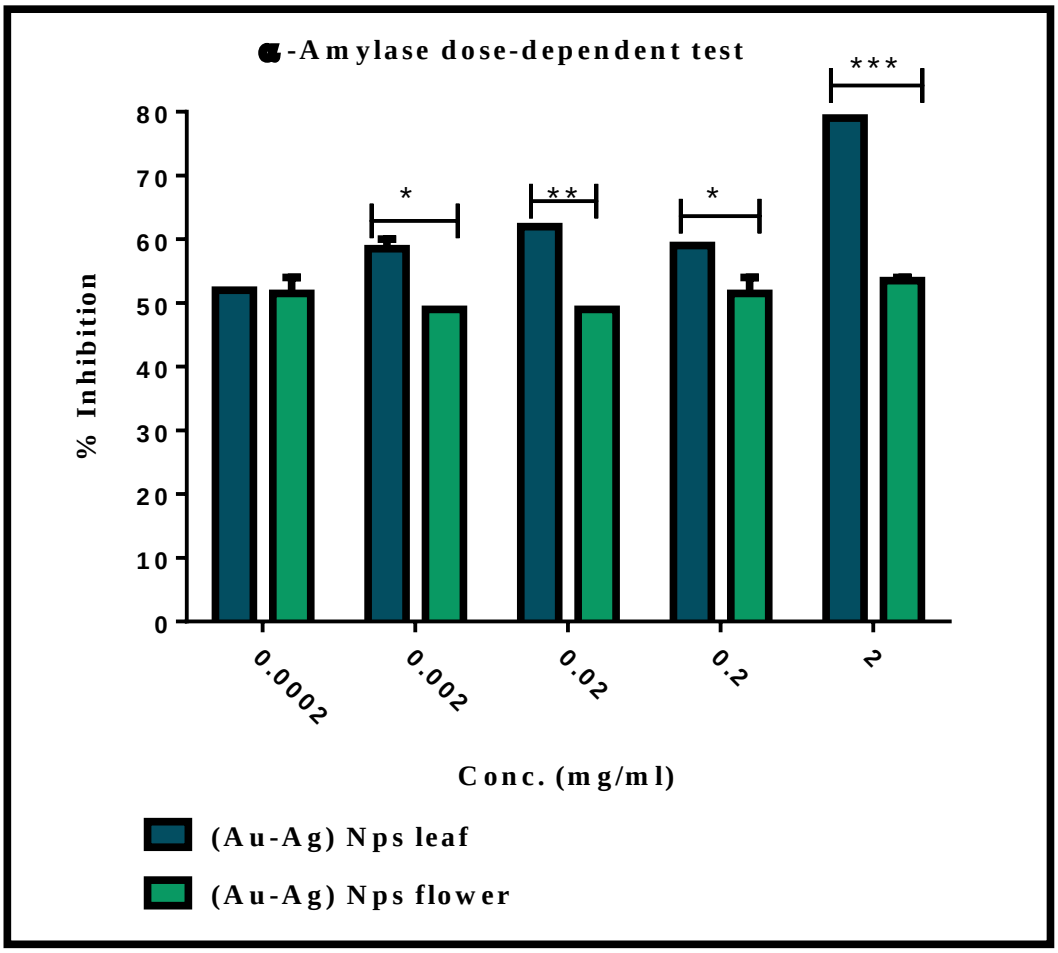

Appendix 42: Inhibitory activities on α-amylase of AgNps synthesised from various *Ocimum* sp. extracts, tested for their hypoglycaemic activity at different dose-response, in a concentration range (0.05-1.6 mg/ml)

*Results expressed as a % mean ± SEM, N = 3, p-value < 0.05, p-value summary * and p-value < 0.01, p-value summary **; OS = O. sanctum, OB = O. basilicum*

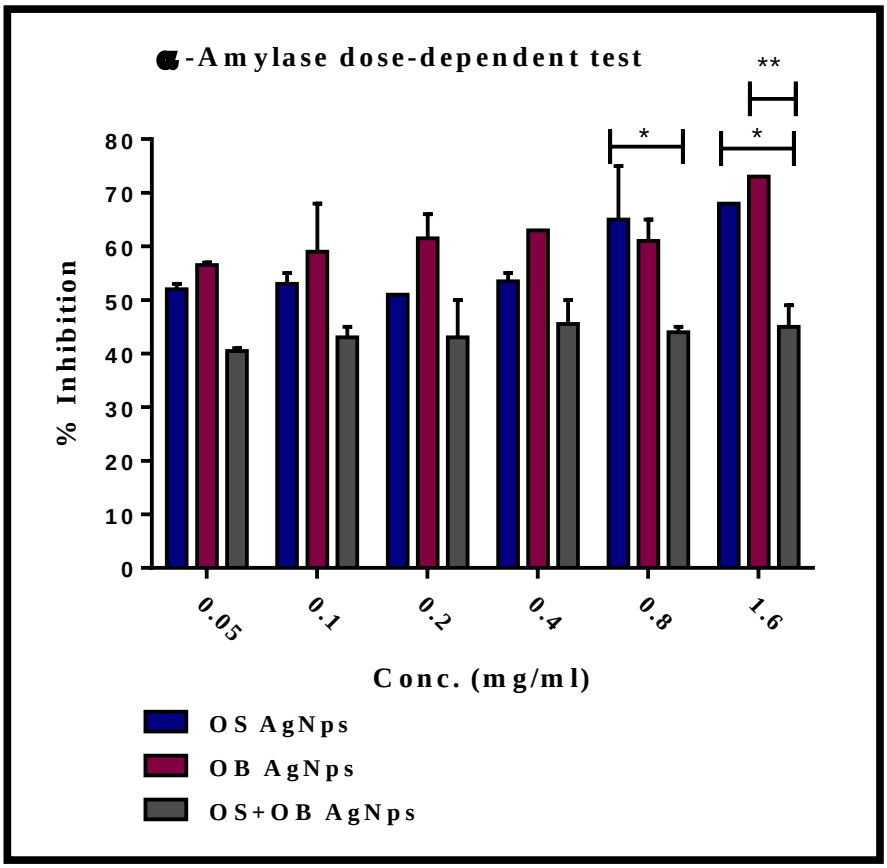

Appendix 43: Inhibitory activities on α-glucosidase of crude *O. basilicum* extracts, tested for their hypoglycaemic activity at different dose-response, in a concentration range (0.0003-0.3 mg/ml)

*Results expressed as a % mean ± SEM, N = 2, p-value < 0.05, p-value summary * and p-value < 0.01, p-value summary **; GHP = German Homoeopathic Pharmacopoeia; Aq. dist. = Aqueous distillation*

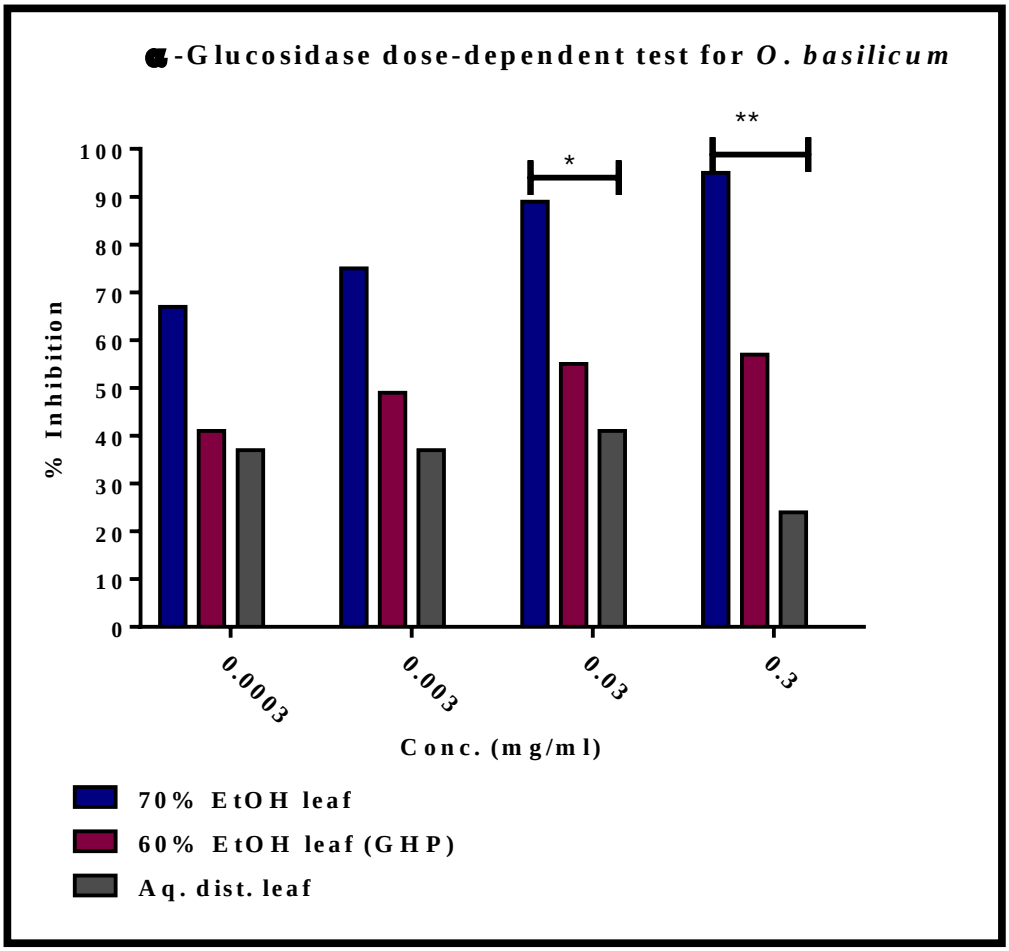

Appendix 44: Inhibitory activities on α-glucosidase activity of crude *O. sanctum* extracts, tested for their hypoglycaemic activity at different dose-response, in a concentration range (0.0003-0.3 mg/ml)

*Results expressed as a % mean ± SEM, N = 2, p-value < 0.05, p-value summary *; OS = O. sanctum; GHP = German Homoeopathic Pharmacopoeia; Aq. dist. = Aqueous distillation*

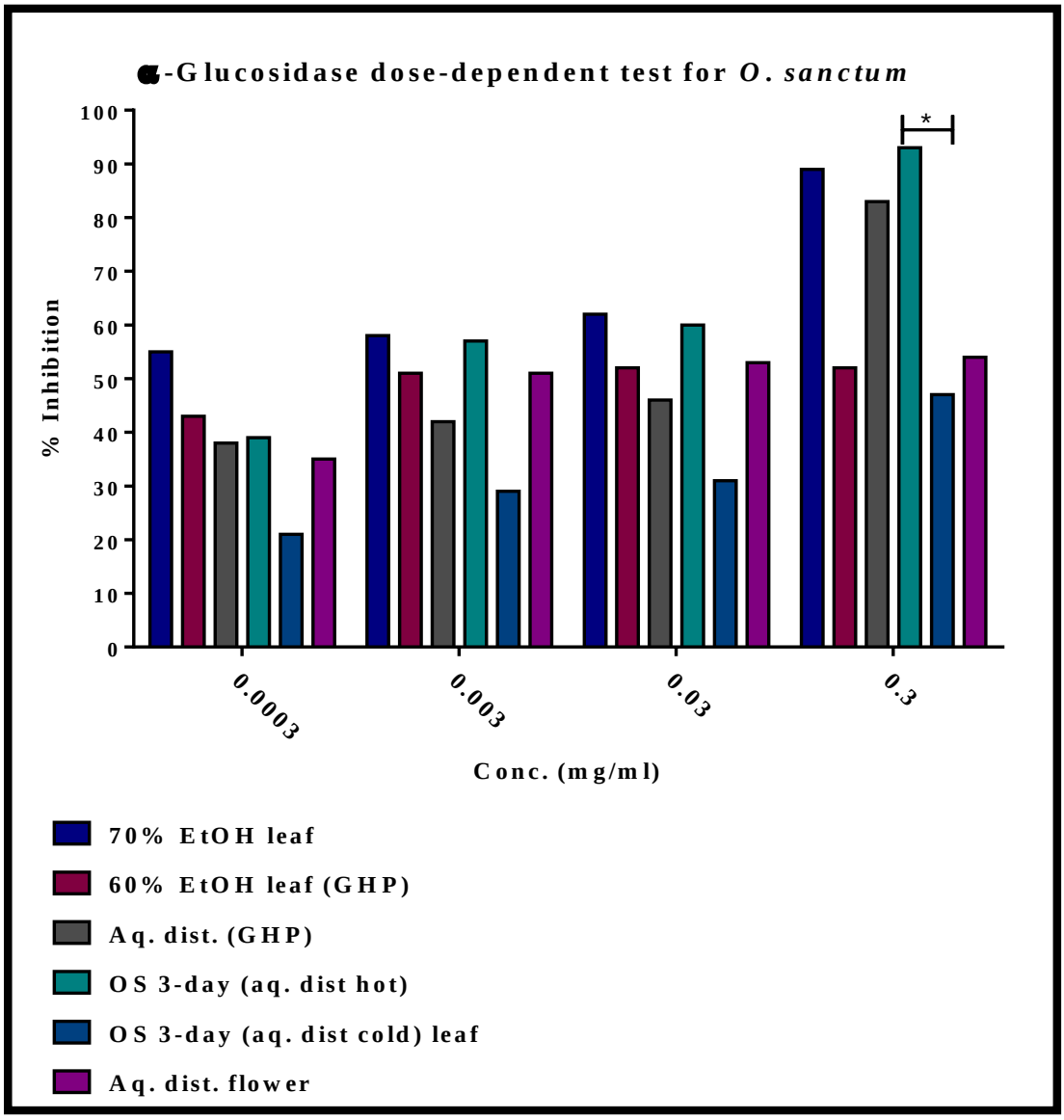

Appendix 45: Inhibitory activities on α-glucosidase activity of bimetallic (Au-Ag) Nps synthesised from *O. basilicum* extracts, tested for their hypoglycaemic activity at different dose-response, in a concentration range (0.0002-0.2 mg/ml)

*Results expressed as a % mean ± SEM; N = 2; p-value < 0.05, p-value summary **

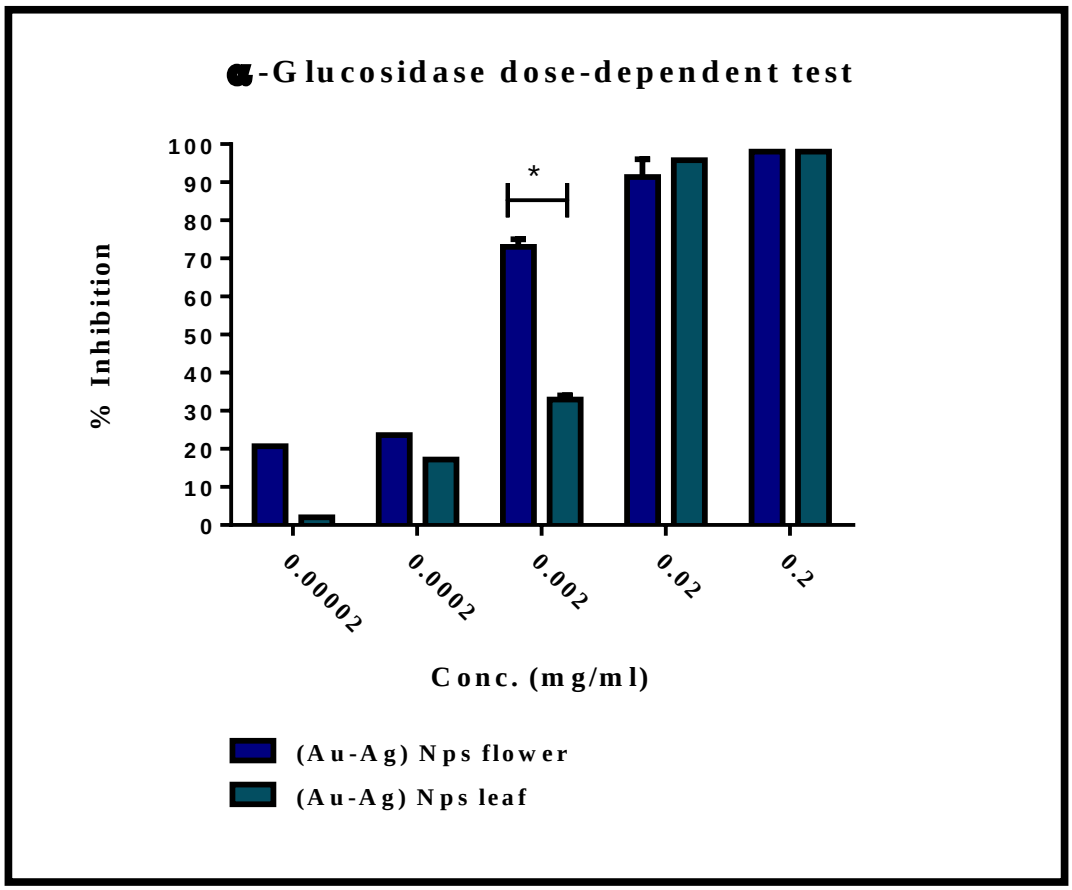

Appendix 46: Inhibitory activities on α-glucosidase activity of AgNps synthesised from various *Ocimum* sp. extracts, tested for their hypoglycaemic activity at different dose-response, in a concentration range (0.0003-3 mg/ml)

Results expressed as a % mean ± SEM; N = 3; OS = O. sanctum, OB = O. basilicum

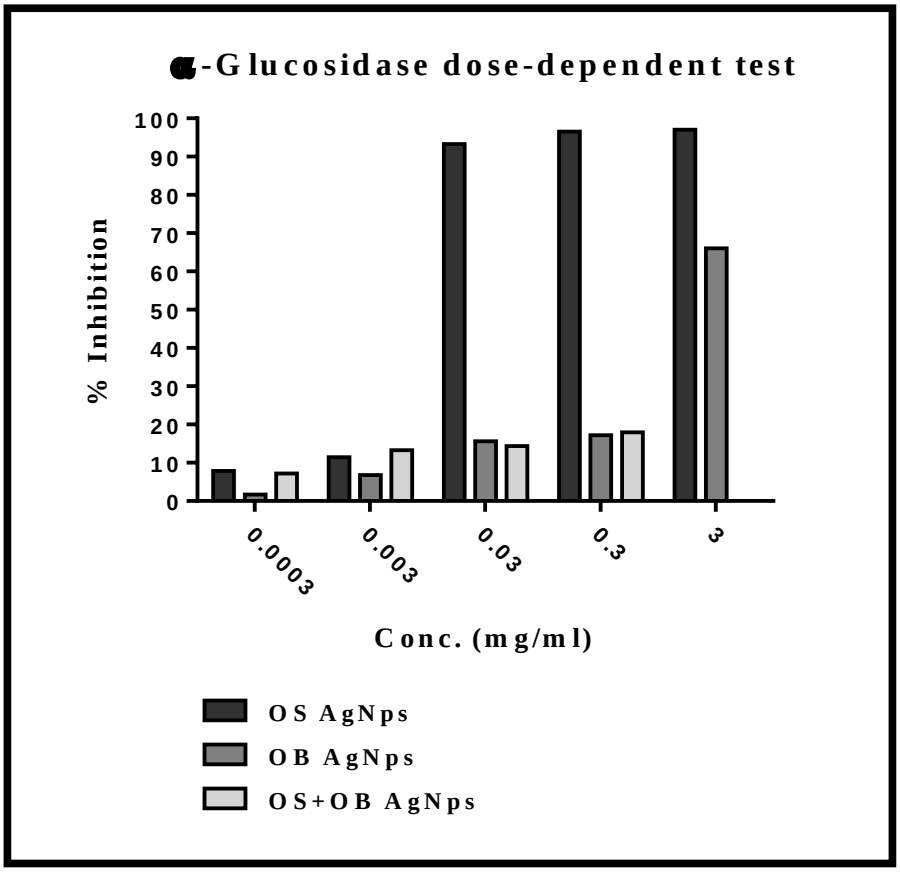

Appendix 47: Interaction of medicinal plants in combination with Glibenclamide

Plant	Study design	Interaction	References
Zingiber officinale	In STZ-induced diabetic rat	Potentiation of effect, lacks trial on patients	Al-Omaria *et al.* 2012
Aloe vera	Placebo-controlled single blinded randomised study in patients	Beneficial and promising effect	Bunyapraphatsara *et al.* 1996
Pleurotus pulmonarius	Alloxan-induced diabetic mice	Synergistic effect	Badole *et al.* 2008
Gymnema sylvestre	Trial in patients	Synergistic effect	Sharma and Kar 2014
Trigonella foenum graceum	STZ-induced diabetic rats	Synergistic effect	Gupta *et al.* 2001
Azadirachta indica	Alloxan-induced diabetic rabbits	No contraindication is reported	Lal *et al.* 2011
Momordica charantia	STZ-induced diabetic rats	Synergistic effect	Lal *et al.* 2011
Allium sativum	Alloxan-induced diabetic rats	No contraindication is reported	Eyo *et al.* 2011
Costus afer	Fasting blood glucose of normal rats. Adult male wistar strain albino rats	Significant reduction in fasting blood sugar of glucose loaded and unloaded rats.	Momoh *et al.* 2011
Ginkgo biloba	Double-blind randomised trial in patients	Contraindication	Kudolo 2001

List of Conferences

Presentation

National

Nominated to participate in the Falling walls laboratory Conference. Presented research entitled: Breaking the wall of… *In vitro* evaluation of the antidiabetic properties and synergistic potential of *Ocimum sanctum* (L.) held in Johannesburg, SA on 13th September 2013.

Presented research entitled: Type 2 Diabetes Mellitus, specifically focusing on the potential use of combining traditional medicines and drug therapy held by the Society of Medical Laboratory Technologists (SMLTSA) on 26th October 2013 at Albert Luthuli, Durban, SA.

Award received for the best oral presentation in Health Science faculty, research entitled: Phytosynthesis of bimetallic Au-Ag nanoparticles using *Ocimum basilicum* (L.) with enhanced antidiabetic and antimicrobial properties, held in Durban University of Technology Institutional Research Day on the 26th November 2014 in Durban, SA.

Poster presentation for the second National Global Change Conference, held in Port Elizabeth (Nelson Mandela Metropolitan University), South Africa on the 3rd December 2014.

Presented a research paper at the conference titled Medical Laboratory Professionals Congress 2015, (SMLTSA), at the Boardwalk conference centre, Port Elizabeth, SA from the 15-17 May 2015.

Selected to participate in the conference titled Nanotech France 2015 for an oral presentation in Paris, France from the 15-17 June 2015.

Selected to participate in the conference titled Recent Advances in Nano Science and Technology (RAINSAT-2015) for an oral presentation in Chennai, India from the 8-10 July 2015.

List of publications

Enhancing antidiabetic and antimicrobial performance of *Ocimum basilicum*, and *Ocimum sanctum* (L.) using silver nanoparticles. Veshara Malapermal, Izel Botha, Suresh Babu Naidu Krishna, Joyce Nonhlanhla Mbatha. *Saudi Journal of Biological Sciences*, 2015. DOI: 10.1016/j.sjbs.2015.06.026.

Biosynthesis of bimetallic Au-Ag nanoparticles using *Ocimum basilicum* (L.) with antidiabetic and antimicrobial properties. V. Malapermal, J.N. Mbatha, R.M. Gengan, K. Anand. *Advanced Materials Letters*, 2015. DOI: 10.5185/amlett.2015.5997.